



PHD

**NMR studies of the cyclodextrin complexes of some 2-arylpropionates and their application to chiral analysis**

Marchant, Carol A.

*Award date:*  
1992

*Awarding institution:*  
University of Bath

[Link to publication](#)

**Alternative formats**

If you require this document in an alternative format, please contact:  
[openaccess@bath.ac.uk](mailto:openaccess@bath.ac.uk)

Copyright of this thesis rests with the author. Access is subject to the above licence, if given. If no licence is specified above, original content in this thesis is licensed under the terms of the Creative Commons Attribution-NonCommercial 4.0 International (CC BY-NC-ND 4.0) Licence (<https://creativecommons.org/licenses/by-nc-nd/4.0/>). Any third-party copyright material present remains the property of its respective owner(s) and is licensed under its existing terms.

**Take down policy**

If you consider content within Bath's Research Portal to be in breach of UK law, please contact: [openaccess@bath.ac.uk](mailto:openaccess@bath.ac.uk) with the details. Your claim will be investigated and, where appropriate, the item will be removed from public view as soon as possible.

NMR STUDIES OF THE CYCLODEXTRIN COMPLEXES OF SOME 2-  
ARYLPROPIONATES AND THEIR APPLICATION TO CHIRAL ANALYSIS

submitted by Carol A. Marchant  
for the degree of PhD  
of the University of Bath  
1992

COPYRIGHT

Attention is drawn to the fact that copyright of this thesis rests with its author. This copy of the thesis has been supplied on condition that anyone who consults it is understood to recognise that its copyright rests with its author and that no quotation from the thesis and no information derived from it may be published without the prior written consent of the author.

This thesis may be made available for consultation within the University Library and may be photocopied or lent to other libraries for the purposes of consultation.

*C Marchant*

UMI Number: U045688

All rights reserved

INFORMATION TO ALL USERS

The quality of this reproduction is dependent upon the quality of the copy submitted.

In the unlikely event that the author did not send a complete manuscript and there are missing pages, these will be noted. Also, if material had to be removed, a note will indicate the deletion.



UMI U045688

Published by ProQuest LLC 2014. Copyright in the Dissertation held by the Author.  
Microform Edition © ProQuest LLC.

All rights reserved. This work is protected against  
unauthorized copying under Title 17, United States Code.



ProQuest LLC  
789 East Eisenhower Parkway  
P.O. Box 1346  
Ann Arbor, MI 48106-1346

UNIVERSITY OF BATH  
LIBRARY

93

17 SEP 1992

Ph.D.

5062355



**for Mum and Dad**

... for it is but just that men, who so often arrogate to their own merit the good of which they are but instruments, should also attribute to themselves absurdities which they could not prevent.

*Vathek* by William Beckford

## ACKNOWLEDGEMENTS

This work was carried out in the School of Pharmacy and Pharmacology, University of Bath, under the supervision of Dr Sarah K. Branch and funded by an SERC quota award.

I would like to thank Sarah for her patience, help and encouragement both during the course of this work and the preparation of this thesis.

I would also like to thank Dave Wood and Harry Hartell for their help and co-operation in the use of NMR facilities both at Bath and on a jointly owned spectrometer in the Department of Chemistry, University of Bristol.

I am indebted to Rose Silvester, Martin Murray and Robin Goodfellow of that department, again for co-operation in the use of NMR facilities and, in addition, for generously sharing their knowledge of NMR spectroscopy and spectrometer with me.

I thank members of the School of Pharmacy and Pharmacology for their considerable technical and administrative support. In particular, I acknowledge the assistance of Lesley Moore in studies of flurbiprofen metabolism *in vivo*.

Martin Kipps, ICI Plant Protection Division, Bracknell, kindly ran the  $^{19}\text{F}$  spectra which appear in this work, and also supplied a copy of the FLOCK sequence.

I am also grateful to Professor Canet of the University of Nancy for correspondence relating to the implementation of the SUFIR method.

Boots provided a gift of racemic and enantiomerically pure samples of ibuprofen and flurbiprofen.

My gratitude to family and friends, who have provided support and understanding throughout, goes without saying.

## ABSTRACT

The stereochemical determination of the non-steroidal anti-inflammatory agents ibuprofen sodium and flurbiprofen sodium in biological media using  $^1\text{H}$  and  $^{19}\text{F}$  NMR respectively has been attempted. Initial studies showed that chiral recognition of resonances in aqueous solutions of drug were achieved in the presence of cyclodextrin. When equivalent solutions were used to spike samples of human or rat urine, however, such discrimination was either altered or eliminated. This observation was thought to be a consequence of structural changes in the complex formed between drug and cyclodextrin brought about by endogenous urinary metabolites. The effect of a number of experimental variables such as pH, temperature and the presence of ionic salts on the chiral discrimination process was investigated.

Complexes of  $\beta$ -cyclodextrin with ibuprofen sodium and flurbiprofen sodium and a number of structurally related 2-arylpropionates were further examined using a range of NMR methods. Chemical shift, J coupling and Job plot data recorded in  $\text{D}_2\text{O}$  and  $\text{d}_6$ -DMSO allowed structures for the inclusion complexes to be proposed.

The nuclear Overhauser effect (nOe) has also been used to provide information relating to the structure of the cyclodextrin inclusion complex. Correlation times of complexes necessitated use of the ROESY experiment. TOCSY correlations present in ROESY spectra hindered their interpretation through the possible additional presence of false cross-peaks. Methods were therefore examined to effect their elimination.

Preliminary measurements of  $^{13}\text{C}$  longitudinal relaxation times for the  $\beta$ -cyclodextrin inclusion complex of ibuprofen sodium have been made using the SUFIR method.

## CONTENTS

### CHAPTER 1

#### Introduction to NMR Bio-fluid Analysis and its Application to Studies of the Enantioselective Metabolism of the Profens

1.1 Introduction	1
1.2 The Profens as Non-steroidal Anti-inflammatory Drugs	2
1.3 Stereoselectivity in Profen Metabolism	3
1.3.1 Stereoselectivity in Drug Absorption	3
1.3.2 Stereoselectivity in Drug Distribution	4
1.3.3 Stereoselectivity of the Drug-Receptor Interaction	6
1.3.4 Stereoselectivity in Drug Metabolism	7
1.3.5 Stereoselectivity in Drug Excretion	11
1.4 Application of NMR Spectroscopy to the Analysis of Biological Fluids	12
1.4.1 Considerations of Experimental Protocol in NMR Studies of Xenobiotic Metabolism	12
1.4.2 NMR Bio-fluid Studies of Profen Metabolism	19
1.5 Determination of Optical Purity by NMR Spectroscopy	22
1.5.1 Derivatization with an Optically Pure Reagent	23
1.5.2 Chiral Lanthanide Shift Reagents	24
1.5.3 Chiral Solvating Agents	26

## **CHAPTER 2**

### **Studies of the Enantioselective Metabolism of the Profens by NMR Bio-fluid**

#### **Analysis**

2.1 Introduction	30
2.2 <sup>1</sup> H NMR Data for the Cyclodextrins	31
2.3 NMR Studies of Ibuprofen and Cyclodextrin Mixtures	34
2.4 Extension of NMR Studies of Ibuprofen Sodium and Cyclodextrin Mixtures to Biological Fluids	45
2.5 NMR Studies of Flurbiprofen and Cyclodextrin Mixtures	52
2.6 Extension of NMR Studies of Flurbiprofen and Cyclodextrin Mixtures to Biological Fluids	57
2.7 Factors Affecting Chiral Recognition of Ibuprofen and Flurbiprofen by Cyclodextrins in NMR Spectroscopy	61
2.7.1 Effect of Variations in Mole Ratio and Concentration	62
2.7.2 Effect of Variations in Temperature	68
2.7.3 Effect of added Salts on Complexation	70
2.7.4 Effect of Variations in Solution pH	71
2.7.5 Effect of Variations in Solvent	73
2.8 Conclusion	76

## **CHAPTER 3**

### **Introduction to Aspects of Cyclodextrin Complexation and NMR Methods for their**

#### **Examination**

3.1 Introduction	78
3.2 Applications of Cyclodextrin Complexation	79
3.2.1 Analytical Chemistry	79

3.2.2 Preparative Chemistry	79
3.2.3 Pharmaceuticals	80
3.3 The Structure of the Cyclodextrins	81
3.3.1 Solid State Studies of the Structure of $\beta$ -cyclodextrin	81
3.3.2 The Structure of $\beta$ -cyclodextrin in Solution	85
3.4 Thermodynamics of Cyclodextrin Complexation	87
3.4.1 The Structural Types of Cyclodextrin Complexes	87
3.4.2 The Contribution of Hydrophobic Interactions to the Cyclodextrin Complexation Process	89
3.4.3 The Contribution of Van der Waals Interactions to the Cyclodextrin Complexation Process	90
3.4.4 The Contribution of Conformational Changes to the Cyclodextrin Complexation Process	90
3.4.5 The Contribution of Activated Cavity Water to the Cyclodextrin Complexation Process	92
3.4.6. The Contribution of Hydrogen Bonds to the Cyclodextrin Complexation Process	92
3.5 X-ray Crystallographic Studies of the Structures of Complexes of some 2-Arylpropionic Acids with $\beta$ -cyclodextrin	93
3.5.1 The $\beta$ -cyclodextrin Complexes of Fenoprofen	93
3.5.2 The $\beta$ -cyclodextrin Complexes of Flurbiprofen	96
3.6 Chiral Discrimination by Cyclodextrins	98
3.6.1 Chiral Discrimination in Chromatographic Analysis	99
3.6.2 Cyclodextrins as Chiral Solvating Agents in NMR	101
3.6.3 Chiral Discrimination in Fractional Crystallisation	102
3.7 NMR Methods	103
3.7.1 Measurement of Longitudinal Relaxation Times	103
3.7.1.1 The Inversion-Recovery Experiment	104

3.7.1.2 DESPOT	105
3.7.1.3 SUFIR	107
3.7.2 Measurement of the Nuclear Overhauser Effect	108
3.7.2.1 The nOe Difference Experiment	110
3.7.2.2 The Transient nOe and NOESY Experiments	111
3.7.2.3 The ROESY or CAMELSPIN Experiment	114

## CHAPTER 4

### NMR Studies of the Complexation of $\beta$ -cyclodextrin with some 2-Arylpropionates

4.1 Introduction	120
4.2 $^1\text{H}$ NMR Studies of the Complexation of $\beta$ -cyclodextrin with some 2-Arylpropionates in $\text{D}_2\text{O}$	122
4.3 $^1\text{H}$ NMR Studies of the Complexation of $\beta$ -cyclodextrin with some 2-Arylpropionates in $\text{d}_6$ -DMSO	129
4.4 $^1\text{H}$ NMR Studies of Conformational Changes of $\beta$ -cyclodextrin upon Complexation with some 2-Arylpropionates in $\text{D}_2\text{O}$	134
4.5 $^1\text{H}$ NMR Studies of the Stoichiometry of the Inclusion Complexes of $\beta$ -cyclodextrin with some 2-Arylpropionates in $\text{D}_2\text{O}$	138
4.6 NMR Studies of Hydrogen Bonding Interactions between $\beta$ -cyclodextrin and some 2-Arylpropionates	150
4.6.1 $^1\text{H}$ NMR Studies of the Complexation of $\beta$ -cyclodextrin with Structural Analogues of the 2-Arylpropionates in $\text{D}_2\text{O}$	151
4.6.2 $^{17}\text{O}$ NMR Studies of the Complexation of Cyclodextrins with the 2-Arylpropionates in $\text{D}_2\text{O}$	152
4.6.3 $^1\text{H}$ NMR Studies of the Complexation of $\beta$ -cyclodextrin with some 2-Arylpropionates in $\text{d}_6$ -DMSO	154



4.7 Application of the Nuclear Overhauser Effect to Studies of the Complexation of $\beta$ -cyclodextrin with some 2-Arylpropionates	156
4.7.1 Studies with the nOe Difference experiment	157
4.7.2 Studies with the ROESY Experiment	165
4.8 Application of Measurements of $^{13}\text{C}$ $T_1$ to the Complexation of $\beta$ -cyclodextrin with some 2-Arylpropionates in $\text{D}_2\text{O}$	185
4.8.1 Implementation of the SUFIR sequence on a JEOL NMR Spectrometer	186
4.8.2 Testing of the SUFIR sequence	189
4.8.3 $^{13}\text{C}$ $T_1$ Measurements of the Complexation of $\beta$ -cyclodextrin with Ibuprofen Sodium in $\text{D}_2\text{O}$ using the SUFIR sequence	194
4.9 Conclusion	199

<u>APPENDIX 4.1: 400MHz <math>^1\text{H}</math> NMR Data and Assignments for the Sodium Salts of some 2-Arylpropionic Acids at a Concentration of 0.014M in <math>\text{D}_2\text{O}</math> at 30°C</u>	202
---	-----

<u>APPENDIX 4.2: 400MHz <math>^1\text{H}</math> NMR Data and Assignments for the Sodium Salts of some 2-Arylpropionic Acids at a Concentration of 0.014M in <math>\text{d}_6</math>-DMSO at 30°C</u>	206
--	-----

## CHAPTER 5

### Experimental Methods

5.1 Chemical Suppliers	208
5.2 Preparation of the Salts of the 2-Arylpropionic Acids	208
5.3 Biological Fluid Studies with Ibuprofen	209
5.3.1 <i>in vivo</i> Studies with Ibuprofen	209

5.3.2 <i>in vitro</i> Studies with Ibuprofen Sodium	209
5.4 <i>in vivo</i> Studies with Flurbiprofen	210
5.5 Preparation of Non-biological NMR Samples	211
5.6 NMR Methods	212
<b><u>REFERENCES</u></b>	<b>218</b>

## CHAPTER 1

### Introduction to NMR Bio-fluid Analysis and its Application to Studies of the Enantioselective Metabolism of the Profens

#### 1.1 Introduction

The analysis of biological fluids by high-field FT NMR in the study of drug metabolic processes is now relatively commonplace. It has been estimated, however, that approximately 25% of drugs currently available have a chiral centre as part of their structure and are formulated as the racemate [1]. Except in rare examples of self-discrimination, NMR spectroscopy is unable to distinguish the two enantiomeric forms of such a drug (or its metabolites). With increasing awareness of the importance of enantioselective metabolism and the need in drug metabolic studies to be able to effect such a distinction, there would appear to be a serious limitation to the applications of NMR bio-fluid analysis in this area. We envisage that this may be remedied by the addition to the bio-fluid of an appropriate chiral shift reagent prior to analysis, and have investigated such a possibility with regard to the 2-arylpropionic acid series of non-steroidal anti-inflammatory drugs (NSAIDs). By way of introduction, this chapter considers our interest in this particular series of drugs, general features of NMR bio-fluid analysis and the results of previously-reported studies relevant to this work. Finally, the choice of an appropriate chiral NMR shift reagent is considered.

Chapter 2 describes the results of our studies of the enantioselective metabolism of the 2-arylpropionic acid NSAIDs using NMR bio-fluid analysis. These results prompted further examination of the nature of the interaction between the drug and the chiral NMR reagents of choice, the cyclodextrins. Results of solution state NMR studies of this interaction are given in Chapter 4. The preceding chapter introduces relevant properties of the cyclodextrins and their

complexes and NMR methods used to examine them. Finally, Chapter 5 describes experimental methods appropriate to the results discussed in Chapters 2 and 4.

## 1.2 The Profens as Non-steroidal Anti-inflammatory Drugs

The 2-arylpropionic acid or profen series of NSAIDs are widely used as analgesics and in the treatment of a range of inflammatory conditions [2]. Their action is associated with the inhibition of the cyclooxygenase enzyme responsible for the conversion of essential fatty acids, stored in the phospholipids of cell membranes and other complex lipids, to prostaglandins [3], although other mechanisms of action of as yet unknown clinical significance have been reported [4]. Their general structure is shown in Figure 1.1.

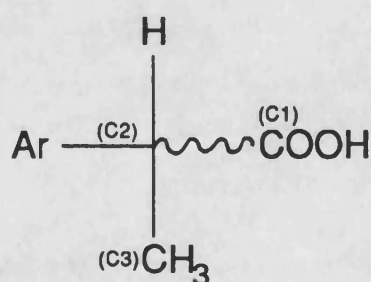


Figure 1.1 The general structure of the profen series of NSAIDs

The compounds have a chiral centre at C2, and therefore exist in both R and S enantiomeric forms (although a few examples with an additional asymmetric substituent of the aryl group, and consequently a total of four stereoisomers *eg* loxoprofen are also known). As therapeutic agents, the profens are generally formulated as the racemate, except in the case of naproxen, where a single

enantiomer, (S(+)), is used. The significance of drug stereochemistry with regard to biological action and consequences is becoming increasingly recognised [1,5-11].

### 1.3 Stereoselectivity in Profen Metabolism

Optical isomers have identical physical and chemical properties in an achiral chemical environment. In a chiral environment, however, this equality does not necessarily remain. Biological systems present such an environment, because of the chiral building blocks, such as amino acids and sugars, which Nature employs. Thus, the administration of a racemic drug to the body inevitably leads to differentiation between the two enantiomers which make up the mixture. The importance of this and other stereochemical considerations in the action of xenobiotics has recently received much attention.

Recognition processes involving chiral molecules are involved in many of the stages which together form the whole of the metabolic process [12-14]. These stages, together with their relevance to the metabolism of the profens, are now considered.

#### 1.3.1 Stereoselectivity in Drug Absorption

Most routes of drug administration (excepting injection) require the absorption of the drug across a lipophilic membrane before it can enter the body. Both passive diffusion and carrier-mediated processes are possible. Passive diffusion depends on differences in aqueous and lipid solubility and as such does not differ for a pair of enantiomers. Carrier-mediated processes require interaction with chiral bio-macromolecules and are therefore associated with stereoselectivity. Carrier mechanisms are, however, only seldomly implicated in the absorption of drug molecules, since these systems were evolved to enable the absorption of essential nutrients, which often bear little structural resemblance to drug

molecules. Differential changes in membrane permeability brought about by the two enantiomers of a drug have also been suggested as a possible mechanism of enantioselective drug absorption [15].

Studies of the enantioselectivity in the absorption of the profen series of drugs have not been reported. The gut has, however, been implicated as a possible site for the stereoselective bio-transformations some of these drugs undergo (Section 1.3.4), so that consideration of route of administration is obviously of importance.

### 1.3.2 Stereoselectivity in Drug Distribution

Following absorption, a drug is circulated around the body in the blood supply. The effective concentration available is dictated by the extent of binding to proteins which are present in the plasma. Albumin and  $\alpha_1$ -acid glycoprotein are the major plasma proteins, which bind predominantly acidic and basic species respectively. The degree of stereoselectivity in binding to such proteins varies considerably with drug, but is generally considered small.

The profens are highly bound to plasma proteins, predominantly albumin , Table 1.1. The data in this table, taken from the review of Lin *et al.* [16], refer to formulated drug, which for all but naproxen is the racemate.

Drug	Plasma protein binding
Fenoprofen	>99
Flurbiprofen	99
Ibuprofen	99
Ketoprofen	98.7
Naproxen	>99

Table 1.1 Clinical pharmacokinetic properties of some NSAIDs [16]

More recently, studies have addressed the stereoselectivity of this binding process, and have found small but significant differences for the two enantiomers of most of the drugs studied [17-23]. The results of these studies are summarised in Table 1.2.

Drug	Stereoselectivity?	Reference
Carprofen	yes	[17]
Fenoprofen	no	[18]
	probably	[19]
Flurbiprofen	yes	[20]
Ibuprofen	yes	[21]
Ketoprofen	yes	[22]
2-Phenylpropionic acid	yes	[23]

Table 1.2 Stereoselectivity in the plasma protein binding of some profens in various species

Whilst detailed examination of the consequences of such differential binding in terms of the pharmacokinetics and therapeutic effects of these drugs have not been studied, competitive binding has been suggested as a possible explanation for differences in pharmacokinetic properties when these drugs are administered as individual enantiomers rather than the racemate [24,25].

Possible stereoselectivity in the uptake of drug from the blood by the tissues remains relatively unexplored in general. The profens are, however exceptional in this regard.

Xenobiotic carboxylic acids, when converted to their coenzyme A (CoA) thioester *in vivo*, may replace natural fatty acids in the formation of triacylglycerides. Possible consequences of such hybrid triglyceride formation are the accumulation of tissue residues of xenobiotics, disturbance of lipid biochemistry and disruption of normal membrane function with possible

concomitant toxicity [26]. As carboxylic acids, the profens are possible substrates for this pathway, and indeed Fears *et al.* [27] have reported the presence of ketoprofen, ibuprofen and fenoprofen in such hybrid triglycerides in *in vitro* studies with rat liver slices. Interestingly, flurbiprofen was not incorporated, presumably because of its inability to form a CoA derivative [28]. More recent studies with ibuprofen [29] and fenoprofen [30] have shown that the uptake of these drugs into adipose tissue in the rat occurs stereospecifically for the R enantiomer. Such stereospecificity may be associated with enantiospecific formation of the CoA thioester of these drugs (Section 1.3.4).

### 1.3.3 Stereoselectivity of the Drug-Receptor Interaction

The enantioselectivity of the drug-receptor interaction has been more fully characterised. The therapeutic action of a drug generally results from the interaction of a drug molecule with one or more specific receptor sites. The chirality of a receptor site allows stereoselective distinction between enantiomers to be made. For any particular action, therapeutic or toxic, the differential responses produced by each of the enantiomers may be expressed in terms of the eudismic ratio. The most active enantiomer at a receptor site is termed the eutomer, and the less active the distomer; the eudismic ratio is the activity ratio of eutomer to distomer. Obviously, the higher the eudismic ratio, the greater the drug enantioselectivity: eudismic ratio values of the order of one hundred are not uncommon for drug substances [5]. Where eudismic ratios differ considerably from unity, the therapeutic action resides almost completely in the eutomer. At best the distomer may be regarded as biologically inactive, at worst it may give rise to a range of undesirable effects, not necessarily related to those of the eutomer, which may include non-competitive antagonistic and toxic responses [1,5-11].



Eudismic ratios for the profen NSAIDs *in vitro* have recently been reviewed by Caldwell *et al.* [31] and are summarised in Table 1.3, taken from that paper. It is readily apparent that it is the S enantiomer which is responsible for the anti-inflammatory action of these drugs.

Drug	Eudismic ratio S/R
Ibuprofen	160
Flurbiprofen	878
Indoprofen	~100
Naproxen	133
	70
Pirprofen	6.4
Carprofen	>16
	>23
Fenoprofen	35

Table 1.3 Stereoselectivity of action of profen NSAIDs at putative sites of action in various species [31]

#### 1.3.4 Stereoselectivity in Drug Metabolism

Enantioselectivity may also be apparent in the bio- transformations initiated by metabolizing enzymes, as a consequence of differential enzymic affinity and rates of metabolism. The metabolites so-formed may thus show differences in molecular structure and stereochemistry depending on the enantiomer from which they were derived, and may therefore elicit different biological responses, including toxicity. It is generally the case, however, that differences in the metabolism of enantiomers is often considerably less than might be expected on the basis of differential receptor binding. This may be related to poorer enzyme specificity, or, more probably, as a result of averaging of any preferences over a number of steps catalysed by a number of isoenzymes [12,13].

The metabolic pathways of the profens will be influenced by the nature of the aryl substituent of each individual drug and by the species to which it is administered [32-39]. A common metabolic pathway is the formation of the glucuronide conjugate, a well-known mechanism for the detoxification of xenobiotic carboxylic acids [40], and it is the enantioselectivity of the glucuronidation process which has received most attention. El Mouelhi *et al.* [41] have shown, for example, the enantioselective glucuronidation of racemic naproxen, ibuprofen and benoxaprofen *in vitro*, using immobilized enzyme preparations which avoided complications from competing metabolic routes. The preferred enantiomer and its extent of preference were found to depend on both drug substrate and species. Nakamura and Yamaguchi [42] have similarly suggested the stereoselective glucuronidation of (S)-2-phenylpropionic acid and hydrolysis of the (R)-2-phenylpropionic acid glucuronide in rat liver preparations.

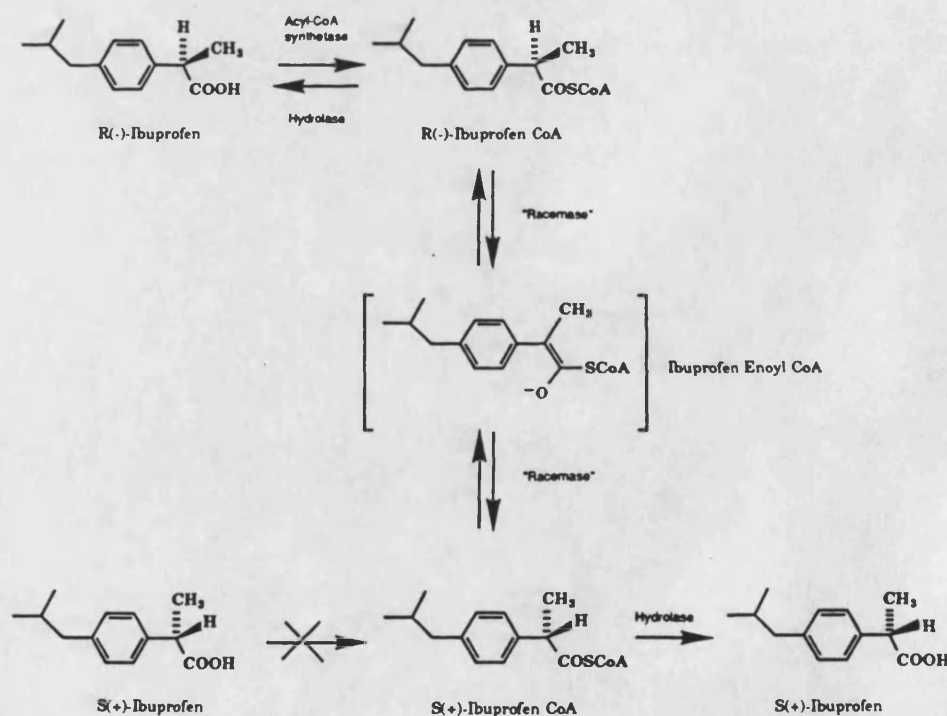


Figure 1.2 Proposed mechanism for the uni-directional metabolic inversion of the profens, illustrated for ibuprofen [54]

In addition to studies of glucuronidation, studies of ibuprofen metabolism *in vivo* in man show a lack of stereoselectivity in formation of the carboxy metabolite [43].

Most interest in the stereoselectivity in profen metabolism has, however, centered on an unusual transformation which inverts the chiral centre at the C2 atom [44]. The reaction is essentially uni-directional, with the R enantiomer converting to the S, Figure 1.2, although small amounts of the R enantiomer formed from the S have been observed in studies of 2-phenylpropionic acid metabolism in rat kidney slices [42] and *in vivo* [45], of ibuprofen metabolism in the rat [46] and possibly in man [24], and also of cicloprofen in the rat [47]. The extent of this chiral inversion depends on both drug substrate and species, and has recently been reviewed by Jamali [48].

The biological consequences of this conversion of inactive to active isomer is readily apparent from comparisons of the eudismic ratios of these drugs measured *in vivo* compared with *in vitro* data, Table 1.4, and has lead to considerable research into its mechanism and site of occurrence.

Drug	Eudismic ratio S/R	
	<i>in vitro</i>	<i>in vivo</i>
Ibuprofen	160	1.3
Flurbiprofen	878	8
Indoprofen	~100	25
Naproxen	133	
	70	21
Carprofen	>16	
	>23	15
Fenoprofen	35	~1

Table 1.4 Differential stereoselectivity of action of profen NSAIDs *in vitro* and *in vivo* [31]

An initial study of the metabolism of deuterium-labelled (R)-ibuprofen in man suggested that reaction proceeded *via* the action of fatty acid dehydrogenase on the CoA thioester of (R)-ibuprofen [49]. Subsequent studies have shown, however, that the CoA thioester formation leads to increased acidity of the H<sub>2</sub> proton, and that in fact reaction proceeds via deprotonation, as opposed to elimination, and subsequent racemization. There is much evidence to suggest that stereospecific action of the acyl-CoA synthetase enzyme on the R enantiomer gives rise to the uni-directional nature of this inversion (and to the enantiospecific uptake of these drugs into adipose tissue, Section 1.3.2). Thus, for example, enantioselective thioester formation has been demonstrated *in vitro* for (R)-ibuprofen [50] and (R)-fenoprofen [51] and, Porubek *et al.* [28] have shown that once formed, the CoA thioesters of flurbiprofen are both able to readily epimerize *in vitro*.

Deprotonation of the CoA thioester could occur either by enzymic or chemical means. The pK<sub>a</sub> of 10.3 observed for the ibuprofen N-acetylcysteamine thioester model compound [46] suggest that chemical deprotonation is unlikely and, indeed, the NMR deuterium exchange experiments of Mayer *et al.* [52,53] show that although chemical deprotonation may be possible under extremely non-physiological conditions, even so the rate of reaction is not sufficient to explain those observed *in vivo*. The failure to observe a detectable deuterium kinetic isotope effect in the isomerization of ibuprofen gives some insight as to the identity of the enzyme system responsible [54], although it remains unknown at present.

The distribution of the epimerizing enzyme in the body also remains unclear. Proposed sites have included the gut (Section 1.3.1), where inversion of (R)-benoxaprofen in the rat [55] and of (R)-ibuprofen in man [56-58] have been observed. A small amount of (R)- to (S)-2-phenylpropionic acid interconversion has also been reported in rat small intestine *in vitro*, although not in the lung,

testes, heart or spleen [42]. The predominant sites for inversion in this study were, however, the liver and kidney, the importance of these organs subsequently being demonstrated *in vivo* [45]. Inversion of (R)-ibuprofen has also been demonstrated in perfused rat liver [59] and in isolated liver preparations [60,61]. Knadler and Hall [62] have also reported inversion of fenoprofen in liver preparations.

### 1.3.5 Stereoselectivity in Drug Excretion

Both drugs and metabolites are susceptible to enantioselective excretion as they are eliminated from the body in the urine and bile. The kidney employs secretory and reabsorption mechanisms in the tubules which form part of its structure to allow removal of waste products in the urine. Both mechanisms may be carrier-mediated, and as such enantioselectivity may be anticipated, although it has not as yet been demonstrated for xenobiotic excretion. Carrier systems have also been implicated in the biliary excretion of several drugs and metabolites, but no enantioselectivity has been established.

The difference in biological fate of the enantiomers of chiral drug compounds has thus been demonstrated at stages throughout the metabolic pathway. These differences may be either pharmaco-dynamic or -kinetic in origin, and raise many questions concerning the propriety of the administration of drugs as racemates, without thorough testing of the metabolism of the individual enantiomers. The profens are particularly interesting in this regard: enantioselectivity has been demonstrated at many stages of their passage through the body and they exhibit a highly unusual, essentially uni-directional chiral inversion mechanism. Perhaps more worrying than interesting, however, is the formulation of these drugs as the racemate, when evidence suggests that the R enantiomer (although often partially converted to the S enantiomer in many

species) is therapeutically inactive and stereospecifically implicated in possible mechanisms of toxicity.

#### 1.4 Application of NMR Spectroscopy to the Analysis of Biological Fluids

The application of high-field FT NMR spectroscopy to the study of biological fluids is now relatively common-place. Although rather insensitive in comparison with other analytical techniques, its advantages include rapid, non-destructive, qualitative and (with addition of a suitable standard and with care) quantitative analysis with minimal sample preparation and, indeed, sample volume required. Applications of the method have recently been reviewed [63-70] and may be divided into two general categories:

1. the monitoring of endogenous metabolites aimed at the understanding of biochemical and toxicological pathways and the diagnosis of various disease states, particularly of organic acid metabolic disorders and of cancer;
2. the analysis of both endogenous and exogenous metabolites following drug administration in the study of xenobiotic metabolic processes.

Discussion is restricted here predominantly to the second of these two categories. Some general considerations in carrying out such studies are given, and specific applications to the study of profen metabolism are reviewed.

##### 1.4.1 Considerations of Experimental Protocol in NMR Studies of Xenobiotic Metabolism

#### 1. Substrate Suitability for NMR Analysis

As a result of the comparative insensitivity of NMR, for  $^1\text{H}$  spectra, for example, concentrations typically of the order of  $100\mu\text{M}$  at  $400\text{MHz}$  are required for measurement. For this reason, low efficacy drugs (hence given in large doses)

which are rapidly excreted as a small number of metabolites are particularly appropriate for this method of analysis. Samples taken following overdose are also readily examined. Thus, changes in endogenous metabolite levels as well as the occurrence of drug and exogenous metabolites have been readily observed by  $^1\text{H}$  NMR in various bio-fluids following paracetamol [71], aspirin [72,73] and alcohol [72] ingestion in overdose. NMR analysis is also recommended where the drug metabolites (or in the case of overdose, even the drug itself) are unknown, since unlike a technique such as chromatography, no presumption about the structure of metabolites need be made prior to analysis. Thus, on the basis of  $^1\text{H}$  NMR of urine samples from various species, new metabolites have been identified for ampicillin sodium in the rat [74], DMF in the mouse [75], NMF in rats and mice [76,77], and by  $^{19}\text{F}$  NMR, novel metabolites for 5'-deoxy-5-fluorouridine [78] and 5-fluorocytosine [79] in man have also been elucidated. Similarly, Vermeersch *et al.* [73] were able to determine by  $^1\text{H}$  NMR analysis of a urine sample that the symptoms of a four month old girl arose from aspirin-poisoning rather than an organic aciduria as first suspected.

In structural terms, drug structures which give signals with relatively simple splitting patterns in regions of the NMR spectrum free of endogenous signals are to be preferred.

## 2. The Choice of Biological Fluid for NMR Analysis

The choice of an appropriate biological fluid for analysis is governed by many factors. Obviously it is essential to choose a fluid into which the drug is excreted and which gives the necessary biological information. The ease of obtaining the sample and its available volume are also considerations. Thus, most work in this area makes use of blood and urine samples. Endogenous composition of the fluid is also important. Fluids containing a large percentage of endogenous bio-macromolecules will give spectra with broad peaks arising from them. In

addition, any drug bound to such bio-macromolecules will similarly give rise to broadened resonances. Although such resonances may be eliminated by the use of a Hahn [80] or Carr-Purcell-Meiboom-Gill (CPMG) [81,82] spin-echo sequence or the use of convolution difference [83], quantitative measurements remain inaccurate. Bell *et al.* [84] have reported the observation of so-called 'NMR invisible lactate' in human plasma. Only after addition of a suitable agent such as ammonium chloride, which disrupts binding of lactate to plasma proteins, was it possible to make a reliable estimation of total lactate concentration by  $^1\text{H}$  NMR. Similarly, Bock [72] used perchloric acid to precipitate plasma proteins, which broadened  $^1\text{H}$  signals from aspirin metabolites as a result of binding, in a sample taken from a human overdose subject. Alternatively, it may be necessary to extract the plasma-bound species with an organic solvent, as has been reported for the determination of esterified and non-esterified cholesterol in serum by  $^1\text{H}$  NMR [64]. The use of sodium 3-(trimethylsilyl)propionate (TSP) as an internal standard in quantitation in such samples is also precluded, as macromolecular binding broadens its resonance. Alanine is suggested as a suitable alternative for use in plasma [64]. In some cases, however, protein binding need not be a problem. Thus, Meynial *et al.* [85] observed two distinct signals in the  $^{19}\text{F}$  NMR spectrum of human serum following administration of the anti-neoplastic agent 5'-deoxy-5-fluorouridine, corresponding to free and plasma-bound drug, allowing quantification of the binding process. Human urine and cerebrospinal fluid are notable in their low protein content.

Bio-fluids which have been used in NMR analysis include blood, urine, cerebrospinal, amniotic and seminal fluids as well as sweat, aqueous humour, milk and bile.



### 3. Sample Preparation for NMR Analysis

At its simplest, sample preparation requires only the addition of 10% deuterated water, as a field-frequency lock, to the biological fluid (of which there may be as little as 0.3ml) prior to analysis. Where the sample is required after use or it is undesirable to contaminate the sample with deuterium, a concentric capillary tube of deuterated water may be used.

The possible need to precipitate bio-macromolecules has already been considered. The predominant component of bio-fluids is, however, water, which gives rise to a very large peak in the  $^1\text{H}$  spectra of these samples, which will not only obscure part of the spectrum, but will also severely restrict sensitivity as a result of the limited dynamic range of the analogue-to-digital converter of the spectrometer. Several solutions to these problems are available. A straight-forward approach is to freeze-dry the sample and to reconstitute it in deuterated solvent. Thus, where necessary, sample concentration may be achieved, but the loss of volatile and unstable constituents from the sample and the absence of exchangeable protons from the resulting spectrum may, however, be undesirable. The extent to which a sample may be concentrated is also limited, because if ionic strength becomes too high, salting out of solute may occur and the tuning of the radio-frequency circuitry of the spectrometer may be affected [86]. Alternatively, spectroscopic techniques, generally referred to as solvent suppression methods, are available. These eliminate the water signal from the spectrum either by selective excitation of all other resonances or by nullifying the water signal at the point of acquisition. Numerous methods are available, but probably the most established have been discussed by Freeman [87] and Sanders and Hunter [83]. None of these methods is ideal for all situations, and it is important to weigh-up the advantages and disadvantages of each for any particular application. Thus, the most straight-forward method of presaturation of the water resonance prior to acquisition is

simple and easy to use, but exchangeable protons and signals close in chemical shift to the water signal may be eliminated from the spectrum.

Where complexity of the sample is a problem, the use of solid phase extraction cartridges is also advocated. This allows removal of endogenous components, simultaneous concentration and, with careful method development, may allow separation of a drug and its metabolites. For example, studies relating to  $^1\text{H}$  NMR determination in human urine of ibuprofen, paracetamol, aspirin, oxpentifylline and naproxen have been reported [86]. Their use, however, does detract from the rapidity of NMR bio-fluid analysis.

Where endogenous peak interference alone is the problem, it may be possible simply to separate overlapping signals by careful adjustment of the sample pH for protons close to an ionisable group [64]. Sample pH must also be considered in multi-nuclear studies with  $^{14}\text{N}$  or  $^{15}\text{N}$ . Protonation of the nitrogen nucleus in such cases leads to line-broadening through chemical-exchange. In extreme cases such broadening may be sufficient for the signal to be unobservable [69].

#### 4. The Observation Nucleus for NMR Analysis

The  $^1\text{H}$  nucleus has high abundance and magnetogyric ratio and is of wide-spread occurrence, and as such should be a good choice of observation nucleus in bio-fluid analysis. The necessity of the elimination of the large water peak from such spectra has already been discussed. The wide-spread occurrence coupled with the narrow chemical shift range of the proton can, however, lead to highly complex, overlapping spectra. This may be alleviated to a certain extent by working at higher magnetic field, where frequency dispersion (and sensitivity) is improved.

The narrow chemical shift range of the proton is almost unique to this nucleus. It may, therefore, be possible to circumvent this problem by the use of another suitable observation nucleus.  $^{19}\text{F}$  and  $^{31}\text{P}$  are particularly attractive in this regard because of their high magnetogyric ratio and 100% natural abundance, but there are comparatively few drug molecules which contain one of these nuclei as part of their structure.

$^{19}\text{F}$  NMR studies of bio-fluids have included work with flucloxacillin [88,89], the anti-cancer fluoropyrimidines [67] and with flurbiprofen [90] in various fluids and species.  $^{19}\text{F}$  chemical shifts have been reported to be sensitive to molecular changes up to 8-10 bonds from the fluorine atom in such experiments [88].

Phosphorus occurs endogenously in compounds involved in the body's energetic cycles.  $^{31}\text{P}$  NMR studies have, therefore, tended to be restricted to the examination of such processes in samples of whole cells, tissues, perfused organs or in the body itself. Concentrated samples of urine from patients undergoing treatment with the cyclophosphamide analogue ifosfamide have been examined by  $^{31}\text{P}$  NMR at 24.3MHz (equivalent to 60MHz for  $^1\text{H}$ ), but the peaks for ifosfamide and a metabolite resulting from dechloroethylation were not well resolved at this low field, and organic extraction of samples was found to be necessary [91].

Although notoriously insensitive,  $^{13}\text{C}$  NMR studies of bio-fluids have also been reported. Nicholson and Wilson [69] report that they were able to obtain reasonable spectra in 20 minutes (125MHz, proton-decoupled, corresponding to 500MHz for  $^1\text{H}$ ) from rat urine following administration of acetazolamide. Nuclear Overhauser enhancements and long relaxation times may preclude quantification. Alternatively, the use of  $^{13}\text{C}$ -labelled xenobiotic may be appropriate. Dohn *et al.* [92] have, for example, followed the metabolism of 3- $^{13}\text{C}$  labelled 1,2-dibromo-3-chloropropane, previously used as a soil fumigant, in the rat, in order to gain greater understanding of its mechanisms of toxicity.

Other nuclei used in bio-fluid analysis include  $^{14}\text{N}$  and  $^{15}\text{N}$ .  $^{14}\text{N}$  is reasonably sensitive, but as a quadrupolar nucleus gives rise to very broad signals, so that only those molecules with highly symmetric electronic environments about the nitrogen centre are ideally studied by this method. Norman and Sadler [93] have examined the reactions of some platinum anti-tumour agents in plasma by this method, in an attempt to achieve essentially physiological conditions for their experiments.

Whilst  $^{15}\text{N}$  is a spin 1/2 nucleus, its natural abundance and magnetogyric ratio are low.  $^{15}\text{N}$ -labelled drugs are, therefore, to be recommended in metabolic studies with this nucleus [94].

A disadvantage of the use of nuclei other than protons, however, is that information relating to endogenous metabolites may be lost. Thus, for example, there are no fluorine-containing endogenous metabolites.

Alternative methods for over-coming resolution problems in  $^1\text{H}$  NMR have included the use of 2D homonuclear and heteronuclear correlation experiments. The  $^1\text{H}$  homonuclear or COSY experiment was first applied to bio-fluid analysis to study the fate of paracetamol in a concentrated urine sample [95]. The overlapping resonances of free paracetamol and its cysteinyl conjugate observed in one-dimensional  $^1\text{H}$  spectroscopy were readily distinguishable in two. The utility of such COSY experiments has since been demonstrated by studies of the metabolism of N-methylformamide (NMF, [76]) and hydrazine [96] in the rat. Heteronuclear 2D correlation experiments have been used to give additional structural information relating to the metabolites of, for example, flucloxacillin in rat urine by  $^{19}\text{F}$ - $^1\text{H}$  correlation [88] and, by  $^{13}\text{C}$ - $^1\text{H}$  correlation, of [3- $^{13}\text{C}$ ]-1,2-dibromo-3-chloropropane also in the rat [92]. These experiments are difficult to quantify and are generally time-consuming. Wade *et al.* [90], for example, were only able to distinguish 6 of the 10 metabolites which they had observed in the  $^{19}\text{F}$  spectrum in a  $^{19}\text{F}$ - $^1\text{H}$  correlation experiment of human urine following a dose of the NSAID

flurbiprofen. The same authors have also recommended the use of  $^1\text{H}\{^{19}\text{F}\}$  spin-echo difference spectroscopy, which edits out all protons not coupled to  $^{19}\text{F}$ , leading to considerable spectral simplification, and envisage its application for other heteronuclei.

#### 1.4.2 NMR Bio-fluid Studies of Profen Metabolism

##### 1. Naproxen

Wilson and Ismail [97] have examined the urine of a female patient with suspected osteoarthritis. Following the administration of a single oral dose of 500mg of naproxen, Figure 1.3, 2ml aliquots of urine were freeze-dried, reconstituted in deuterated water and analysed by  $^1\text{H}$  NMR at 250MHz, with presaturation to suppress the residual HDO signal.

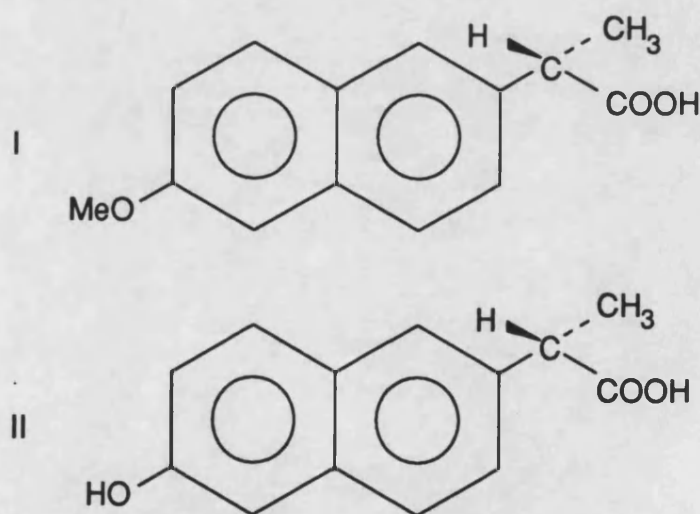


Figure 1.3 Structure of (I) naproxen and (II) its O-desmethyl metabolite

Urine collected 0-5.5 hours following dosing showed several drug- related resonances associated with the methyl, methoxy and aromatic protons, and additionally a signal from the anomeric proton of glucuronic acid, consistent with

the formation of glucuronide conjugates. Stepwise gradient elution of acidified urine from a solid phase extraction cartridge with deuteromethanol and acidified deuterated water allowed separation of endogenous metabolites, and the collection of exogenous metabolites in two fractions, which by  $^1\text{H}$  NMR were found to contain 1. unchanged naproxen and its O-desmethyl metabolite, Figure 1.3, both present as the glucuronide and 2. unchanged naproxen as its glucuronide.

Wilson and Nicholson [86] have since reported the isolation of pure naproxen and O-desmethyl naproxen glucuronides, in sufficient yield for  $^{13}\text{C}$  NMR, by additional concentration and solid phase extraction of such samples.

## 2. Ibuprofen

$^1\text{H}$  NMR at 250MHz was used to examine the urine of a healthy male following administration of a single therapeutic dose of 400mg ibuprofen, Figure 1.4, [86,98]. 2ml of urine was freeze-dried and reconstituted with 1ml of deuterated water, with the residual HDO peak suppressed in the resulting spectrum by presaturation.

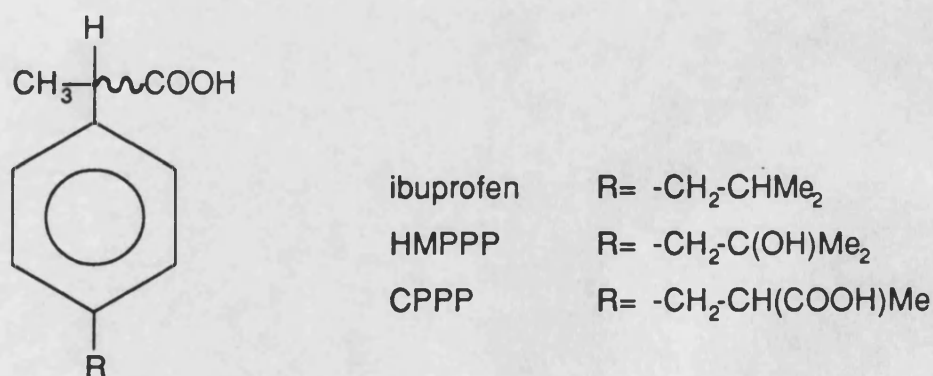


Figure 1.4 Structure of ibuprofen and its metabolites HMPPP and CPPP

The urine sample collected 2-4 hours after dosing showed several signals arising from the drug and its metabolites: in the aromatic region around 7.25ppm, from 0.8-1.5ppm and a doublet at 5.4 ppm, indicating the presence of glucuronides. A large singlet at 1.18ppm was identified as the metabolite 2-[4-(2-hydroxy-2- methylpropyl)phenyl]propionic acid (HMPPP, Figure 1.4). Passage of the acidified sample through a solid phase extraction cartridge lead to considerable improvement of the spectrum, and by using stepwise gradient elution, it was possible to separate the ibuprofen metabolites into two fractions: 1. the glucuronides of HMPPP and 2-[4-(2-carboxypropyl)phenyl]propionic acid (CPPP, Figure 1.4) and 2. ibuprofen glucuronide. The subsequent separation of the glucuronides of HMPPP and CPPP was possible, but difficult.

### 3. Flurbiprofen

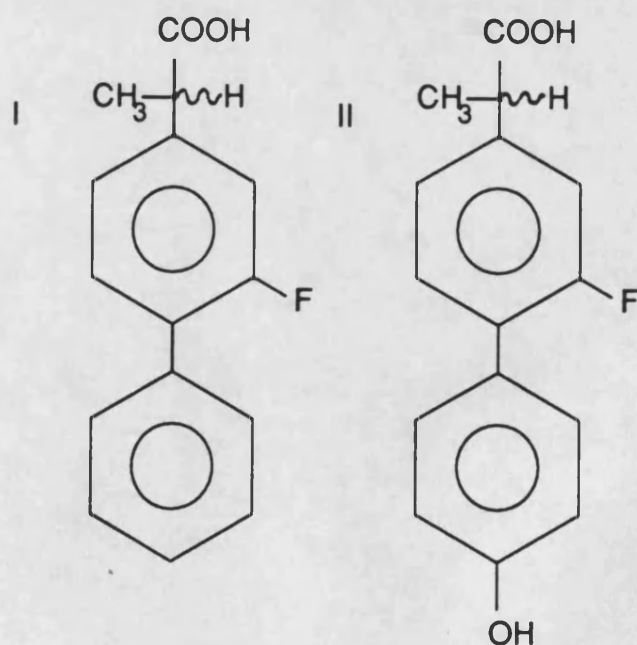


Figure 1.5 Structure of (I) flurbiprofen and (II) its metabolite 2-(2-fluoro-4'-hydroxy-4-biphenyl)propionic acid

The metabolism of flurbiprofen, Figure 1.5, has been studied following oral dosing of 150mg flurbiprofen or 800mg of a slow release formulation by a male volunteer [90].  $^1\text{H}$  NMR analysis of the collected urine showed few clearly identifiable signals from the drug or its metabolites, except for a resonance at 1.5ppm arising from a methyl group. In the  $^{19}\text{F}\{^1\text{H}\}$  spectrum, however, exogenous signals were very clearly seen. Two major metabolites were identified by alkaline hydrolysis as glucuronides, one of unchanged flurbiprofen. In addition, eight minor metabolites were detected, and were thought to be sulphates and glucuronides of reported metabolites. Solid phase extraction allowed separation of the metabolites into two fractions, which on the basis of  $^1\text{H}$  and  $^{19}\text{F}$  NMR and FAB-MS were found to contain 1. flurbiprofen and 2-(2-fluoro-4'-hydroxy-4-biphenyl)propionic acid, Figure 1.5, as their glucuronides and 2. flurbiprofen glucuronide.

A  $^{19}\text{F}\text{-}^1\text{H}$  correlated spectrum and  $^1\text{H}\{^{19}\text{F}\}$  spin-echo difference spectroscopy of samples gave additional structural information, and were consistent with metabolism taking place on the non-fluorinated ring of the drug.

### 1.5 Determination of Optical Purity by NMR Spectroscopy

NMR has found wide-spread use in the determination of enantiomeric excess [99-102]. Since enantiomeric species are chemically and magnetically equivalent in an achiral chemical environment, in order for chiral discrimination to be realised in an NMR experiment, inequivalence *via* a diastereomeric relationship must be introduced either through derivatization or intermolecular association with an optically active reagent.



### 1.5.1 Derivatization with an Optically Pure Reagent

Derivatization requires the reaction of the enantiomeric mixture to be determined with an optically pure reagent prior to analysis. It is therefore necessary for the molecule under investigation to possess functional groups suitable for such reactions as part of its structure. The optical purity of the derivatizing reagent is essential for accurate determination by this method, and care must also be taken that variable rates and extents of formation of the diastereomer from each enantiomer do not occur, and that stereochemical configurations are maintained throughout. The derivatizing reagent may be chosen so as to contain a resonance signal suitable for NMR analysis, and ideally also contains a phenyl ring or other highly magnetically anisotropic groups to increase the chemical shift non-equivalence of resonances arising from the different enantiomers. Conformational preferences of the reagent which can maximise the effects of such groups are also advantageous. Mosher's reagent, ( $\alpha$ -methoxy- $\alpha$ -trifluoromethylphenylacetic acid) or MTPA [103], is the most widely used chiral derivatizing agent (CDA) for NMR studies, and has been used for the determination of the enantiomeric purity of alcohols and amines. Other CDAs which have been used to determine enantiomeric excess by NMR have recently been discussed by Yamaguchi [99]. Chiral splittings in the 0.01- 0.15ppm range in such studies may be anticipated. In cases where chemical shift non-equivalence is small, the addition of a lanthanide shift reagent may lead to enhanced separation [104]. The formation of a diastereomeric derivative may additionally allow deduction of the absolute configuration of the analyte.

The derivatization reaction need not necessarily result from covalent linking of analyte and reagent. Thus, Parker and Taylor [105] have recently reported the determination of electron- deficient or strained alkenes and allenes by reaction with the platinum or palladium complexes (diop) $M^0$ -C<sub>2</sub>H<sub>4</sub> (diop=2,2-

dimethyl- 4,5-bis(diphenylphosphinomethyl)-1,3-dioxolane). The facile displacement of the ethene ligand gives complexes which may readily be examined by  $^{31}\text{P}$  NMR, thus exploiting the sensitivity and wide chemical shift range of this nucleus. As with other CDAs, care must be taken that there is no enantioselectivity in binding. It is envisaged that this may be a problem where the chiral centre of the analyte is close to the binding site or a substituent is capable of additionally binding to the metal.

### 1.5.2 Chiral Lanthanide Shift Reagents

Another commonly used method for the determination of optical purity by NMR, first reported by Whitesides and Lewis [106], requires the use of a chiral lanthanide shift reagent (CLSR) [101,102,107], which gives rise to a differential lanthanide induced shift for the two enantiomers of a molecule. The CLSR generally consists of three molecules of a bidentate  $\beta$ -diketonate derivative of d-camphor complexed to a lanthanide ion such as europium or praeosodymium in non-competitive solvents such as carbon tetrachloride or deuterated benzene. The possible expansion of the coordination sphere of the lanthanide ion allows chiral discrimination to be achieved by substrate binding. Solutions are thought to contain a complex series of equilibria, usually in fast exchange, but are not as yet fully understood. It is not clear, for example, whether chiral discrimination results predominantly from a difference in stabilities of the diastereomeric complexes formed by each enantiomer, or from an intrinsic difference in magnetic environment of the complexes themselves. The choice of lanthanide ion and chiral ligand in any given application also remains somewhat empirical. It is known, however, that complexes of europium and ytterbium give rise to downfield shifts, whereas those of praeosodymium are upfield, and on the basis of experimental data, Fraser [101] has suggested the following protocol: For the determination of the

optical purity of an unknown sample, experiments with at least four CLSRs should be attempted.  $\text{Eu}(\text{dcm})_3$ ,  $\text{Pr}(\text{hfbc})_3$ ,  $\text{Yb}(\text{hfbc})_3$  and  $\text{Eu}(\text{hfbc})_3$  (dcm =dicampholyl-d-methanato-, hfbc =heptafluoropropylhydroxy- methylene-d-camphorato-) are the most likely to give success. Variations in temperature and achiral substrate derivatization are a last resort. Splittings up to 0.2ppm may be expected.

Since the lanthanide complexes are hard acids, the best results with CLSRs are observed for hard bases. For weaker bases. binding may be enhanced by the introduction of a fluorine atom in the biketonate ligand of the CLSR, thus increasing its acidity (and solubility) [108]. Studies with soft bases such as alkenes and aromatics require the additional presence of a silver (I)  $\beta$ -diketonate [109]. Evidence suggests that the silver ion is ion- paired with a lanthanide (III) tetrakis chelate anion formed *in situ*, and that binding of the substrate to the reagent is through the silver ion.

Although most CLSRs are appropriate for use in apolar solvents, the use of some in aqueous systems has also been reported.  $\text{Na}[\text{Eu}(\text{III})(\text{R or S})\text{pdta}(\text{H}_2\text{O})_3]$  (pdta=1,2- propanediaminetetraacetate) has been used in deuterated water to determine the enantiomeric purities of chelating ligands such as  $\alpha$ -amino and  $\alpha$ -hydroxy acids as well as carboxylic acids [110,111]. Kabuto and Sasaki [111] have, for example, reported a 0.03ppm splitting of the methyl resonance of 2-phenylpropionic acid in  $\text{D}_2\text{O}$  by this method.  $\beta$ -hydroxy acids [112] as well as  $\alpha$ - [113] may also be studied in aqueous solution by the use of europium chloride and an excess of an additional chiral acid also capable of chelation. The stoichiometry and structure of the resulting lanthanide complex which allows chiral recognition has been studied [114]. Complexes with a 3:1 ligand to metal ratio would appear to be of primary importance, presumably as a result of steric crowding around the lanthanide ion forcing ligands into a more stereochemically rigid position. The method may be extended to the self-resolution of non-racemic mixtures of appropriate ligands. A further chiral lanthanide reagent, based on the ligand (S)-

carboxymethyloxysuccinate (CMOS) and suitable for use in D<sub>2</sub>O, has been reported by Peters *et al.* [115]. Substrates included amino acids and a range of polycarboxylates.

Chiral shift reagents based on cobalt have also been reported for use in aqueous solution. Cobalt (II) adenosine 5'-triphosphate has been used to determine, for example, the enantiomeric excess of norepinephrine [116]. Chiral discrimination is thought to occur by substrate binding to adenosine 5'-triphosphate stabilised by ring stacking and electrostatic interactions between the ammonium and phosphate groups. The optical purity of 2-(5,6-dihydroxy-1,2,3,4-tetrahydro-1-naphthyl)imidazoline and 2-(5,6-dimethoxy-1,2,3,4-tetrahydro-1-naphthyl)imidazoline have also been determined by this method [117].

### 1.5.3 Chiral Solvating Agents

Chiral Solvating Agents (CSAs) [100,102] were developed following the observation by Pirkle [118] that chiral discrimination of 2,2,2-trifluoro-1-phenylethanol was observed in its <sup>19</sup>F NMR spectrum in the presence of the asymmetric solvent 1-(-)-phenethylamine. The compounds which have been used as CSAs are structurally diverse, but the most popular are probably the aryltrifluoromethylcarbinols and 1-arylethylamines. The CSAs are used in optically enriched, and preferably optically pure, form and often in large molar excesses. Simplistically, their mechanism of action may be considered to involve binary association between molecules of the analyte and the reagent, resulting from hydrogen bond interactions between the two, with discrimination of enantiomers generally enhanced where the CSA contains a magnetically anisotropic aryl group directly attached to its asymmetric centre. Although chemical shift differences are generally smaller than for the CLSRs, spectra do not suffer from the disadvantage of line-broadening associated with the latter, and are more useful in the determination of absolute configuration. Small splittings may,

however, be enhanced by the additional presence of an achiral lanthanide shift reagent where necessary [119].

The CSA category may also be considered to encompass NMR enantiomeric excess determination by diastereomeric ion-pair formation. Thus, Baxter and Richards [120] have reported the determination of the optical purity of the antischistosomal agent 2- N- isopropylaminomethyl-6-methyl-7-nitro -1,2,3,4-tetrahydro- quinoline following the formation of a diastereomeric salt with MTPA in ethyl acetate. Whilst the method was successful in deuteriochloroform, in a polar solvent such as deuteromethanol ion-pairing was disrupted. Parker and Taylor [121] have recently suggested the use of O-acetyl mandelic acid as an improved reagent for the analysis of chiral amines and aminoalcohols, because of the improved solubility of ion-pairs of this acid in apolar solvents, and because, with the substrates examined, splittings were larger than those observed for MTPA or mandelic acid.

Where molecular association occurs between two molecules of the analyte itself, self-induced non-equivalence in NMR spectra may additionally be observed. Thus, Dobashi *et al.* [122] have reported the observation of non-equivalence in the  $^1\text{H}$  NMR spectrum of N-acetylvaline *tert*-butyl ester enantiomers in carbon tetrachloride. The authors propose a dimeric structure resulting from intermolecular N-H to C=O hydrogen bonding as being responsible for this observation.

An important class of CSAs, because of their effectiveness in water and certain other polar solvents, are the cyclodextrins [123]. These are water-soluble oligomers containing from 6 to 12 glucose units connected through  $\alpha(1,4)$  linkages, the most common being those with 6,7 and 8 units, referred to as  $\alpha$ -,  $\beta$ - and  $\gamma$ -cyclodextrin respectively. The toroidal structure of these molecules, shown in Figure 1.6, allows inclusion of a range of hosts in the molecular cavity, the diameter of which depends on the number of glucose units in the macrocycle. This

cavity is hydrophobic in nature as a result of the methylenic and glycosidic linkages which forms its walls, and it is therefore generally hydrophobic molecules, or parts thereof, which are preferentially included.

In 1977, MacNicol and Rycroft [125] reported the inequivalence in the  $^{19}\text{F}$  NMR spectra of the trifluoromethyl groups of  $\alpha,\alpha$ -bis(trifluoromethyl)-benzenemethanol and 1-methyl-4-[2,2,2-trifluoro-1-(trifluoromethyl)ethyl]-benzene, Figure 1.7, in the presence of  $\beta$ -cyclodextrin. They suggested that interactions of the two enantiomers of a compound with the chiral cyclodextrins would lead to the formation of diastereomeric complexes which could be distinguished by NMR, and demonstrated this by their observation of a 4.3Hz chemical shift difference (measured at a frequency of 94.15MHz) in the  $^{19}\text{F}$  signal for the two enantiomers of 1-phenyl-2,2,2-trifluoroethanol in the presence of  $\alpha$ -cyclodextrin in deuterated water.

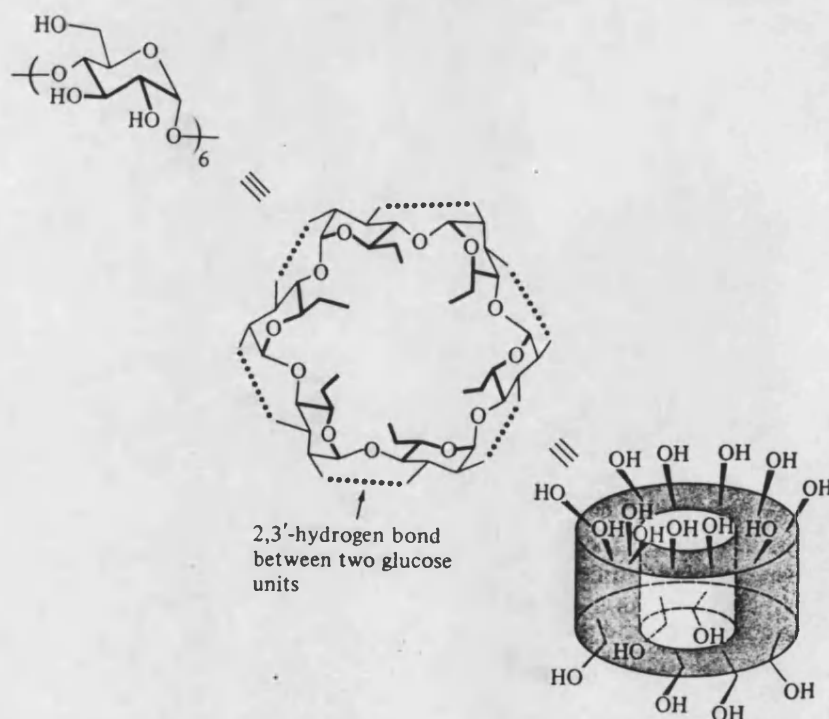


Figure 1.6 Structure of the cyclodextrins, illustrated for  $\alpha$ -cyclodextrin [124]

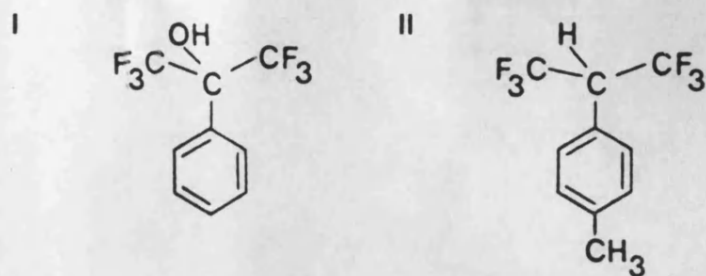


Figure 1.7 Structure of (I)  $\alpha, \alpha$ -bis(trifluoromethyl)benzenemethanol and (II) 1-methyl-4-[2,2,2-trifluoro-1-(trifluoromethyl)ethyl]benzene [125]

Subsequently, chiral discrimination of a range of substrates in the presence of cyclodextrins and their derivatives have been reported. The majority of these studies have employed deuterated water as solvent [126-140], although deuterated dimethylsulphoxide has also been used [140,141]. The applicability of this method to a given substrate and the most appropriate choice of cyclodextrin remains somewhat empirical. This is perhaps a reflection of the conclusions of some workers that the different magnetic environments of the diastereomeric cyclodextrin complexes, rather than their formation constants, are primarily responsible for the chiral recognition process [128,129]. Experimental variables which have been shown to affect the recognition process include pH [128], temperature [125,141] and the presence of salts [125]. These factors will be considered in greater detail in Chapter 2.

## CHAPTER 2

### Studies of the Enantioselective Metabolism of the Profens by NMR Bio-fluid

#### Analysis

#### 2.1 Introduction

Chapter 1 referred to the aim of this work, which was to examine the enantioselectivity of profen metabolism, particularly with regard to the chiral inversion mechanism, by NMR studies of biological fluids. Ibuprofen and flurbiprofen were chosen as model compounds, since the metabolites of these drugs excreted in urine have already been elucidated by NMR [86,90,98]. On this basis, and because of its ready availability, urine was also chosen as the medium of study here.

It was our intention that the two stereochemistries of the unchanged drug in the biological fluid be distinguished by the addition of an appropriate water-soluble chiral NMR reagent. Two possible reagents capable of resolving a mono-functionalised carboxylic acid were identified, namely  $\text{Na}[\text{Eu(III)}(\text{R or S})\text{pdta}(\text{H}_2\text{O})_3]$ , which was used by Kabuto and Sasaki [111] with 2-phenylpropionic acid, and the cyclodextrins, which have shown chiral recognition with ibuprofen [126] and pirprofen [128]. The commercial availability of the cyclodextrins, and the many literature reports of interactions of the profens with them [142-145], made these the reagents of choice.

Prior to the addition of such a reagent, however, it would first be necessary to free that part of the unchanged drug present as its glucuronide conjugate. In the body hydrolysis of the conjugate is brought about by the action of the  $\beta$ -glucuronidase enzyme [40]. Decomposition under basic conditions, as was used by Wade *et al.* [90] in their study of the metabolism of flurbiprofen by NMR was, however, considered a simpler method for use in this work.



Initial studies were aimed at assessing the viability of the proposed method by examining discrimination of the enantiomers of ibuprofen and flurbiprofen by NMR in deuterated water in the presence of cyclodextrins, before extending the method to biologically relevant conditions.

## 2.2. $^1\text{H}$ NMR Data for the Cyclodextrins

The NMR spectra for ibuprofen and flurbiprofen were recorded in a 1:1 mole ratio in the presence of a range of cyclodextrins in  $\text{D}_2\text{O}$ . The cyclodextrins which were available to us were the  $\alpha$ -,  $\beta$ - and  $\gamma$ -cyclodextrin oligomers, and the  $\beta$ -cyclodextrin derivative 2,6-di-O-methyl- $\beta$ -cyclodextrin (DMCD, Figure 2.1). The  $^1\text{H}$  NMR spectra of the  $\alpha$ -,  $\beta$ - and  $\gamma$ -cyclodextrin were consistent with reported data [126] and showed no significant level of impurity. Chemical shifts and coupling constants are summarised in Table 2.1.

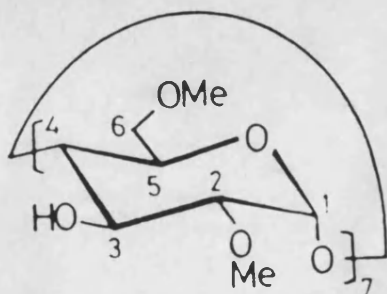


Figure 2.1 Structure of DMCD

The  $^1\text{H}$  spectrum of DMCD in  $\text{D}_2\text{O}$ , shown in Figure 2.2 with assignments from Kobayashi [146], clearly showed significant levels of impurity, however. This is most clearly seen for the glycosidic H1 resonance around 5.33ppm. The high level of impurity was not unexpected. Indeed, Irie *et al.* [147] have reported the analysis of a number of commercial preparations of DMCD by plasma-

Cyclodextrin	H1	H2	H3	H4	H5	H6
$\alpha$	5.141 (d,3.4)	3.721 (dd,10.0,3.4)	4.068 (dd,10.0,8.8)	3.672 (t,9.2)	overlapping multiplets 4.022-3.907	
$\beta$	5.158 (d,3.7)	3.738 (dd,9.8,3.7)	4.050 (t,9.4)	3.670 (t,9.0)	overlapping multiplets 4.009-3.930	
$\gamma$	5.196 (d,3.9)	3.742 (dd,9.9,3.8)	4.020 (t,9.5)	3.674 (t,9.4)	overlapping multiplets 3.988-3.927	

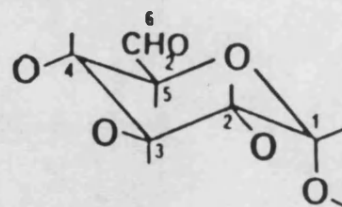


Table 2.1 400MHz  $^1\text{H}$  NMR data for the cyclodextrins at a concentration of 0.014M in  $\text{D}_2\text{O}$  at  $30^\circ\text{C}$

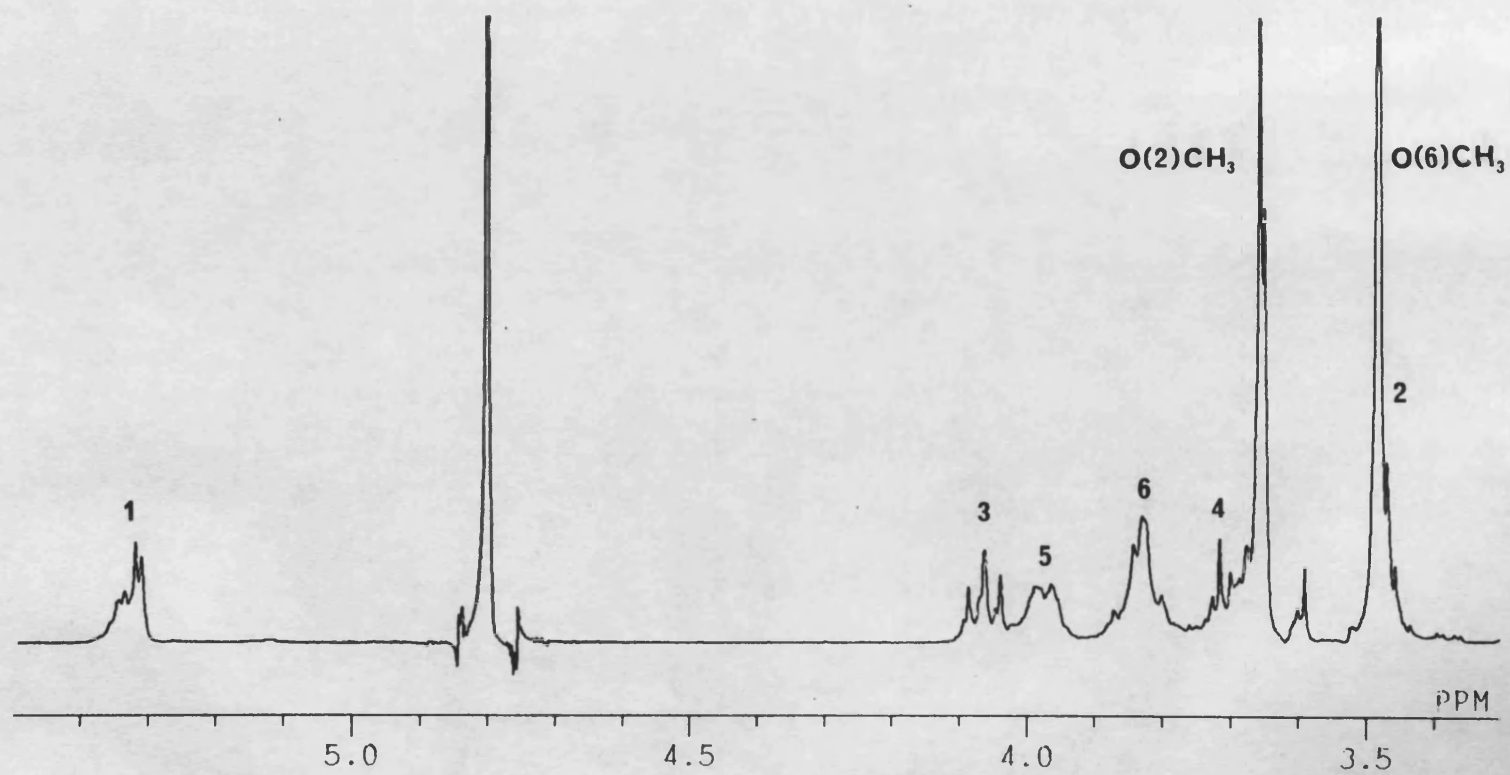


Figure 2.2 400MHz  $^1\text{H}$  NMR spectrum of a 0.014M solution of DMCD in  $\text{D}_2\text{O}$  at 30°C

desorption MS and have shown them to be markedly impure, with  $\beta$ -cyclodextrin molecules carrying 13 and 15 methyl substituents as the primary contaminants. It was not possible to accurately assess the purity of the DMCD samples used in this work by  $^1\text{H}$  NMR, however, because as a complex mixture of closely related components, there are many overlapping and unresolved resonances, at least in  $\text{D}_2\text{O}$  [148]. No attempt at purification was made, because of the difficulty of identifying impurities in such samples and subsequent purification [148-150]. This was considered reasonable since most impurities differ in structure from DMCD itself only by the presence or absence of one or two methyl groups, and because no quantitative measurement was made concerning interaction of the drug molecule with DMCD.

### 2.3 NMR Studies of Ibuprofen and Cyclodextrin Mixtures

The  $^1\text{H}$  NMR data for ibuprofen sodium (Figure 2.3), chosen over the free acid because of its higher aqueous solubility, in  $\text{D}_2\text{O}$  is summarised in Table 2.2.

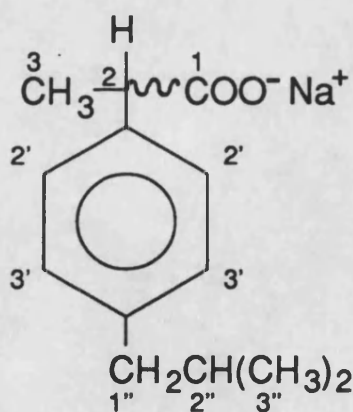


Figure 2.3 Structure of ibuprofen sodium

Chemical shift/ppm (Coupling constant/Hz)	Assignment
7.351 (d,8.3)	H2'
7.296 (d,8.1)	H3'
3.692 (q,7.2)	H2
2.562 (d,7.1)	H1''
1.922 (m,6.8)	H2''
1.470 (d,7.1)	H3
0.958 (d,6.8)	H3''

Table 2.2 400MHz  $^1\text{H}$  NMR data for a 0.014M solution of ibuprofen sodium in  $\text{D}_2\text{O}$  at  $30^\circ\text{C}$

The chemical shifts of the pair of doublets associated with the aromatic protons are calculated on the basis of a strongly coupled AB spin system, using equations given in most basic NMR texts [151]. These have been used for the simple *para*-disubstituted aromatic ring system throughout this work where the frequency difference of the two  $^1\text{H}$  resonances is less than six times greater than the coupling constant between them [152].

The assignment of the ibuprofen sodium spectrum from chemical shifts, coupling patterns and integrals is straight-forward, except in the case of the aromatic signals. The presence of the inductively electron-withdrawing carboxylate functionality on the alkyl chain *ortho* to H2' might be expected to lead to a down-field shift of this resonance compared to H3'. This was confirmed by nOe difference spectroscopy (see Chapter 4).

The duplication and the magnitude of splitting of these signals observed in the presence of a mole equivalent of  $\alpha$ -,  $\beta$ - and  $\gamma$ - cyclodextrin and DMCD are indicated in Table 2.3. The H2 resonance is, however, masked by the cyclodextrin signals, so that information regarding its duplication is not available. The largest duplications are seen for  $\beta$ -cyclodextrin, the results for which reproduce those of Casy and Mercer [126], who reported splittings of 3Hz and 5Hz at 400MHz for the

H3 and low field aromatic signals respectively. Whilst no chiral recognition is apparent in the presence of  $\gamma$ -cyclodextrin, splitting of the H3'' signal is observed for  $\alpha$ -cyclodextrin and DMCD, although the former is very small.

Ibuprofen sodium resonance	Chiral splitting in presence of cyclodextrin/ppm			
	$\alpha$	$\beta$	$\gamma$	DMCD
H2'	0	0.009	0	0
H3'	0	0	0	0
H2	obscured	obscured	obscured	obscured
H1''	0	0	0	0
H2''	0	0	0	0
H3	0	0.006	0	0
H3''	0.001	0	0	0.006

Table 2.3 Chiral duplication of 400MHz  $^1\text{H}$  resonances of a 0.014M solution of ibuprofen sodium in the presence of a mole equivalent of cyclodextrin in  $\text{D}_2\text{O}$  at 30°C

The cyclodextrin chiral recognition process necessarily requires some form of interaction between cyclodextrin and drug. Inclusion of a substrate in the cyclodextrin cavity is the most commonly observed complexation process [146]. The formation of such an inclusion complex may be apparent from changes in chemical shift of both drug and cyclodextrin NMR resonances on mixing of the two. That each species only gives rise to a single set of resonances in such a mixture of ibuprofen sodium and cyclodextrin (except where duplication of drug signals is apparent), indicates that complexation is a fast exchange process, and as a result, resonances will be a population weighted average of those for the free and complexed species. Table 2.4 summarises the shifts of the ibuprofen sodium  $^1\text{H}$  resonances in the presence of cyclodextrin, and Table 2.5 the corresponding shifts



Ibuprofen sodium resonance	Cyclodextrin			
	$\alpha$	$\beta$	$\gamma$	DMCD
H2'	+0.022	-0.016,-0.007	-0.003	-0.015
H3'	+0.026	-0.160	-0.086	-0.263
H2	obscured	obscured	obscured	obscured
H1''	+0.058	-0.014	-0.031	-0.062
H2''	+0.070	-0.011	-0.049	-0.029
H3	+0.005	+0.015,+0.009	+0.011	+0.062
H3''	+0.066,+0.065	+0.029	-0.023	+0.055,+0.050

Table 2.4 Changes in 400MHz  $^1\text{H}$  NMR chemical shifts of resonances of a 0.014M solution of ibuprofen sodium in the presence of a mole equivalent of cyclodextrin in  $\text{D}_2\text{O}$  at  $30^\circ\text{C}$

in the cyclodextrin signals. The residual HDO resonance was used as an internal reference standard for comparison of these spectra.

Resonance	$\alpha$ -cyclodextrin	$\beta$ -cyclodextrin	$\gamma$ -cyclodextrin	DMCD
H1	0	-0.029	-0.020	
H2	0	-0.033	-0.021	
H3	+0.010	-0.111	-0.041	~-0.080
H4	+0.002	-0.009	-0.014	
H5	*	>-0.179	>-0.066	~-0.175
H6	*	*	*	

Table 2.5 Changes in 400MHz  $^1\text{H}$  NMR chemical shifts of resonances of cyclodextrin at a concentration of 0.014M in the presence of a mole equivalent of ibuprofen sodium in  $\text{D}_2\text{O}$  at 30°C

Common referencing methods have been discussed by Brevard and Granger [153]. The use here of an external reference contained in a capillary or of a reference sample contained in a separate tube was considered inappropriate for the accurate measurement of chemical shift. The use of an internal standard was also ruled out, since it was thought that this might interfere with the complexation process. Thus, Brereton *et al.* [154] reported that they were unable to use trifluoroacetate as an internal reference for their  $^{19}\text{F}$  NMR studies of the inclusion of fluoro- and difluoro- *trans*- cinnamates by  $\alpha$ -cyclodextrin, as the reference was itself found to include within the cyclodextrin. The use of the HDO resonance as reference here was considered a reasonable alternative in view of the low concentration of the solutions used, such that necessarily most HDO molecules are associated with bulk solvent, and because all spectra were acquired at a fixed temperature of 30°C.

The shifts of the aromatic system in Table 2.4 are calculated on the basis that no cross-over of these signals occurs on formation of the cyclodextrin complex. This has been confirmed at least in the case of  $\beta$ -cyclodextrin (see



Chapter 4). Determination of small changes in chemical shift of the cyclodextrin H5 and H6 resonances in the presence of ibuprofen sodium was not possible as a result of the overlapping nature of these resonances. Where larger changes were, however, observed, these are given approximately in Table 2.5.

The large shifts of the cyclodextrin H3 and H5 signals which point into the molecular cavity indicate the occurrence of inclusion for  $\beta$ - and  $\gamma$ -cyclodextrin. Approximate calculations for the H3 and H5 resonances of DMCD show similar evidence for the inclusion process. Such upfield shifts are consistent with the inclusion of an aromatic ring as was shown by Demarco and Thakkar [155], who applied the theory of Johnson and Bovey [156,157] to inclusion complex formation. The shielding component of the secondary magnetic field arising from the aromatic ring current normal to the plane of the benzene ring is greater than the deshielding component in its plane at any distance from its centre, so that unless the guest molecule assumes some preferred fixed orientation in the cyclodextrin cavity, an up-field shift of the inwardly pointing cyclodextrin signals is observed. In contrast, the  $\alpha$ -cyclodextrin molecule shows a down-field shift of the H3 proton in the presence of ibuprofen sodium, which implies that inclusion of the aromatic ring does not occur for this host.

Analysis of the shifts in drug signals is less straight forward, since both insertion into the cyclodextrin cavity and interaction near its rim have been suggested as causes of the larger shifts on complexation. Thus, Djedaïni *et al.* [158] and Backensfeld *et al.* [159] both observed large down-field shifts of the  $^1\text{H}$  NMR signals of the indole unit compared with those of the *p*-chlorobenzoyl unit upon inclusion of indomethacin (Figure 2.4) in  $\beta$ -cyclodextrin and hydroxypropyl- $\beta$ - and  $\gamma$ -cyclodextrin respectively. Backensfeld and co-workers [159] argued that the indole ring was too large for insertion in the cyclodextrin cavity and that the large shifts in its signals arose from the butting of the indole moiety on the margin of the cyclodextrin ring on inclusion of the *p*-chlorobenzoyl ring. Djedaïni *et al.*

[158], however, interpreted their results as occurring as a consequence of the inclusion of part of the indole ring in the cyclodextrin cavity. It would therefore appear difficult to unequivocally correlate such shifts with complex structure. Additionally, in relation to the ibuprofen sodium structure, precedents for the insertion of both aromatic rings and aliphatic chains are also known. Kotake and Janzen [160], for example, were able to observe inclusion of both the *t*-butyl substituent and the phenyl ring of some nitroxide radicals with  $\beta$ -cyclodextrin by ESR. The same authors have also used ESR to demonstrate the relative preferences of  $\gamma$ -cyclodextrin for various structural units [161].

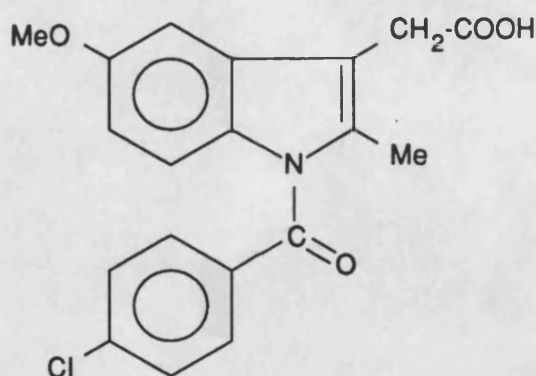


Figure 2.4 Structure of indomethacin

Two classes of complex may be distinguished from the changes in chemical shift of the ibuprofen sodium signals, given in Table 2.4. Firstly, in the presence of  $\beta$ - and  $\gamma$ -cyclodextrin and DMCD a large upfield shift of one of the aromatic signals (regardless of whether signal cross-over occurs or not), which is bigger than any other shift, is observed. For the  $\alpha$ -cyclodextrin solution the shift of the H2'' resonance of the ibuprofen sodium isobutyl chain is larger than that for any other cyclodextrin. In addition, this resonance and that for the isobutyl H1'' show a down-field shift in contrast to that of the other hosts. These observations

suggest that in the case of  $\alpha$ -cyclodextrin, inclusion of the isobutyl chain is favoured over that of the aromatic ring, whereas for the other cyclodextrins examined here, aromatic inclusion is preferred. This is presumably a result of the greater compatibility of inclusion of the isobutyl chain either partially or fully into the smaller cavity of the  $\alpha$ -cyclodextrin macrocycle. Since the isobutyl chain lies far from the chiral centre of the drug molecule, this perhaps contributes to the minimal chiral duplication of the ibuprofen sodium signals in the presence of  $\alpha$ -cyclodextrin. For the larger  $\gamma$ -cyclodextrin oligomer, it is reasonable to assume that binding of the aromatic ring is not sufficiently tight for chiral recognition between guest and host to occur. Requirements for chiral discrimination are considered further in Chapters 3 and 4.

The differences in magnitude of shifts in both drug and cyclodextrin signals for this series of complexes may be associated with differences in formation constant or the intrinsic magnetic environment of the complex. Chiral discrimination may similarly be ascribed to small differences in the formation constant of the complexes of each enantiomer or to structural differences of the two diastereomeric complexes. The ibuprofen sodium/DMCD complex is particularly interesting in this regard. Figure 2.5 (i) and (ii) shows the  $H_3''$  resonance of ibuprofen sodium and its duplication in the presence of DMCD. The unequal peak sizes observed for the complex are consistent with resonances arising from the two methyl groups of the isobutyl substituent remaining equivalent in the diastereomeric complex of one enantiomer, but becoming inequivalent in the complex of the other with partial peak overlap. This was confirmed by analysis of the sodium salts of the two pure ibuprofen enantiomers in the presence of DMCD, Figure 2.5 (iii) and (iv). The complex of the S enantiomer is that which shows an inequivalence of the two methyl groups. This distinction of the two methyl groups highlights the importance of the differential magnetic environment in such complexes. Other authors have similarly attributed chiral discrimination in NMR

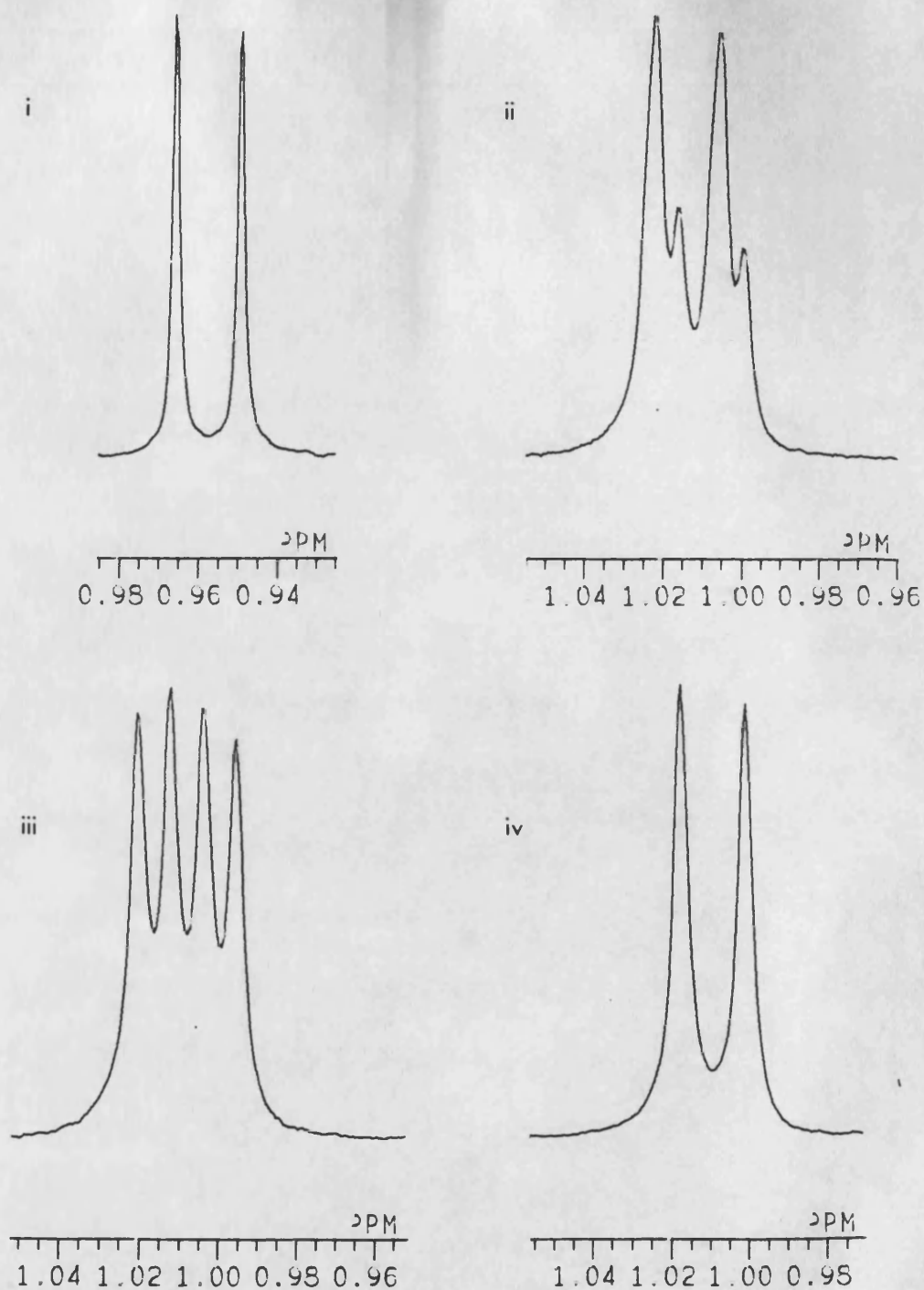


Figure 2.5 400MHz <sup>1</sup>H<sup>3</sup> resonance of a 0.014M solution of (i) ibuprofen sodium, (ii) ibuprofen sodium in the presence of a mole equivalent of DMCD, (iii) S(+)-ibuprofen sodium in the presence of a mole equivalent of DMCD and (iv) R(-)-ibuprofen sodium in the presence of a mole equivalent of DMCD in D<sub>2</sub>O at 30°C

spectra by cyclodextrins primarily to magnetic rather than thermodynamic differences of the diastereomers [128,129].

The inequivalence of the two isobutyl methyl resonances observed for the ibuprofen sodium/DMCD complex must also raise the question as to whether the pair of doublets forming the H3" signal for the ibuprofen sodium/ $\alpha$ -cyclodextrin complex is indeed the result of a chiral discrimination process or of the inequivalence of the two methyl resonances in both of the ibuprofen sodium/ $\alpha$ -cyclodextrin diastereomeric complexes. This could ideally be elucidated by examination of the  $^1\text{H}$  NMR spectra for the individual ibuprofen sodium enantiomers in the presence of  $\alpha$ -cyclodextrin, as in the case of DMCD, but the splitting of the resonances with  $\alpha$ -cyclodextrin was considered too small for this distinction to be made.

With use of an appropriate resolution enhancement function, it was possible to obtain baseline separation of the chiral splitting of the ibuprofen sodium H3" resonance in the presence of DMCD, and of the low field aromatic and H3 signals in the presence of  $\beta$ -cyclodextrin. Under such conditions, additional duplications of some ibuprofen sodium resonances were identified, but since these were not observable under routine processing conditions were considered insignificant.

Resolution enhancement may lead to distortion of peak integrals and a loss of accurate quantitative information. To ensure that quantitation was not precluded by the use of such a function here, a series of solutions prepared from different ratios of the pure ibuprofen enantiomers to fixed total concentration in the presence of a mole equivalent of  $\beta$ -cyclodextrin were examined and their enantiomeric purity determined. Ibuprofen sodium salts were formed *in situ* by use of alkaline  $\text{D}_2\text{O}$  as solvent. The  $^1\text{H}$  H3 resonance of these solutions was chosen for quantitation since the low field aromatic resonance showed some fine structure associated with deviation from first order coupling behaviour. For simplicity, a

comparison of peak heights of the H3 signal of each of the two enantiomers was made, and the enantiomeric purity compared with the known value. Table 2.6 shows the results of this study.

S% by weight	S% by NMR
76.5	76.2
56.0	55.7
50	50.1
39.6	41.2
20.4	32.1

Table 2.6 Determination of the enantiomeric purity of ibuprofen sodium at a concentration of 0.040M in the presence of a mole equivalent of  $\beta$ -cyclodextrin in 0.07M NaOD in D<sub>2</sub>O by 400MHz <sup>1</sup>H NMR at 25°C

In general, the ratio of (S)- to (R)-ibuprofen found by NMR is in close agreement with the expected value. Only one solution showed any significant deviation between the two, which suggests that it may be the consequence of an inaccuracy in the weighing of a small quantity of enantiomer. Examination of solutions of the supposedly pure enantiomers confirmed that each contained less than 5% of the other.

For the ibuprofen sodium/DMCD mixture, peak heights were found to be inadequate for the determination of the enantiomeric purity from the H3" resonance, since the overlapping peaks which give rise to the low field doublet lead to broadening of this signal in comparison to that at higher field (Figure 2.5). The measurement of peak integrals is therefore required.

#### 2.4 Extension of NMR Studies of Ibuprofen Sodium and Cyclodextrin Mixtures to Biological Fluids

The  $^1\text{H}$  NMR spectrum of a freeze-dried human urine sample reconstituted in  $\text{D}_2\text{O}$ , with some concentration, is shown in Figure 2.6. Many of the resonances from endogenous metabolites have previously been identified, and the most prominent are labelled here [65,86,98]. It can be seen from this spectrum that there are several areas free of these endogenous metabolites, and therefore suitable for study of xenobiotic metabolism.

Figure 2.6 also shows an identical sample spiked with 0.65mg of ibuprofen sodium, which is of the order of the concentration to be expected *in vivo*. The drug resonances, which are all within 0.01ppm of their shifts in  $\text{D}_2\text{O}$ , are indicated where they are clearly identifiable, and it is readily apparent that the H3" signal would be most suited to any attempt at chiral discrimination because of its large height and separation from endogenous peaks. The comparative prominence of the H3" signal of ibuprofen and its metabolites in urine samples can similarly be seen in Figure 2.7, which shows the  $^1\text{H}$  NMR spectrum of a human urine sample following ingestion of 400mg ibuprofen, and confirms the work of Wilson and Nicholson [86,98]. Reconstitution of an equivalent sample in alkaline  $\text{D}_2\text{O}$  allows glucuronide hydrolysis to be achieved as expected. This is most readily apparent from the disappearance of the H3 resonance of ibuprofen glucuronide from the  $^1\text{H}$  spectrum under such conditions. The H3 resonance of the resulting free ibuprofen is obscured beneath that of the other metabolites, and is thus ruled out for use in determinations of enantiomeric purity (Figure 2.7).

The only cyclodextrin which allowed reasonable chiral discrimination of the isobutyl methyl resonance was the ibuprofen sodium/DMCD system, and the reproduction of this recognition was therefore attempted in urine.

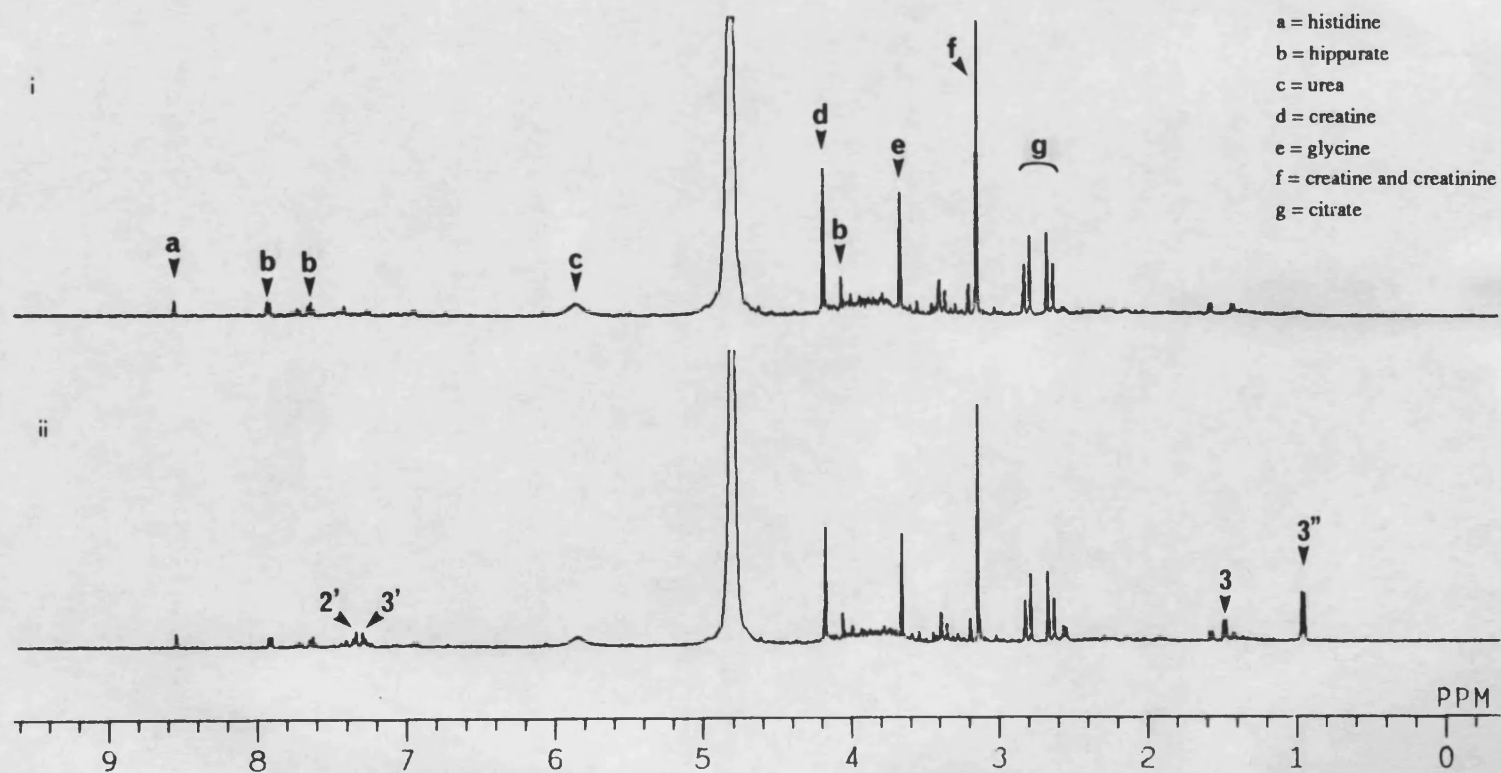


Figure 2.6 400MHz  $^1\text{H}$  NMR spectrum of (i) freeze-dried human urine reconstituted in  $\text{D}_2\text{O}$  and (ii) as (i) with added ibuprofen sodium at  $30^\circ\text{C}$



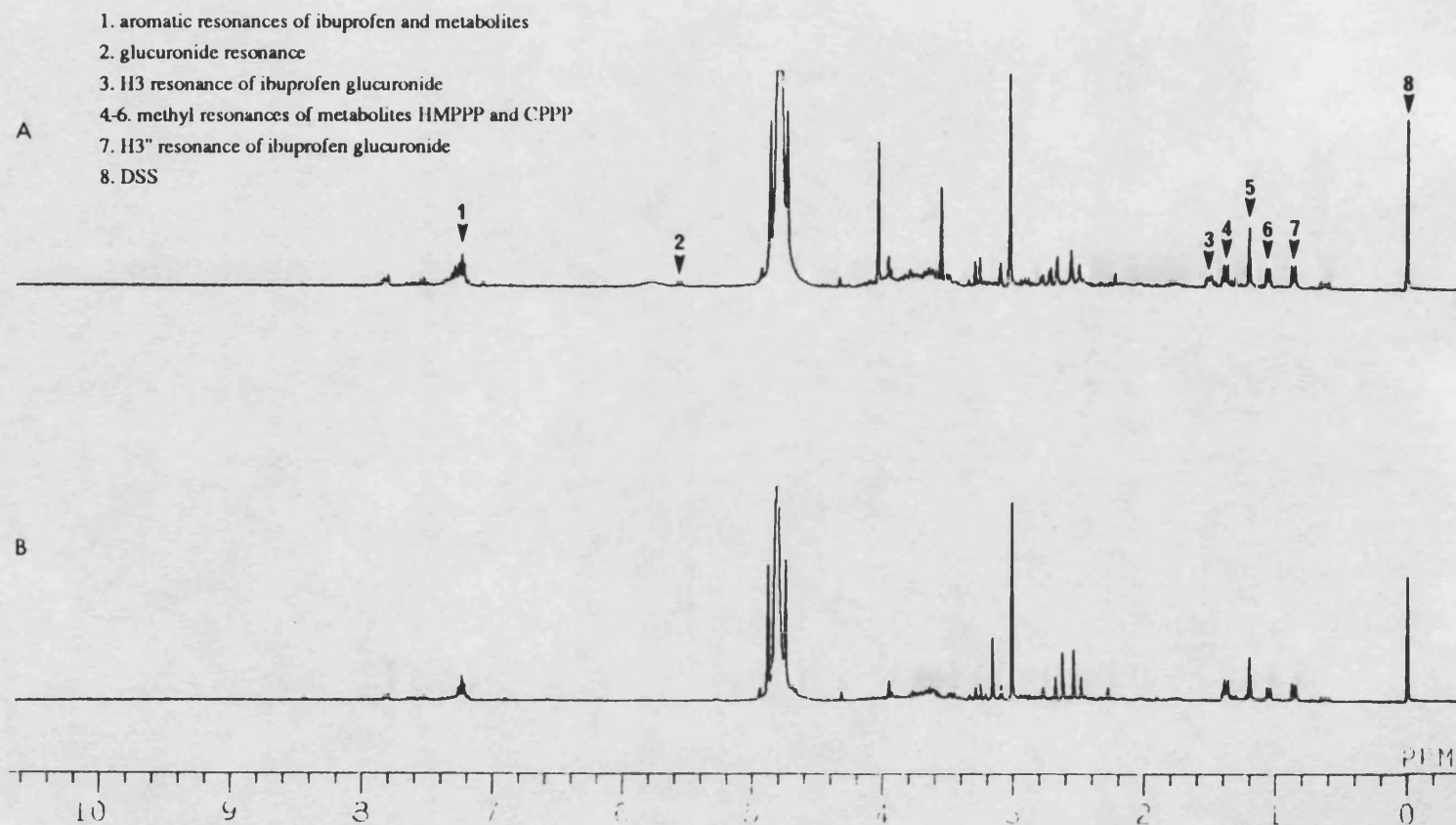


Figure 2.7

270MHz  $^1\text{H}$  NMR spectrum of a freeze-dried human urine sample following ingestion of ibuprofen, reconstituted in (A)  $\text{D}_2\text{O}$  and (B) 0.07M NaOD in  $\text{D}_2\text{O}$

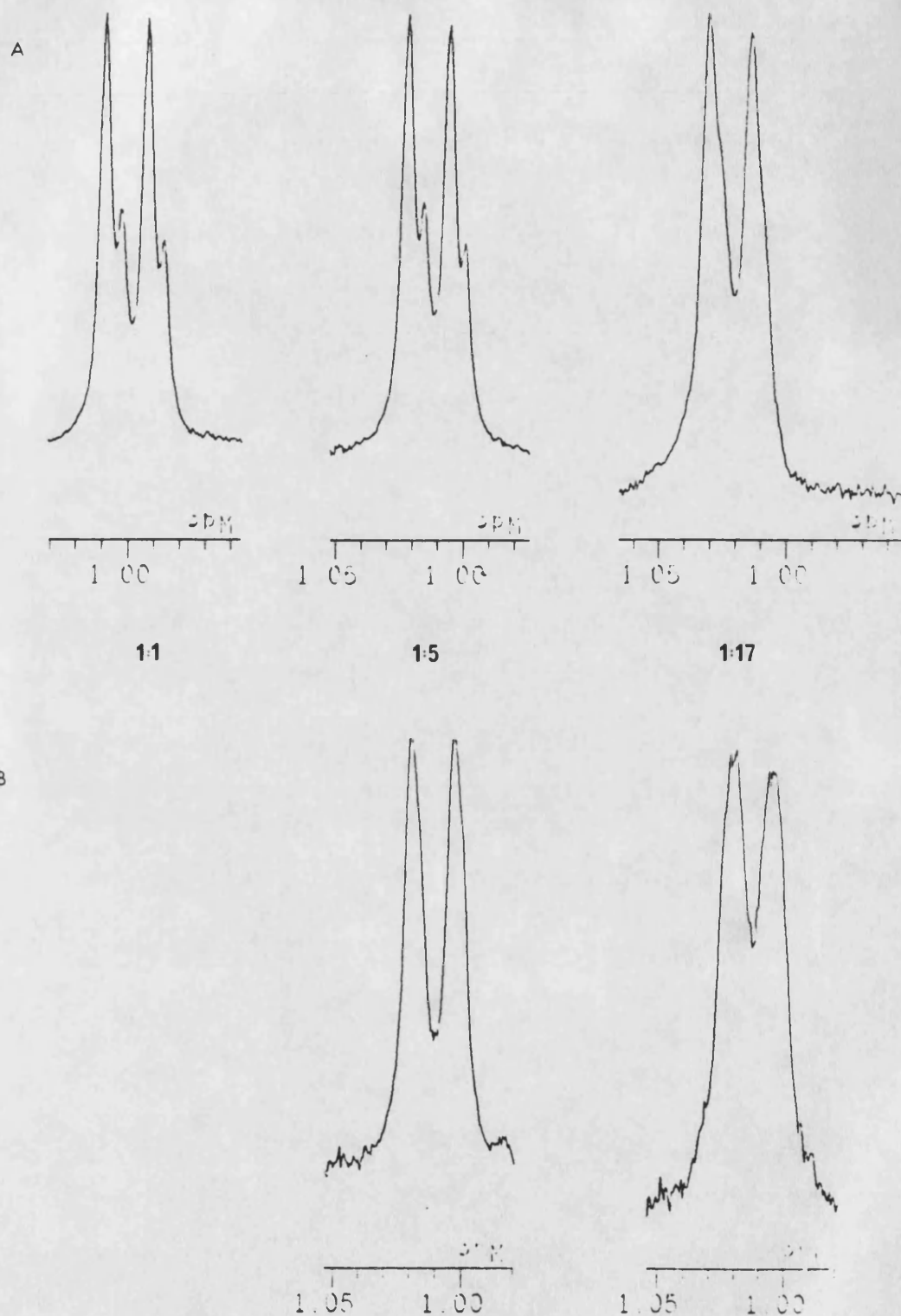


Figure 2.8 400MHz  $^1\text{H}$   $\text{H}3''$  resonance of a 0.0044M solution of ibuprofen sodium in the presence of varying equivalents of DMCD (A) in  $\text{D}_2\text{O}$  and (B) in freeze-dried human urine in  $\text{D}_2\text{O}$  at  $30^\circ\text{C}$

Figure 2.8 shows the chiral splitting of the H3" resonance of ibuprofen sodium in D<sub>2</sub>O with increasing equivalents of DMCD added. Above a 1:17 ratio of drug to cyclodextrin the splitting is lost. That shifts in <sup>1</sup>H resonances of the drug observed in the presence of a mole equivalent of DMCD are not enhanced at high mole ratio of cyclodextrin suggests that this is the result of some disruption of the inclusion process, possibly as a result of associative complexation of the cyclodextrin molecules at high concentration. The viscosity of such a concentrated solution may also lead to enhanced rates of relaxation and consequent line-broadening and loss of resolution.

Figure 2.8 also shows the isobutyl methyl resonance for equivalent solutions used to reconstitute samples of the same freeze-dried urine specimen as that used in Figure 2.6. A greater than 1:1 ratio of ibuprofen sodium to DMCD was chosen to allow for competitive inclusion by the many endogenous urinary components. Even at a mole ratio of 1:5, for which a 0.006ppm splitting was observed in D<sub>2</sub>O, no chiral recognition of the H3" resonance is apparent in the urine sample. Several possible explanations for this observation may be considered.



Figure 2.9 Part of the 400MHz <sup>1</sup>H spectrum of a freeze-dried human urine sample reconstituted in D<sub>2</sub>O at 30°C, showing overlap of the sarcosine N-methyl and citrate resonances

1. The increased viscosity and particulate nature of the urine sample compared to that of D<sub>2</sub>O may lead to an increase in relaxation rate and loss of homogeneity respectively, which results in peak broadening and a loss of resolution.

Some measure of the effective resolution of the spectra can, however, be achieved by observation of the sarcosine N-methyl signal which overlaps with that arising from one of the citrate doublets (Figure 2.9). Their separation is 0.005ppm in blank urine, which suggests that the 0.006ppm splitting of the ibuprofen sodium/DMCD system in such a medium should be readily apparent if achieved. In fact, the resolution of the sarcosine and citrate resonances is still apparent in the presence of the 1:5 ibuprofen sodium/DMCD solution, but is lost for the 1:17 mole ratio solution, most probably as a result of line-broadening in such a highly concentrated and viscous sample.

2. The level of DMCD may not be sufficient to eliminate disruption of the ibuprofen complexation process by competing endogenous metabolites. Inspection of the aromatic resonances of ibuprofen in urine samples spiked with the drug shows, however, their chiral duplication in the presence of 5 and/or 17 mole equivalents of DMCD and indicates that significant levels of complexation of the drug with the cyclodextrin remain, Figure 2.10.

3. Chiral discrimination of these aromatic resonances was not observed in equivalent samples prepared in D<sub>2</sub>O, which suggests that rather than preventing inclusion of the ibuprofen molecule in the DMCD cavity, some endogenous urinary component gives rise to a change in structure, and hence nuclear magnetic properties, of the resulting complex.

The protonation of the ibuprofen salt might, for example, give rise to some such alteration of complex structure. The pH of a human urine sample is, however, typically in the range 4.8-7.8 [162], and since the pK<sub>a</sub> of ibuprofen is 4.63 [142],

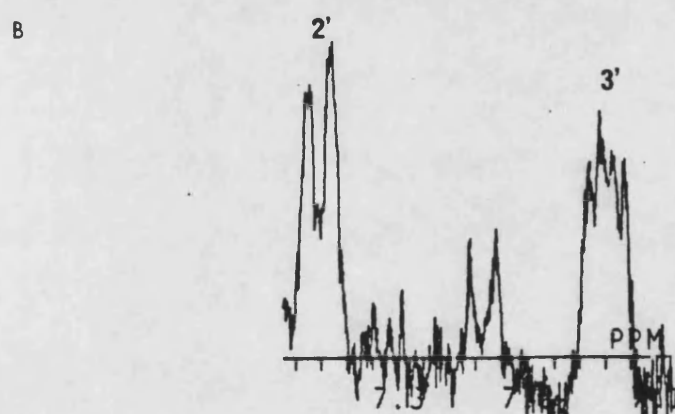
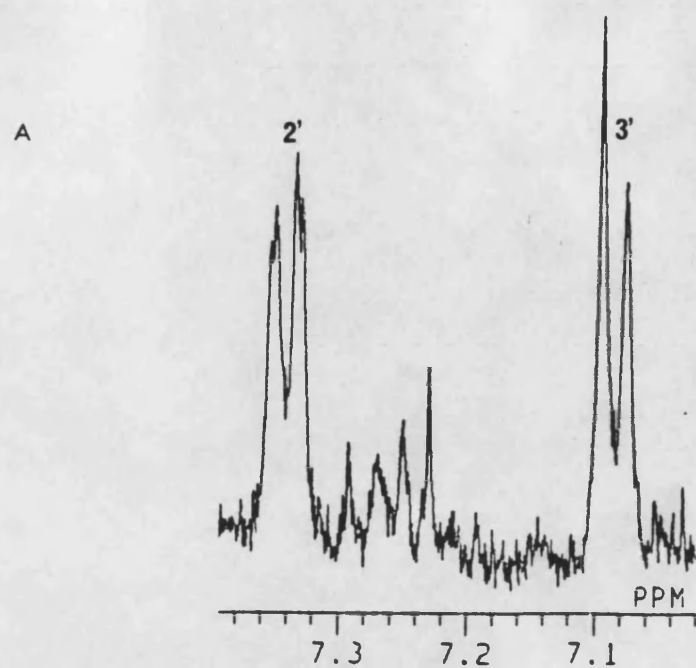


Figure 2.10 Part of the 400MHz <sup>1</sup>H NMR spectrum of freeze-dried human urine spiked with 0.65mg of ibuprofen sodium and reconstituted in D<sub>2</sub>O in the presence of (A) 5 equivalents and (B) 17 equivalents of DMCD at 30°C

the carboxylate group of the ibuprofen molecule should remain at least approximately 50% ionised. It must be noted, however, that deviation from this pKa value may occur as a result of the deuterated solvent environment [163] and upon inclusion of the drug in the cyclodextrin macrocycle [123].

Since the desired duplication of the ibuprofen H3'' resonance in the presence of DMCD is not achieved and the aromatic resonances of the drug, which do show duplication, are not resolved from those of its metabolites *in vivo*, Figure 2.7 and the work of Wilson and Nicholson [86,98], it is concluded that the nature of the biological medium precludes the use of DMCD as a chiral reagent for the determination of the enantiomeric purity of ibuprofen in such studies.

The significance of the effects of medium would presumably have been less had the initial chiral splitting in D<sub>2</sub>O been larger and thus more robust. Methods of enhancing the enantioselectivity of the ibuprofen sodium/cyclodextrin system are considered further in Section 2.7 below.

## 2.5 NMR Studies of Flurbiprofen and Cyclodextrin Mixtures

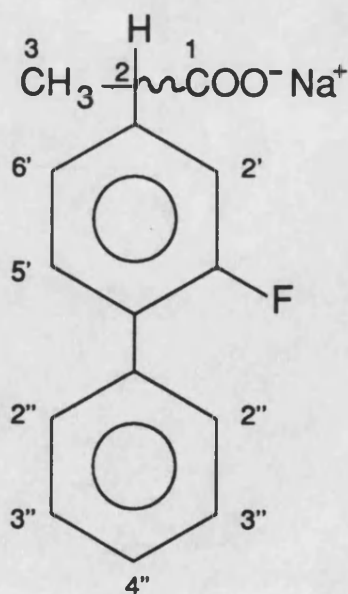


Figure 2.11 Structure of flurbiprofen sodium

The  $^1\text{H}$  NMR spectrum of flurbiprofen sodium (Figure 2.11) in  $\text{D}_2\text{O}$  is considerably more complex than that of ibuprofen sodium, because of the biaryl ring system and the additional complication of coupling to the  $^{19}\text{F}$  nucleus. Table 2.7 summarises the data. Assignments are based on coupling patterns and peak integrals, and since there is some discrepancy between our interpretation and that of Wade *et al.* [90], they were confirmed by a COSY-45 experiment (Chapter 4).

In the presence of a mole equivalent of  $\alpha$ -cyclodextrin, the chemical shifts of the drug signals show a small down-field shift, whereas those of the cyclodextrin move slightly up-field (Tables 2.8 and 2.9 respectively). Again, chemical shifts for the cyclodextrin H5 and H6 protons could not be accurately determined because of their overlapping nature, but changes upon addition of flurbiprofen sodium were clearly small. Such data are not consistent with any significant level of inclusion complex formation, so that as for ibuprofen sodium, the cavity of the  $\alpha$ - cyclodextrin macrocycle would appear to be too small for favourable accommodation of the flurbiprofen molecule.

Chemical shift/ppm (Coupling constant/Hz)	Assignment
7.708 (d,8.3)	H2''
7.612 (t,7.4)	H3''
7.559 (t,8.2)	H5'
7.534 (tt,7.3,1.6)	H4''
7.318 (dd,7.9,1.6)	H6'
7.283 (dd,12.2,1.7)	H2'
3.773 (q,7.2)	H2
1.522 (d,7.3)	H3

Table 2.7 400MHz  $^1\text{H}$  NMR data for a 0.014M solution of flurbiprofen sodium in  $\text{D}_2\text{O}$  at 30°C



Resonance	Change in chemical shift/ppm
H2''	+0.025
H3''	+0.022
H5'	+0.019
H4''	+0.014
H6'	+0.011
H2'	+0.012
H2	+0.006
H3	+0.007

Table 2.8 Change in 400MHz  $^1\text{H}$  chemical shift of resonances of a 0.014M solution of flurbiprofen sodium in the presence of a mole equivalent of  $\alpha$ -cyclodextrin in  $\text{D}_2\text{O}$  at  $30^\circ\text{C}$

In the case of  $\beta$ - and  $\gamma$ -cyclodextrin and DMCD, however, large up-field shifts of the H3 and H5 cyclodextrin proton signals are observed in accordance with the inclusion of an aromatic substrate (Table 2.9). Shifts in the drug signals are also apparent but, as a result of extensive overlap of the aromatic resonances, are not readily assigned in most cases. Some broadening of the aromatic signals, resulting in a loss of small couplings and fine structure, is also seen. This may be accounted for by the reduced rate of tumbling of the aromatic ring system of the flurbiprofen molecule on complexation with the cyclodextrin, leading to enhanced rates of relaxation. The rate of exchange of the drug between free and complexed states could also have some effect on the linewidths of drug resonances if it were to be intermediate between the two extremes of slow and fast exchange. Since other resonances do not appear to be affected, however, it is believed that the complexation process remains in the fast exchange limit.

As a result of the complexity of the aromatic resonance coupling pattern, chiral recognition of the flurbiprofen molecule leading to duplication of the  $^1\text{H}$  NMR signals is most readily observed for the H3 and H2 (where visible) protons. Even so, in the latter case chiral splitting was difficult to determine with accuracy as a result of partial peak overlap of signals arising from each drug enantiomer.



Cyclodextrin	Change in chemical shift/ppm					
	H1	H2	H3	H4	H5	H6
$\alpha$	-0.012	-0.014	-0.030	-0.014	*	*
$\beta$	-0.075	-0.102	-0.177	-0.041	>-0.246	*
$\gamma$	-0.055	-0.050	-0.109	-0.043	>-0.118	*
DMCD			$\sim$ -0.157		$\sim$ -0.223	

Table 2.9 Change in 400MHz  $^1\text{H}$  chemical shift of a 0.014M solution of cyclodextrin in the presence of a mole equivalent of flurbiprofen sodium in  $\text{D}_2\text{O}$  at  $30^\circ\text{C}$

Table 2.10 summarises the splittings of these signals in the presence of cyclodextrins.

Cyclodextrin	Splitting/ppm	
	H2	H3
$\alpha$	0	0
$\beta$	-0.016	0.010
$\gamma$	obscured	0.004
DMCD	partially obscured	0.002

Table 2.10 Chiral splitting of 400MHz  $^1\text{H}$  H2 and H3 resonances of a 0.014M solution of flurbiprofen sodium in the presence of a mole equivalent of cyclodextrin in  $\text{D}_2\text{O}$  at 30°C

Splittings are observed for the  $\beta$ - and  $\gamma$ -cyclodextrin and DMCD solutions, which are those shown to favour inclusion of the aromatic ring system of flurbiprofen. As for ibuprofen sodium, chiral recognition of flurbiprofen sodium is greatest with  $\beta$ -cyclodextrin again because of the compatibility of the sizes of the flurbiprofen molecule and the  $\beta$ -cyclodextrin cavity (Chapter 3). That methylation of the  $\beta$ -cyclodextrin molecule appears to hinder this discrimination process, and also alters the nature of that with ibuprofen sodium may be associated with the marked difference in conformational properties of  $\beta$ -cyclodextrin and DMCD [164-166]. The structure of the flurbiprofen sodium complex with cyclodextrins will be considered in more detail in Chapters 3 and 4.

The  $^{19}\text{F}$  NMR spectra of flurbiprofen in the presence of  $\alpha$ -,  $\beta$ - and  $\gamma$ -cyclodextrin and DMCD were also examined for evidence of inclusion and chiral discrimination of the flurbiprofen molecule. Table 2.11 shows the shifts and splittings of the  $^{19}\text{F}\{^1\text{H}\}$  singlet resonance. Note that these samples were prepared by dissolution of the free acid flurbiprofen (and cyclodextrin) in approximately 0.07M NaOD in  $\text{D}_2\text{O}$  rather than by use of the flurbiprofen sodium salt.

Cyclodextrin	Splitting/ppm
$\alpha$	0
$\beta$	0.007
$\gamma$	0
DMCD	0.019

Table 2.11 Chiral splitting of the 254MHz  $^{19}\text{F}\{^1\text{H}\}$  resonance of a solution of 0.011M flurbiprofen in the presence of a mole equivalent of cyclodextrin in 0.07M NaOD in  $\text{D}_2\text{O}$

The largest splitting was observed for DMCD, and was sufficiently large that use of a sine-bell window function, in place of the exponential function routinely used, allowed baseline resolution of the resonance from each enantiomer and the possibility of quantitation.

## 2.6 Extension of NMR Studies of Flurbiprofen and Cyclodextrin Mixtures to Biological Fluids

Since the splitting of the  $^{19}\text{F}\{^1\text{H}\}$  resonance in the flurbiprofen/DMCD system was the greatest of those observed, and because of the ease of analysis of bio-fluids by  $^{19}\text{F}$  NMR, as a result of the lack of interfering endogenous metabolites, we chose to examine flurbiprofen metabolism by  $^{19}\text{F}\{^1\text{H}\}$  NMR, using DMCD as chiral solvating agent. The rat was chosen as the species for study in the first instance.

Figure 2.12 shows the  $^{19}\text{F}\{^1\text{H}\}$  NMR spectrum of a urine sample collected 0-7.5 hours following oral administration of a 10mg/kg dose of a suspension of flurbiprofen in 1% aqueous tween 80. The signal-to-noise ratio of this spectrum remains low despite the accumulation of 9000 scans, corresponding to an experiment time of 5 hours. The improvement in sensitivity as a result of sample

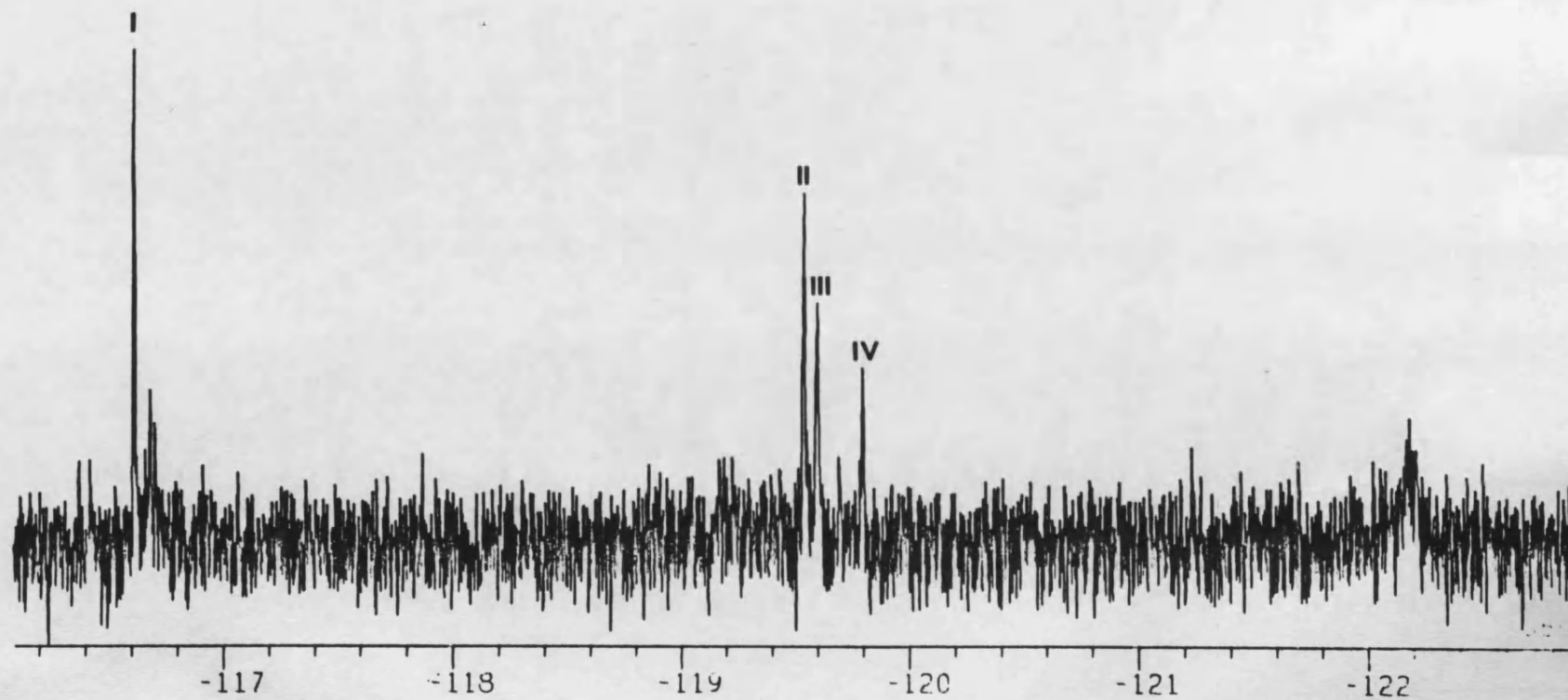
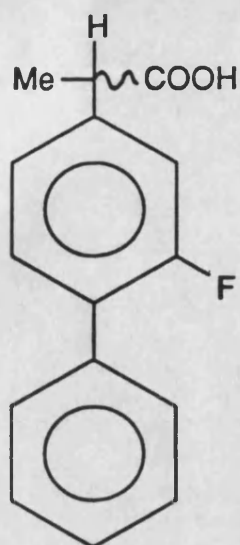


Figure 2.12 376MHz $^{19}\text{F}$ { $^1\text{H}$ } spectrum of rat urine following oral administration of flurbiprofen. The sample has been freeze-dried and reconstituted in 0.07M NaOD in  $\text{D}_2\text{O}$

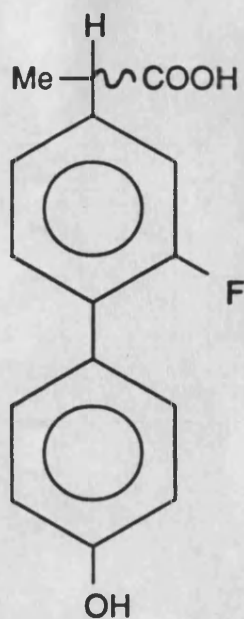
concentration is limited by the small volume of urine a rat typically produces. In this study, for example, 2-4ml was collected in the first 7.5 (day-time) hours with an increased production of 6-8ml overnight.

The sample has been freeze-dried and reconstituted in approximately 0.07M NaOD in D<sub>2</sub>O, to allow hydrolysis of any glucuronides present. Significant levels of a number of metabolites are clearly present. Spiking of an equivalent blank urine sample with flurbiprofen suggested that the resonance of the drug should appear in the region of metabolite (iv), but since it was expected to be present at considerably lower levels in comparison to other metabolites [34], and therefore in this case was probably not detected, we identify (iv) as more likely arising from the metabolite 2-(2-fluoro-4'-hydroxy-4-biphenyl)propionic acid, Figure 2.13, which is known to lie very close in chemical shift to the free drug [90]. Resonances (ii) and (iii) lie within 0.3ppm down-field of metabolite (iv) and probably arise from other known metabolites, Figure 2.13. The remaining prominent signal at -116.62ppm shows an unexpectedly large down-field shift in relation to other resonances (approximately 3ppm) which suggests that it is most likely the product of metabolic transformation of the fluorophenyl as opposed to phenyl aromatic ring. This proposal is supported by the effect on <sup>19</sup>F chemical shift of the introduction of a hydroxyl substituent to the fluorobenzene ring, Table 2.12. Data in this table suggest that metabolite (i) may then be the result of oxidative metabolism at the 5' position of flurbiprofen. Such a metabolite has not previously been identified in metabolic studies of flurbiprofen, however.

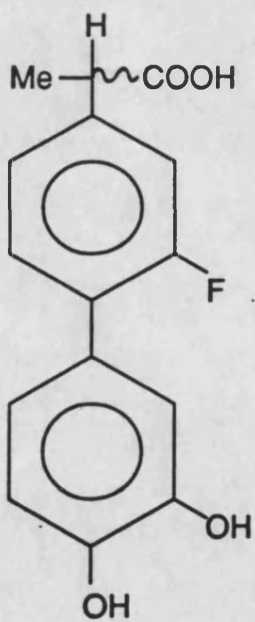
The experiment was repeated with an increased dosage of 75mg/kg (oral LD<sub>50</sub>=88mg/kg, [168]) for improved sensitivity. Dissolution of the dose was achieved in an equivalent of aqueous sodium hydroxide to avoid the inaccuracies of the administration of a suspension. The higher dose was, however, found to induce diarrhoea in the rat which received it, and was therefore considered inappropriate for further studies.



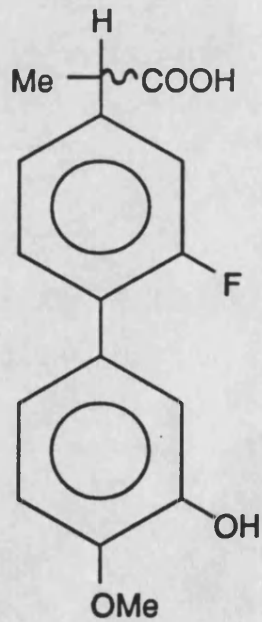
1.7%



59.1%



8.0%



8.5%

Figure 2.13 Proportions of flurbiprofen and its metabolites found in rat urine [34]



Compound	$^{19}\text{F}$ chemical shift/ppm
fluorobenzene	-113.07 - -114.97
<i>o</i> -fluorophenol	-138.1
<i>m</i> -fluorophenol	-111.57 - -112.67
<i>p</i> -fluorophenol	-123.54 - -124.00

Table 2.12  $^{19}\text{F}$  chemical shift data (relative to  $\text{CFCl}_3$ ) for fluorobenzene and the fluorophenols. Ranges represent the results of a number of studies in a range of solvents [167]

Attempts to reproduce the duplication of the flurbiprofen  $^{19}\text{F}$  resonance observed in  $\text{D}_2\text{O}$  in the presence of DMCD were unsuccessful in the biological fluid as in the case of ibuprofen. Thus, a freeze-dried rat urine sample reconstituted in alkaline  $\text{D}_2\text{O}$  and with 0.35mg of a flurbiprofen spike added failed to show duplication of the  $^{19}\text{F}\{^1\text{H}\}$  resonance in the presence of DMCD, added in excess (approximately 16.4 equivalents), to avoid competitive binding of other urinary constituents. A down field shift of the  $^{19}\text{F}$  resonance suggested that some interaction of the flurbiprofen and cyclodextrin was present, and that discrimination of the flurbiprofen enantiomers was not achieved for reasons similar to those outlined for ibuprofen sodium (Section 2.4).

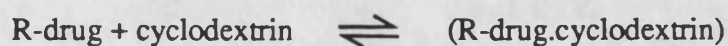
## 2.7 Factors Affecting Chiral Recognition of Ibuprofen and Flurbiprofen by Cyclodextrins in NMR Spectroscopy

Since the action of cyclodextrins as chiral solvating agents appeared to be diminished in urine samples, methods were investigated to enhance the chiral recognition process in an attempt to minimise the effect of changing from an aqueous to biological medium. Such experiments also allow some insight into the importance of various aspects of the recognition process. The  $\beta$ -cyclodextrin complexes of ibuprofen sodium and flurbiprofen sodium were chosen for these

studies, as a result of the considerably lower cost of  $\beta$ -cyclodextrin compared to that of the other cyclodextrins used in this work.

### 2.7.1 Effect of Variations in Mole Ratio and Concentration

Complexation of a chiral drug with a cyclodextrin molecule can be represented as a pair of rapidly-exchanging, competing equilibrium processes of the form:



for which the equilibrium constants  $K_R$  and  $K_S$  may be given by:

$$K_R = \frac{[(\text{R-drug.cyclodextrin})]}{[\text{R-drug}] \times [\text{cyclodextrin}]} \quad (2.1)$$

$$K_S = \frac{[(\text{S-drug.cyclodextrin})]}{[\text{S-drug}] \times [\text{cyclodextrin}]} \quad (2.2)$$

These expressions presuppose that the stoichiometry of the complex is 1:1 drug:cyclodextrin, as is most commonly the case [123]. If it is further assumed that  $K_R=K_S$ , the system may be simplified to:



with an equilibrium constant  $K$  such that:

$$K = \frac{[(\text{drug.cyclodextrin})]}{[\text{drug}] \times [\text{cyclodextrin}]} \quad (2.3)$$



Perturbation of the equilibrium by addition of further cyclodextrin will lead to increased formation of complex, such that the ratio of free to complexed drug will be reduced, and where chiral discrimination is present in the NMR spectrum as a result of the differential magnetic environment experienced by each enantiomer within the cyclodextrin cavity, this will be enhanced. Table 2.13 shows the effect on  $^1\text{H}$  drug resonances of increasing the drug: $\beta$ -cyclodextrin mole ratio from 1:1 to 1:3 for flurbiprofen sodium and ibuprofen sodium. Whilst the expected increase in splitting of stereochemically-recognised signals is observed, its size is in all cases small. Similarly, the splitting of the H3"  $^1\text{H}$  resonance of ibuprofen sodium in the presence of DMCD was not found to improve at a 1:5 mole ratio of drug to cyclodextrin, whereas much higher levels of cyclodextrin were found to lead to loss of chiral recognition in the  $^1\text{H}$  NMR spectrum altogether (Section 2.4).

Mole ratio drug: $\beta$ -cyclodextrin	Splitting/ppm			
	Ibuprofen sodium		Flurbiprofen sodium	
	H2'	H3	H3	H2
1:1	0.009	0.005	0.008	0.012
1:3	0.011	0.007	0.009	~0.016

Table 2.13 The effect of mole ratio on the chiral discrimination of 400MHz  $^1\text{H}$  resonances of 0.0056M solutions of ibuprofen sodium and flurbiprofen sodium in the presence of varying mole ratios of  $\beta$ -cyclodextrin in  $\text{D}_2\text{O}$  at 30°C

It was thought that the limited effect of the changes in drug to cyclodextrin mole ratio might be a consequence of extensive binding of the drug to the cyclodextrin, such that increased concentrations of  $\beta$ -cyclodextrin would then not significantly alter the ratio of bound to free drug. In order to further investigate this proposal, changes in  $^1\text{H}$  NMR chemical shift of the drug resonances in each

solution from those in the absence of cyclodextrin were calculated. Table 2.14 shows the results for ibuprofen sodium. The increase in change of chemical shift in the presence of 3 mole equivalents of cyclodextrin over that in the presence of 1 is small, and thus supports the argument above.

Ibuprofen sodium resonance	Change in chemical shift/ppm	
	Mole ratio ibuprofen sodium: $\beta$ -cyclodextrin 1:1	1:3
H2'	-0.011 & -0.020	-0.013 & -0.024
H3'	-0.154	-0.186
H2	obscured	obscured
H1''	-0.017	-0.019
H2''	-0.015	-0.018
H3	+0.010 & +0.005	+0.012 & +0.005
H3''	+0.023	+0.028

Table 2.14 Changes in 400MHz  $^1\text{H}$  chemical shift of resonances of a 0.0055M solution of ibuprofen sodium in the presence of varying mole ratios of  $\beta$ -cyclodextrin in  $\text{D}_2\text{O}$  at  $30^\circ\text{C}$

If it is again assumed that the formation constants for each diastereomeric complex are equal, then the observed drug chemical shift  $\delta d_o$  in each solution will be given by:

$$\delta d_o = (1-f)\delta d_f + f\delta d_c \quad (2.4)$$

where  $\delta d_f$  and  $\delta d_c$  are the drug chemical shift in the free and complexed state respectively, and  $f$  is the mole fraction of the drug in the complex.

Thus,

$$\delta d_o - \delta d_f = f(\delta d_c - \delta d_f) \quad (2.5)$$

so that since  $(\delta d_c - \delta d_f)$  is a constant, the change in drug chemical shift on addition of the cyclodextrin is directly proportional to the mole fraction  $f$  of complex. For two solutions for which the changes in shift are denoted by  $\delta d_1$  and  $\delta d_2$ , then

$$\frac{\delta d_1}{\delta d_2} = \frac{f_1}{f_2} \quad (2.6)$$

where  $f_1$  and  $f_2$  are the mole fractions of complex for each solution.

Analysis of the data in Table 2.14 reveals the following linear relationship between the two data sets,

$$\delta d_1 = 0.828\delta d_2 - 0.000141$$

The constant term in this expression is sufficiently small that it may be neglected, which gives:

$$\delta d_1 = 0.828\delta d_2 \quad (2.7)$$

with correlation coefficient 0.99995, where  $\delta d_1$  and  $\delta d_2$  refer to the 1:1 and 1:3 drug:cyclodextrin solutions respectively.

Comparison of equation (2.7) with equation (2.6) suggests that the assumption required for the derivation of the former is valid for the ibuprofen sodium/ $\beta$ -cyclodextrin system, that is, that chiral recognition occurs as a result of differences in magnetic shielding in each diastereomeric complex, and not from differences in the formation constant for each complex.

Then, for the two ibuprofen sodium/ $\beta$ -cyclodextrin solutions examined here,

$$\frac{f_1}{f_2} = 0.828$$

which allows calculation of the equilibrium constant for complex formation  $K$ , assuming a 1:1 stoichiometry of the ibuprofen sodium: $\beta$ -cyclodextrin complex (which is later demonstrated, Section 4.5) such that:

$$K = 4080 \text{ M}^{-1}$$

A similar analysis of the flurbiprofen sodium/ $\beta$ -cyclodextrin system is precluded by the complexity of the aromatic region of the  $^1\text{H}$  NMR spectrum of flurbiprofen sodium in the presence of the cyclodextrin. Changes in chemical shift of the H3 resonance with different mole ratios of  $\beta$ -cyclodextrin do, however, suggest levels of complexation comparable with those of ibuprofen sodium.

Equilibrium constants for the  $\beta$ -cyclodextrin complexes of ibuprofen and flurbiprofen in aqueous solution have previously been calculated to be  $10800 \text{ M}^{-1}$  and  $4340 \text{ M}^{-1}$  (at  $25^\circ\text{C}$ ) respectively. These values, although of a similar order of magnitude to the equilibrium calculated here, are not, however, strictly comparable with measurements of the salts of the drug.

Increased concentrations of host and guest at fixed mole ratio may also be expected to lead to raised levels of complexed to free drug and enhanced chiral splittings. Table 2.15 shows the effect on the  $^1\text{H}$  resonances of ibuprofen sodium and flurbiprofen sodium of increasing concentrations in the range 5.5-56mM in the presence of a mole equivalent of  $\beta$ -cyclodextrin. The splittings of the H3 and H2' signal of ibuprofen sodium are essentially independent of concentration over the range studied.

Concentration/mM	Chiral splitting/ppm			
	ibuprofen sodium		flurbiprofen sodium	
	H2'	H3	H3	H2
~5.5	0.009	0.005	0.008	0.012
~14	0.009	0.006	0.010	~0.016
~55	0.010	0.006	0.016	0.018

Table 2.15 Effect of concentration on the chiral splitting of 400 MHz  $^1\text{H}$  resonances of ibuprofen sodium and flurbiprofen sodium in the presence of a mole equivalent of  $\beta$ -cyclodextrin in  $\text{D}_2\text{O}$  at  $30^\circ\text{C}$

Our results have already suggested that the mole fraction  $f$  of the  $\beta$ -cyclodextrin complex for ibuprofen sodium will be the same for each enantiomer of the racemate drug. Then the observed chemical shift of the R and S enantiomers, in the presence of cyclodextrin,  $\delta R_o$  and  $\delta S_o$ , will be given by:

$$\delta R_o = (1-f)\delta R_f + f\delta R_c \quad (2.8)$$

$$\delta S_o = (1-f)\delta S_f + f\delta S_c \quad (2.9)$$

where subscripts f and c denote the free and complexed states respectively.

Thus, from equations (2.8) and (2.9), since  $\delta R_f = \delta S_f$

$$\text{chiral splitting} = \delta R_o - \delta S_o = f(\delta R_c - \delta S_c) \quad (2.10)$$

and since  $(\delta R_c - \delta S_c)$  is a constant,

$$\text{chiral splitting} \propto f \quad (2.11)$$

In order therefore to achieve a significant increase in the chiral splitting of a resonance, it is necessary to bring about a corresponding increase in the mole

fraction of the complex. From our calculations above, we determine that approximately 81% of the ibuprofen sodium is complexed in the solution of the lowest concentration examined here. It is therefore not surprising that increased concentrations of solution did not bring about a marked improvement in chiral discrimination, since even in weak solutions recognition is already close to its maximum value.

For the H3 resonance of flurbiprofen sodium a doubling of the chiral splitting following a ten-fold increase in concentration was observed in addition to a large increase of that of the H2 resonance. On the basis of preceding discussions, this increase was unexpectedly large, and was therefore suspected of being a consequence of some change in the complexation process at high concentrations, presumably as a result of molecular association. Interpretation of such differences in behaviour are difficult, however, because of the complexity of the equilibrium process.

### 2.7.2 Effect of Variations in Temperature

Solution temperature can significantly alter the position of the equilibrium processes described above. At temperatures which favour complexation, improved performance of the cyclodextrin as a chiral solvating agent may be anticipated. Thus, MacNicol and Rycroft [125] reported increased prochiral recognition of an aromatic substrate by  $\beta$ -cyclodextrin as the temperature was decreased.

The effect of both high and low temperatures on the duplication of the H3 and H2' resonances of ibuprofen sodium in the presence of a mole equivalent of  $\beta$ -cyclodextrin are shown in Table 2.16. Enhanced chiral splitting at lower temperatures (although necessarily limited by the freezing point of the aqueous solvent) is clearly observed, and is indicative of increased levels of complexation and therefore the exothermicity of the complexation process. Cyclodextrin

complexation is indeed commonly associated with a negative change in enthalpy. The thermodynamics of complexation will be considered in greater detail in Chapters 3 and 4.

Temperature/°C	Chiral splitting/ppm	
	H2'	H3
5	0.011	0.008
30	0.009	0.006
45	0.007	0.005
75	0.005	0.003

Table 2.16 Effect of temperature on the chiral splitting of 400MHz  $^1\text{H}$  resonances of a 0.014M solution of ibuprofen sodium in the presence of a mole equivalent of  $\beta$ -cyclodextrin in  $\text{D}_2\text{O}$

An enhancement of the splitting of the H2 and H3 resonances of a 1:1 mole ratio of flurbiprofen sodium and  $\beta$ -cyclodextrin at reduced temperature is also found (Table 2.17), but is again small.

Temperature/°C	Chiral splitting/ppm	
	H3	H2
5	0.016	0.018
30	0.010	-0.016

Table 2.17 Effect of temperature on the chiral splitting of the 400MHz  $^1\text{H}$  resonances of a 0.014M solution of flurbiprofen sodium in the presence of a mole equivalent of  $\beta$ -cyclodextrin in  $\text{D}_2\text{O}$

### 2.7.3 Effect of Added Salts on Complexation

During the course of their work, MacNicol and Rycroft [125] also observed that chiral discrimination by cyclodextrins may be improved by the presence of inorganic salts such as the chlorides of sodium and lithium. The authors suggest that the salt leads to a type of 'salting out' of the guest into the cyclodextrin cavity and possibly a change in structure of the complex itself. Other studies have also related the importance of ionic species in the complexation process [123].

We investigated the effect of 5M sodium chloride on the splittings of the ibuprofen sodium and flurbiprofen sodium  $\beta$ - cyclodextrin systems.

The ibuprofen sodium spectrum shows a very slight reduction of the splitting of the low-field aromatic doublet (0.008ppm), whilst that of the H3 resonance is lost completely, with some asymmetry of the H3" resonance becoming apparent. This differential effect upon the chiral splittings of the low-field aromatic and H3 resonances suggests that the salt leads to some structural change within the complex.

The H3 resonance of 1:1 flurbiprofen sodium: $\beta$ - cyclodextrin in 5M sodium chloride, in contrast, shows a slight increase in splitting to 0.011ppm compared to that in D<sub>2</sub>O solution, although its cause remains unclear. The H2 resonance is insufficiently resolved from neighbouring cyclodextrin resonances to determine either the presence or extent of chiral duplication under such conditions.

That the presence of salts may give rise to structural changes in the cyclodextrin complex, at least in the case of ibuprofen sodium, renders their use as additives to enhance chiral duplication unpredictable. Their sometimes detrimental effect, observed here for ibuprofen sodium must have important implications regarding the use of cyclodextrins in biological media which contain large amounts of inorganic salts. Thus, such salts must be considered a possible source of the alteration of chiral recognition effects in the urine samples examined previously.



#### 2.7.4 Effect of Variations in Solution pH

pH has been shown to have a significant effect on the formation of inclusion complexes by cyclodextrins. Thus, Uekama *et al.* [128] observed that chiral recognition of the NSAID pirprofen, Figure 2.14, by  $\beta$ -cyclodextrin was increased in acidic as opposed to alkaline solution. The authors suggested that this was a consequence of differential binding modes. In alkaline solution, the carboxylic acid group is deprotonated, and inclusion occurs preferentially at the more hydrophobic pyrroline site. In acidic solution, however, protonation of this pyrroline ring favours inclusion of the phenylpropionic functionality, which, lying closer to the chiral centre, leads to improved chiral discrimination.

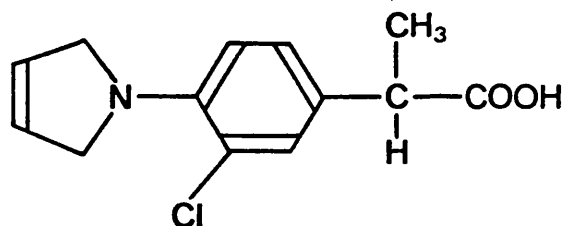


Figure 2.14 Structure of pirprofen [128]

The effect of pH on the chiral recognition by cyclodextrins in the  $^1\text{H}$  NMR spectra of ibuprofen and flurbiprofen were investigated here. We attempted to examine each of the three possible ionisation states of the inclusion complexes, by dissolution of:

1. the free acid NSAID and  $\beta$ -cyclodextrin in  $\text{D}_2\text{O}$ ;
2. the salt of the NSAID and  $\beta$ -cyclodextrin in  $\text{D}_2\text{O}$ ;
3. the salt of the NSAID and  $\beta$ -cyclodextrin in approximately 1M NaOD in  $\text{D}_2\text{O}$ , allowing significant levels of deprotonation of the  $\beta$ -cyclodextrin macrocycle (pKa 12.3 [169]).

Observations for mixtures of salt and cyclodextrin in D<sub>2</sub>O have already been described above. Dissolution of mixtures of the free acid and  $\beta$ -cyclodextrin in D<sub>2</sub>O were not achieved despite agitation for two hours in an ultrasonic bath. This may be a consequence of either a thermodynamic or kinetic phenomenon [123]. Certainly, in the case of flurbiprofen dissolution is limited by the low solubility of the  $\beta$ -cyclodextrin complex [143].

Dissolution of a mole equivalent of ibuprofen sodium and  $\beta$ -cyclodextrin in NaOD/D<sub>2</sub>O leads to a substantial change in the <sup>1</sup>H NMR spectrum of the drug to that observed in D<sub>2</sub>O. Table 2.18 summarises the duplication of drug resonances in both cases.

A reduction in splitting of the H3 and low-field aromatic resonance is accompanied by an increase in that of the H3'' doublet (although this may be a distinction of a prochiral rather than chiral nature, Section 2.3). Additionally, the H2 resonance is now visible and is seen to show chiral duplication. This simultaneous observation of both increases and decreases in signal splitting within the spectrum suggests that the result of raised solution pH is to bring about a change in complex structure.

Ibuprofen sodium resonance	Chiral splitting/ppm	
	D <sub>2</sub> O	Alkaline D <sub>2</sub> O
H2'	0.009	0.005
H2	obscured	0.012
H3	0.006	0.003
H3''	0	0.008

Table 2.18 Chiral splitting of 400MHz resonances of a 0.014M solution of <sup>1</sup>H ibuprofen sodium in the presence of a mole equivalent of  $\beta$ -cyclodextrin in approximately 1M NaOD in D<sub>2</sub>O at 30°C

A mixture of flurbiprofen sodium and  $\beta$ -cyclodextrin failed to dissolve completely in alkaline  $D_2O$  following shaking in an ultrasonic bath for two hours.

#### 2.7.5 Effect of Variations in Solvent

The thermodynamic stability and structure of a cyclodextrin complex will depend greatly on the solvent in which it is dissolved. The formation of complexes is best achieved in aqueous solvents, DMSO or DMF [123]. Since deuterated DMF is very expensive, and because the non-deuterated molecule gives rise to three resonances in its  $^1H$  NMR spectrum which would be difficult to suppress simultaneously to obtain an adequate dynamic range, ibuprofen sodium and flurbiprofen sodium complexes have been investigated only in  $d_6$ -DMSO. The comparison of spectra in deuterated and non-deuterated water has also been made.

##### 1. Deuterated versus Non-deuterated Water

The hydroxylic protons of cyclodextrins are in fast exchange in aqueous solution. In deuterated water, this will mean their replacement by deuterons, which will, for example, lead to differing thermodynamic stability of the complex should the exchangeable hydroxyl groups be involved in the donation of a hydrogen bond to an included drug. Additionally, changes in solvation of the complex may be anticipated.

Table 2.19 summarises the chiral splittings of those resonances in the  $^1H$  NMR spectra of ibuprofen and flurbiprofen sodium which are readily observed to undergo recognition in the presence of a mole equivalent of  $\beta$ -cyclodextrin when dissolved in  $D_2O$  and 60% $H_2O$ /40% $D_2O$ . Suppression of the intense solvent resonance in the latter case was achieved by presaturation. Discrimination in these two solvent systems is essentially equal, indicating that isotope effects are minimal.

Solvent	Chiral splitting/ppm			
	ibuprofen sodium H2'	H3	flurbiprofen sodium H3	H2
60% $\text{H}_2\text{O}$ /40% $\text{D}_2\text{O}$	0.010	0.006	0.010	0.014
$\text{D}_2\text{O}$	0.009	0.006	0.010	-0.016

Table 2.19 Chiral splittings of 400MHz  $^1\text{H}$  resonances of 0.014M solutions of ibuprofen sodium and flurbiprofen sodium in the presence of a mole equivalent of  $\beta$ -cyclodextrin in  $\text{D}_2\text{O}$  and 60% $\text{H}_2\text{O}$ /40% $\text{D}_2\text{O}$  at 30°C

## 2. Studies in $\text{d}_6$ -DMSO

$\beta$ -cyclodextrin dissolves more readily in  $\text{d}_6$ -DMSO than in  $\text{D}_2\text{O}$ , although resonances in its  $^1\text{H}$  NMR spectrum are more difficult to distinguish, particularly where the solvent has absorbed atmospheric water which obscures the H2 and H4 resonances. The spectrum is shown in Figure 2.15, with assignments taken from Yamamoto *et al.* [170] The hydroxyl proton resonances, which were absent from the  $\text{D}_2\text{O}$  spectrum as a result of their facile exchange, are now clearly visible.

Although duplication of the flurbiprofen sodium H3  $^1\text{H}$  resonance in the presence of a mole equivalent of  $\beta$ -cyclodextrin is lost in  $\text{d}_6$ -DMSO, significant splittings of the low field aromatic and isobutyl H2" and H3" groups of ibuprofen sodium are observed, Table 2.20. The H3" resonance must be a consequence of both enantiomer recognition and of prochiral discrimination of the individual methyl groups within each enantiomer, since the signal has a five line structure. As a result, the chiral splitting could not be determined without further peak assignment. The H2  $^1\text{H}$  resonance was obscured by cyclodextrin signals in the case of both ibuprofen sodium and flurbiprofen sodium.

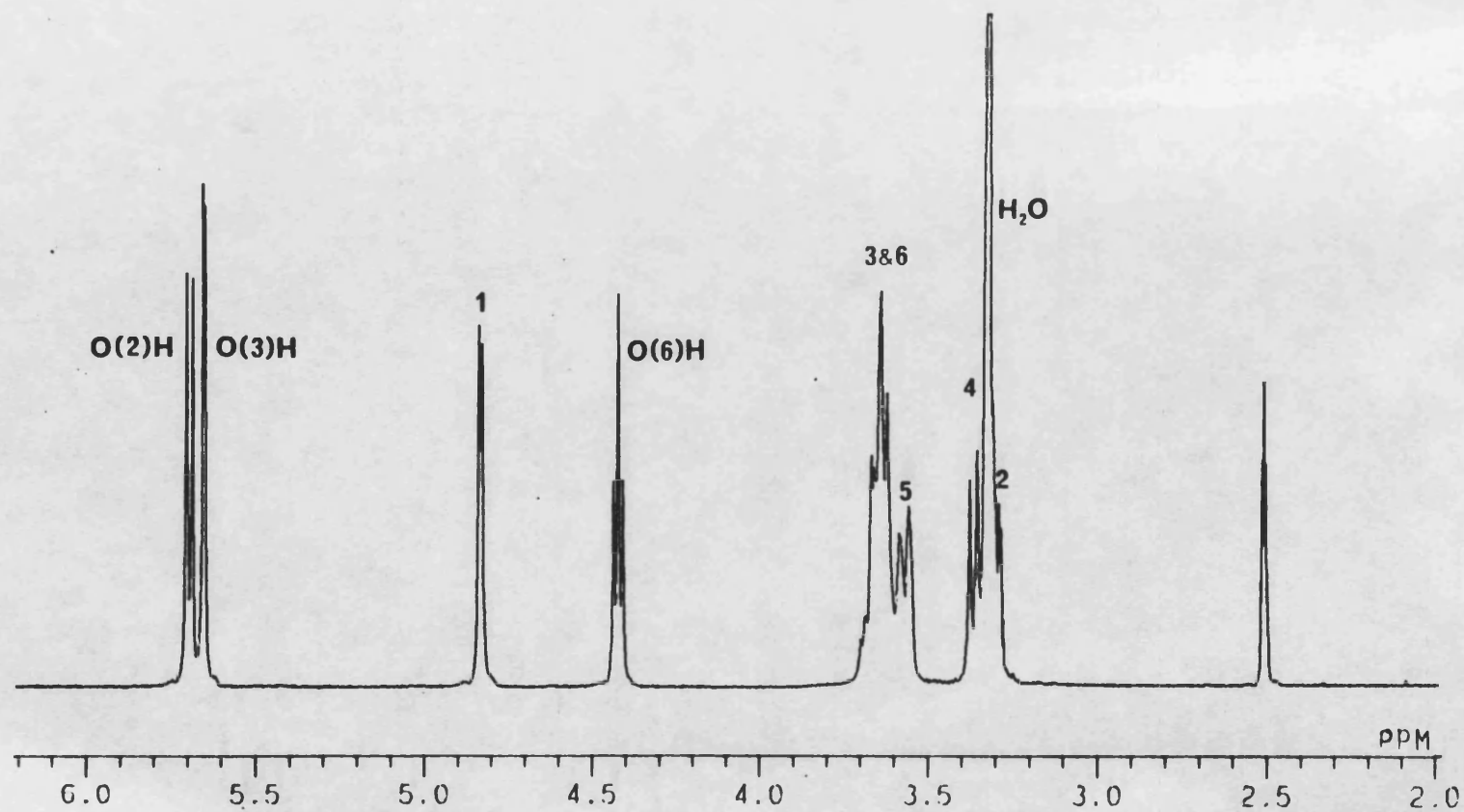


Figure 2.15 400MHz  $^1\text{H}$  spectrum of a 0.014M solution of  $\beta$ -cyclodextrin in  $\text{d}_6$ -DMSO at 30°C

Ibuprofen sodium resonance	Chiral splitting/ppm
H2'	0.005
H2''	0.006
H3''	undetermined (see text)

Table 2.20 Chiral splitting of 400MHz  $^1\text{H}$  resonances of a 0.014M solution of ibuprofen sodium in the presence of a mole equivalent of  $\beta$ -cyclodextrin in  $\text{d}_6$ -DMSO at 30°C

The differences in splitting patterns observed between mixtures of ibuprofen sodium and  $\beta$ -cyclodextrin in  $\text{D}_2\text{O}$  and  $\text{d}_6$ -DMSO suggest that a change of solvent can bring about a significant structural change in the complex formed between the two. For flurbiprofen sodium it is not clear whether loss of chiral duplication is a consequence of such a structural change of the corresponding  $\beta$ -cyclodextrin complex or of its reduced thermodynamic stability. Certainly, shifts in both the resonances of drug and cyclodextrin indicate that some interaction between drug and cyclodextrin remains in DMSO. Further consideration of the structures of the complexes with  $\beta$ -cyclodextrin in DMSO will be given in Chapter 4.

## 2.8 Conclusion

The NMR spectra of the NSAIDs ibuprofen sodium and flurbiprofen sodium were examined in the presence of a range of cyclodextrins in  $\text{D}_2\text{O}$ . The desired chiral recognition was observed for certain combinations of drug and cyclodextrin, but attempts to reproduce these results in biological media were unsuccessful, and studies relating to the enantioselective metabolism of the profens could not, therefore, be pursued.

The effects of experimental variables such as pH, temperature and solvent were examined with a view to enhancing the cyclodextrin discrimination process, but whilst many had a marked effect, none brought about the significant increase desired. Alteration of many of these variables was thought to bring about a structural change of the complex which results from interaction between the drug and cyclodextrin, but the nature of this change was unclear. Further studies were therefore aimed at the gaining of a greater understanding of the structure of the cyclodextrin complex and its response to changes in its environment. It was hoped that these would reduce the degree of empiricism associated with the use of cyclodextrins as agents for chiral recognition, not only in NMR, but in the many other areas in which the chirality of the cyclodextrin is exploited. Chapter 3 discusses properties of the cyclodextrin molecule and its complexes which provide a useful basis for this work.

## CHAPTER 3

### Introduction to Aspects of Cyclodextrin Complexation and NMR Methods for their Examination

#### 3.1 Introduction

In order to gain a greater understanding of the cyclodextrin chiral recognition process, it is appropriate to consider initially in more detail the structural aspects of these compounds. Since  $\beta$ -cyclodextrin is that host used in these studies, this discussion will be restricted to its conformational properties both in the solid state and in solution. The structural forms of the complexes this macrocycle is able to form with other guest molecules will then be considered together with the energetic processes which favour the formation of such complexes. The results of previous structural studies of the complexes of  $\beta$ -cyclodextrin with 2-arylpropionic acids are then discussed in view of their relevance to this work. Factors thought to be of importance in the cyclodextrin chiral recognition process are also reviewed.

The work reported in Chapter 4 has been aimed at further elucidation of the solution structure of the cyclodextrin complexes of the 2-arylpropionic acids, and the possible concomitant chiral recognition, using NMR spectroscopy. A large part of this work centres on the interpretation of chemical shift and changes in its value on complexation. Use has also been made, however, of measurements of the nuclear Overhauser effect, in both the laboratory and rotating frame, and of the longitudinal relaxation time. Aspects of their measurement are therefore reviewed here to clarify the discussions which follow. By way of introduction, however, the practical applications of the cyclodextrin complex, many of which make use of the chirality of the carbohydrate, are first considered to give some perspective to the



importance of the complexation and chiral recognition properties of the cyclodextrins.

### 3.2 Applications of Cyclodextrin Complexation

The ability of cyclodextrins to complex with a wide range of substrates [123], both organic and inorganic, has been exploited in many areas, which may be broadly divided into three categories. These categories may be subdivided into those which make use only of the ability of the cyclodextrin to form complexes, and those which additionally exploit the chirality of the cyclodextrin molecule. Thus, the interaction of the two enantiomers of a compound with the cyclodextrin leads to the formation of two physically and chemically distinct diastereomeric complexes.

#### 3.2.1 Analytical Chemistry

The use of cyclodextrins as chiral solvating agents in the determination of enantiomeric excess by NMR spectroscopy has already been referred to in Chapters 1 and 2. The chiral discriminatory properties of cyclodextrins have also been exploited in the field of chromatography, where they are being increasingly used both as chiral mobile phase additives in HPLC [171] and TLC [172], and as chiral stationary phases in HPLC [173], SFC [174] and GC [175] in the resolution of a range of enantiomeric molecules. The selectivity of binding of cyclodextrins also extends to other isomeric forms, and has, for example, been of use in the HPLC separation of a series of structural isomers [176], which were otherwise difficult to separate on conventional columns because of their similarity.

#### 3.2.2 Preparative Chemistry

Cyclodextrin-based chromatographic methods have allowed not only the determination of the enantiomeric purity of many chiral molecules, but in some

cases have also allowed small scale preparative separation of the two enantiomers to be achieved [177,178]. For preparation of enantiomerically enriched compounds on a larger scale, fractional crystallisation of the two diastereomeric complexes formed between the two optical isomers of a molecule and a cyclodextrin have been used. The method was first introduced by Cramer and Dietsche [179], and is of particular use for those compounds which do not contain a functional group appropriate for the more commonly used method of derivatization to the diastereomeric salt.

Cyclodextrins have also been used in an alternative approach to the preparation of enantiomerically pure species, that is as chiral catalysts in the field of asymmetric synthesis [180,181].

The organic asymmetric catalytic properties of cyclodextrins have also promoted their use as models of biological systems, for example in studies of the action of enzymes. Such applications have recently been reviewed by Dugas [124].  $\alpha$ -cyclodextrin has been proposed as being particularly appropriate for such studies, since it is believed to undergo conformational changes on complexation which parallel those observed on interaction of a substrate molecule with a biological receptor [182]. The validity of this induced fit mechanism of cyclodextrin complexation will be considered in more detail in Section 3.4.4.

### 3.2.3 Pharmaceuticals

The physical and chemical properties of the cyclodextrin complex of a molecule may be markedly different from those of the uncomplexed species. Thus, modification of many undesirable qualities of a drug may be achieved by its formulation as the cyclodextrin complex. Such properties include its solubility, taste, smell and stability. The use of cyclodextrins in the pharmaceutical industry has recently been reviewed by Duchene and Wouessidjewe [183]. Such technology

is equally applicable in related industries including those of cosmetics and food [184,185].

### 3.3 The Structure of The Cyclodextrins

The structure of the cyclodextrins has already been referred to in Chapter 1 (Section 1.5.3). They are generally formed from the degradation of starch by the cyclodextrin glycosyltransferase enzyme isolated from *Bacillus macerans* [186]. The  $\alpha$ ,  $\beta$  and  $\gamma$  oligomers containing 6, 7 and 8 glucose units respectively are formed in greatest yield, although evidence also exists supporting the formation of small amounts of higher oligomers [187]. Indeed, the crystalline structure of the comparatively rare  $\delta$ -cyclodextrin, composed of 9 glucose units, has recently been described [188]. Cyclic structures of smaller size have not been isolated and indeed are thought to be unlikely on steric grounds [189,190]. Many chemical derivatives of these native cyclodextrins have been prepared since their original isolation, in attempts to enhance certain of their properties. Thus, the 2,6-di-O-methyl- $\beta$ -cyclodextrin derivative used in Chapter 2 has a considerably higher aqueous solubility than the underivatized  $\beta$ -cyclodextrin as a result of a reduction of intermolecular interactions and increased amorphicity associated with the impurities in the crude form [183]. The work which follows in Chapter 4, however, concentrates on the complexing properties of  $\beta$ -cyclodextrin, which although considerably less soluble in water than the  $\alpha$  and  $\gamma$  oligomers and the most commonly available derivatives, is also considerably less expensive, and therefore more widely used. Its structure and conformation are now considered.

#### 3.3.1 Solid State Studies of the Structure of $\beta$ -cyclodextrin

$\beta$ -cyclodextrin has been shown to crystallise in two forms from aqueous solution, which may be distinguished by the number of water molecules in the structure, or more easily by comparison of the unit cell parameters of the crystal,

since the former would often seem to be difficult to determine with sufficient accuracy as a result probably of partial occupancies of many of the water sites [191]. The crystal form depends largely on the history of the crystals. Thus, transition of one form (form II) to the other (form I) has been observed to occur over a period of four weeks. Most studies have used the form I crystal [191-196] and it is therefore that which is considered here. The form II crystal differs mainly in the distribution of the disordered water molecules in the  $\beta$ -cyclodextrin cavity [196].

### 1. The Structure of the Glucopyranose Unit

The X-ray diffraction study of the  $\beta$ -cyclodextrin form I crystal [192,193,196] showed that the glucopyranose units were all in the  ${}^4C_1$  chair conformation with essentially similar dimensions. The distance of the C4 and C1 atoms from the C2-C3-C5-O5 plane, Figure 3.1, are however increased and reduced respectively compared to those found for  $\alpha$ -cyclodextrin as a result of the greater radius of the  $\beta$ -cyclodextrin macrocycle.

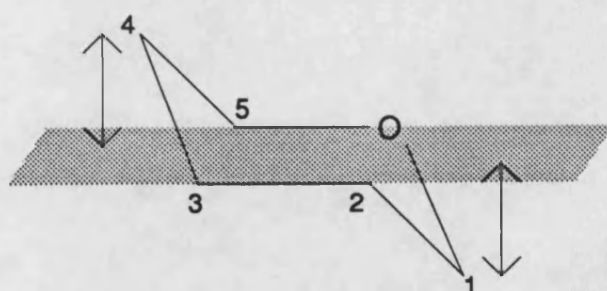


Figure 3.1 The structure of the glucopyranose unit in the  $\beta$ -cyclodextrin crystal: the distances of C1 and C4 from the C2-C3-C5-O5 plane

The greatest differences between the glucopyranose units are observed for the O5-C5-C6-O6 torsion angle. Three staggered conformations about the C5-C6 bond may be envisaged: the *trans*, the (+)gauche and the (-)gauche. These are illustrated in Figure 3.2.

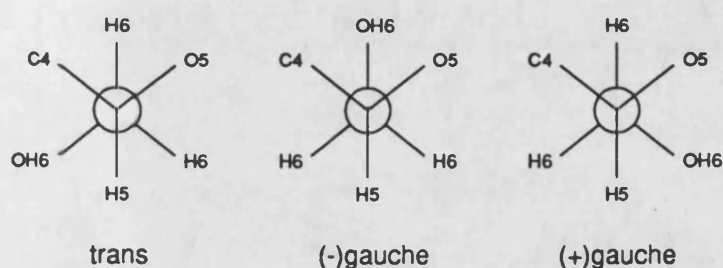


Figure 3.2 Staggered conformations about the C5-C6 bond in cyclodextrins

Of these, the *trans* conformation has never been observed in the crystal structures of the cyclodextrins and their complexes. It has been suggested that this is a consequence of the resulting unfavourable steric interaction between the OH6 group and the adjacent glucopyranose ring and/or of the gauche effect [197]. Of the two gauche conformations, the (-)gauche form which directs the OH6 group away from the cyclodextrin cavity is generally preferred, although the formation of a hydrogen bond between this group and some molecule within the cyclodextrin cavity may lead to orientation in the (+)gauche conformation [197].

In agreement with these observations, in the hydrated  $\beta$ -cyclodextrin crystal four of the seven OH6 groups take up the (-)gauche conformation, two the (+)gauche and one is disordered over the two. In the (+)gauche conformation, the OH6 groups are observed to hydrogen bond with water molecules in the  $\beta$ -

cyclodextrin cavity. The hydrogen bonding pathways will be considered in greater detail below.

## 2. Structure of the Cyclodextrin Macrocycle

The O4 atoms of each glucopyranose unit lie in a regular heptagonal arrangement with the angle between the plane of the O4-C6-O4' atoms and that of the O4 heptagon lying in the range 82.9°-120.6°. As a result, the structure of the macrocycle may be described as open, circular but slightly conical, with the secondary hydroxyls lining the slightly wider rim of the cyclodextrin cavity. Lindner and Saenger [193] give the width of the annular aperture of this cavity as 6.2Å.

The conformation of the macrocycle is stabilised by a ring of hydrogen bonds between the O2 and O3 atoms of neighbouring glucopyranose units, although it was not possible from the X-ray study to assign the directional sense of these, since the position of the hydrogen atoms could not be located. Similarly, 6.5 water molecules were found to be highly disordered over 8 sites within the cyclodextrin cavity, but the hydrogen atoms associated with these again could not be found.

## 3. Structure of the Hydrogen Bonding Network

Most of the information regarding the hydrogen bonding network within the  $\beta$ -cyclodextrin crystal has been gained by neutron diffraction studies at both room [191] and reduced [194] temperature of a sample exchanged with, and crystallised from, D<sub>2</sub>O. These studies show the hydrogen bonding scheme to be highly complex with circular arrangements and extended hydrogen bond chains being observed. Of most interest, however, are the interglucose hydrogen bonds which have already been suggested as a source of stabilisation for the cyclodextrin

structure. DSC and low temperature (120K) neutron diffraction studies [194] show these to be dynamically (as opposed to statistically) disordered flip-flop bonds which concertedly interchange at room temperature as shown in Figure 3.3.

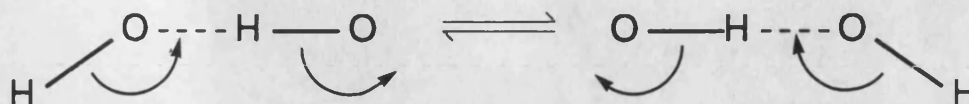


Figure 3.3 The concerted interchange of hydrogen bonding networks within the  $\beta$ -cyclodextrin crystal

At low temperature, the flip-flop nature of these bonds disappears, although bonding between the O2 atom on glucopyranose ring 4 and O3 on ring 5 remains disordered. Additionally, these bonds have been shown to be bifurcated with a weak binding to the inter-residue glycosyl O4 atom, which represents a rare example of the acceptance of a hydrogen bond by a glycosidic oxygen.

### 3.3.2 The Structure of $\beta$ -Cyclodextrin in Solution

Amongst many other techniques, NMR spectroscopy has been used to study the structure of  $\beta$ -cyclodextrin in solution and its relationship to that in the solid state.

#### 1. Structure of the Glucopyranose Ring

The  $^1\text{H}$  NMR spectrum of  $\beta$ -cyclodextrin in  $\text{D}_2\text{O}$  shows a single set of signals for all seven glucopyranose units of the structure, which indicates that on the NMR time-scale each of these units is equivalent. Thus, the three-bond  $^1\text{H}$  coupling constants  $J_{1,2}$ ,  $J_{2,3}$ ,  $J_{3,4}$  and  $J_{4,5}$  for  $\beta$ -cyclodextrin have been determined,

and have been found to be consistent with a  ${}^4C_1$  chair conformation of each of the glucopyranose rings [198]. Additionally, measurement of  ${}^{13}\text{C}$  longitudinal relaxation times for the  $\beta$ -cyclodextrin molecule, and interpretation of these in terms of its motion indicate rapid internal rotation about the C5-C6 bond in solution, so that, in contrast to the solid state structure, no marked conformational preference is exhibited [199].

## 2. Structure of the Macrocycle

Lipkind *et al.* [200] used nOe measurements following pre-irradiation of the glycosidic protons and three-bond carbon-proton coupling constants near the glycosidic linkage, in conjunction with theoretical calculations to determine torsional angles for  $\beta$ -cyclodextrin in  $\text{D}_2\text{O}$  which describe the relative orientation of glucopyranose rings within the macrocycle. These compare favourably with equivalent angles found in the solid state [193], and indicate that on average the conformation of the  $\beta$ -cyclodextrin macrocycle in solution is comparable with that in the crystal. Measurements of  ${}^3J_{\text{CH}}$  for  $\beta$ -cyclodextrin have also been made by Mulloy *et al.* [201] in their work relating such coupling constants to the dihedral angle between two sugar units.

## 3. Structure of the Hydrogen Bonding Network

Onda *et al.* [202] have studied the intramolecular hydrogen bonding interactions of cyclodextrins in  $\text{d}_6\text{-DMSO}$  by  ${}^1\text{H}$  NMR. They observed that the resonances of the secondary hydroxyl groups of  $\beta$ -cyclodextrin were down-field of that of the primary hydroxyls and of all OH resonances of methyl  $\alpha$ -D-glucoside, Figure 3.4, and concluded that this must be a consequence of formation of intramolecular hydrogen bonds in the macrocycle. This conclusion was supported by the temperature dependence of these resonances, which further



indicated that the bonds were predominantly a consequence of donation from the OH3 proton to the OH2 group of the neighbouring residue.

Determination of orientation of the secondary hydroxyl groups from a Karplus type relationship equating  $^3J_{\text{HO}(2,3)\text{CH}}$  to the dihedral angle across the HO-CH bond were in agreement with this proposal. The results of this study, which are considered in more detail in Chapter 4, Section 4.6.3, support earlier work on the analysis of  $^3J_{\text{HOCH}}$  [203] and the effect of  $^2\text{H}$  substitution on  $^1\text{H}$  and  $^{13}\text{C}$  chemical shifts [204] in  $\beta$ -cyclodextrin.

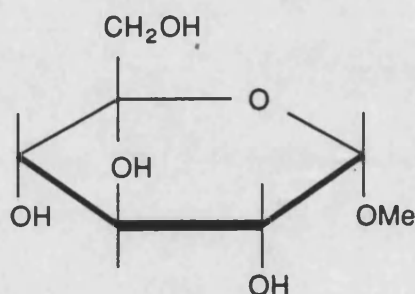


Figure 3.4 Structure of methyl  $\alpha$ -D-glucoside

It is therefore concluded that whilst the main structural form of the  $\beta$ -cyclodextrin macrocycle remains relatively unperturbed on dissolution, the introduction of free rotation about the C5-C6 bond and the change in directional preferences of the hydrogen bonding network of the secondary hydroxyl functions indicate significant differences between the solid and solution state.

### 3.4 Thermodynamics of Cyclodextrin Complexation

#### 3.4.1 The Structural Types of Cyclodextrin Complexes

Cyclodextrin complexes may be broadly divided into three structural types, illustrated in Figure 3.5, and termed axial, equatorial or lid-type complexes

depending on the orientation of the longer molecular axis of the guest to that of the cyclodextrin cavity [205]. In some cases it has been shown that complex type depends on the choice of solvent [206-209]. The axial complex is that most commonly observed, particularly for *para*-substituted benzenes, whilst the lid-type complex has been observed only for a limited number of substrates [205-211], and rarely in aqueous solution.

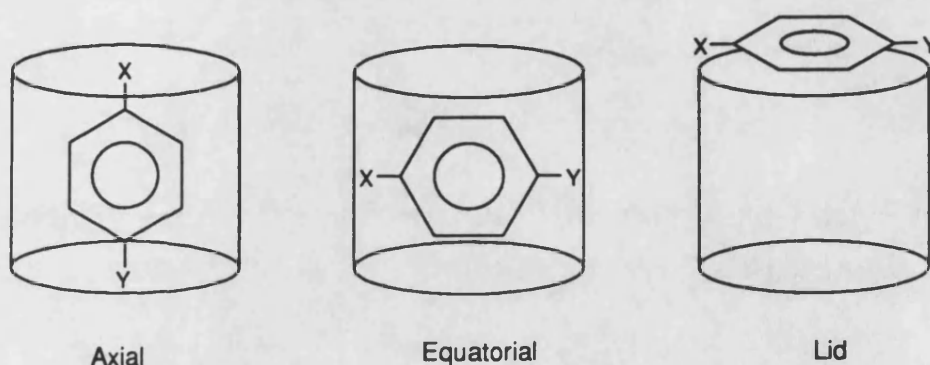


Figure 3.5 Structural types of cyclodextrin complexes, illustrated schematically for a *p*-substituted aromatic substrate

Most studies which have addressed the solution thermodynamics of cyclodextrin complexation have been concerned with complexes of the axial and equatorial types, which may be collectively termed inclusion complexes, as a result of the penetration of the cyclodextrin cavity by the substrate. The results of such studies are briefly reviewed here because of their importance in understanding the complexation process.

The solution thermodynamics of cyclodextrin complexation, generally studied in aqueous solution, have recently been reviewed by Clarke *et al.* [186].

The process is usually associated with a favourable negative enthalpy (0 to -10 kcal/mol) and a negative entropy (0 to -20 cal/(mol.deg)), although positive entropies of complexation are also known. Several physical processes have been proposed as contributing to these observations, although the relative importance of each of these necessarily depends on the nature of the particular substrate and the choice of cyclodextrin.

#### 3.4.2 The Contribution of Hydrophobic Interactions to the Cyclodextrin Complexation Process

The hydrophobic effect [212], which has been shown to have important consequences regarding the structure of biological macromolecules, describes the tendency to association of apolar species dissolved in an aqueous solution. Dissolution of an apolar molecule in water leads to a highly ordered solvent envelope with increased hydrogen bonding around the solute molecule. This process is characterised by a negative enthalpy and a very large negative change in entropy, and is thus energetically disfavoured. This unfavourability may be reduced by association of the apolar molecules which reduces contact between solute and solvent.

The hydrophobicity of the cyclodextrin cavity is comparable with that of the octanol molecule [213]. Thus, interaction of the cyclodextrin with an apolar substrate might reasonably be expected to be influenced by the hydrophobic effect, and indeed many complexes are found to be weaker in non-aqueous solvents where the degree of such hydrophobic interactions will be less [186]. Hydrophobicity alone cannot, however, be the driving force of the cyclodextrin complexation process, since such interactions are generally associated with a very favourable change of entropy [214], in contrast to that usually observed for cyclodextrin complexation [186].

### 3.4.3 The Contribution of Van der Waals Interactions to the Cyclodextrin Complexation Process

Van Etten *et al.* [215] have reported an approximately linear relationship between the logarithm of the dissociation constants for a series of cyclodextrin complexes and the molar refraction of the substrate, a measure of its polarisability. This observation indicates the importance of permanent dipole-induced dipole interactions and London dispersion forces in determining complex stability. Additionally, X-ray crystallographic studies have revealed interatomic distances between guest and cyclodextrin which are consistent with the occurrence of Van der Waals interactions [186].

Recently, the dipole moments of a range of cyclodextrins have been calculated and been found to be of a significant size [216,217]. They are the result of contributions from the individual glucopyranose residues, and are generally directed from the secondary to the primary hydroxyl end of the cyclodextrin molecule, although asymmetry of the structure may cause some deviation from the cavity axis. Whilst the contribution of these dipole moments to stabilisation of a cyclodextrin complex will depend largely on the polarity and polarisability of the guest substrate, it has also been suggested that for substrates with significant polarity the dipole moment of the cyclodextrin dictates the orientation of the guest within the cavity. Thus, guests with large dipoles align preferentially with their dipole moment anti-parallel to that of the cyclodextrin.

### 3.4.4 The Contribution of Conformational Changes to the Cyclodextrin Complexation Process

Saenger and co-workers [182,218-222] have examined each of the three crystalline forms of  $\alpha$ -cyclodextrin obtained from aqueous solution by X-ray crystallography, and have found that both forms I [218-220] and II [221,222]

display significant asymmetry of the macrocycle with one of the glucopyranose rings rotated to lie more nearly normal to the axis of the cyclodextrin, which thus disrupts inter-residue hydrogen bonding between the OH2 and OH3 hydroxyls. This strained conformation is not found in the crystalline inclusion complexes of  $\alpha$ -cyclodextrin, and it has therefore been proposed that this apparent relaxation of conformation on complexation (so-called induced fit) might provide an important favourable contribution to the stabilisation of the cyclodextrin complex. The form III  $\alpha$ -cyclodextrin structure, which is more symmetrical and can only be formed in the presence of barium chloride, is considered as representative of the transition state of this change [182].

Whilst other experimental techniques, reviewed by Clarke *et al.* [186], have similarly suggested changes in conformation of the  $\alpha$ -cyclodextrin molecule on formation of an inclusion complex,  $^{13}\text{C}$  CPMAS NMR studies of Gidley and Bociek [223,224] in this area are particularly elegant. These authors were able to identify resonances associated with the C1 and C4 atoms of the rotated glucopyranose ring of the  $\alpha$ -cyclodextrin molecule in the solid state [223]. They found that these resonances were, however, absent from a frozen aqueous solution of  $\alpha$ -cyclodextrin [224], which suggests that the strained conformation of the  $\alpha$ -cyclodextrin macrocycle observed in crystalline samples does not contribute significantly to that present in solution. Additionally, the theoretical calculations of Tabushi *et al.* [225] indicate that rather than promoting complex stability, the conformational change of  $\alpha$ -cyclodextrin on complexation is associated with a slight increase in energy of approximately 4 kcal/mol. Thus, the existence and significance of changes in conformation of the  $\alpha$ -cyclodextrin macrocycle upon substrate inclusion remain unclear.

In contrast, X-ray crystallographic studies of hydrated  $\beta$ - and  $\gamma$ -cyclodextrin show structures which are more symmetrical than that of  $\alpha$ -

cyclodextrin forms I and II, such that conformational changes on complexation for these oligomers are minimal [226].

#### 3.4.5 The Contribution of Activated Cavity Water to the Cyclodextrin Complexation Process

The enthalpy and entropy changes associated with the formation of cyclodextrin complexes with a wide range of cyclodextrin hosts have been shown to be linearly related by a compensation temperature  $T_c$  [186]. This relationship implies a common mechanism of formation, which some have suggested is a consequence of solvent effects [186]. Others have, however, proposed that this observation may be a result of the predominance of dipolar interaction between host and guest [227] or of changes in the structure of the cyclodextrin [228]. Certainly changes of solvation of both guest and host must be anticipated since the generally tight fit of the substrate in the cyclodextrin, as judged from crystal structure determinations and molecular models, necessarily restricts the number of molecules of water of solvation surrounding the substrate in the complex [186].

It has been suggested by Griffiths and Bender [229] that those water molecules which solvate the hydrophobic cyclodextrin cavity are unable to realise their full hydrogen bonding potential, and as such may be regarded as enthalpy rich. The expulsion of such high energy water on complexation of the cyclodextrin cavity may thus contribute to the favourable enthalpic process associated with inclusion. This proposal has been supported by the calculations of Tabushi *et al.* [225].

#### 3.4.6 The Contribution of Hydrogen Bonds to the Cyclodextrin Complexation Process

The hydroxyl groups of the cyclodextrin molecule provide an ideal site for hydrogen bonding interactions with a suitable substrate, and indeed the formation

of such bonds have been observed in the X-ray crystallographic studies of crystalline complexes (see for example Section 3.5) and have been proposed to exist in solution [230]. That many stable complexes are formed with substrates incapable of either donating or accepting such a hydrogen bond suggests, however, that hydrogen bonding does not provide an important contribution to complex stability. A recent study by Buvári and Barcza [230] with  $\beta$ -cyclodextrin and a wide range of substrates in aqueous solution similarly concluded that although hydrogen bonding interactions between host and guest certainly enhance the stability of the complex, their rôle is not dominant.

### 3.5 X-ray Crystallographic Studies of the Structures of Complexes of some 2-Arylpropionic Acids with $\beta$ -cyclodextrin

The Cambridge Crystallographic Database [231] currently lists five X-ray crystallographic studies of the inclusion complexes formed between  $\beta$ -cyclodextrin and 2-arylpropionic acids. These complexes are of the individual enantiomers and the racemate of the NSAIDs flurbiprofen [232-234] and fenoprofen [235,236], whose structures are represented in Figure 3.6.

The results of these studies are briefly reviewed here for the insight they allow us to the possible solution state structures of these complexes, and indeed for some sense of relative steric proportions of the guest and host molecules used in this work.

#### 3.5.1 The $\beta$ -cyclodextrin Complexes of Fenoprofen

Crystals prepared from an aqueous mixture of racemic fenoprofen and  $\beta$ -cyclodextrin show a 3:1 occupancy ratio of (S)- to (R)-fenoprofen. Hamilton and Chen [236] suggest that this chiral recognition is a reflection of the preferential binding of the S enantiomer by the macrocycle. Structurally, the (S)- and (R)-fenoprofen complexes in the racemate crystal are the same as those observed in

crystalline complexes of the individual enantiomers [235], except for small differences in the (R)- fenoprofen complex, which may be attributed to additional packing requirements in the presence of the (S)-fenoprofen complex.

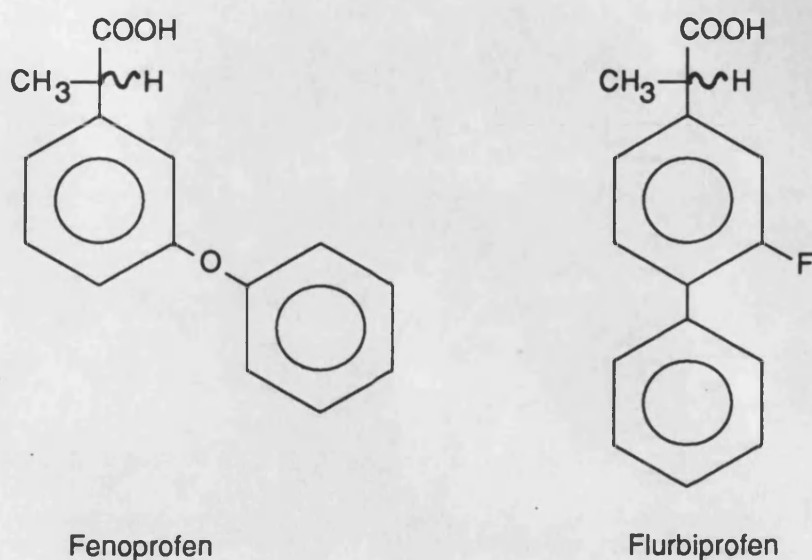


Figure 3.6 Structures of flurbiprofen and fenoprofen

The S and R enantiomers in the racemate complex crystallise in separate dimeric units. Both consist of two  $\beta$ -cyclodextrin units with their secondary hydroxyl faces joined by extensive intermolecular hydrogen bonding between the OH3 groups. A single fenoprofen molecule is included by each of the cyclodextrin macrocycles in the manner shown in Figure 3.7.

There is a fundamental difference between the two complex structures: the (R)-fenoprofen complex is described as head-to-head, with the phenoxy substituents of each molecule lying adjacent, whereas that of the S enantiomer is head-to-tail, with the phenoxy group of one molecule close to the propionic substituent of the other. This difference is attributed by Hamilton and Chen [235] to three basic interactions:-

1. the fit of the guest in the cyclodextrin cavity;



2. the relative strengths of phenyl/phenyl and phenyl/methyl hydrophobic forces in the centre of the  $\beta$ -cyclodextrin dimer;
3. the hydration requirements of the carboxylic acid group.

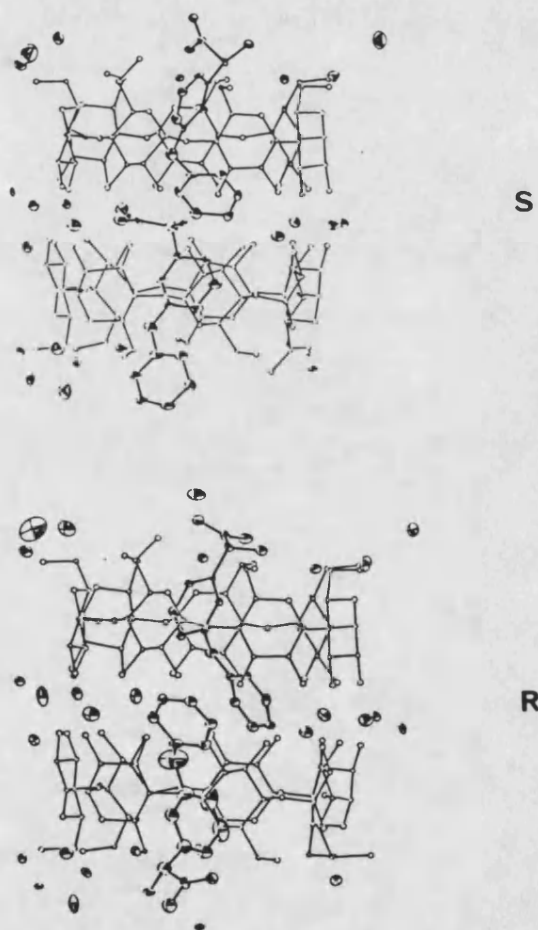


Figure 3.7 Dimeric structure of the (S)-fenopropfen and (R)-fenopropfen complexes of  $\beta$ -cyclodextrin in a crystal prepared from the racemate [235]

As a result of the different stereochemical orientations of the carboxylic acid group in each fenoprofen enantiomer, and steric restrictions imposed by the bulky aromatic ring system, it is not possible for each optical isomer to achieve the same hydrogen bonding interactions in the complex. Thus, the carboxylic acid groupings of the R enantiomers are restricted to hydrogen bonding with waters of crystallisation, whereas one of the S enantiomers hydrogen bonds to the primary hydroxyl group of a neighbouring  $\beta$ -cyclodextrin molecule, whilst the other hydrogen bonds to secondary hydroxyl groups at the  $\beta$ -cyclodextrin dimer interface. In this way, Armstrong's criteria for chiral recognition [236] (which were formulated for use in chromatographic analysis with cyclodextrins, Section 3.6.1) are satisfied.

### 3.5.2 The $\beta$ -cyclodextrin Complexes of Flurbiprofen

X-ray crystallographic studies of hydrated flurbiprofen  $\beta$ -cyclodextrin complexes have been reported for both the (S)- flurbiprofen enantiomer [233,234] and the racemate [232,234]. Crystals precipitated from an aqueous solution of  $\beta$ -cyclodextrin saturated with racemic flurbiprofen show no preference for inclusion of either flurbiprofen enantiomer. As for the fenoprofen  $\beta$ -cyclodextrin crystal, the structure of the complex is dimeric with extensive intermolecular hydrogen bonding joining the secondary hydroxyl faces of two cyclodextrin molecules in each unit. Again, the glucopyranose rings maintain a  ${}^4C_1$  chair conformation and inter-residue hydrogen bonding gives a round regular structure to each macrocycle. One  $\beta$ -cyclodextrin molecule includes a flurbiprofen molecule of S stereochemistry and the other one of R. The orientation of these flurbiprofen molecules within these macrocycles is such that the fluorobenzene ring lies at the centre of the cyclodextrin cavity so that the two phenyl rings are directed toward the dimer interface, are partially inserted in the adjacent cyclodextrin molecule, and possibly interact via a hydrophobic interaction. The steric restrictions of the

cyclodextrin cavity are thought to be responsible for the reduction in the angle between the planes of the two aromatic rings from that of  $54.4^\circ$  in the uncomplexed state to  $34.8^\circ$  and  $37.4^\circ$  for the S and R enantiomers in the complexed state respectively. Close contact between the fluoro- substituent and the glycosidic oxygen also suggest that van der Waals interactions may contribute to complex stability.

Hydrogen bonding interactions in the complex are such that the carboxylic acid group of the R enantiomer hydrogen bonds with a primary hydroxyl group of an adjacent cyclodextrin molecule, whereas the S enantiomer forms two such bonds to cyclodextrin primary hydroxyl groups and additionally bonds to a water molecule. The absence of hydrogen bonds between the carboxylic acid group and the cyclodextrin secondary hydroxyl has been suggested as the reason for the failure to observe chiral separation of the two enantiomers in the formation of the crystal. In comparison with the fenoprofen  $\beta$ -cyclodextrin complex, Hamilton and Chen [236] believe that the reduced flexibility of the flurbiprofen biphenyl system compared to that of the *meta* phenoxyphenyl of fenoprofen gives rise to this difference in behaviour. Despite this lack of chiral separation of the flurbiprofen optical isomers, some element of chiral discrimination must be present, however, to ensure that the dimeric structure includes a single molecule of each enantiomer.

The geometry of the racemate complex is generally similar to that observed for the (S)-flurbiprofen complex, except for slight differences in orientation of the cyclodextrin primary hydroxyl groups and the distribution of waters of crystallisation. Differences in hydrogen bonding interactions of the carboxylic acid group shown in Figure 3.8 may be understood in terms of the change in orientation of the functionality on replacement of the R enantiomer in the racemate by the S, which disfavors the formation of the hydrogen bond to the cyclodextrin primary hydroxyl.

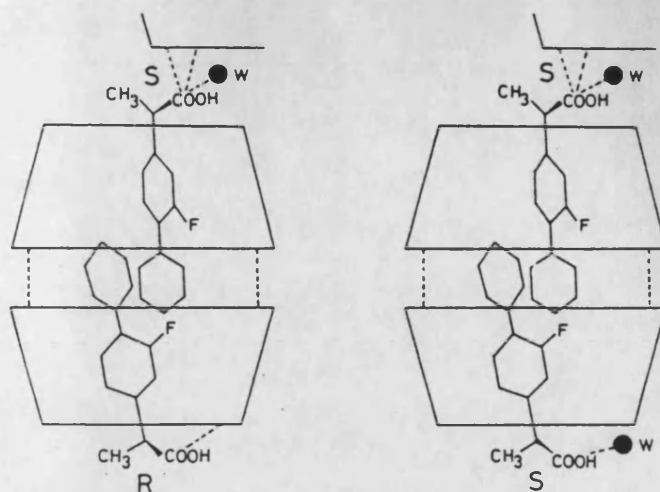


Figure 3.8 Schematic representation of the differences in hydrogen bonding of the carboxylic acid group of flurbiprofen in the  $\beta$ -cyclodextrin complexes of the racemate and the *S* enantiomer [234]

### 3.6 Chiral Discrimination by Cyclodextrins

The ability of a cyclodextrin molecule to recognise the two enantiomers of a chiral substrate in any given process depends upon some difference in structural or physical properties of the two diastereomeric complexes thus formed. Since many processes which make use of the chirality of cyclodextrins often exploit differences in different physical properties, it is difficult to generalise about which substrates and cyclodextrins are best suited to these methods.

### 3.6.1 Chiral Discrimination In Chromatographic Analysis

The extensive studies by Armstrong and co-workers [173,237] directed towards the use of cyclodextrins as chiral stationary phases in HPLC have allowed the deduction of the following empirical rules for those chiral substrates which are most likely to be resolved:-

1. The substrate should include into the cyclodextrin macrocycle;
2. The complex so-formed should be tight, promoting increased binding and restricted rotation of the guest;
3. The chiral centre of the guest, or substituents off it, should lie near to the mouth of the cyclodextrin and interact with it, either sterically or through hydrogen bond formation. Interactions with the uni-directional secondary hydroxyl group hydrogen bonding network of the cyclodextrin are thought to be particularly important;
4. Guests generally have a rigid  $\pi$  system  $\alpha$  or  $\beta$  to the chiral centre, groups off of the chiral centre which are capable of hydrogen bonding, and a second  $\pi$  system or amino group, which perhaps restricts the possible conformations of the guest.

These rules relate to use of the column in the reverse phase mode, and will be a reflection of the difference in distribution of the two enantiomers between the stationary and mobile phase. Stationary phases which have been derived for use in normal phase HPLC have been prepared by derivatization of the cyclodextrin chiral stationary phase with aromatic isocyanates or acid chlorides to give the carbamate and ester derivatives respectively [237]. As such, interaction with chiral analytes is thought to occur predominantly at the  $\pi$  bonding sites of these derivatives, as in a Pirkle-type stationary phase [238], and are therefore not considered further here.

Derivatized cyclodextrins are also used as chiral GC stationary phases, and are preferred to the crystalline native forms as a result of their higher

chromatographic efficiency [237]. This is a consequence of their composition; the complex mixture of isomers and varying degrees of substitution gives rise to highly viscous liquids which are more amenable to use as GC stationary phase coatings. The work of Armstrong *et al.* [239] has suggested that the penetration of the guest into the cyclodextrin cavity is not as deep as that in solution. Resolution is, however achieved because of a lack of competing solvent effects. König *et al.* [240] have also observed that whilst inclusion may have a similar importance to that proposed in liquid chromatography, some of the chiral compounds which these authors were able to resolve appeared to be too large for inclusion to occur. They also noted that whilst hydrogen bonding interactions may be present for some GC chiral stationary phases, enantioselectivity is also possible for analytes which do not contain functional groups capable of hydrogen bonding. Cyclodextrin chiral stationary phases in GC, including their possible mechanism of resolution, have recently been reviewed by Schurig and Nowotny [175].

Enantiomeric resolution in reversed phase liquid chromatography using cyclodextrins as a mobile phase additive has recently been discussed by Sibilska and Zukowski [171]. They identify three interactions which may contribute to the method:-

1. differences in stability of the cyclodextrin/analyte complex
2. differences in adsorption of these diastereomeric complexes on the achiral stationary phase;
3. differences in adsorption of the analyte on a dynamically generated cyclodextrin stationary phase.

These authors conclude that whilst practical applications of the method are being increasingly reported, understanding of the relative importance of each of these mechanisms, together with suitable properties of the analyte, have yet to be determined.

### 3.6.2 Cyclodextrins as Chiral Solvating agents in NMR

The cyclodextrins are being increasingly used as CSAs for the determination of enantiomeric excess by NMR spectroscopy. Most studies have, however, been concerned only with practical applications of the method, with little consideration given to understanding of the cyclodextrin chiral recognition process. It is possible, however, to deduce several empirical rules, some of which have already been exploited in Chapter 2.

1. Many reports of the use of cyclodextrins as CSAs have also noted significant shifts of the cyclodextrin H3 and H5  $^1\text{H}$  resonances which line the macromolecular cavity [126,127,130,137,138], indicative of the occurrence of inclusion complexation. This is perhaps a somewhat unsurprising observation since chiral recognition necessarily requires some interaction between the analyte and the cyclodextrin, and that cyclodextrin complexation usually involves the formation of an inclusion complex has already been referred to above (Section 3.4.1). It would, however, seem reasonable to assume that any factors which favour the inclusion process, such as the use of aqueous as opposed to organic solvent [186] and the manipulation of parameters such as those investigated in Chapter 2, would promote chiral recognition.

2. Several authors have reported that chiral recognition of the substrate by the cyclodextrin is the consequence of a difference in structure and not stability of the resulting diastereomeric complexes [128,129]. There is as yet, however, insufficient data in the literature to confirm this as a general rule.

3. Murakami *et al.* [130] were able to observe enhanced chiral recognition in the  $^1\text{H}$  NMR spectra of mandelic acid, methyl mandelate and N-acetyl- $\alpha$ -phenylglycine in the presence of 3-acetylamino-3-deoxy- $\beta$ -cyclodextrin in comparison to that in the presence of the primary substituted derivative and native

$\beta$ -cyclodextrin. This observation was attributed to an inversion of configuration of C2 and C3 of one of the sugar residues. Although the use of derivatized cyclodextrins as CSAs has been limited, probably because of difficulties associated with their preparation, we believe that they will find increasing use in this field. Thus, studies have also suggested that derivatized cyclodextrins tend to enhance structural differences of diastereomeric inclusion complexes as a result of their increased asymmetry [165,166].

Determination of specific interactions such as hydrogen bonding within the substrate/cyclodextrin complex and their significance in the NMR chiral discrimination process in the solution state remains relatively unexplored.

### 3.6.3 Chiral Discrimination in Fractional Crystallisation

Factors governing the resolution of a chiral substrate by cyclodextrins depend largely on experimental method. Thus, Drabowicz *et al.* [241] reported resolution of sulphurous acid derivatives prepared by grinding the cyclodextrin and analyte in the solid state, followed by washing with ether and decomposition in a mixture of methylene chloride and water. The success of such a process must be a consequence of the differential formation of each of the diastereomeric analyte/cyclodextrin complexes.

More commonly a classical fractional crystallisation method is used, whereby complexation is achieved in solution and the inclusion complex subsequently allowed to crystallise. Thus, this method may additionally incorporate differences in solubility of the two cyclodextrin complexes. Despite this, Michon and Rassat [242] were able to associate the preferential precipitation of (+)-fenchone/ $\beta$ -cyclodextrin from a mixed aqueous/DMSO solvent system with the greater formation constant of the (+)- versus (-)-fenchone  $\beta$ -cyclodextrin complex. Mikolajczyk and Drabowicz [243] were further able to interpret their data relating to the resolution of chiral benzyl-, phenyl- or *p*-tolyl-alkyl



sulphoxides using  $\beta$ - cyclodextrin in terms of a model involving inclusion of the aromatic ring in the cyclodextrin cavity, a hydrogen bond interaction between a cyclodextrin hydroxyl functionality and the sulphoxide oxygen and a steric interaction between the alkyl substituent and the rim of the cyclodextrin molecule.

### 3.7 NMR Methods

That the use of cyclodextrins as CSAs in NMR spectroscopy remains largely empirical prompted us to further examine the chiral recognition properties of the cyclodextrins in solution using NMR spectroscopy (Chapter 4). We describe here some of the less commonly used NMR methods which form part of this work.

#### 3.7.1 Measurement of Longitudinal Relaxation Times

Studies of the rates of relaxation of a nuclear spin system can yield useful information regarding the dynamics of a molecule in the solution state. Measurement of the transverse relaxation time  $T_2$  requires use of a spin-echo sequence such as that of Carr, Purcell, Meiboom and Gill (CPMG) [81,82] in order to eliminate the adverse effects of magnetic field inhomogeneities, diffusion and inaccuracies in pulse widths. Even so, measurements of  $T_2$  remain difficult, particularly in samples where homonuclear J coupling provides an additional complication [244]. We concentrate here, therefore, on the more routine determination of longitudinal relaxation time  $T_1$ . Recent methods designed to reduce the time required to measure NMR relaxation parameters are described.

It is generally assumed that longitudinal relaxation is a first-order process, characterised by a longitudinal relaxation time  $T_1$  such that:-

$$\frac{dM_z}{dt} = \frac{M_0 - M_z}{T_1} \quad (3.1)$$

where  $M_0$  is the equilibrium longitudinal magnetisation and  $M_z$  is the longitudinal magnetisation at some time  $t$  following application of a radio-frequency pulse to

the nuclear spin system. This expression forms the basis of experimental methods for the determination of  $T_1$ .

### 3.7.1.1 The Inversion-Recovery Experiment

The inversion-recovery experiment [245] is the classical sequence for the measurement of longitudinal relaxation time. It requires the use of the sequence shown in Figure 3.9.

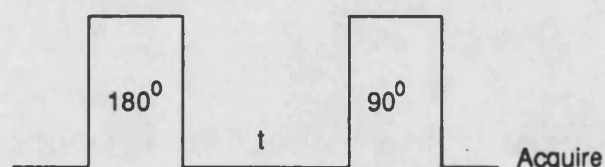


Figure 3.9 The inversion-recovery sequence for the measurement of longitudinal relaxation times

A number of data sets with differing  $t$  are acquired. The initial  $180^\circ$  pulse inverts the equilibrium magnetisation  $M_0$ , which from equation 3.1 relaxes back to a value  $M_z$  in time  $t$  such that:-

$$\ln(M_0 - M_z) = \ln 2M_0 - \frac{t}{T_1} \quad (3.2)$$

$M_z$  is then read by the application of a  $90^\circ$  pulse and subsequently allowed to relax to equilibrium during the pulse delay which must therefore be of the order of  $5T_1$ .  $M_0$  corresponds to  $M_z$  for  $t > 5T_1$ , and its measurement allows a semi-logarithmic plot of  $\ln(M_0 - M_z)$ , or in practice,  $\ln(I_0 - I_z)$ , where  $I_0$  and  $I_z$  are the measured peak intensities corresponding to  $M_0$  and  $M_z$ , against  $t$  to be made, from

which  $T_1$  may be found. Alternatively, an approximation to its value can be readily determined from the time  $t$  at the null point at which  $M_z=0$ , which from equation 3.2 occurs for a value  $t_{\text{null}}$  such that:-

$$T_1 = \frac{t_{\text{null}}}{\ln 2} \quad (3.3)$$

Imperfections in the inversion pulse in the standard inversion recovery experiment can be avoided by the use of a composite pulse or the residual transverse magnetisation removed by use of a homospoil pulse or suitable phase cycling [87,246]. Phase cycling may also be used to eliminate the effects of multiple quantum coherences which may be generated [245].

The inversion recovery experiment is generally regarded as the most accurate method for the measurement of longitudinal relaxation times [244], but suffers from the disadvantage of the necessity of acquiring a number of data sets with long pulse delays, which for insensitive nuclei, where extensive signal averaging is required, leads to unacceptably long experiment run times. Several faster methods have been introduced to circumvent this difficulty, most notably those of progressive saturation [247] and saturation recovery [248]. These methods and many others have been discussed by Martin *et al.* [244]. Two of the most recent methods, DESPOT and SUFIR, were considered for use in the measurement of  $^{13}\text{C}$  longitudinal relaxation times of the low concentration cyclodextrin complex solutions examined in this work.

### 3.7.1.2 DESPOT

The DESPOT (Driven Equilibrium Single Pulse Observation of  $T_1$ ) method was originally introduced by Christensen *et al.* [249], but has more recently been re-evaluated by Homer and co-workers [250,251]. The sequence has the form

$$(\theta\text{-FS-}t)_m\text{-(}\theta\text{-A-FS-}t^*)_n$$

where an initial series of  $m$  pulses is used to set up a steady state prior to some number  $n$  of the acquisition (A) sequence. FS represents application of a homospoil pulse for the elimination of residual transverse magnetisation, and the pulse delays  $t$  and  $t^*$  are such that the total inter-pulse delay  $t_i$  is constant throughout so that the steady state is maintained, that is,

$$t_i = FS + t = A + FS + t^* \quad (3.4)$$

Consider the longitudinal magnetisation once the steady state has been achieved,  $M_S$ . Following application of the pulse of angle  $\theta$ , the longitudinal ( $M_L$ ) and transverse ( $M_T$ ) components are such that:-

$$M_T = M_S \sin \theta, \quad M_L = M_S \cos \theta \quad (3.5)$$

Following the homospoil pulse, only the longitudinal component remains. This will begin to relax to its equilibrium value  $M_0$  and at the end of the period  $t_i$  will have reached a value  $M_{ii}$  given by:-

$$M_{ii} = M_0 - (M_0 - M_S \cos \theta) e^{-t_i/T_1} \quad (3.6)$$

Since the system is in a steady state,

$$M_S = M_{ii} \quad (3.7)$$

Thus, at constant  $t_i$  and over a range of  $\theta$ , a plot of  $M_S$  against  $M_S \cos \theta$  gives  $T_1$ . In practice, since the NMR signal is detected in the transverse plane, the measured intensity  $I_S$  of signals will be related to  $M_S$  through:-

$$I_S \propto M_S \sin \theta$$

so that the regression will, in fact, be of  $I_S/\sin \theta$  versus  $I_S \cos \theta/\sin \theta$ .

Reasonable results with this method have been obtained with as little as two data points, in which case,

$$\ln \frac{I_1 \sin \theta_2 - I_2 \sin \theta_1}{I_1 \sin \theta_2 \cos \theta_1 - I_2 \sin \theta_1 \cos \theta_2} = - \frac{t_i}{T_1} \quad (3.8)$$

where  $I_1$  and  $I_2$  are the intensities corresponding to flip angles  $\theta_1$  and  $\theta_2$  respectively.

Homer and co-workers [250,251] have described the protocol for the successful use of the DESPOT method, and have highlighted the need to implement a sufficient number of dummy pulses to establish the stationary state, to use a  $t_i$  value such that  $t_i/T_1$  is approximately 0.2 and to systematically increase  $\theta$  between data sets. Additionally, the sample must be restricted to the effective volume of the excitation coils and a pulse offset value determined to ensure proportionality between the pulse width and its flip angle.

### 3.7.1.3 SUFIR

The SUFIR (SUper Fast Inversion Recovery) method has been described by Canet *et al.* [252]. The sequence has the form shown in Figure 3.10. and requires acquisition into separate memory blocks at two stages in the cycle.

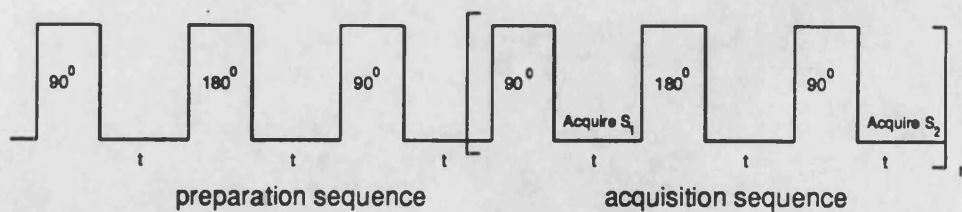


Figure 3.10 The SUFIR sequence for the measurement of longitudinal relaxation times

If it is assumed that immediately prior to each pulse no transverse magnetisation remains, the effect of the sequence may be determined from

equation 3.1. Figure 3.11 shows the orientation and magnitude of magnetisation at each stage of the sequence.

The initial preparation sequence gives rise to the steady state of the acquisition sequence for which the two signals  $S_1$  and  $S_2$  are given by:-

$$S_1 = M_0(1-y) \quad (3.9)$$

$$S_2 = M_0(1-y)^2 \quad (3.10)$$

where  $y = e(-t/T_1)$ , which eliminating  $M_0$  from equations 3.9 and 3.10 gives:-

$$T_1 = \frac{-t}{\ln(1-S_2/S_1)} \quad (3.11)$$

Thus,  $T_1$  may be calculated from a single experiment. For optimum accuracy, the authors recommend a  $t$  value such that  $t=0.5-3T_1$  and that sufficient transients be accumulated to ensure good signal to noise in the resulting spectra. Additionally, composite  $180^\circ$  pulses are recommended to avoid errors during inversion. The eight step phase cycle proposed by the authors eliminates the effects of misadjustment of the  $90^\circ$  pulse width and residual transverse magnetisation.

### 3.7.2 Measurement of the Nuclear Overhauser Effect

The nuclear Overhauser effect (nOe) [253] describes the change in intensity of the resonance of one nucleus as a result of a perturbation of the population of the nuclear energy levels at some other, which need not necessarily be found within the same molecule. It is a consequence of the dipolar cross-relaxation which may occur between two such spin systems, and where additional pathways of relaxation are operative, may be related to internuclear distance. Consequently it is an important tool in the determination of molecular structure in solution.

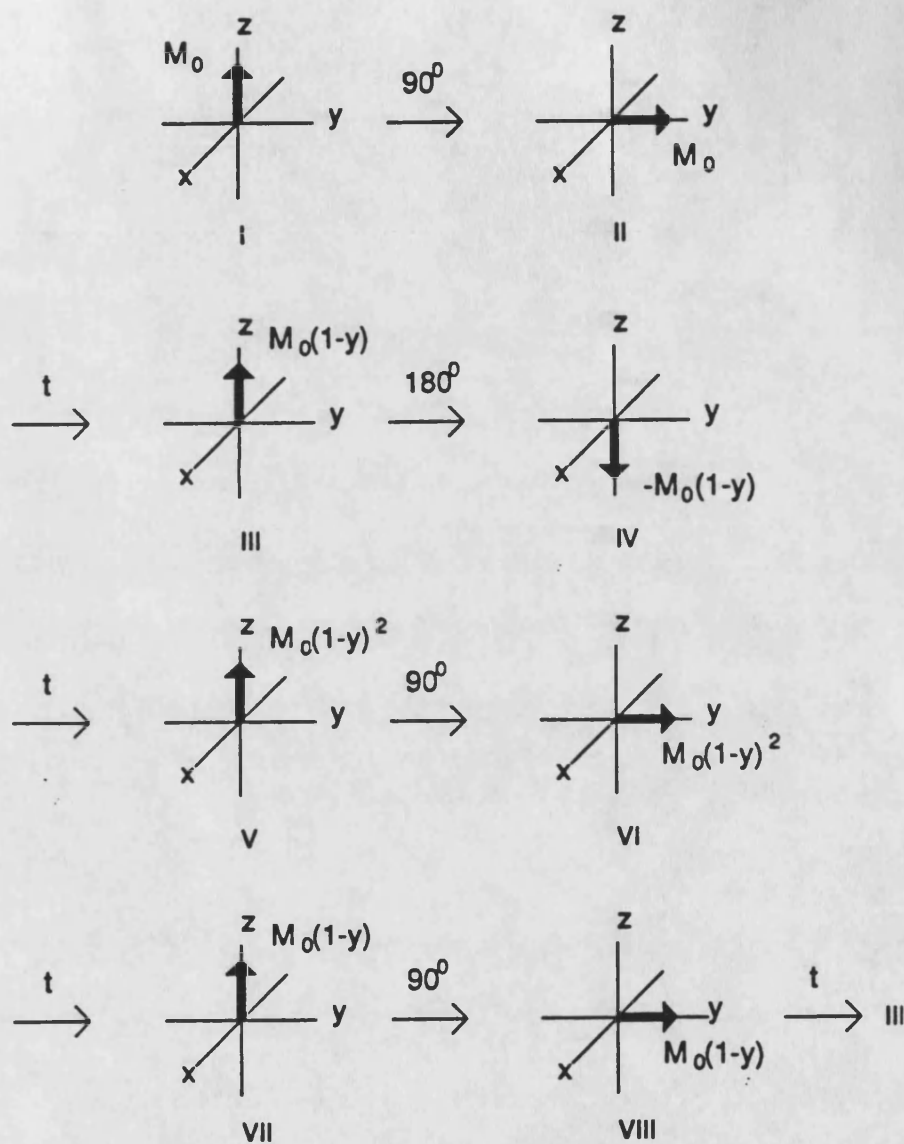


Figure 3.11 A vector model representation of the SUFIR sequence

### 3.7.2.1 The nOe Difference Experiment

In order to observe an nOe, it is necessary to compare resonance intensities in a control spectrum acquired in the absence of perturbation, with the nOe spectrum in which one resonance has been selectively perturbed prior to acquisition. Since the nOe resulting from the perturbation may be small, it is then most readily visible if these two spectra, or the FIDs from which they are derived, are subtracted. This is the nOe difference experiment [254]. Selective saturation with a weak radio-frequency field is the most common method of generating the nOe. In practice, for convenience and improved spectral subtraction, this field is not absent from the control spectrum, but is positioned in an area of the spectrum free from resonances. Thus, the nOe difference sequence may be represented as shown in Figure 3.12.

Presaturation of the selected resonance is continued for several  $T_1$ s to ensure that the nOe has adequate time to be established. Several other precautions are also generally taken to improve spectral subtraction and thus allow small nOes to be observed [83,253,255]. The effect of fluctuations of temperature during acquisition are generally avoided by use of the spectrometer variable temperature unit to control sample temperature. The deuterium lock unit reduces drifting of the magnetic field, and it is therefore desirable to study samples in a solvent which gives rise to a strong and sharp deuterium resonance which facilitates its operation, although the choice of solvent may also be influenced by its effect on molecular correlation time. Non-viscous solvents are more likely to give solutions in the extreme narrowing limit. Finally, the nOe and control spectra are not acquired consecutively, but cycle between nOe and control acquisitions in blocks of a small number of scans. In terms of sample preparation, it is desirable to reduce competing relaxation pathways, which if highly efficient may significantly reduce the size of an nOe or eliminate it completely. Steps should therefore be taken to



remove paramagnetic ions and possibly oxygen dissolved in the solvent. Dilute solutions also restrict the contribution of intermolecular relaxation mechanisms.

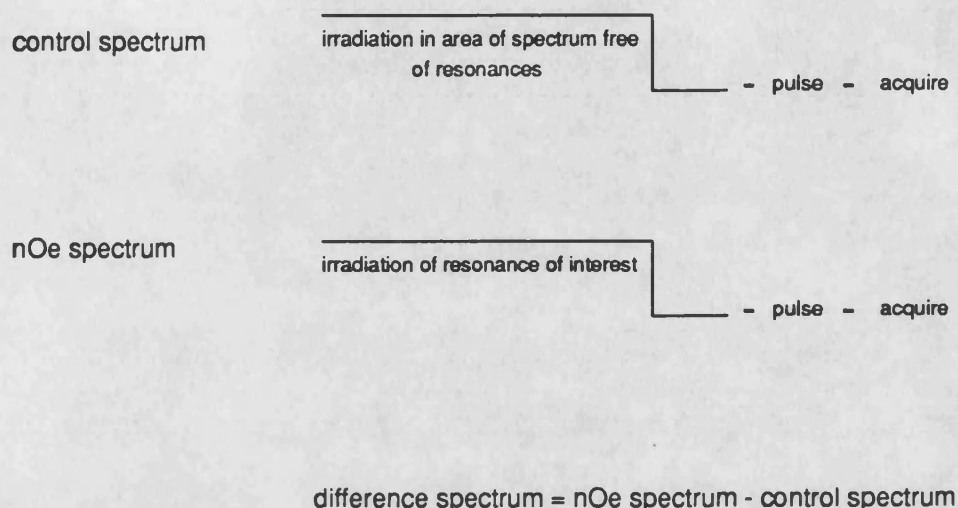


Figure 3.12 The nOe difference experiment

### 3.7.2.2 The Transient nOe and NOESY Experiments

The transient nOe experiment [256] provides an alternative method for the measurement of nOes in one dimensional NMR spectroscopy. A selective  $180^\circ$  pulse, generated by use of a soft pulse or the DANTE sequence [257], is used in place of saturation to perturb the population difference of the nuclear energy levels of a single resonance. A series of spectra acquired with increasing  $t$  allows the build-up rate of the nOe, which may be related to internuclear distance, to be measured. The method has, however, been largely superseded by its two dimensional equivalent, the NOESY (Nuclear Overhauser Effect Spectroscopy) experiment.

The NOESY experiment [258] has the form shown in Figure 3.13:- where  $t_1$  is the two dimensional incremental time delay and  $t_m$  the constant period called the mixing time during which the transient nOe develops. A basic understanding of the experiment may be achieved with the vector model [246], Figure 3.14.

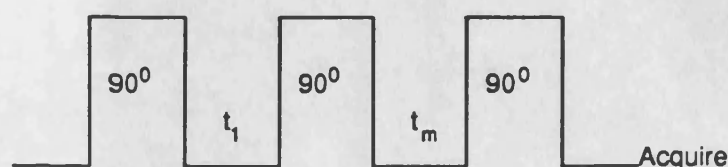


Figure 3.13 The NOESY experiment

The initial  $90^\circ$  pulse rotates the bulk magnetisation  $M_0$  into the xy plane. Evolution during  $t_1$  then follows. At the end of this period, the magnetisation vector will lie at some angle  $\theta$ , to the y axis. This vector may be resolved into two perpendicular components, lying along the x and y axes, the size of which depend on  $\theta$ , which in turn is a function of the precessional frequency of the nucleus and the value of  $t_1$ . In this way, amplitude modulation of the components at the end of the  $t_1$  period leads to frequency labelling of the vector. The second  $90^\circ$  pulse then flips the magnetisation component lying along the y axis down onto the -z axis, whilst the remaining transverse magnetisation is removed by phase cycling or the use of a homospoil pulse. Cross relaxation of the z component of magnetisation of this nucleus and that of some other during the mixing time  $t_m$  that follows then leads to a transfer of magnetisation which may be read by the final  $90^\circ$  pulse and results in the observation of cross-peaks in the NOESY spectrum between closely spaced nuclei.

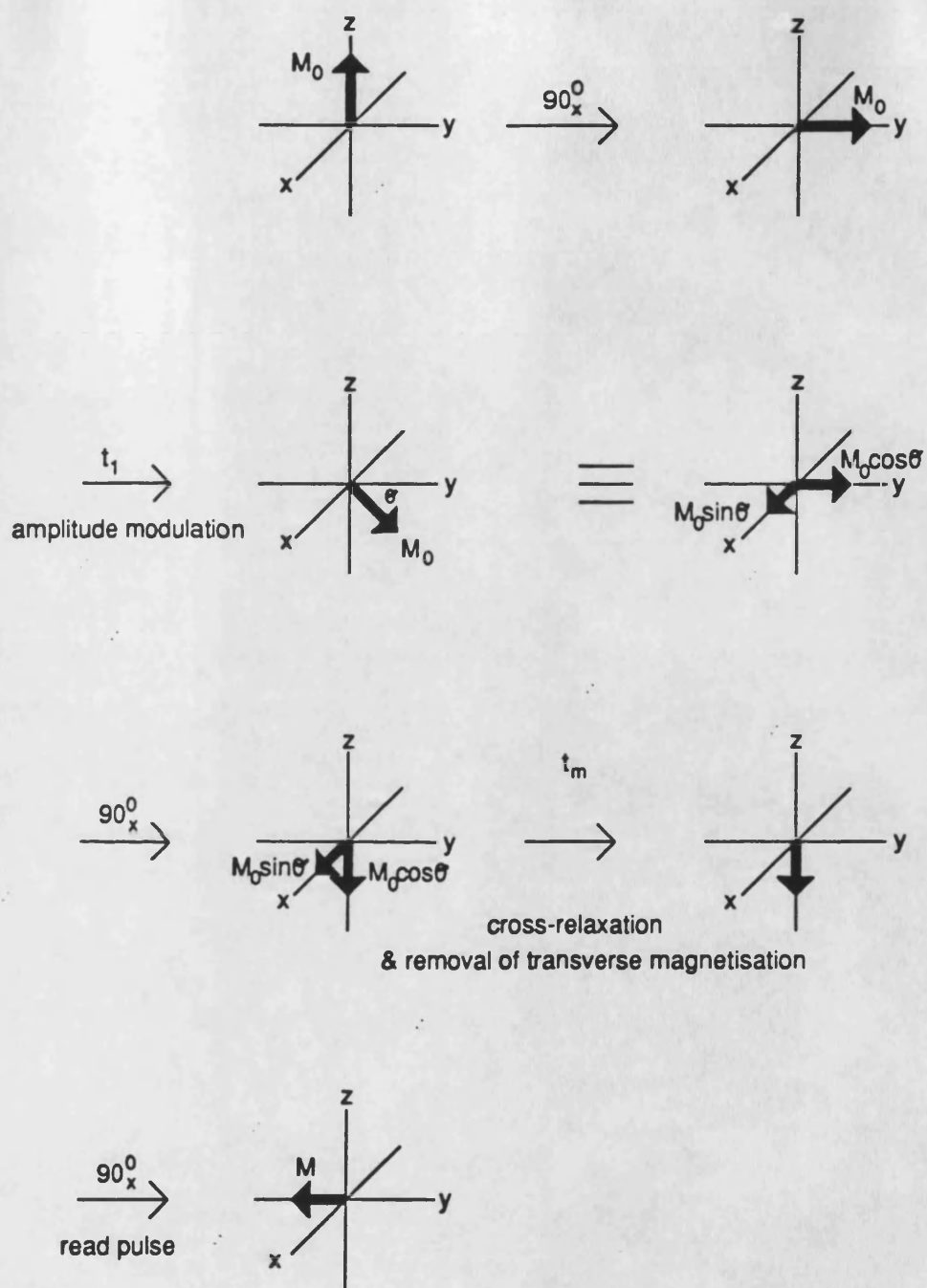


Figure 3.14

A vector model representation of the NOESY experiment

For qualitative studies the mixing time  $t_m$  is generally of the order of  $T_1$  which allows sufficient time for the transient nOe to develop. Quantitative work generally requires NOESY data acquired over a series of  $t_m$  [259], although a single spectrum acquired with short  $t_m$  and following the so-called initial rate approximation may yield distance information directly [246].

Methods suitable for the elimination of cross-peaks arising from coherence transfer pathways which may confuse spectral interpretation have recently been discussed [253].

### 3.7.2.3 The ROESY or CAMELSPIN Experiment

The CAMELSPIN (Cross relaxation Appropriate for Mini- molecules EmuLated by SPIN-locking) experiments [260] in one or two dimensions are analogous to the transient nOe and NOESY methods described above, but are a consequence of cross- relaxation in the transverse plane rather than along the longitudinal axis.

The one dimensional experiment requires the collection of two data sets as in the case of nOe difference spectroscopy: one in which the transverse or rotating frame nOe (rOe) is generated, and the other used as a control, Figure 3.15.

The spin-lock field is typically of the order of 1-10kHz [253] and is either applied continuously [260] or intermittently at high power [261]. Its importance in the generation of the rOe can be understood from Figure 3.16.

The  $180^\circ$  pulse of the rOe sequence selectively inverts one of the resonances so that it lies along the z axis. The  $90^\circ$  pulse then flips magnetisation along the longitudinal axis to the transverse plane. Application of the spin-lock field in a direction perpendicular to this pulse then serves two purposes [253]:-

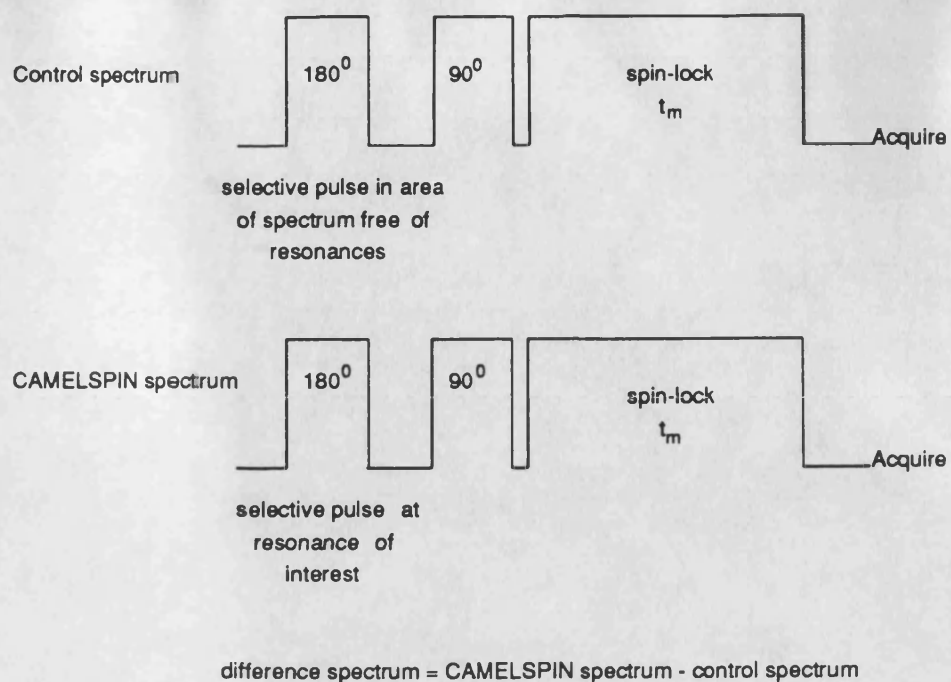


Figure 3.15 The one dimensional CAMELSPIN experiment

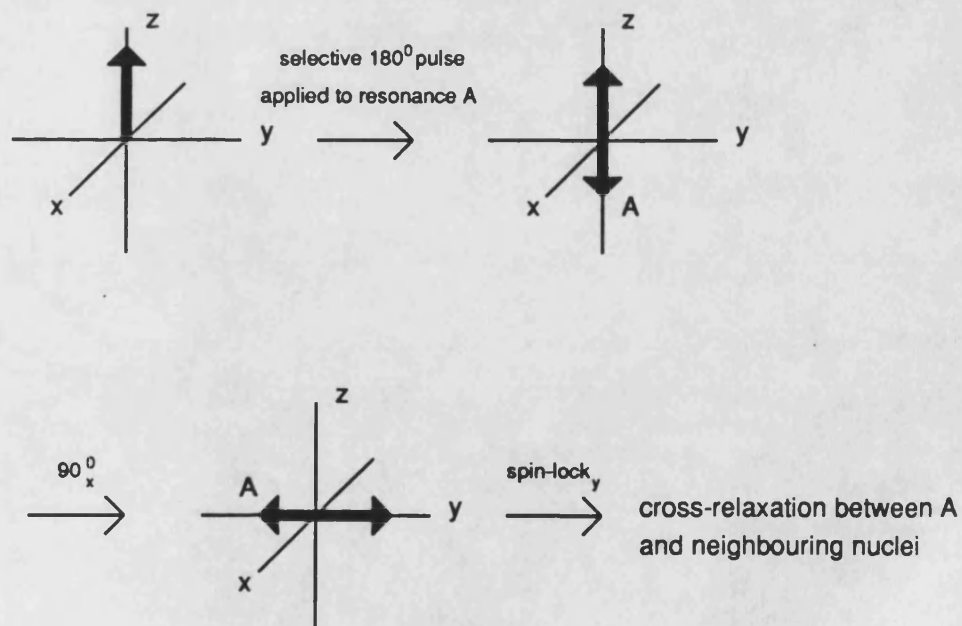


Figure 3.16 A vector model representation of the one dimensional CAMELSPIN experiment

1. It generates a magnetic field along the y axis which functions in a manner analogous to the static field along the z axis. Pseudo longitudinal relaxation relative to this  $B_1$  field gives rise to the rOe in the event of cross-relaxation.
2. It serves to prevent relative precession of vectors in the transverse plane which would otherwise lead to overall cancellation of the rOe.

More commonly the rOe is observed in a two dimensional experiment, often referred to as ROESY [262] (Rotating frame Overhauser Effect Spectroscopy), the acquisition sequence for which is shown in Figure 3.17.

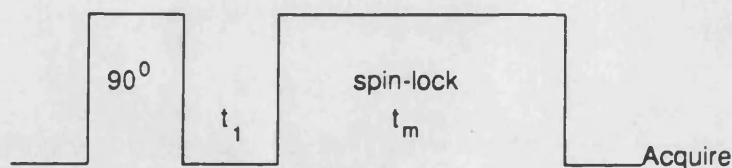


Figure 3.17 The two dimensional CAMELSPIN or ROESY experiment

There are several advantages associated with measurement of the rOe as opposed to the nOe. Thus, chemical exchange may be readily distinguished from the rOe by its difference in phase, and spin diffusion, which can hamper the acquisition of nOe data for large macromolecules, is limited in the rOe experiment [263]. Its greatest use, however, is in the examination of medium sized molecules in the molecular weight range 800-2000 [253,260]. Such molecules are typically characterised by a correlation time  $t_c$  such that  $\omega_0 t_c \sim 1$  and lie on or near the cross-over point between the positive nOe of the small molecule in the extreme narrowing condition and the negative nOe associated with larger molecules. Thus,

the nOe observed for such molecules is generally zero or very small. In contrast, the rOe is positive and of a reasonable magnitude irrespective of molecular correlation time and therefore size. This may be understood qualitatively in terms of  $\omega_0$  [253]. For the nOe,  $\omega_0$  characterises the precessional frequency about the longitudinal axis and thus is of the order of hundreds of MHz for the  $^1\text{H}$  nucleus. In the rOe experiment, precession is about the weak  $B_1$  field, giving frequencies of the order of kHz. As a result all molecules necessarily satisfy the extreme narrowing condition  $\omega_0 t_c \ll 1$  and give rise to a positive rOe.

Disadvantages of observation of the rOe arise primarily from interactions which either obscure the rOe or confuse its interpretation. Most may be distinguished by their phase properties, so that it is essential to acquire two dimensional spectra in the phase sensitive mode. The cross-peaks most commonly observed for medium sized molecules relative to a diagonal of positive double absorption phase are then summarised in Table 3.1.

Elimination of the TOCSY interaction is particularly desirable, since such correlations are often large and may obscure underlying ROESY cross-peaks, and additionally give false ROESY cross-peaks through the TOCSY-ROESY or ROESY-TOCSY pathways [264]. Methods proposed for their reduction have included the use of a low power spin-lock field [262] and of an intermittent spin-lock field composed of a train of small flip angle pulses [261] (although Bax [265] has questioned this proposal). In practice it is difficult to remove such interactions completely, however, and more commonly they are identified by their dependence on carrier frequency. Thus, the ROESY cross-peak is generally little affected by small changes in the carrier frequency, in contrast to the TOCSY (and consequently ROESY-TOCSY and TOCSY-ROESY) cross-peak [264].

The other main disadvantage of the ROESY method is concerned with practical difficulties in the generation of a uniform excitation pulse and spin-lock field. Deviations from uniformity reduce the efficiency of the experiment and



Cross-peak	Cause	Phase Properties *
ROESY	transverse cross-relaxation between nuclei close in space	negative, in-phase, double absorption
COSY	coherence transfer between J coupled nuclei	doubly antiphase, double dispersion
TOCSY	magnetisation transfer between J coupled nuclei	positive, in-phase, double absorption
ROESY-TOCSY or TOCSY-ROESY	consecutive operation of the ROESY and TOCSY mechanisms	negative, in-phase, double absorption

\* Relative to a diagonal of positive, double absorption phase

Table 3.1 Cross-peaks commonly observed in the ROESY experiment: their phase properties and cause



7

additionally complicate quantitative interpretation of spectra [253]. Practical aspects of the ROESY experiment will be considered in greater detail in Chapter 4.

## CHAPTER 4

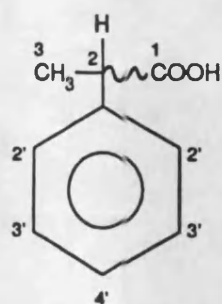
### NMR Studies of the Complexation of $\beta$ -Cyclodextrin With Some 2-

#### Arylpropionates

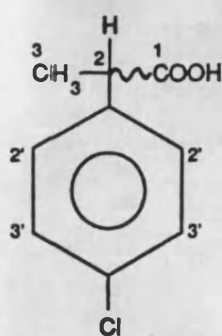
#### 4.1 Introduction

Chapter 2 referred to the use of cyclodextrins as chiral solvating agents (CSAs) in NMR spectroscopy. Our results showed that the sodium salts of the NSAIDs ibuprofen and flurbiprofen chosen for study exhibited chiral recognition in the form of peak duplication in their NMR spectra in the presence of various cyclodextrins and under a range of experimental conditions. In all cases, however, the splitting was small ( $<0.02\text{ppm}$ ) and less than ideal for use as a method of measurement of enantiomeric excess. The use of cyclodextrins as CSAs remains largely empirical, and in an attempt to gain greater understanding of their applicability, a study of the interaction of a range of 2-arylpropionic acids with  $\beta$ -cyclodextrin by NMR spectroscopy has been undertaken, the results for which are reported here. NMR was chosen as the technique for studies of this system, because of its unique ability to probe molecular structure in solution. Yamamoto and Inoue have recently reviewed the application of NMR spectroscopy to the cyclodextrin inclusion process [266]. Interactions of molecules with cyclodextrins in the solution state, aside from their relevance to the use of cyclodextrins as CSAs, are additionally of interest in regard to their action, for example, as catalysts, enzyme mimics and formulation agents for pharmaceuticals, as was discussed in Chapter 3.

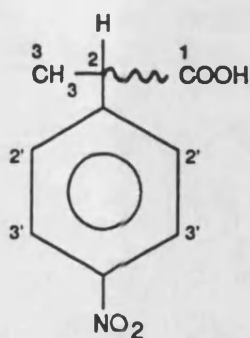
The structures of the compounds used in this study are shown in Figure 4.1. Flurbiprofen, ibuprofen and naproxen are used as NSAIDs [2], whilst 2-phenylpropionic acid, 2-(4-chlorophenyl)- and 2-(4-nitrophenyl)-propionic acid were chosen as simple, readily available structural analogues of the 2-



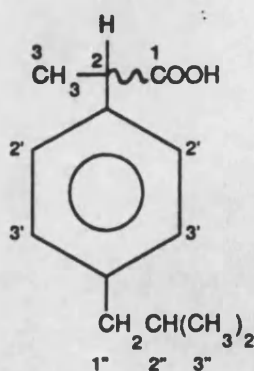
2-phenylpropionic acid



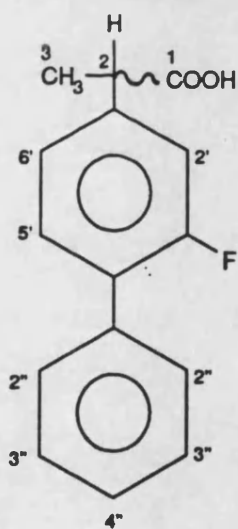
2-(4-chlorophenyl)propionic acid



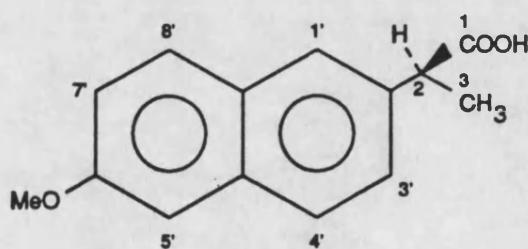
2-(4-nitrophenyl)propionic acid



ibuprofen



flurbiprofen



naproxen

Figure 4.1 Structure of the 2-arylpropionic acids



arylpropionic acid series of drugs. Throughout this work, these compounds were used as the racemate, excepting naproxen, which is available commercially only as the therapeutically active S enantiomer. Additionally, all compounds were used in the form of their sodium salts as a result of the improved aqueous solubility over the free acid.

#### 4.2 $^1\text{H}$ NMR Studies of the Complexation of $\beta$ -Cyclodextrin with some 2-Arylpropionates in $\text{D}_2\text{O}$

Several common features of the interaction of ibuprofen sodium and flurbiprofen sodium with various cyclodextrins in  $\text{D}_2\text{O}$  were discussed in Chapter

2. Thus,

1. Changes in  $^1\text{H}$  NMR chemical shift of both drug and cyclodextrin resonances were indicative of the formation of an inclusion complex.
2. The presence of a single set of resonances for the cyclodextrin and the drug (in the absence of its chiral recognition) demonstrated that the equilibrium between the free and complexed species was in the fast exchange limit.
3. The observation of chiral recognition of the drug molecule by the cyclodextrin was dependent on the choice of cyclodextrin.

For the four additional substrates examined here, namely, the sodium salts of naproxen, 2-phenylpropionic acid and 2-(4-chlorophenyl)- and 2-(4-nitrophenyl)-propionic acid, in all cases an inclusion complexation interaction in the fast exchange limit was again observed in the  $^1\text{H}$  NMR spectra recorded in the presence of a mole equivalent of  $\beta$ -cyclodextrin in  $\text{D}_2\text{O}$ , although broadening of some guest resonances may represent approach towards a more intermediate rate of exchange. Table 4.1 summarises changes in chemical shift of the  $^1\text{H}$  NMR resonances of  $\beta$ -cyclodextrin upon addition of a mole equivalent of each of the

Substrate	Change in chemical shift/ppm of $\beta$ -cyclodextrin resonance					
	H1	H2	H3	H4	H5	H6
ibuprofen sodium	-0.029	-0.033	-0.111	-0.009	> -0.179	*
flurbiprofen sodium	-0.075	-0.102	-0.177	-0.041	> -0.246	*
naproxen sodium	-0.058	-0.065	-0.154	-0.050	> -0.240	*
sodium 2-phenylpropionate	-0.017	-0.022	-0.039	-0.021	> -0.050	*
sodium 2-(4-chlorophenyl)propionate	-0.033	-0.050	-0.099	-0.032	> -0.096	*
sodium 2-(4-nitrophenyl)propionate	-0.031	-0.047	-0.106	-0.027	> -0.103	*

Table 4.1 Changes in 400MHz  $^1\text{H}$  chemical shift of the resonances of a 0.014M solution of  $\beta$ -cyclodextrin in the presence of a mole equivalent of sodium 2-arylpropionate in  $\text{D}_2\text{O}$  at  $30^\circ\text{C}$

sodium 2-arylpropionate substrates examined. Data relating to the sodium salts of ibuprofen and flurbiprofen, already reported in Chapter 2, are reproduced here for comparison. All spectra are again referenced to the residual HDO resonance of the solvent.

In addition to providing evidence for the formation of an inclusion complex, we suggest that the large up-field shifts in the H3 and H5 resonances of the cyclodextrin may also give some indication of the structure of this complex. Thus, by comparison of the magnitude of these resonances in the presence of each substrate, three categories of guest molecule may be identified:

1. Sodium 2-phenylpropionate:

The up-field shifts of the cyclodextrin H3 and H5 resonances are both small. We attribute this to the low formation constant of the inclusion complex of this substrate.

2. Ibuprofen sodium, sodium 2-(4-chlorophenyl)propionate, sodium 2-(4-nitrophenyl)propionate:

The up-field shift of the cyclodextrin H3 resonance is comparable in the presence of each of these substrates and considerably larger than that observed in the presence of sodium 2-phenylpropionate. We suggest that this is a consequence of a similarity of structure of the inclusion complex for each of these substrates and of a comparable formation constant, considerably greater than that of the  $\beta$ -cyclodextrin complex formed with sodium 2-phenylpropionate. This greater stability may be associated with a number of factors, including increased van der Waals interactions in the complex as a result of the bulk of the *para* substituent, and in the case of sodium 2-(4-nitrophenyl)propionate, the possibility of hydrogen bonding between the nitro group and the hydroxylic groups of the cyclodextrin [267].

This argument neglects the widely differing electronic effect of each of the *para* substituents of these substrates on the aromatic ring current, which in view of the work of Demarco and Thakkar [155], described in Chapter 2, might be considered an important influence on the cyclodextrin H3 resonance. It is noted, however, that Yamamoto *et al.* [268] similarly neglected the electronic properties of aromatic substituents in their calculations, based on the theory of Johnson and Bovey [156,157], relating to the structure of cyclodextrin inclusion complexes. Certainly, it is clear that ring current effects alone cannot account for variations in shifts of the cyclodextrin <sup>1</sup>H resonances observed here, since changes in chemical shift in the presence of sodium 2-(4-chlorophenyl)propionate are markedly different from those of sodium 2-phenylpropionate, despite the minimal electronic influence of an aromatic chloro substituent.

Despite the similarity of the cyclodextrin H3 resonance in the presence of each of the substrates in this category, a large difference of chemical shift of the cyclodextrin H5 resonance is observed in the presence of ibuprofen sodium in comparison with sodium 2-(4-chlorophenyl)- and 2-(4-nitrophenyl)-propionate. This may be attributed to the differential effect of the *para* substituent on the cyclodextrin H5 resonance, either through a direct interaction, or indirectly through its influence on the level of penetration of the substrate in the cyclodextrin cavity, and is therefore suggestive of their proximity. This observation allows us to propose a structure of the inclusion complex with these *para* substituted substrates shown schematically in Figure 4.2.

### 3. Flurbiprofen sodium and naproxen sodium:

These substrates induce a very large up-field shift in both the cyclodextrin H3 and H5 resonances, which may be interpreted, at least in part, as a consequence of the greater formation constant of the inclusion complex of these more highly hydrophobic substrates.

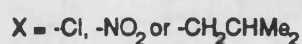
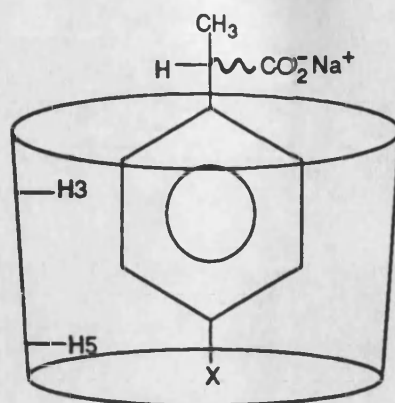


Figure 4.2 Proposed structure of the  $\beta$ -cyclodextrin inclusion complex of some 2-arylpropionates in  $\text{D}_2\text{O}$

Shifts in  $^1\text{H}$  resonances of the cyclodextrin, other than those of the H3 and H5 protons, may be attributed to conformational changes on formation of the inclusion complex.

Changes in chemical shift of the  $^1\text{H}$  sodium 2-arylpropionate resonances in the presence of a mole equivalent of  $\beta$ -cyclodextrin are shown in Figure 4.3. They are given as ranges where exact determination of chemical shift in the presence of  $\beta$ -cyclodextrin was not achieved.  $^1\text{H}$  NMR data for these salts are given in Appendix 4.1 at the end of this chapter. NOe difference, COSY-45, ROESY and homonuclear decoupling experiments, in addition to the Job plots discussed in Section 4.5, were used to confirm assignments where they were thought to be ambiguous.

Inspection of Figure 4.3 reveals that trends in the changes of chemical shifts of the salt resonances are less apparent than were those of the cyclodextrin. It is suggested that this is a consequence of the greater sensitivity of guest resonances to variations in depth of penetration of the cyclodextrin cavity [269].



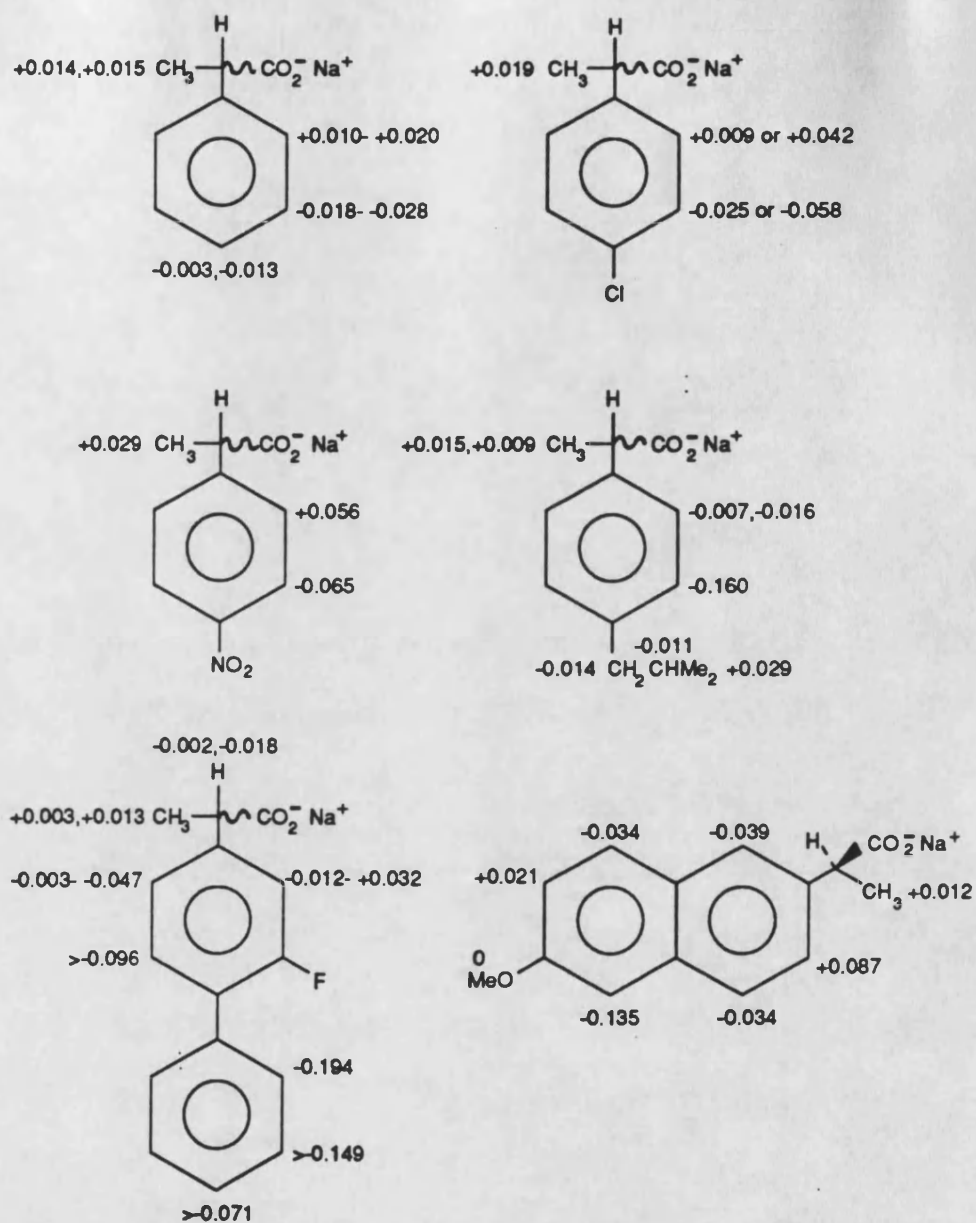


Figure 4.3 Changes in 400MHz  $^1\text{H}$  chemical shift of the resonances of a 0.014M solution of some 2-arylpropionates in the presence of a mole equivalent of  $\beta$ -cyclodextrin in  $\text{D}_2\text{O}$  at  $30^\circ\text{C}$

Although determination of the H2' and H3' resonances of sodium 2-phenylpropionate in the presence of  $\beta$ -cyclodextrin was not possible because of strong coupling between these two nuclei, it remains clear that changes in chemical shift of resonances of this substrate are in most cases small. This is consistent with the low formation constant previously proposed for its inclusion complex.

A common structure for the  $\beta$ -cyclodextrin inclusion complexes of ibuprofen sodium, sodium 2-(4-chlorophenyl)- and 2-(4-nitrophenyl)-propionate was also suggested above. For these substrates, we note a common up-field shift of the H3' resonance, which is larger than that for any other resonance in the molecule. In terms of the structure of Figure 4.2, this suggests that such an up-field shift may be associated with aromatic protons deep in the cyclodextrin cavity. On this basis it is proposed that it is the central portion of the naproxen sodium molecule which lies within the cyclodextrin cavity.

Changes in chemical shift of the  $^1\text{H}$  resonances of the fluorophenyl aromatic ring and H3 group of flurbiprofen sodium in the presence of a mole equivalent of  $\beta$ -cyclodextrin are comparable with those of ibuprofen sodium and sodium 2-(4-chlorophenyl)- and 2-(4-nitrophenyl)-propionate. This suggests a structure for the  $\beta$ -cyclodextrin inclusion complex of flurbiprofen sodium similar to that of these substrates and shown schematically in Figure 4.2.

$^1\text{H}$  resonances of the non-fluorinated phenyl ring also show a large up-field shift in the presence of cyclodextrin, however. Since the biphenyl ring system is too large to be wholly accommodated within a single cyclodextrin molecule, this suggests that the flurbiprofen sodium molecule interacts simultaneously with more than one cyclodextrin macrocycle, either through the formation of a complex of 1:2 guest:host stoichiometry, or through dimerisation of the 1:1 complex in a manner analogous to that observed in its crystal structure.

It has also been suggested by Imai *et al.* [270], who used  $^{13}\text{C}$  NMR to examine the interaction between  $\beta$ -cyclodextrin and flurbiprofen in 0.05M NaOD,

that changes in chemical shift may also be attributed in part to ring current effects associated with the constraints of the inclusion process on the torsional angle between the two phenyl rings. We do not believe, however, that this effect is a primary cause of the observed changes in chemical shift of the  $^1\text{H}$  resonances of flurbiprofen sodium in the presence of  $\beta$ -cyclodextrin, since the phenyl rings do not appear equally affected.

The chiral duplication of drug resonances in the presence of  $\beta$ -cyclodextrin has already been described in Chapter 2 for ibuprofen sodium and flurbiprofen sodium. For the additional racemic substrates examined here, only the sodium 2-phenylpropionate molecule shows duplications. Splittings of 0.001ppm and 0.010ppm are observed for the H3 and H4' resonances respectively.

#### 4.3 $^1\text{H}$ NMR Studies of the Complexation of $\beta$ -cyclodextrin with some 2-Arylpropionates in $d_6$ -DMSO

During the course of this work, interaction between the 2- arylpropionates and  $\beta$ -cyclodextrin was also examined in  $d_6$ -DMSO. Sodium 2-(4-nitrophenyl)propionate was, however, found to be unsuitable for study in this solvent, as a result of its rapid decomposition (in both the presence and absence of  $\beta$ -cyclodextrin). Two decomposition products were formed in significant amounts, and were identified as 4-ethylnitrobenzene and 4'-nitroacetophenone, on the basis of  $^1\text{H}$  NMR data. These products are a consequence of decarboxylation and subsequent autoxidation of the salt, and are favoured for this substrate as a result of stabilisation of the intermediate carbanionic and radical species by the electron-withdrawing nitro group. Presumably this decomposition pathway is not observed in aqueous solvents because of improved solvation and stabilisation of the carboxylate functionality.

$^1\text{H}$  NMR data for all other substrates, referenced to the residual solvent resonance at 2.5ppm, are given in Appendix 4.2 at the end of this chapter.

Assignment of the aromatic resonances of naproxen sodium and flurbiprofen sodium was achieved by comparison with the corresponding data for solutions in  $D_2O$ . The electronic influence of the isobutyl and chloro substituents of ibuprofen sodium and sodium 2-(4-chlorophenyl)propionate on the resonances of sodium 2-phenylpropionate determined in  $D_2O$  were used to assign the aromatic resonances of ibuprofen sodium and sodium 2-(4-chlorophenyl)propionate from those of sodium 2-phenylpropionate in  $d_6$ -DMSO.

Changes in chemical shift of the  $^1H$  2-arylpropionate resonances in the presence of a mole equivalent of  $\beta$ -cyclodextrin are given in Figure 4.4. These changes are calculated assuming where necessary that no change of relative position of aromatic resonances occurs on addition of cyclodextrin. We believe that this is a reasonable assumption, since spectra appear little changed from that of the free salt.

The small shifts of resonances given in the figure are suggestive of low levels of complexation between substrate and cyclodextrin. Changes in chemical shift of the cyclodextrin H5 resonance in the presence of a mole equivalent of the salts, shown in Table 4.2, further support this conclusion. Although these are difficult to measure with great accuracy as a result of the broad nature of the doublet resonance, they are clearly reduced from the large values observed in  $D_2O$ . The cyclodextrin H3 resonance which also showed large changes in chemical shift in  $D_2O$  in the presence of a guest substrate is obscured by the over-lying signal of the H6 resonance in  $d_6$ -DMSO, Figure 2.15.

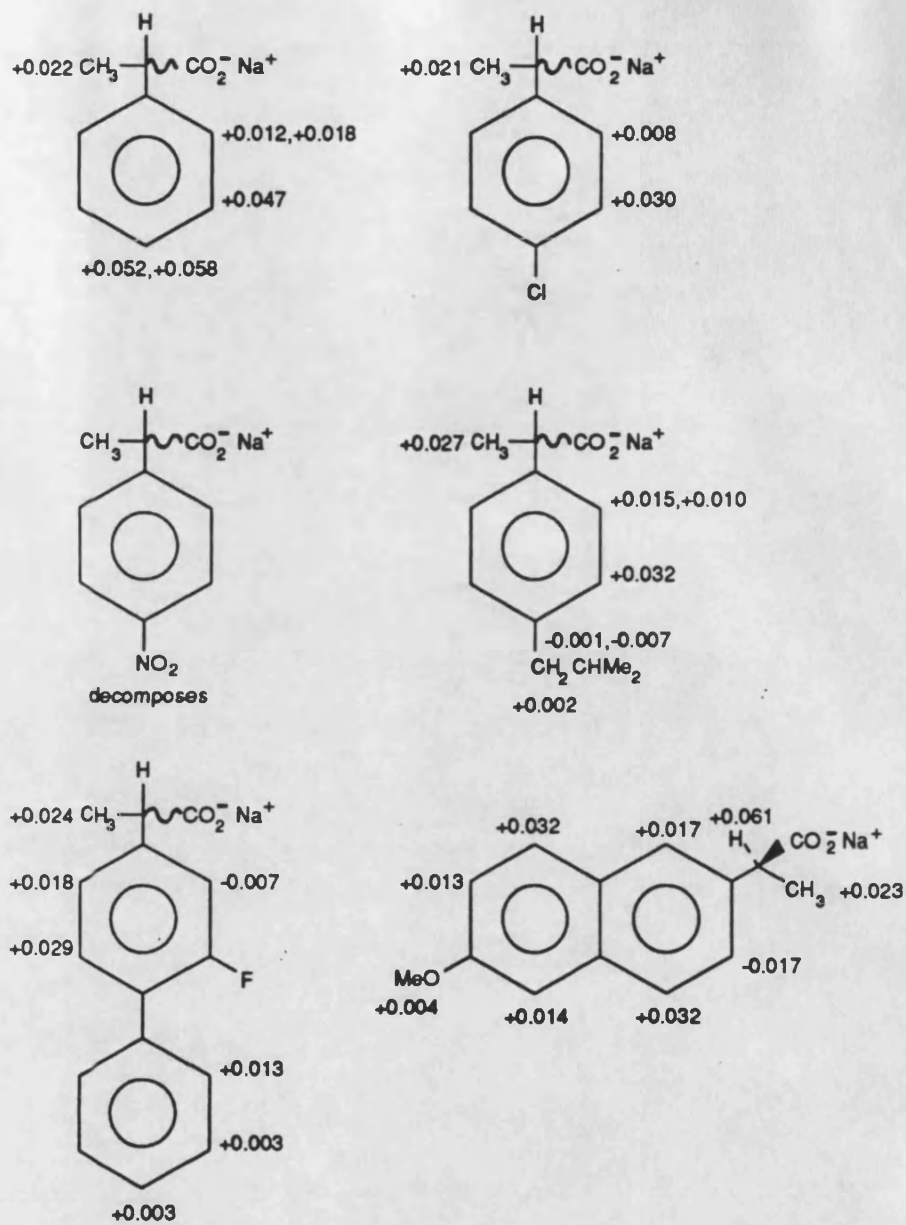


Figure 4.4 Changes in 400MHz  $^1\text{H}$  chemical shift of the resonances of a 0.014M solution of some 2-arylpropionates in the presence of a mole equivalent of  $\beta$ -cyclodextrin in  $\text{d}_6$ -DMSO at  $30^\circ\text{C}$

Substrate	Shift of cyclodextrin resonance/ppm	
	H1	H5
sodium 2-phenylpropionate	-0.009	-0.001
sodium 2-(4-chlorophenyl)propionate	-0.011	-0.001
ibuprofen sodium	-0.014	-0.002
flurbiprofen sodium	-0.006	+0.006
naproxen sodium	-0.010	+0.004

Table 4.2 Changes in 400MHz  $^1\text{H}$  chemical shift of resonances of a 0.014M solution of  $\beta$ -cyclodextrin in the presence of a mole equivalent of some 2-arylpropionates in  $\text{d}_6$ -DMSO at 30°C

Although the reduced stability of cyclodextrin inclusion complexes in DMSO has been described [186], we do not believe that this is the sole cause of these small changes in chemical shift. Thus, the change in chemical shift of the cyclodextrin H1 resonance in the presence of a mole equivalent of 2-arylpropionate in  $\text{d}_6$ -DMSO, also shown in Table 4.2, although reduced from its value in  $\text{D}_2\text{O}$ , remains significant, and may again be associated with conformational changes of the cyclodextrin on formation of the inclusion complex. Additionally, chiral splittings in the presence of  $\beta$ -cyclodextrin of the H2' and H4' resonances of sodium 2-phenylpropionate, both of magnitude 0.006ppm, and of resonances of ibuprofen sodium, described in Chapter 2, further indicate extensive interaction between the two species, almost certainly through the formation of an inclusion complex. Certainly, the formation of a lid-type complex seems unlikely, since such interactions have been observed only rarely, and generally for substrates which disfavour inclusion on steric grounds, or contain more than one hydrogen bonding functionality capable of interacting with the cyclodextrin hydroxyl groups [205-211].

The presence of large amounts of the inclusion complex coupled with a minimal shift of the cyclodextrin H5 resonance is, however, inconsistent with the aromatic ring current arguments of Demarco and Thakkar [155]. We believe this is a consequence of the failure of these authors to take account of the effect on chemical shift of the elimination of the solvation envelopes of the host cavity and guest which necessarily accompanies the formation of the inclusion complex (see Chapter 3). The significance of such solvent effects in cyclodextrin inclusion complexation has also been described by Sunamoto *et al.* [271], but remains largely overlooked.

The complexity of changes in chemical shift observed for the  $^1\text{H}$  resonances of the 2-arylpropionates in the presence of  $\beta$ -cyclodextrin in  $\text{D}_2\text{O}$  has already been referred to. In  $d_6$ -DMSO, such changes in shift appear more straightforward. Thus, for sodium 2-phenylpropionate, sodium 2-(4-chlorophenyl)propionate and ibuprofen sodium changes in chemical shift of the H3 and aromatic H2' and H3' resonances are of a similar magnitude, which suggest a common structure and comparable formation constant for the  $\beta$ -cyclodextrin inclusion complex for each of these substrates. The minimal changes of chemical shift of the cyclodextrin H5 resonance and the obscured nature of the H3 resonance restricts information regarding the nature of this structure. The greater size of the shift in the H3' aromatic resonance of the substrate would, however, suggest that it is this end of the aromatic molecule which penetrates the cyclodextrin cavity most deeply. Certainly, there would appear to be some fundamental difference in the structure of the inclusion complex between the aqueous and organic solvent, however, since at least in the case of ibuprofen sodium it is different resonances which undergo duplication in the presence of the cyclodextrin.

That the stability of the sodium 2-phenylpropionate complex is not substantially weaker than the complexes of other guests as was thought to be the case in  $\text{D}_2\text{O}$  suggests that the additional stability associated with the presence of

substituents in this molecule was most likely a consequence of hydrophobic interactions which are less significant in the organic solvent.

Changes in chemical shift of the H3 and H5' and H6' aromatic resonances of flurbiprofen sodium in the presence of  $\beta$ -cyclodextrin in  $d_6$ -DMSO are comparable with the corresponding resonances for these 2-phenylpropionates, and suggest a similarity of structure of the inclusion complex. Changes in chemical shift of the H3'' and H4'' resonances are negligible in comparison to the large values observed in  $D_2O$  and indicate that this phenyl ring no-longer interacts significantly with the cyclodextrin. This suggests that an important contribution to the driving force for its inclusion in aqueous solvent is the dimerisation of the cyclodextrin host through the formation of intermolecular hydrogen bonding interactions, which are less favoured in the strongly hydrogen bonding DMSO. Shifts of the  $^1H$  resonances of naproxen sodium in the presence of a mole equivalent of  $\beta$ -cyclodextrin in  $d_6$ -DMSO also suggest a stability of the order of that of the other substrates studied, although structural comparisons are difficult.

#### 4.4 $^1H$ NMR Studies of Conformational Changes of $\beta$ -cyclodextrin upon Complexation with some 2-Arylpropionates in $D_2O$

Conformational changes of the cyclodextrin molecule upon inclusion of a guest substrate have been suggested as a contributory factor to the energetic favourability of the complexation process, particularly for  $\alpha$ -cyclodextrin, as was discussed in Chapter 3. Thus, changes in chemical shift of the  $^1H$  resonances of those protons on the external surface of the  $\beta$ -cyclodextrin molecule in the presence of a mole equivalent of sodium 2-arylpropionate in  $D_2O$  have already been suggested as indicative of conformational changes of the cyclodextrin. Further analysis of  $^1H$  NMR data allows additional insight into these changes.

Conformational changes of the cyclodextrin may be broadly divided into two classes:



1. Intra-residue conformational changes of the glucopyranose ring,
2. Inter-residue conformational changes as a result of reorientation of these glucopyranose rings about the glycosidic linkage.

Inter-residue conformational changes of oligosaccharides are generally determined by measurement of inter-residue nOes and long-range carbon-proton coupling constants [200,201]. Since measurement of long-range heteronuclear coupling constants is generally an insensitive technique, and was not therefore considered appropriate for the low concentrations of solutions used in this work, changes in inter-residue conformation of  $\beta$ -cyclodextrin on complexation with the 2-arylpropionates were not examined. Recent methods describing the inverse detection of long-range heteronuclear coupling constants provide a suitable solution to this difficulty, however [272,273].

Information regarding changes in the conformation of the glucopyranose ring itself upon guest inclusion may be gained from the measurement of  $^1\text{H}$  coupling constants. A sine bell window function was used in place of the standard exponential window to reprocess the data of Section 4.2 with enhanced resolution, which allowed for the determination of some coupling constants which were not previously accessible because of extensive peak overlap. Such constants represent a population-average of those of the cyclodextrin in the free and complexed states, and are summarised in Table 4.3, together with those for methyl  $\alpha$ -D-glucoside, taken from the work of Wood *et al.* [274], and the predicted values for a  $^4\text{C}_1$  glucose ring, taken from the work of Hervé du Penhoat *et al.* [275], and calculated on the basis of the empirical equations of Altona and Haasnoot [276].

Comparison of the theoretical coupling constants and those of  $\beta$ -cyclodextrin in both the free and complexed state confirms that the glucose residues are held in an essentially classical chair conformation throughout.

Added substrate	H <sub>1,2</sub>	H <sub>2,3</sub>	H <sub>3,4</sub>	H <sub>4,5</sub>	H <sub>5,6</sub>	H <sub>6,6</sub>
none	3.7	9.8	9.0	9.3	*	*
sodium 2-phenylpropionate	3.8	9.9	9.0	9.7	4.4,2.2	12.4
sodium 2-(4-chlorophenyl)propionate	3.7	9.7	9.5	9.6	4.3,2.2	12.5
sodium 2-(4-nitrophenyl)propionate	3.7	9.7	9.5	9.6	4.3,2.6	12.6
ibuprofen sodium	3.7	9.8	8.8	9.8	3.4,2.3	*
naproxen sodium	3.8	10.0	8.6	*	3.2,1.9	12.4
flurbiprofen sodium	3.7	9.9	8.3	*	*	*

Substrate	H <sub>1,2</sub>	H <sub>2,3</sub>	H <sub>3,4</sub>	H <sub>4,5</sub>	H <sub>5,6</sub>	H <sub>6,6</sub>
calculated	3.6	9.9	9.4	9.8		
methyl $\alpha$ -D-glucoside	3.7	9.8	8.8	10.0	5.7,2.3	12.3

Table 4.3 Magnitude of 400MHz  $^1\text{H}$  NMR coupling constants of a 0.014M solution of  $\beta$ -cyclodextrin in the presence of some 2-arylpropionates in  $\text{D}_2\text{O}$  at 30°C

Variations in  $J_{5,6}$  may be interpreted in terms of preferential population of the rotameric forms described in Chapter 3. Thus, Wood *et al.* [274] observed a reduction in the coupling constants  $J_{5,6a}$  and  $J_{5,6b}$  for  $\alpha$ -cyclodextrin in comparison to those of methyl  $\alpha$ -D-glucoside, and interpreted this in terms of the increased proportion of the (-)gauche conformer in the cyclodextrin.

We were unable to measure  $J_{5,6}$  for  $\beta$ -cyclodextrin itself since resonances of the cyclodextrin H5 and H6 protons were not sufficiently well resolved even with the use of a resolution enhancement function. Our results have suggested, however, that the cyclodextrin complexes only weakly with sodium 2-phenylpropionate and that therefore  $J_{5,6}$  values observed in the presence of this substrate may be taken as a measure of  $J_{5,6}$  for the cyclodextrin in its free state. It can be seen from Table 4.3 that for ibuprofen sodium and naproxen sodium a reduction in magnitude of  $J_{5,6}$  for  $\beta$ -cyclodextrin in the presence of a mole equivalent of sodium 2-arylpropionate is apparent in comparison to coupling constants of  $\beta$ -cyclodextrin in the presence of sodium 2-phenylpropionate and of methyl  $\alpha$ -D-glucoside and again indicates an increased preference for the (-)gauche rotamer. Since this rotamer is associated with the OH6 group being directed away from the cyclodextrin cavity, this observation rules out interaction between the cyclodextrin primary hydroxyl group and the included guest, and may be a consequence of the steric requirements of the guest substrate or of the expulsion of water molecules from the macrocyclic cavity upon formation of the inclusion complex.

In the presence of sodium 2-(4-chlorophenyl)- and 2-(4-nitrophenyl)-propionate, however, it can be seen from Table 4.3 that  $J_{5,6}$  for  $\beta$ -cyclodextrin show little change from their values in the presence of sodium 2-phenylpropionate. Earlier analysis of chemical shift data has indicated that significant levels of complexation of these substrates occurs in aqueous solution. Interpretation of this contrasting behaviour of  $J_{5,6}$  then lends support to the common structure for the  $\beta$ -

cyclodextrin complex proposed in Section 4.2. Approach from the secondary hydroxyl face of the cyclodextrin by the guest substrates sodium 2-(4-chlorophenyl)- and 2-(4-nitrophenyl)propionate leaves the primary hydroxyl face, and therefore  $J_{5,6}$ , relatively unperturbed. For ibuprofen sodium, however, an equivalent structure of the inclusion complex leads to disturbance of the primary hydroxyl face as a result of proximity of the comparatively bulky *para*-isobutyl substituent.

#### 4.5 $^1\text{H}$ NMR Studies of the Stoichiometry of the Inclusion Complexes of $\beta$ -Cyclodextrin with some 2-Arylpropionates in $\text{D}_2\text{O}$

The preceding discussions have required many important assumptions. Thus, for example, in the interpretation of chemical shift data and in the calculations of Chapter 2, it has generally been assumed that the inclusion process involves interaction of a single substrate molecule with one of cyclodextrin. Since a 1:1 host:guest stoichiometry is indeed that most commonly observed for the inclusion complexes of the cyclodextrins [123], this is perhaps reasonable. Our results have suggested, however, that at least in the case of flurbiprofen sodium in aqueous solution, other complex stoichiometries may also be of some importance.

Investigation of the stoichiometry of the complexes examined in this work was therefore undertaken, using the Job or continuous variation method [277,278]. This procedure has been used by several authors in the determination of the stoichiometry of the inclusion complexes formed between cyclodextrins and a number of guest substrates by NMR [126,127,158].

The Job method requires that two species A and B interact to give a single complex of fixed stoichiometry. It can be shown that for a series of solutions of fixed total concentration, but varying mole ratio of A and B, that the maximum concentration of the complex occurs for that solution which contains the two components at a mole ratio corresponding to the stoichiometry of the complex.

Measurement of some parameter proportional to the amount of complex formed for such a series of solutions then readily yields its stoichiometry.

Classically, spectrophotometry has been widely used to monitor the concentration of complex in such studies, but NMR may be used equally well. Thus, consider the general complexation equilibrium of substrate S with cyclodextrin CD,



If it is assumed that no discrimination of the two enantiomers of a chiral substrate by the cyclodextrin is present, then from equation 2.5 (Section 2.7.1) the mole fraction of S in the complexed state is given by:

$$f = \frac{\delta S_o - \delta S_f}{\delta S_c - \delta S_f} \quad (4.1)$$

where  $\delta S_f$  and  $\delta S_c$  denote the chemical shift of some resonance of the substrate in the free and complexed states respectively and  $\delta S_o$  is its value observed in solution. The concentration of complex in solution is then given by,

$$[S \cdot \text{CD}_a] = f[S]_t \quad (4.2)$$

where  $[S]_t$  denotes the total concentration of the substrate, both free and complexed, which from equation 4.1 gives,

$$[S \cdot \text{CD}_a] = [S]_t \times \frac{\delta S_o - \delta S_f}{\delta S_c - \delta S_f} \quad (4.3)$$

and since  $(\delta S_c - \delta S_f)$  is a constant,

$$[S \cdot \text{CD}_a] \propto (\delta S_o - \delta S_f)[S]_t \quad (4.4)$$

For the Job method, all solutions are of fixed total concentration, so that,

$$[S \cdot \text{CD}_a] \propto F(\delta S_o - \delta S_f) \quad (4.5)$$

where  $F$  represents the mole fraction of this concentration of substrate added to the solution.  $F(\delta S_o - \delta S_f)$  is then used as a measure of the concentration of complex in solution. A corresponding argument may be applied to the resonances of the cyclodextrin macrocycle.

Figures 4.5-4.10 show the results of Job plot studies of the complexation of  $\beta$ -cyclodextrin with the sodium 2-arylpropionates in  $D_2O$  for various substrate and cyclodextrin  $^1H$  NMR resonances. Those resonances which showed the largest shifts and no duplication and were well separated from other signals were found to be most suitable for this study. Samples were prepared by quantitative mixing of solutions of equal concentration of the sodium 2-arylpropionate and  $\beta$ -cyclodextrin in  $D_2O$ . In order to facilitate the dissolution of  $\beta$ -cyclodextrin, the concentration of each of these solutions was reduced from that of preceding experiments, and as a result, analysis of cyclodextrin resonances was therefore also generally to be preferred because of the greater signal-to-noise ratio associated with these signals. This difference in solution concentration, combined with acquisition of NMR data at ambient temperature as opposed to  $30^\circ C$ , was thought to be responsible for the observation that changes in chemical shift of both cyclodextrin and substrate  $^1H$  resonances in the Job solution corresponding to a 1:1 mole ratio of the two components showed some deviation from those values given in Table 4.1 and Figure 4.3.

Although the Job experiment often required the analysis of undesirably small changes in chemical shift of both substrate and cyclodextrin resonances, it was possible to assign a 1:1 stoichiometry to all of the  $\beta$ -cyclodextrin inclusion complexes of the sodium 2-arylpropionates studied, excepting that formed with sodium 2-phenylpropionate. Changes in chemical shift of those resonances of host and guest which could be readily determined in this case were too small to allow distinction between different complex stoichiometries, again presumably a consequence of the weak interaction between the two. It seems unlikely, however,

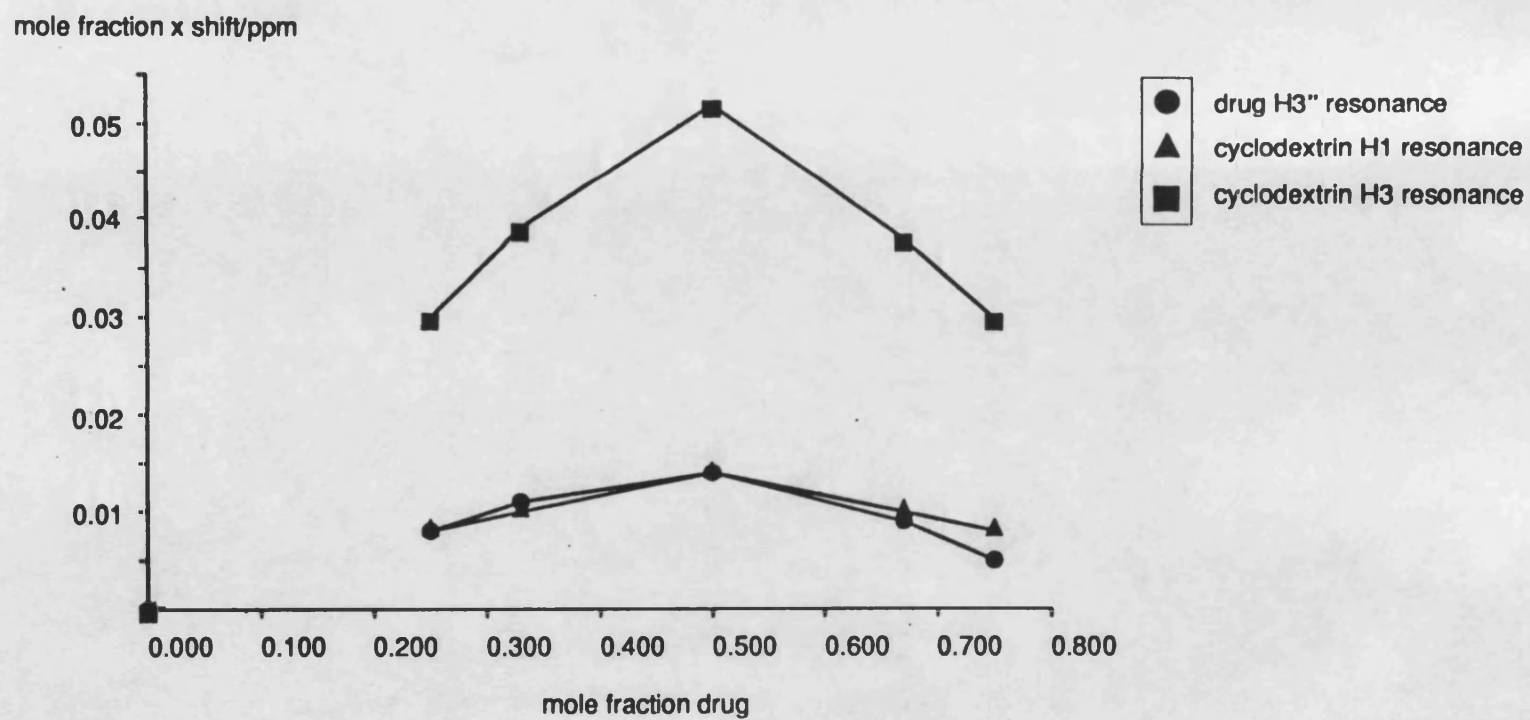


Figure 4.5 Selected resonances from a 270MHz  $^1\text{H}$  Job plot study of the complexation of ibuprofen sodium with  $\beta$ -cyclodextrin in  $\text{D}_2\text{O}$

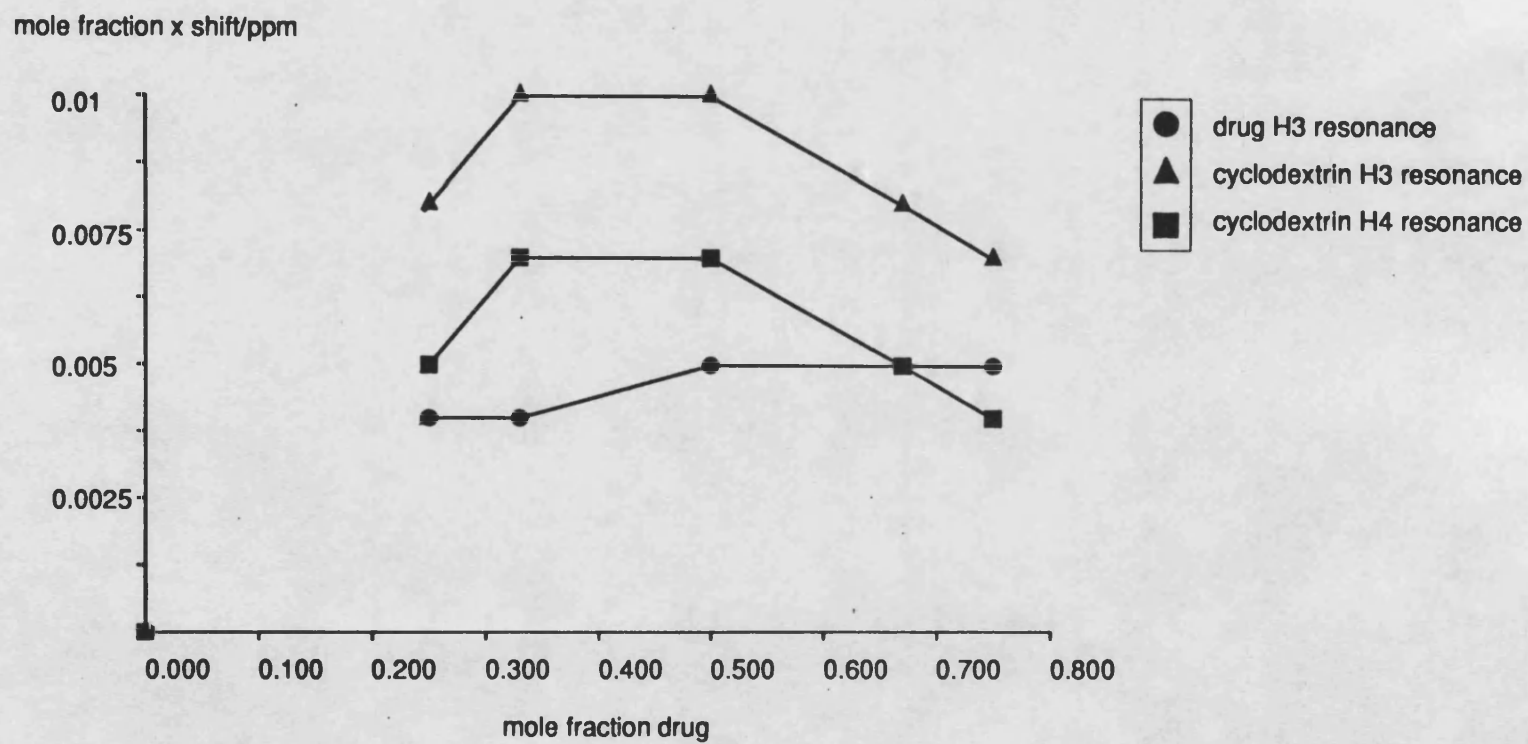


Figure 4.6 Selected resonances from a 270MHz  $^1H$  Job plot study of the complexation of sodium 2-phenylpropionate with  $\beta$ -cyclodextrin in  $D_2O$



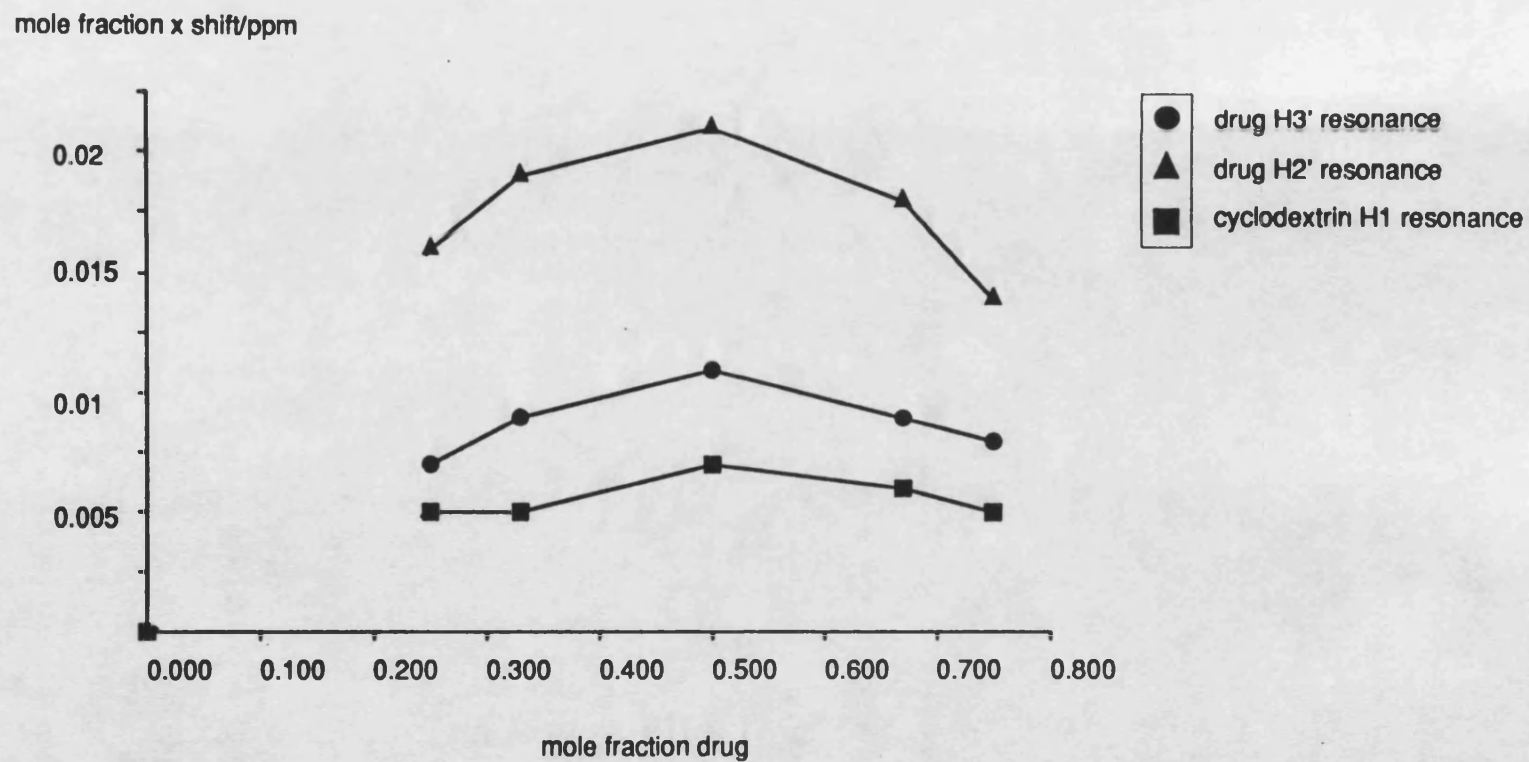


Figure 4.7 Selected resonances from a 270MHz  $^1\text{H}$  Job plot study of the complexation of sodium 2-(4-nitrophenyl)propionate with  $\beta$ -cyclodextrin in  $\text{D}_2\text{O}$

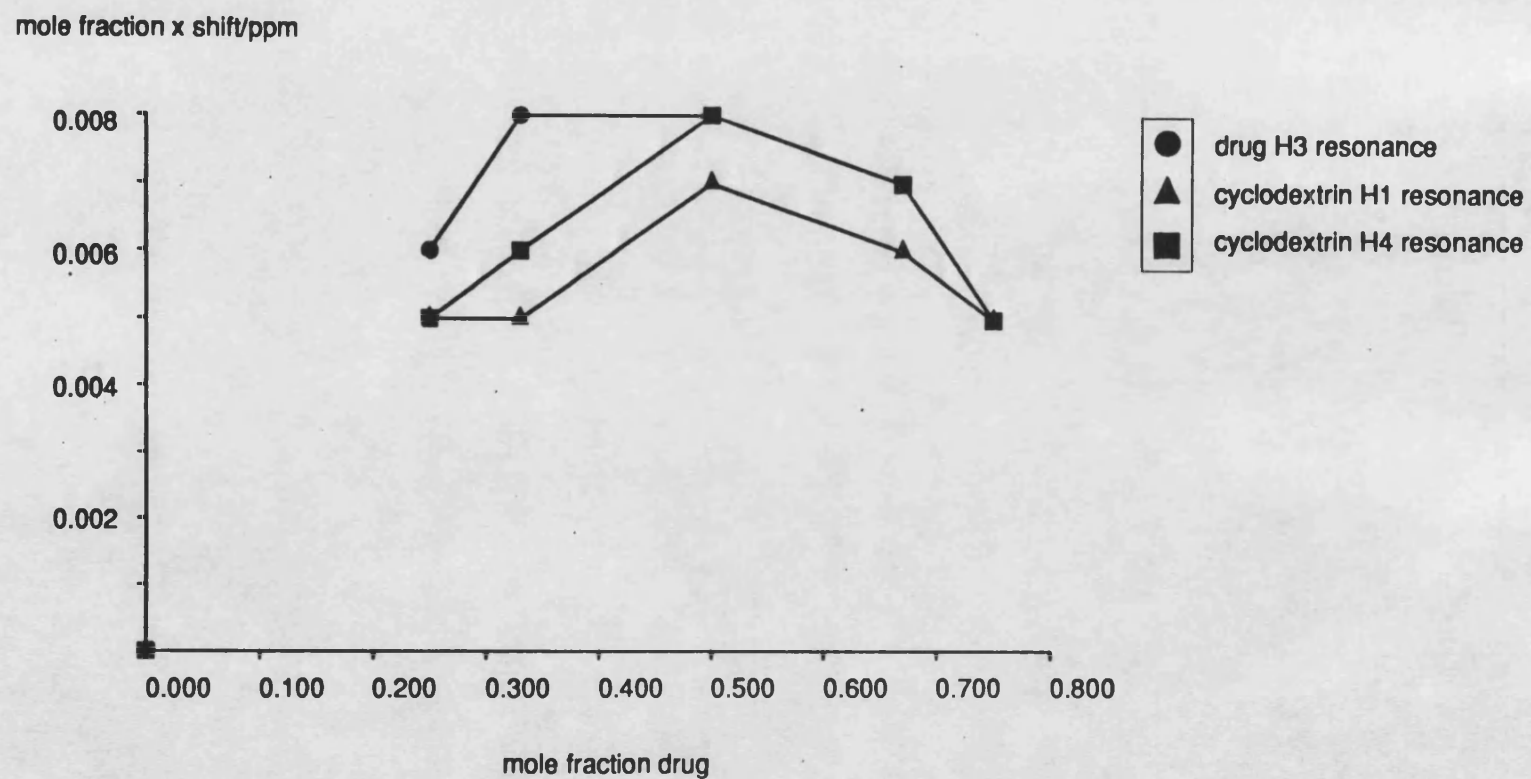


Figure 4.8 Selected resonances from a 270MHz  $^1\text{H}$  Job plot study of the complexation of sodium 2-(4-chlorophenyl)propionate with  $\beta$ -cyclodextrin in  $\text{D}_2\text{O}$

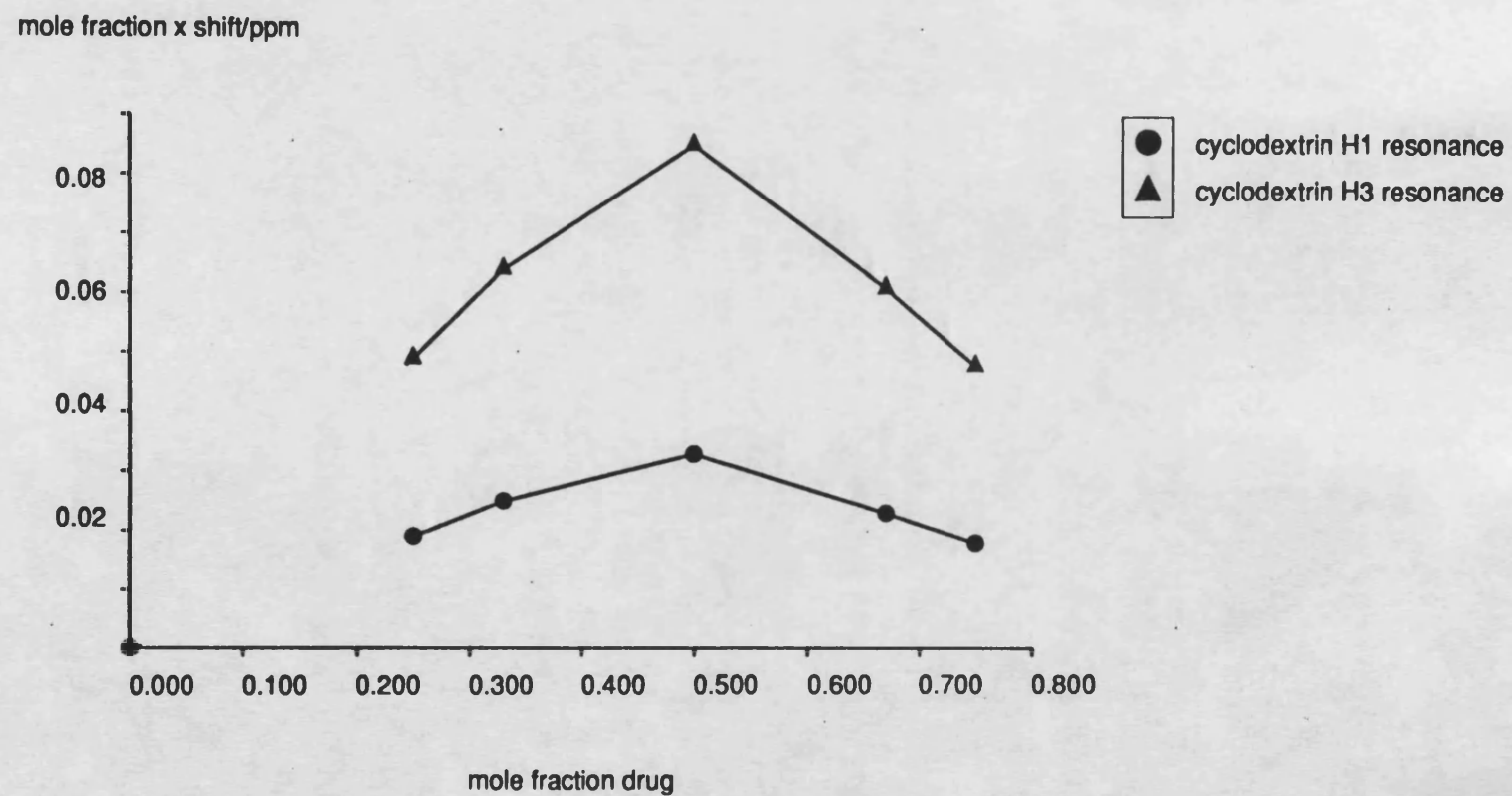


Figure 4.9 Selected resonances from a 270MHz  $^1\text{H}$  Job plot study of the complexation of flurbiprofen sodium with  $\beta$ -cyclodextrin in  $\text{D}_2\text{O}$

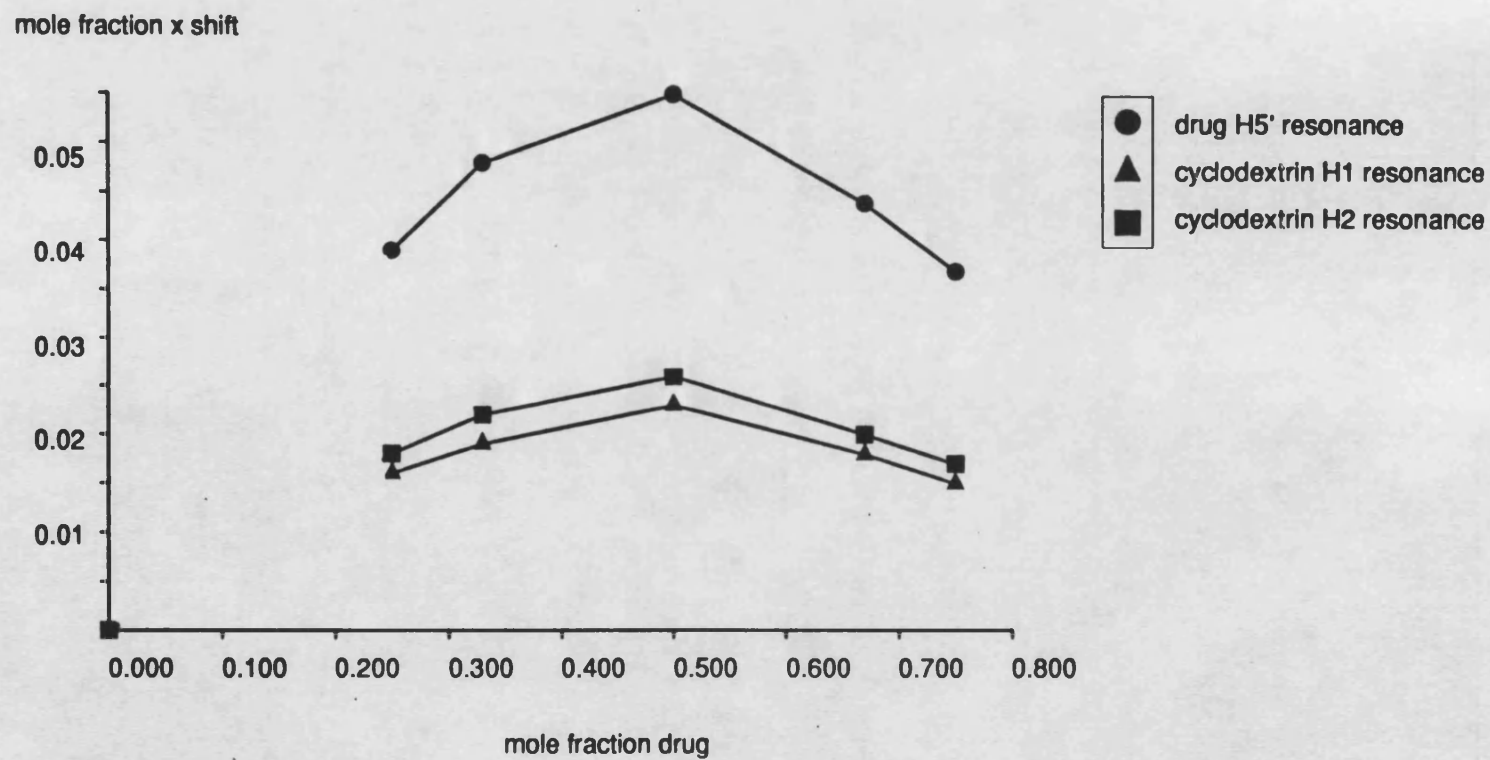


Figure 4.10 Selected resonances from a 270MHz  $^1\text{H}$  Job plot study of the complexation of naproxen sodium with  $\beta$ -cyclodextrin in  $\text{D}_2\text{O}$

that the stoichiometry of this complex should differ from that of the other substrates examined, particularly in view of the structural similarity of the sodium 2-phenylpropionate molecule to that of, for example, sodium 2-(4-chlorophenyl)propionate. Solutions were, however, further examined by  $^{13}\text{C}$  NMR to support this argument, on the basis that this nucleus, with its wider chemical shift range, might be more sensitive to the formation of the inclusion complex [279]. It was possible to detect only the  $^{13}\text{C}$  resonances of the cyclodextrin macrocycle in a reasonable experiment time of approximately one hour per sample. These resonances were referenced to a solution of DSS in  $\text{D}_2\text{O}$  (the use of a reference sample contained in a separate NMR tube being more acceptable for the wider chemical shift ranges associated with heteronuclei, see Chapter 2), but were found to show no significant variation in chemical shift between solutions.

The determination of a 1:1 stoichiometry for the inclusion complexes studied here does not allow distinction between interaction of individual molecules and the formation of dimeric structures such as those observed in the crystalline complexes of flurbiprofen and fenoprofen with  $\beta$ -cyclodextrin (Section 3.5). Further examination of the Job plot for points of inflection, which are not generally visible to the eye, may effect such a distinction [278], but since changes in chemical shift were generally small, such detailed analysis was not considered appropriate.

Our results have already suggested that the complexation of flurbiprofen sodium with  $\beta$ -cyclodextrin involves interaction of the guest with more than one cyclodextrin molecule. On the basis of the 1:1 stoichiometry found here, a dimeric structure for this complex, similar to that observed in the crystal, is therefore suggested. A study of the  $^1\text{H}$  NMR spectrum of  $\beta$ -cyclodextrin in  $\text{D}_2\text{O}$  over a range of concentrations incorporating those of the Job plot showed that resonances were essentially independent of concentration which suggests that, at least in the absence of guest substrate, there is little tendency to dimerisation of the

macrocycle [280,281]. We propose on steric grounds that in such a structure it is the non-fluorinated phenyl rings of the substrate which would most likely lie adjacent at the cyclodextrin interface. This suggestion is supported by the unusual observation of large up-field shifts in  $^1\text{H}$  resonance of all protons of this aromatic ring. The promotion of dimerisation in the presence of flurbiprofen sodium is then a consequence of a favourable hydrophobic interaction between the two phenyl rings at the interface or of the partial inclusion of each of these phenyl rings into the cavity of the neighbouring cyclodextrin molecule. For the salts of the other 2-phenylpropionates it is difficult to envisage a comparable structure with such stabilising features, and it is therefore assumed for these complexes that the 1:1 stoichiometry given by the appropriate Job plot is indicative of a monomeric structure of the cyclodextrin inclusion complex. The interaction of naproxen sodium is less clear-cut. Thus, for example, Samai has reported the association of the 1:1 inclusion complexes of the structurally related compounds naphthalene [280], 2-methoxynaphthalene [280] and 1-cyanonaphthalene [269] with  $\beta$ -cyclodextrin in aqueous solutions at concentrations comparable with those used in this work.

During the course of this work, an important premise of the use of the Job method in NMR spectroscopy was also examined, that is, that resonances of species in the uncomplexed (and complexed) state are independent of concentration (equation 4.4). The concentration independence of the chemical shifts of the  $^1\text{H}$  resonances of  $\beta$ -cyclodextrin has already been described. Ibuprofen sodium and naproxen sodium were chosen as representative of the 2-arylpropionate substrates. It was found that whilst ibuprofen sodium similarly showed a concentration independence in its  $^1\text{H}$  NMR spectrum, significant changes in the chemical shift of the resonances of naproxen sodium were observed (Table 4.4). Such dependence is presumably a consequence of molecular association through a  $\pi$ - $\pi$  stacking or hydrophobic interaction and further emphasises the

1. ibuprofen sodium

Resonance	Chemical shift/ppm		
	0.0077M	0.014M	0.055M
H2'	7.352	7.351	7.352
H3'	7.297	7.296	7.295
H2	3.693	3.692	3.694
H1''	2.563	2.562	2.561
H2''	1.924	1.922	1.922
H3	1.471	1.470	1.472
H3''	0.958	0.958	0.958

2. naproxen sodium

Resonance	Chemical shift/ppm		
	0.0055M	0.014M	0.052M
H8'	7.940	7.929	7.881
H4'	7.912	7.901	7.854
H1'	7.848	7.839	7.809
H3'	7.575	7.570	7.549
H5'	7.453	7.438	7.366
H7'	7.308	7.296	7.244
OMe	4.034	4.024	3.977
H2	3.867	3.864	3.851
H3	1.572	1.570	1.565

Table 4.4 400MHz <sup>1</sup>H NMR data for ibuprofen sodium and naproxen sodium at varying concentrations in D<sub>2</sub>O at 30°C

complexity of interaction between the 2-arylpropionates and  $\beta$ -cyclodextrin in aqueous solution.

#### 4.6 NMR Studies of Hydrogen Bonding Interactions between $\beta$ -Cyclodextrin and some 2-Arylpropionates

Factors contributing to the thermodynamic stability of cyclodextrin inclusion complexes in aqueous solution have been discussed in Chapter 3. It is generally considered that hydrogen bonding between host and guest does not provide a major contribution to complex stability. In contrast, differential hydrogen bonding between the host and the two enantiomers of a guest substrate is thought to be an important process in the chiral recognition of the guest by the cyclodextrin. It was our aim therefore to attempt to determine the presence or absence of such interactions in the  $\beta$ -cyclodextrin inclusion complexes of the 2-arylpropionates.

A common potential site of hydrogen bonding of each of the substrates is the carboxylate group. We also identify the nitro group of sodium 2-(4-nitrophenyl)propionate and the methoxy group of naproxen sodium as additional sources of interaction.

Direct observation of the  $^1\text{H}$  resonances of the hydroxyl groups of  $\beta$ -cyclodextrin, for further investigations of the presence of hydrogen bonding interactions with an included guest, was not possible since these signals are absent from spectra recorded in  $\text{D}_2\text{O}$ , as a result of the fast exchange which they undergo with the solvent. Whilst it has been shown that they may be detected in non-deuterated water, Symons *et al.* [282] report that careful control of both pH and temperature is required to slow the exchange process sufficiently for resonances of a reasonable sharpness to be obtained. The acidic pH recommended by these authors was not considered compatible with the 2-arylpropionate substrates used in this study. Other experimental methods were therefore examined.



#### 4.6.1 <sup>1</sup>H NMR Studies of the Complexation of $\beta$ -Cyclodextrin with Structural Analogues of the 2-Arylpropionates in D<sub>2</sub>O

Structural analogues of 2-phenylpropionic acid were selected to investigate the importance of the carboxylic group in the  $\beta$ -cyclodextrin inclusion process. Their structures, together with that of 2-phenylpropionic acid, are shown in Figure 4.11.

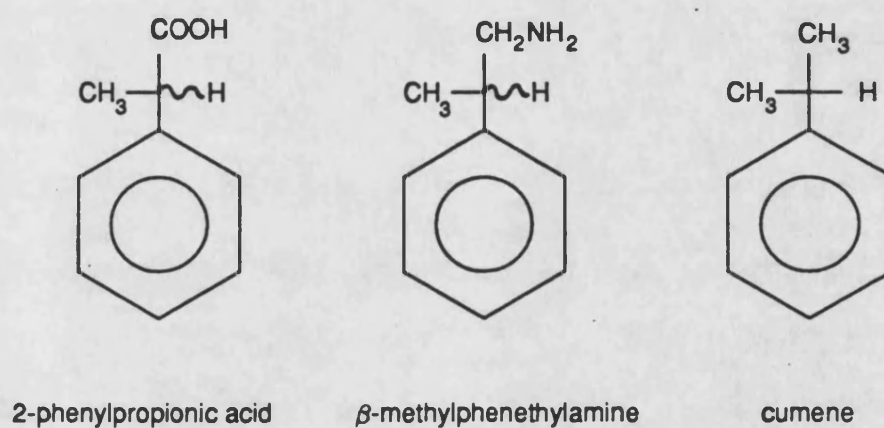


Figure 4.11 2-phenylpropionic acid and some structural analogues

Mixtures of a 1:1 mole ratio of cumene or  $\beta$ -methylphenethylamine and  $\beta$ -cyclodextrin in D<sub>2</sub>O at concentrations of approximately 0.014M failed to dissolve readily, however, and were therefore transferred to an ultra-sonic bath for 1 1/2 hours. At the end of this period, dissolution of only the mixture of  $\beta$ -methylphenethylamine and  $\beta$ -cyclodextrin was achieved, but precipitation followed on subsequent cooling to room temperature. Investigations of the inclusion properties of the structural analogues of 2-phenylpropionic acid were not therefore pursued.

#### 4.6.2 <sup>17</sup>O NMR Studies of the Complexation of Cyclodextrins with the 2-Arylpropionates in D<sub>2</sub>O

The recent studies of Uedairi *et al.* [283,284] have highlighted the relationship between the <sup>17</sup>O longitudinal relaxation time, T<sub>1</sub>, of the water resonance in aqueous solutions of carbohydrates and the mean number of equatorial OH groups of these substrates. Thus, these authors have shown that for α- and γ-cyclodextrin the T<sub>1</sub> of pure water and of a solution of the carbohydrate of concentration m, represented by T<sub>0</sub> and T respectively, are related by the expression,

$$T_0 = 1 + \frac{n_{\text{dm}} \times m}{T \times 55.5} \quad (4.6)$$

where n<sub>dm</sub> is the dynamic hydration number of the oligosaccharide. n<sub>dm</sub> has, in turn, been shown to be linearly dependent on the number of equatorial hydroxyl groups in the carbohydrate.

We postulated that a hydrogen bonding interaction between the cyclodextrin host and an included guest might bring about changes in the hydration sphere of the macrocycle, and consequently the <sup>17</sup>O T<sub>1</sub> of the solvent. To test this hypothesis we chose to examine the interaction of naproxen sodium with γ-cyclodextrin, since this cyclodextrin is considerably more soluble than its β oligomer and therefore allowed the use of the more highly concentrated solutions in which the anticipated effect would be most prominent. <sup>1</sup>H NMR studies confirmed inclusion of the naproxen sodium molecule in this macrocycle.

<sup>17</sup>O T<sub>1</sub> measurements of deuterated water and of solutions of naproxen sodium, γ-cyclodextrin and a 1:1 mole ratio mixture of the two in D<sub>2</sub>O were made using the standard inversion-recovery sequence described in Chapter 3. Its use was possible despite the low natural abundance and magnetogyric ratio of the <sup>17</sup>O nucleus, since rapid quadrupolar relaxation allowed fast pulsing of the sample, and

because the solvent analyte was present in high concentrations. The results of these measurements are shown in Table 4.5.

Added substrate	$^{17}\text{O}$ $T_1$ in ms
none	6.3,6.6
$\gamma$ -cyclodextrin	5.8
naproxen sodium	6.0
1:1 naproxen sodium: $\gamma$ -cyclodextrin	5.9

Table 4.5 54MHz  $^{17}\text{O}$   $T_1$  of  $\text{D}_2\text{O}$  in the presence of 0.078M naproxen sodium and/or  $\gamma$ -cyclodextrin at 30°C

The observed reduction in  $T_1$  in the presence of  $\gamma$ -cyclodextrin gives from equation 4.6 a dynamic hydration number of 79.9, which is reasonably consistent with the value of 77.3 found by Uedairi and co-workers [284], considering that our value was calculated from a single data point. This indicates that hydration of the sugar is little different in deuterated versus non-deuterated solvent.

We had anticipated that the reduction of  $^{17}\text{O}$   $T_1$  from that of pure solvent in the presence of naproxen sodium would be negligible in comparison to that in the presence of  $\gamma$ -cyclodextrin as a result of the considerably smaller molecular size of the former. In this way, it was our intention to interpret relaxation parameters determined in the presence of a 1:1 mole ratio mixture of salt and cyclodextrin solely in terms of the hydration properties of the carbohydrate. In practice, it can be seen from Table 4.5 that a reduction in  $T_1$  in the solution of naproxen sodium comparable with that in the presence of  $\gamma$ -cyclodextrin is observed. The magnitude of this reduction then obviated any attempt to interpret the  $T_1$  measured for a 1:1 mole ratio mixture of naproxen sodium and  $\gamma$ -cyclodextrin in terms of the hydration properties of the macrocycle. It is therefore concluded that measurement of solvent  $^{17}\text{O}$   $T_1$  is an inappropriate parameter for the determination of hydrogen bonding interactions in the cyclodextrin inclusion complex. That the individual

effects of naproxen sodium and  $\gamma$ -cyclodextrin on  $D_2O$   $^{17}O$   $T_1$  values is not, however, additive in a mixture of the two is suggestive of the formation of significant amounts of the inclusion complex.

#### 4.6.3 $^1H$ NMR Studies of the Complexation of $\beta$ -Cyclodextrin with some 2-Arylpropionates in $d_6$ -DMSO

An alternative approach was to examine the  $\beta$ -cyclodextrin inclusion complex interaction in a non-exchanging solvent.  $^1H$  NMR studies in  $d_6$ -DMSO have already been described in Chapter 2 and Section 4.3. Little attention has been given, however, to the effect of added substrate on the hydroxyl resonances of the cyclodextrin. Changes in chemical shift of these resonances in the presence of a mole equivalent of 2-arylpropionate are shown in Table 4.6.

Substrate	Change in chemical shift/ppm	
	OH2&3	OH6
sodium 2-phenylpropionate	>+0.276	+0.023
sodium 2-(4-chlorophenyl)propionate	>+0.273	+0.035
ibuprofen sodium	>+0.292	+0.010
flurbiprofen sodium	>+0.233	+0.019
naproxen sodium	>+0.306	+0.016

Table 4.6 Change in 400MHz  $^1H$  chemical shift of hydroxyl resonances in a 0.014M solution of  $\beta$ -cyclodextrin in the presence of a mole equivalent of some 2-arylpropionates in  $d_6$ -DMSO at 30°C

Although OH2 and OH3 resonances of the cyclodextrin are indistinguishable in the presence of added substrate, a significant down-field shift of these signals remains readily apparent. Such shifts are consistent with the formation of a hydrogen bond between the secondary hydroxyl groups of the cyclodextrin and an included guest and suggest a common orientation of the two in the inclusion complex in which the hydrogen bond accepting carboxylate functionality lies at the secondary hydroxyl face of the cyclodextrin (although in

the case of naproxen sodium a hydrogen bonding interaction with the methoxy substituent cannot be ruled out). Such a structure is in agreement with that proposed to exist in aqueous solution in Section 4.2. Indeed, the presence of host-guest hydrogen bonding in DMSO is suggestive of an equivalent interaction in aqueous solvent as a result of the lesser tendency of the latter to disrupt solute hydrogen bonding. The magnitude of down-field shifts of cyclodextrin hydroxyl resonances are additionally indicative of a comparable stability of the inclusion complex for each substrate.

Alternatively, shifts in the hydroxyl resonances may be interpreted in terms of an exchange mechanism in the presence of the 2-arylpropionate salt. Marked broadening of hydroxyl resonances suggests that such a process is certainly contributory to observed changes in chemical shift of the cyclodextrin hydroxyl groups.

The temperature dependence of chemical shift of hydroxyl resonances of the cyclodextrin in the presence of selected substrates was also examined in this work. Linear regression analysis of chemical shift data with temperature gives the  $d\delta/dT$  values summarised in Table 4.7.

Substrate	$10^3 \times d\delta/dT$ in ppm/ $^{\circ}\text{C}$		
	OH2	OH3	OH6
none	-5.3	-4.1	-5.6
sodium 2-phenylpropionate	-5.3		-5.6
ibuprofen sodium	-5.4		-5.7
naproxen sodium	-5.2		-5.6

Table 4.7 Temperature dependence of 400MHz  $^1\text{H}$  resonances of a 0.014M solution of  $\beta$ -cyclodextrin in the presence of a mole equivalent of some 2-arylpropionates in  $d_6$ -DMSO

Temperature dependence of the hydroxyl resonances of  $\beta$ -cyclodextrin is in agreement with the results of Onda and co-workers [202], who interpreted the

lesser sensitivity of chemical shifts of the secondary hydroxyl resonance to changes in temperature to the preferential formation of intramolecular hydrogen bonds by these groups. In addition, relative magnitudes of the OH2 and OH3  $d\delta/dT$  values may be associated with proton donation within this hydrogen bonding network arising from the OH3 group.

In the presence of a mole equivalent of guest substrate broadening and overlap of the OH2 and OH3 resonances prevents distinction between these two group, so that a single  $d\delta/dT$  value may be calculated. This value remains less than that of the primary hydroxyl groups in all cases and is indicative of the continued presence of intramolecular hydrogen bonding of the secondary hydroxyl groups in the presence of guest substrate. Indistinction of the OH2 and OH3 groups prevents the determination of the directional sense of this bonding, however.

#### 4.7 Application of the Nuclear Overhauser Effect to Studies of the Complexation of $\beta$ -Cyclodextrin with some 2- Arylpropionates

The preceding discussions of structural properties of the  $\beta$ -cyclodextrin inclusion complexes of the sodium 2-arylpropionates have relied on a somewhat subjective interpretation of the results of various NMR experiments. A more direct approach to structural information in NMR spectroscopy is, however, achieved by the measurement of the nuclear Overhauser effect (nOe), methods for which have been described in Chapter 3. Indeed, several authors have reported use of both one- and two- dimensional nOe experiments in the elucidation of the structure of cyclodextrin inclusion complexes with various substrates [127,267,285,286].

#### 4.7.1 Studies with the nOe Difference Experiment

Initial nOe studies of the  $\beta$ -cyclodextrin inclusion complexes of the 2-arylpropionates were carried out using the nOe difference method and with ibuprofen sodium as the chosen substrate, since earlier experiments had suggested extensive formation of a simple monomeric complex with 1:1 guest:host stoichiometry in aqueous solution. Additionally,  $^1\text{H}$  resonances of the ibuprofen sodium salt in the presence of a mole equivalent of  $\beta$ -cyclodextrin in  $\text{D}_2\text{O}$  are well resolved and thus facilitate the acquisition and interpretation of the nOe difference spectrum.

Several practical difficulties were encountered in the implementation of the nOe difference experiment. Thus, for example, the presence of any nOe within the cyclodextrin resonances upon irradiation of drug signals was difficult to observe as a result of the former's overlapping nature.

Figure 4.12 shows the nOe difference spectrum resulting from the converse process, that is irradiation of the cyclodextrin H3, H5 and H6  $^1\text{H}$  resonances. Although small positive enhancements of the ibuprofen sodium H3' resonance are apparent following saturation of these cyclodextrin signals, in general other resonances of the drug do not exhibit such intermolecular nOes. Inoue *et al.* [285] have pointed out that the molecular size of the cyclodextrin molecule and its inclusion complexes is such that nOes lie close to the cross-over point between the positive and negative nOe regimes and that therefore nOes for such species are often small or even zero. It would therefore seem that this absence of any additional nOes for the  $\beta$ -cyclodextrin complex of ibuprofen sodium is most likely a consequence of their inherently small size.

We attempted to circumvent this problem by increasing the temperature at which the nOe difference spectrum was acquired to  $75^\circ\text{C}$  as opposed to  $30^\circ\text{C}$ , thus decreasing the molecular correlation time and pushing the system into the extreme narrowing limit, where nOes of increasing positive magnitude are to be expected.





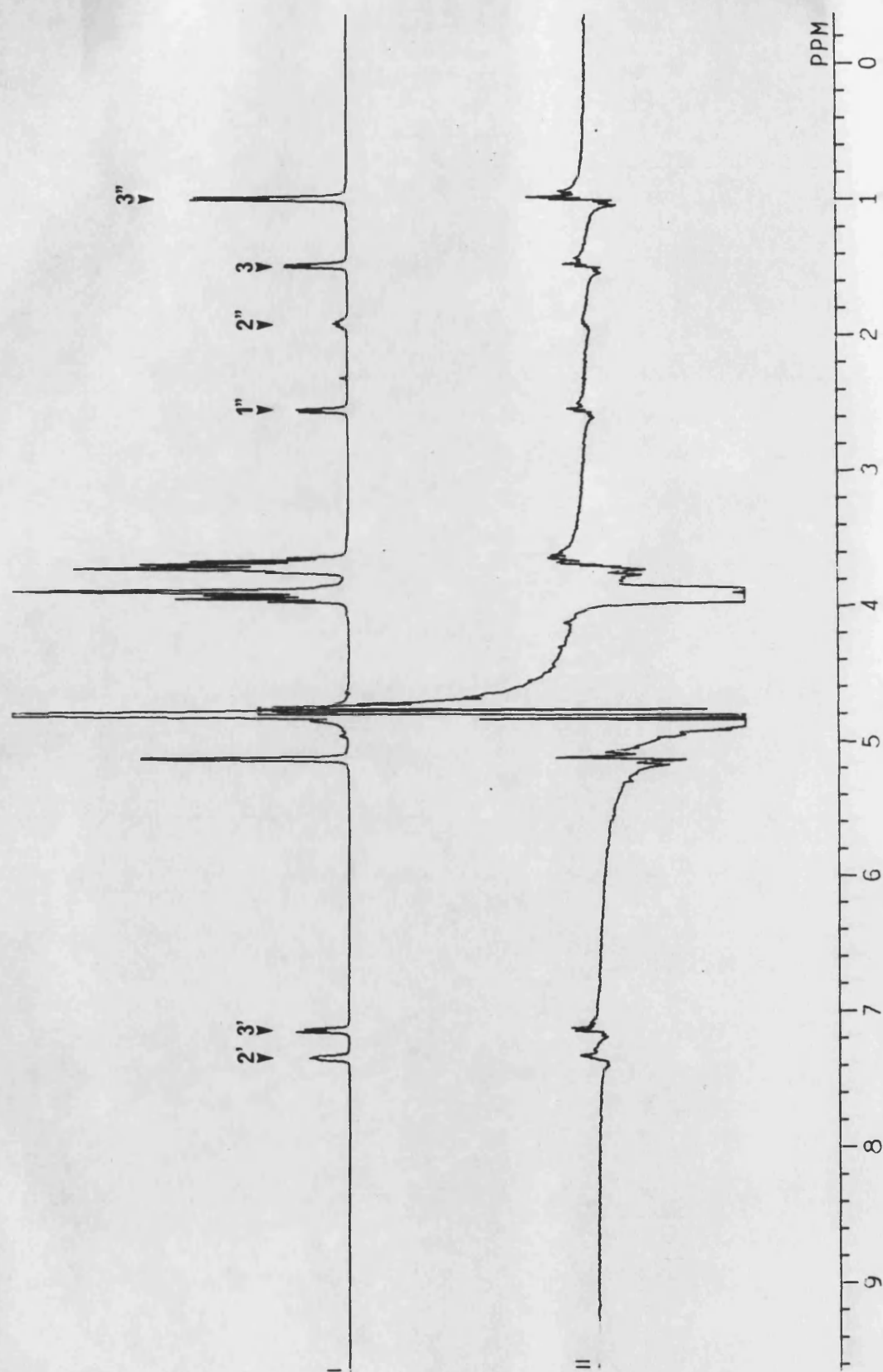




Figure 4.12 400MHz <sup>1</sup>H nOe difference experiment for a 0.014M solution of ibuprofen sodium in the presence of a mole equivalent of  $\beta$ -cyclodextrin in D<sub>2</sub>O at 30°C  
Control spectrum (I) and difference spectra following irradiation of cyclodextrin H3 (ii), H6 (iii) and H5 (iv) resonances

An additional consequence of this change in temperature was to decrease the amount of complex present in solution, but since chiral duplication of the ibuprofen anion H2' and H3 resonances was apparent even at this raised temperature, clearly significant levels of the inclusion complex remain. Indeed, this small reduction in complexation was in practice advantageous. Thus, at 30°C, a COSY-45 experiment of a 1:1 mole ratio solution of ibuprofen sodium and  $\beta$ -cyclodextrin in D<sub>2</sub>O showed that the H2 of the ibuprofen anion lies obscured in the region of the cyclodextrin H5 resonance, itself only partially resolved from other cyclodextrin resonances, so that selective irradiation of the H5 resonance in an nOe experiment, without accompanying perturbation of the ibuprofen anion H2 resonance, may be difficult to achieve. In contrast, at 75°C, a COSY-45 experiment showed that the down-field shift of the cyclodextrin H5 resonance, which may be associated with the reduced levels of complexation, allowed these resonances to be readily distinguished (although the H2 resonance of the ibuprofen anion remained obscured below the cyclodextrin H2 signal), Figure 4.13.

Irradiation of the cyclodextrin H3 and H5 resonances in an nOe difference experiment at 75°C lead to increased clarity of positive enhancements at both drug aromatic resonances, Figure 4.14. Additionally, both difference spectra showed enhancements of all resonances of the isobutyl substituent of the drug. Irradiation of the cyclodextrin H3 resonance also showed a positive enhancement of the H3 resonance, and thus supports the orientation of the ibuprofen anion in the  $\beta$ -cyclodextrin already proposed to exist in D<sub>2</sub>O (Section 4.2) and d<sub>6</sub>-DMSO (Section 4.6.3). In view of the almost universal enhancement of drug resonances we were, however, concerned that the effect of the increase in temperature, in addition to the desired change in molecular correlation time of the complex, might also be to promote permutations of its structure, to which activation barriers may be present at lower temperatures. A lowering of the sample temperature in the nOe difference experiment, which would have the opposed effect of increasing the molecular

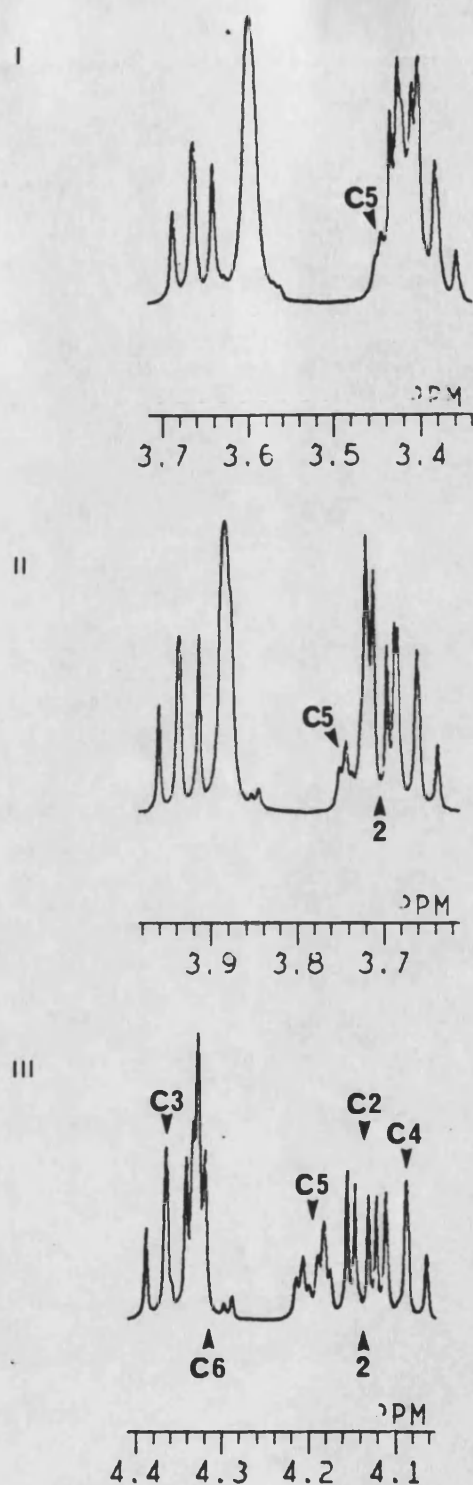


Figure 4.13 Part of the 400MHz  $^1\text{H}$  spectrum of a 0.014M solution of ibuprofen sodium in the presence of a mole equivalent of  $\beta$ -cyclodextrin in  $\text{D}_2\text{O}$  at (i) 50°C, (ii) 30°C and (iii) 75°C, showing the relative positions of the cyclodextrin H5 and drug H2 resonances. C denotes cyclodextrin resonances



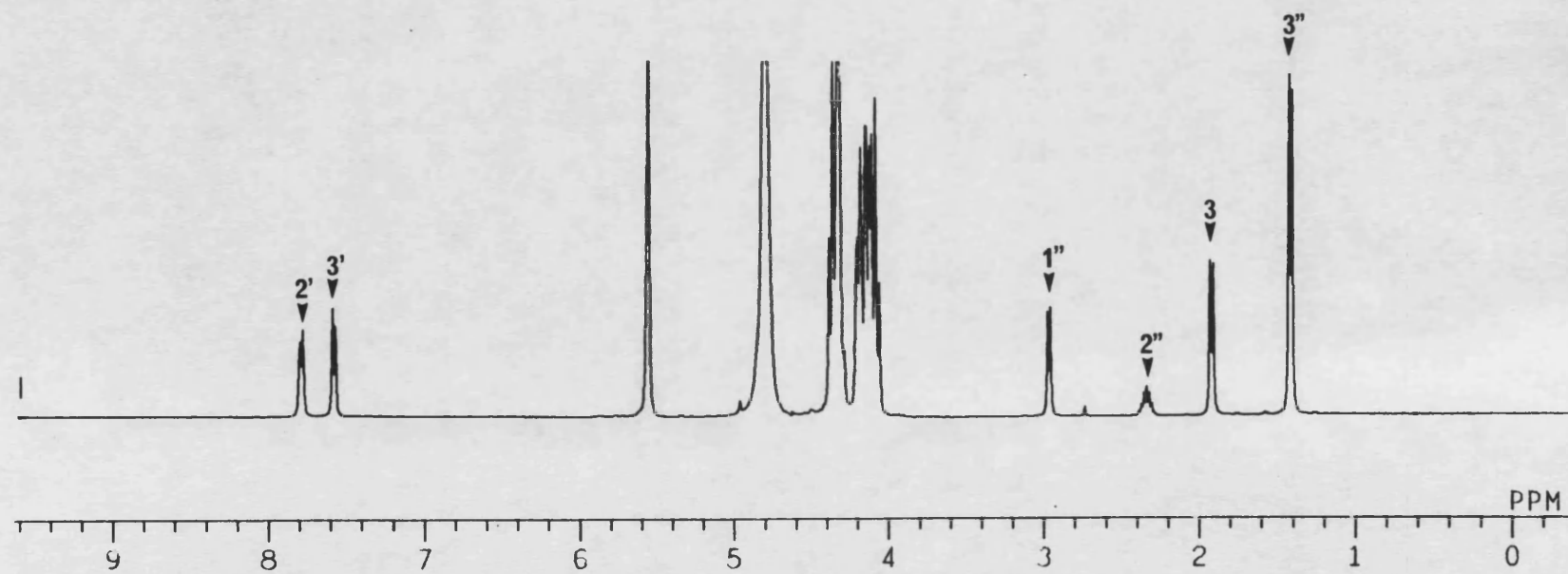




Figure 4.14 400MHz  $^1\text{H}$  nOe difference experiment for a 0.014M solution of ibuprofen sodium in the presence of a mole equivalent of  $\beta$ -cyclodextrin in  $\text{D}_2\text{O}$  at  $75^\circ\text{C}$ . Control spectrum (i) and difference spectra following irradiation of cyclodextrin H5 (ii) and H3 (iii) resonances

correlation time of the complex, pushing it into the negative nOe regime, whilst simultaneously promoting complexation, was considered inappropriate. Thus, the possible reduction in temperature is limited by the freezing point of the aqueous solvent and additionally, at 5°C, it is observed that the cyclodextrin H5 resonance is increasingly obscured beneath that of the cyclodextrin H2 resonance, Figure 4.13.

An alternative approach to increasing the molecular correlation time of the system was to examine complexation of ibuprofen sodium with  $\beta$ -cyclodextrin in a solvent of greater viscosity than D<sub>2</sub>O. Such studies in d<sub>6</sub>-DMSO, which has the added advantage of providing a lock signal more suited to the difference method [253], were, however, unsuccessful, owing to restrictions imposed by the overlap of the H3 and H6 resonances of the cyclodextrin, which therefore ruled out their selective saturation in an nOe difference experiment. Irradiation of low and high field aromatic resonances of ibuprofen sodium was however able to confirm assignment of these resonances in the presence of  $\beta$ -cyclodextrin (Section 4.3), through the observation of positive nOe enhancements of the H3' and isobutyl H1'' and H2'' signals respectively. In contrast, small negative nOes were found for the aromatic and isobutyl H1' and H2' resonances of ibuprofen sodium upon irradiation of the cyclodextrin H5 signal, but in the absence of data relating to irradiation of the cyclodextrin H3 and H6 resonances, interpretation of these nOes in terms of the structure of the  $\beta$ -cyclodextrin complex is unclear. Differences in sign of nOes of the ibuprofen sodium <sup>1</sup>H resonances may be associated with their arising in the free and complexed states.

A further approach was to measure the nOe in the rotating frame, the advantages of which in the study of mini-molecules have already been described in Chapter 3. The 2D ROESY experiment was chosen in preference to the 1D ROE difference method, since the selective inversion required for the latter was



considered inappropriate for application to the partially obscured resonances observed in the spectrum of a 1:1 mole ratio solution of  $\beta$ -cyclodextrin and ibuprofen sodium in  $D_2O$ , and with other guest substrates examined in this work.

#### 4.7.2 Studies with the ROESY Experiment

The spin-lock field introduces considerable difficulties in the practical implementation of the ROESY experiment. Thus, this field must have the same frequency as, and be phase coherent with, the initial  $90^\circ$  excitation pulse and the receiver and must therefore be generated through the transmitter channel [253,287]. Although this requirement has the advantage that the decoupler channel remains available for solvent suppression purposes, where necessary, the high power levels typically used in excitation through the transmitter channel are incompatible with the continual application of the spin-lock over mixing times of the order of hundreds of milliseconds. Such incompatibility may be circumvented by two simple modifications of the basic ROESY experiment, denoted here VPHROEH and VPHROESYH, according to their usage in JEOL spectrometer software.

##### 1. The VPHROESYH Sequence

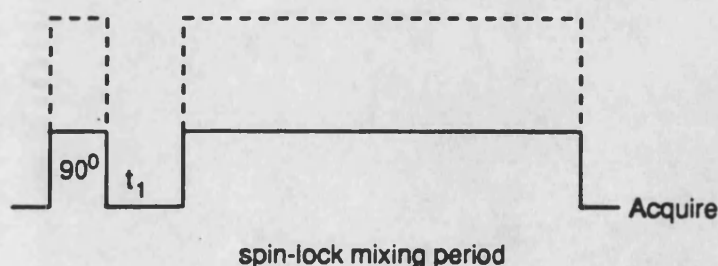


Figure 4.15 The VPHROESYH sequence

The VPHROESYH sequence, Figure 4.15 is based on the original experiment of Bothner-By *et al.* [260]. A reduced power level, which represents a compromise between the requirements of uniform excitation by the initial  $90^\circ$  pulse and the continual application of the spin-lock field, is used throughout.

## 2. The VPHROEH Sequence

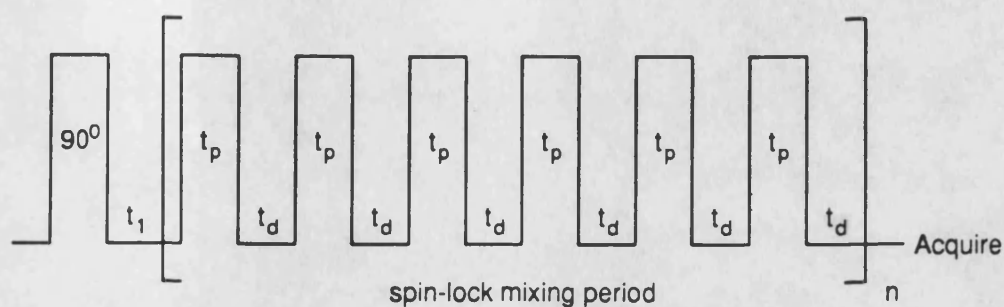


Figure 4.16 The VPHROEH sequence

An alternative approach which allows the use of raised power levels is the VPHROEH sequence, Figure 4.16, derived from the work of Kessler *et al.* [261]. The spin-lock field is here applied intermittently as a series of pulses of duration  $t_p$  separated by short delays of duration  $t_d$ , where the duty cycle,  $t_p/t_d$ , is typically of the order of 10%. The resulting field has a strength  $t_p/(t_p+t_d)$  of the corresponding continuous field [265].

In order to suppress interference from competing TOCSY pathways, Kessler *et al.* [261] advocate that  $t_p$  should correspond to a pulse angle significantly different from  $180^\circ$ , and themselves used  $t_p$  equivalent to a  $32^\circ$  pulse. The subsequent theoretical studies of Bax [265] have suggested however that this method offers no advantage in terms of the reduction of TOCSY correlations over the VPHROESYH experiment.

More advanced experiments requiring the use of rapid power level switching [253] or the use of z-filters [288,289] have been described, but were not considered to offer significant advantages over the VPHROEH and VPHROESYH methods.

Initial studies with the ROESY experiment examined a 1:1 mole ratio solution of ibuprofen sodium and  $\beta$ -cyclodextrin in  $D_2O$ . Spectrometer manufacturer's literature recommended the use of the VPHROEH sequence with a reduced power level setting corresponding to a spin-lock field of 0.5kHz for a 10% duty cycle. Under such conditions, however, the spin-lock field was not of sufficient strength to prevent the relative precession of those resonances furthest from the carrier (at 4.644ppm). This was apparent from the first slice in the imaginary data set, used to set the phase of the spectrum in the  $f_2$  frequency domain, for which it was not possible to simultaneously obtain all resonances in phase, Figure 4.17.

At maximum power this problem was eliminated as is apparent from the corresponding imaginary data slice, Figure 4.17. The 1.4kHz strength of the spin-lock field generated in this case remains low in comparison to the fields of 1-5kHz generally preferred for use in the ROESY experiment [253], however, and the VPHROESYH sequence was therefore chosen for use in this work, since the continual application of the spin-lock field in this sequence allowed field strengths of a considerably greater magnitude to be achieved. Typically, field strengths of the order of 3.8-5.3kHz were used.

Figure 4.18 shows the ROESY spectrum of a 1:1 mole ratio mixture of ibuprofen sodium and  $\beta$ -cyclodextrin in  $D_2O$  acquired under such conditions, with a mixing time of 400ms. The diagonal is phased positive double absorption and shown in black. A number of ROESY correlations of negative double absorption phase and shown coloured red are readily apparent. Additionally, however, two

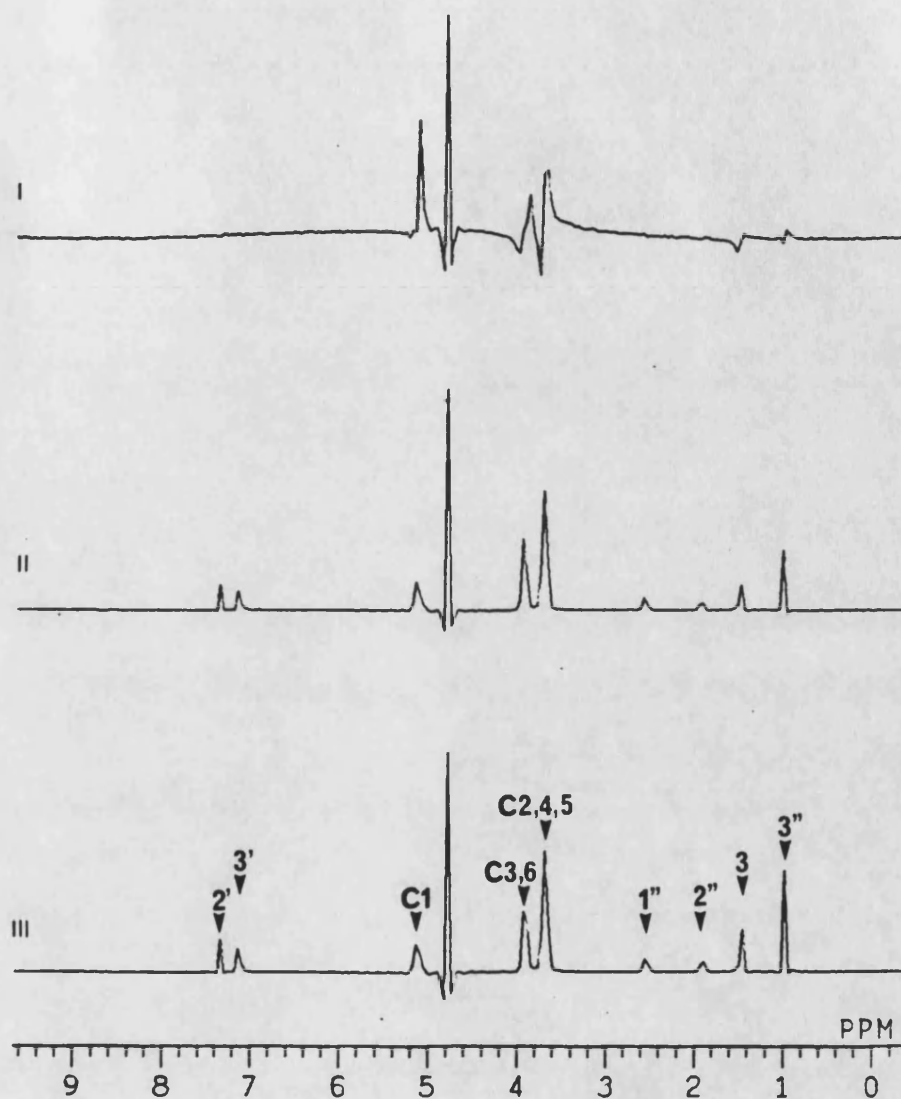


Figure 4.17 Imaginary data slices taken from ROESY data sets recorded at 400MHz on a 0.055M solution of ibuprofen sodium in the presence of a mole equivalent of  $\beta$ -cyclodextrin in  $D_2O$  at 30°C. (i) VPHROEH sequence with spin-lock field of 0.5kHz, (ii) VPHROEH sequence with spin-lock field of 1.4kHz and (iii) VPHROESYH sequence with spin-lock field of 5kHz. The mixing time is 400ms. C denotes cyclodextrin resonances

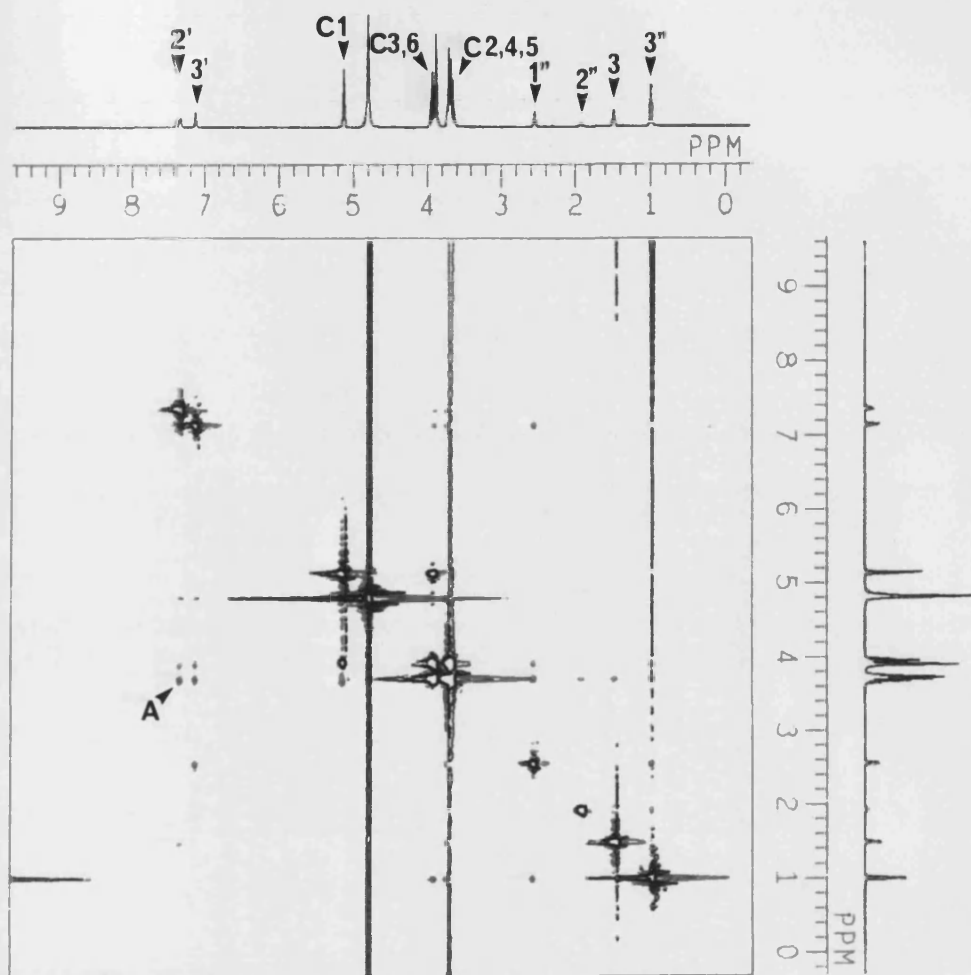


Figure 4.18 400MHz ROESY spectrum of a 0.055M solution of ibuprofen sodium in the presence of a mole equivalent of  $\beta$ -cyclodextrin in  $D_2O$  at 30°C. C denotes cyclodextrin resonances

intramolecular TOCSY correlations (positive double absorption, shown in black) within the cyclodextrin resonances may also be identified. These correlations are not unexpected, since the carrier position (in the centre of the spectrum) is little removed from these resonances [264]. Such positioning of the carrier is unavoidable, however, if spectral resolution is to be maintained.

The presence of such TOCSY interactions further suggests that the combined TOCSY-ROESY or ROESY-TOCSY correlation pathways may be a complicating feature in the interpretation of this spectrum. In order to distinguish the true from the false ROESY correlation it was therefore necessary to investigate the carrier offset dependence of the observed ROESY correlations [264]. Neuhaus and Williamson state that for  $B_1$  and static fields in the 1-5kHz and 200-500MHz ranges respectively, significant changes in intensity of false ROESY correlations should be apparent when the carrier is moved by as little as a few hundred Hz [253].

In practice, the most noticeable change on repositioning the carrier frequency 300-400Hz to high and low field for the ibuprofen sodium/ $\beta$ -cyclodextrin system is seen for cross-peak A of Figure 4.18, which changes phase on moving the carrier to low field. The observation of this necessarily intramolecular TOCSY correlation indicates that in addition to a possible intermolecular ROESY correlation between the cyclodextrin and the aromatic ring of the included guest, there is a significant contribution to this cross-peak as a result of interaction between the H2' and H2 resonances of the drug molecule, the latter of which has already been shown to lie obscured in this region of the spectrum.

In general, however, although movement of the carrier appears to eliminate the TOCSY correlation to the cyclodextrin H1 resonance, that between the H3 or H6 and H2, H4 or H5 resonances remains prominent throughout, which indicates

that carrier off-sets in excess of the recommended value are required in this instance.

Indeed, when the carrier is off-set to high field of all  $^1\text{H}$  resonances [246], corresponding to a shift of approximately 1800Hz, this TOCSY correlation is no longer readily apparent although all other intermolecular ROESY correlations remain. There are, however, several difficulties associated with this extreme positioning of the carrier frequency. Firstly, the necessary increase in frequency width to incorporate all resonances within the spectral window leads to a marked decrease in resolution (here 31.25Hz). Additionally, this increase in spectral width requires an accompanying increase in the rate of sampling of the FID, which for a constant matrix size may lead to severe truncation of the FID. Thus, the ROESY spectrum measured under such conditions here was noisier and showed raised levels of sinc wiggling, characteristic of such truncation [253], which made it difficult to deduce the complete elimination of cyclodextrin TOCSY interactions. Presumably, careful optimisation of window functions for transformation would alleviate this problem.

Lowering of power levels of the spin-lock field provides an alternative approach to the elimination of the TOCSY interaction in ROESY spectra [262]. Examination of the 1:1 mole ratio solution of ibuprofen sodium and  $\beta$ -cyclodextrin in  $\text{D}_2\text{O}$  using the VPHROESYH sequence with the carrier returned to 4.644ppm, but with the spin-lock power lowered to as little as 1kHz, showed that the TOCSY interaction within the cyclodextrin resonances was still apparent, although considerably reduced in intensity.

That equivalent ROESY correlations are present in all spectra, including that with the carrier off-set to high-field where TOCSY interactions appear to have been eliminated, suggests that these correlations are true ROESY cross-peaks in contrast to those which might arise through a false ROESY/TOCSY pathway. These correlations are assigned in Table 4.8.

Ibuprofen sodium resonance	Cyclodextrin resonance
H3"	H3 and/or H6 H5
H1"	weak correlations?
H2'	H3 and/or H6 H5 and/or drug H2
H3'	H3 and/or H6 H5

Table 4.8 Assignment of correlations observed in 400MHz ROESY spectra of a 0.055M solution of ibuprofen sodium in the presence of a mole equivalent of  $\beta$ -cyclodextrin in D<sub>2</sub>O at 30°C

Due to the overlapping nature of the cyclodextrin resonances in these spectra it was necessary to assume when assigning correlations that they arose only from those protons lining the cavity and its rim. It can also be seen from Table 4.8, however, that resolution in the 2D matrix was not sufficient to allow discrimination between the H3 and H6 resonances of the cyclodextrin. This indistinction can be seen more clearly from Figure 4.19 which compares resolution in the high resolution <sup>1</sup>H spectrum with a typical first imaginary data slice taken from one of the ROESY spectra described above. The ROESY experiment was therefore repeated with the matrix size doubled to its maximum possible size compatible with the spectrometer memory capabilities, giving a resolution of 7.81Hz over a standard spectral width of 4000Hz, which then allowed discrimination of the cyclodextrin H3 and H6 resonances to be achieved, Figure 4.19. Additionally, since preliminary studies also made use of a solution of comparatively high concentration of 0.055M in both host and guest, to facilitate rapid data acquisition, solution concentration was reduced to 0.014M in this



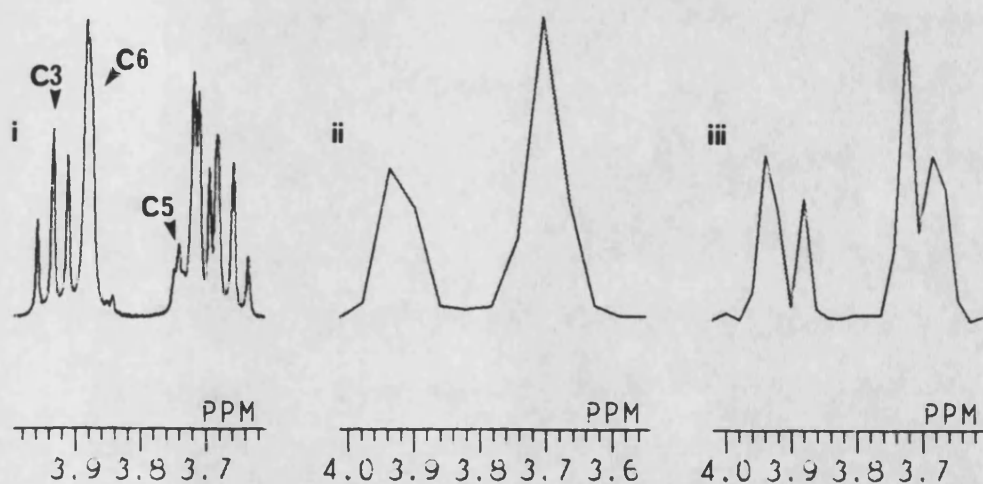


Figure 4.19 Comparison of resolution in 400MHz  $^1\text{H}$  spectra of a 1:1 mole ratio solution of ibuprofen sodium and  $\beta$ -cyclodextrin in  $\text{D}_2\text{O}$  at  $30^\circ\text{C}$ . (i) high resolution spectrum (resolution = 0.24Hz), (ii) imaginary slice from ROESY data set (resolution = 15.6Hz) and (iii) imaginary slice from ROESY data set (resolution = 7.81Hz). C denotes cyclodextrin resonances

experiment to ensure that correlations were not the result of some associative process possibly present at higher concentration. Expansion of this data set revealed that:

1. Correlations previously assigned to the cyclodextrin H3 and/or H6 resonances are composed of two cross peaks, one strong and one weak (see, for example, Figure 4.20). These were assigned respectively to the H6 and H3 protons.
2. Despite increased resolution in the ROESY spectrum, it was not possible to either confirm or eliminate the additional contribution of a ROESY correlation between the H2' resonance of ibuprofen sodium and that of the cyclodextrin H5 signal to cross-peak A of Figures 4.18 and 4.20, which has already been assigned in part as arising from intramolecular correlation between the ibuprofen sodium H2 and H2' resonances. Correlation of the ibuprofen sodium H2' resonance to cyclodextrin H6 would, however, suggest the additional presence of such an interaction.

The interpretation of these correlations, which it is to be noted are not inconsistent with those observed in the high temperature nOe experiment, in terms of a unique structure of the  $\beta$ -cyclodextrin inclusion complex of ibuprofen sodium as has been previously suggested to exist in aqueous solution is not straightforward. The strong intensity of ROESY correlations of the aromatic resonances of ibuprofen sodium to the cyclodextrin H5 and H6 signals in comparison to those to H3 would suggest only partial insertion of the aromatic ring into the macrocyclic cavity, so that it lies close to the primary hydroxyl entrance. A similar interpretation of the correlations of the isobutyl H3" signal would then suggest an orientation of the ibuprofen sodium molecule in the  $\beta$ -cyclodextrin cavity equivalent to that previously proposed (Section 4.2 and Section 4.6.3). Interpretation of ROESY cross peak intensity without regard to its dependence on

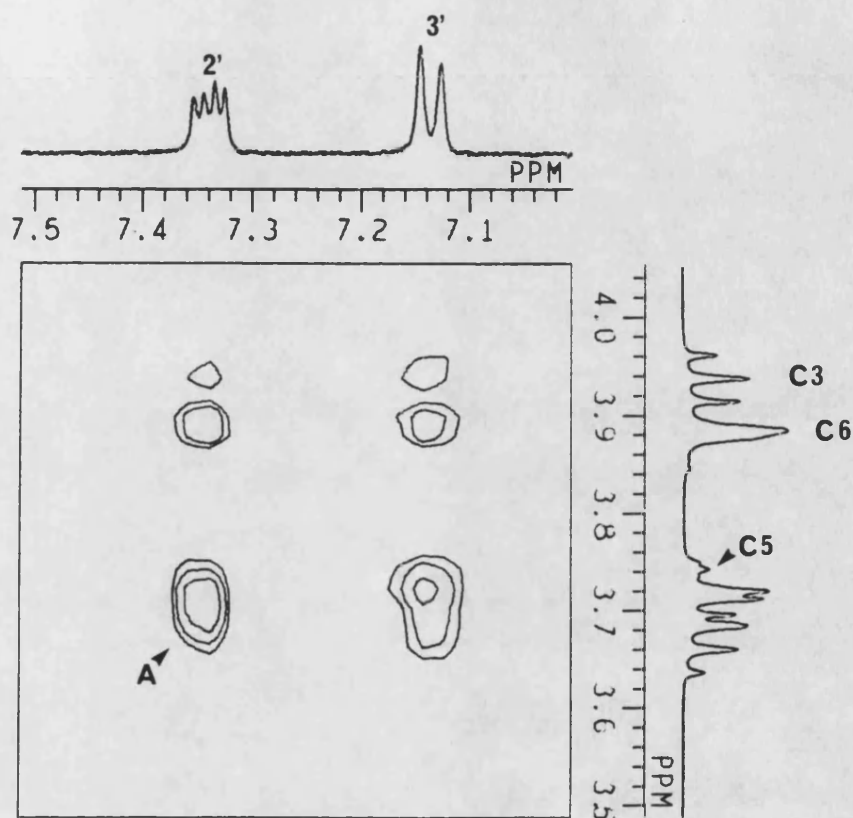


Figure 4.20 Expansion of part of the 400MHz ROESY spectrum of a 0.014M solution of ibuprofen sodium in the presence of a mole equivalent of  $\beta$ -cyclodextrin in  $D_2O$  at 30°C. C denotes cyclodextrin resonances

non-uniform excitation and resonance off-set effects must, however, be regarded with caution [253]. Additionally, it must be remembered that the H3 proton may necessarily lie geometrically further from any molecule within the cyclodextrin cavity, as a result of the greater diameter of the secondary hydroxyl entrance of this cavity.

The ROESY experiment was also used to investigate the complexation of  $\beta$ -cyclodextrin with other of the 2-arylpropionates. Overlap of the cyclodextrin H3, H5 and H6 resonances, both with each other and with the H2 resonance of the guest substrate, was found to be a recurring difficulty in the interpretation of these spectra. Additionally, poor resolution of aromatic signals of some substrates in the presence of  $\beta$ -cyclodextrin further complicated interpretation.

A 1:1 mole ratio solution of sodium 2-(4-chlorophenyl)propionate and  $\beta$ -cyclodextrin in D<sub>2</sub>O was examined using the ROESY experiment to enable unequivocal assignment of the aromatic resonances of the salt, in addition to providing structural information in relation to the inclusion complex.

A COSY-45 experiment of this solution showed that the H2 resonance of the salt was obscured below the cyclodextrin H2 resonance but was conveniently separated from the H3, H5 and H6 resonances of the cyclodextrin which are of interest here. The cyclodextrin H3 and H6 resonances were, however, overlapping and indistinguishable in the resulting ROESY spectrum acquired using the VPHROESYH sequence and a spin-lock field of 3.8kHz over a mixing period of 400ms, Figure 4.21.

A number of correlations were observed in this spectrum. Thus, cross-peaks were identified which were consistent with intramolecular ROESY correlations between the H2 resonance of the 2-arylpropionate and its aromatic and H3 groups. Additionally, intramolecular ROESY and TOCSY correlations were observed within the cyclodextrin resonances. The correlations of greatest interest were, however, the intermolecular ROESY correlations between host and guest;

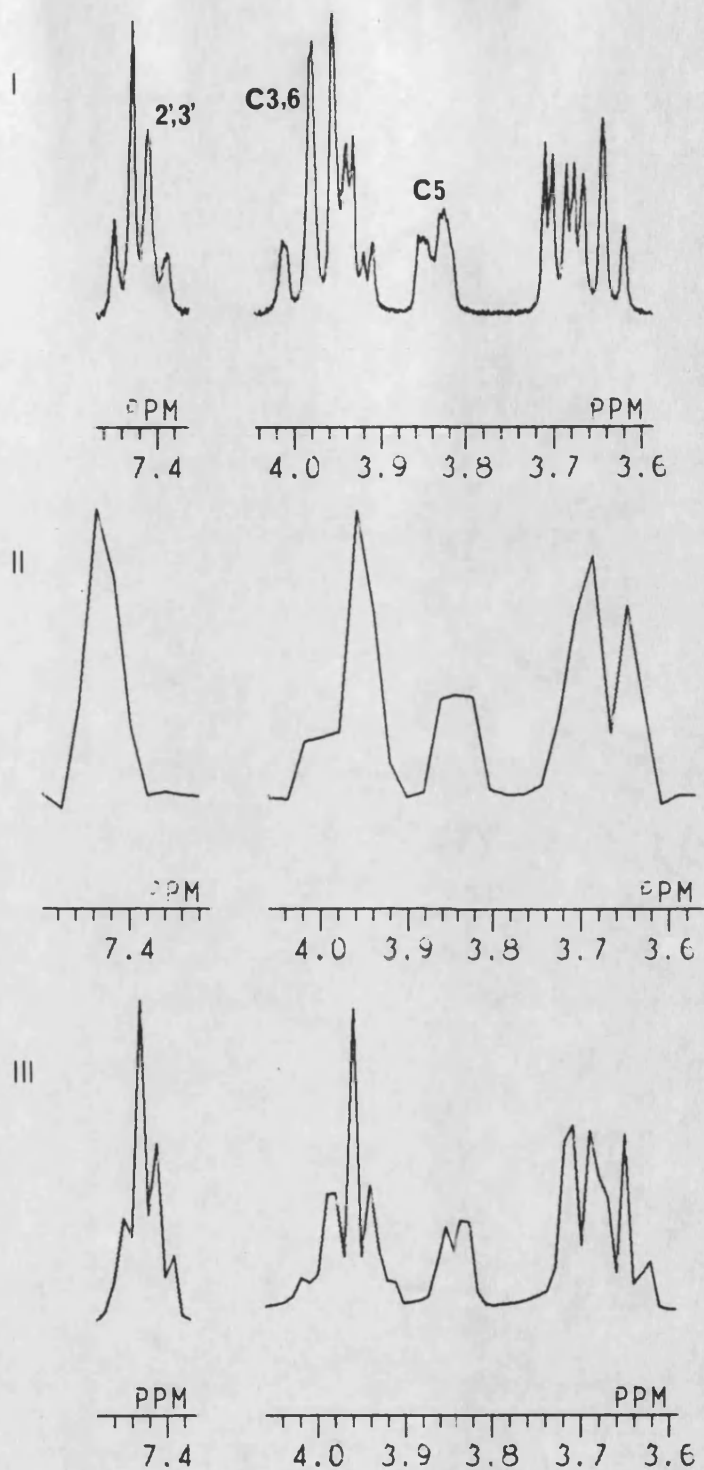


Figure 4.21 Comparison of resolution in 400MHz  $^1\text{H}$  spectra of a 1:1 mole ratio solution of sodium 2-(4-chlorophenyl)propionate and  $\beta$ -cyclodextrin in  $\text{D}_2\text{O}$  at  $30^\circ\text{C}$ . Part of (i) high resolution spectrum (resolution = 0.24Hz), (ii) imaginary slice from ROESY data set (resolution = 7.81Hz) and (iii) imaginary slice from folded ROESY data set (resolution = 3.90Hz). C denotes cyclodextrin resonances

cross-peaks were observed between the aromatic resonances of the guest and the H5 and H3 and/or H6 resonances of the host and between the methyl resonance of the former and the H3 and/or H6 resonance of the cyclodextrin.

A ROESY spectrum acquired under identical conditions but with a mixing time of 800ms reproduced these correlations. Furthermore slices taken through these spectra showed an increase in their intensity with mixing time in comparison to diagonal peaks and suggests that longer mixing times in the ROESY experiment may be generally beneficial in terms of enhanced sensitivity in the study of the complexes of  $\beta$ -cyclodextrin. In contrast, at a shorter mixing time of 200ms a reduced intensity of these correlations was observed, and indicated that mixing times of this order of magnitude, which have been used by other authors [285] in the examination of cyclodextrin complexes, may not be ideal for the examination of those complexes studied in this work.

Resolution of the aromatic H2' and H3' resonances of sodium 2-(4-chlorophenyl)propionate was not achieved in these spectra, despite the use of the largest 2D matrix compatible with the memory capability of the spectrometer. Thus, whilst ROESY correlations between the aromatic resonances of the salt and those of the cyclodextrin clearly supported inclusion of the aromatic ring into the macrocyclic cavity, no further structural information in respect of the complex was established, and additionally assignment of the aromatic resonances of the guest was not confirmed. It was therefore necessary to repeat the ROESY experiment with folding of the H3 resonance in order to achieve sufficient resolution in the 2D matrix to distinguish the H2' and H3' resonances of the salt, Figure 4.21. For maximal reduction in the spectral window upon folding, it was necessary to move the carrier frequency to low field by approximately 340Hz. Large TOCSY correlations were still however apparent within the non-glycosidic group of cyclodextrin resonances. Furthermore, it was not possible to clearly discern ROESY correlations to the aromatic region of the sodium 2-(4-

chlorophenyl)propionate molecule, despite an 8-fold increase in the number of scans used to acquire the data set in comparison to earlier experiments. Imperfect filter cut-off was clearly not the cause of this loss in cross-peak intensity, since filter width was twice that of the spectral window. Small distortions in baseline as a result of non-optimal settings of delays prior to acquisition present a more probable cause.

Folding of the H3 resonance of the guest substrate was also required in studies of complexation of a 1:1 mole ratio solution of flurbiprofen sodium and  $\beta$ -cyclodextrin in  $D_2O$ , again to achieve adequate resolution of the aromatic resonances of the guest together with partial resolution of the H3 and H6 resonances of the cyclodextrin. In this case, the H2 resonance of the flurbiprofen sodium molecule was well resolved from all cyclodextrin resonances even in the absence of spectral folding, Figure 4.22.

Thus, a standard ROESY experiment acquired with a spectral width of 4000Hz using the VPHROESYH sequence with a spin-lock field of 5kHz and a mixing time of 400ms revealed correlations with the same broad classification as was described for the solution of sodium 2-(4-chlorophenyl)propionate and  $\beta$ -cyclodextrin in  $D_2O$ , namely: ROESY correlations of the H2 resonance of flurbiprofen sodium with its H3 and aromatic H2' and H6' resonances, ROESY and TOCSY correlations within the cyclodextrin resonances and intermolecular ROESY correlations between the aromatic resonances of the guest and the H5 and H3 and/or H6 resonances of the cyclodextrin and between the H3 signal of the guest and the H3 and/or H6 resonances of the cyclodextrin. Cross-peaks were observed between the cyclodextrin resonances and each of the three peaks into which the aromatic region of the flurbiprofen sodium molecule was coarsely resolved, Figure 4.23, these peaks incorporating (i) the H2", (ii) the H5', H3", H4" and (iii) H2' and H6' resonances (Figure 4.22). In order to eliminate the possible contribution of TOCSY pathways to the observed intermolecular ROESY

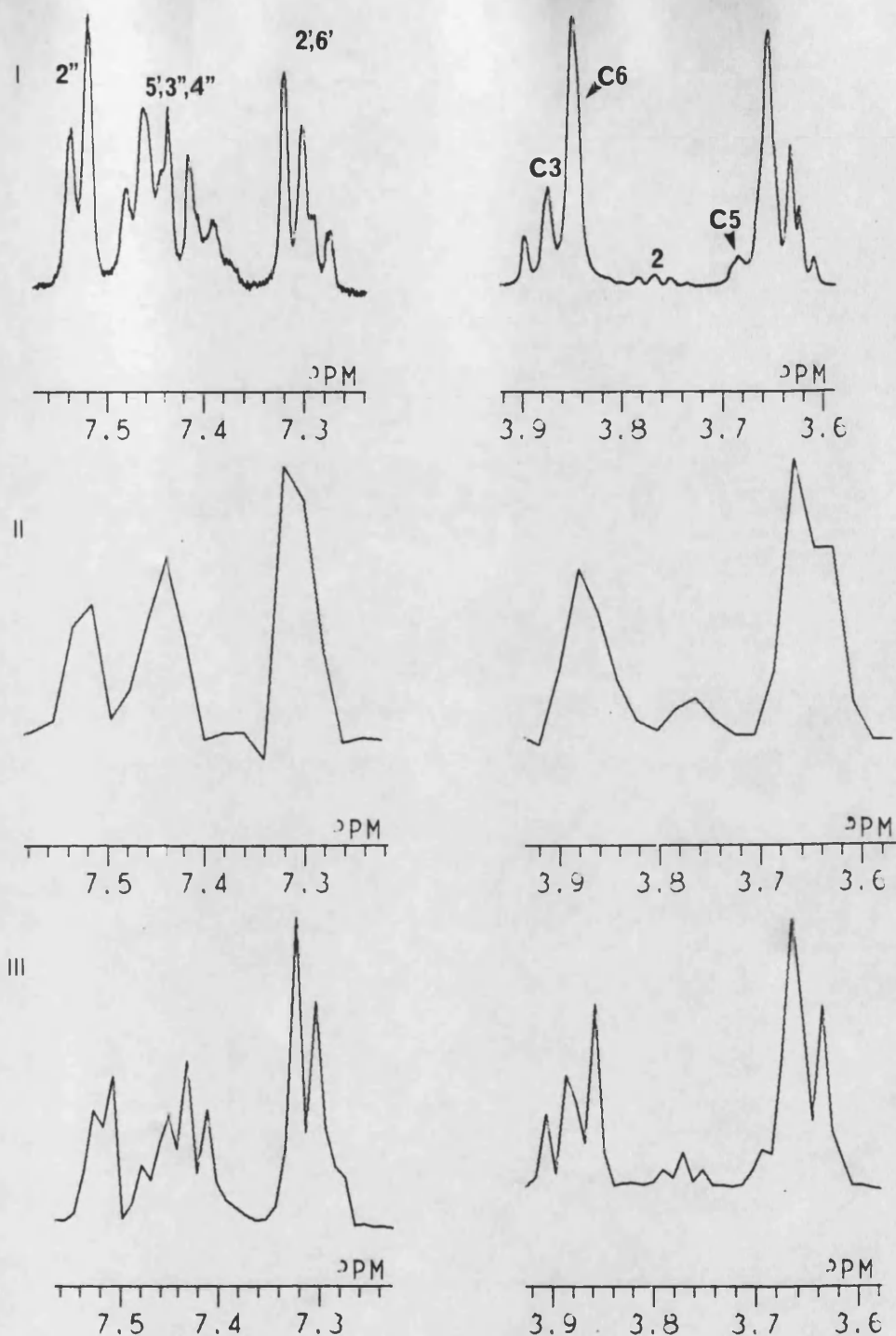


Figure 4.22 Comparison of resolution in 400MHz  $^1\text{H}$  spectra of a 0.014M solution of flurbiprofen sodium in the presence of a mole equivalent of  $\beta$ -cyclodextrin in  $\text{D}_2\text{O}$  at  $30^\circ\text{C}$ . (i) high resolution spectrum (resolution = 0.24Hz), (ii) imaginary slice from ROESY data set (resolution = 7.81Hz) and (iii) imaginary slice from folded ROESY data set (resolution = 3.88Hz). C denotes cyclodextrin resonances



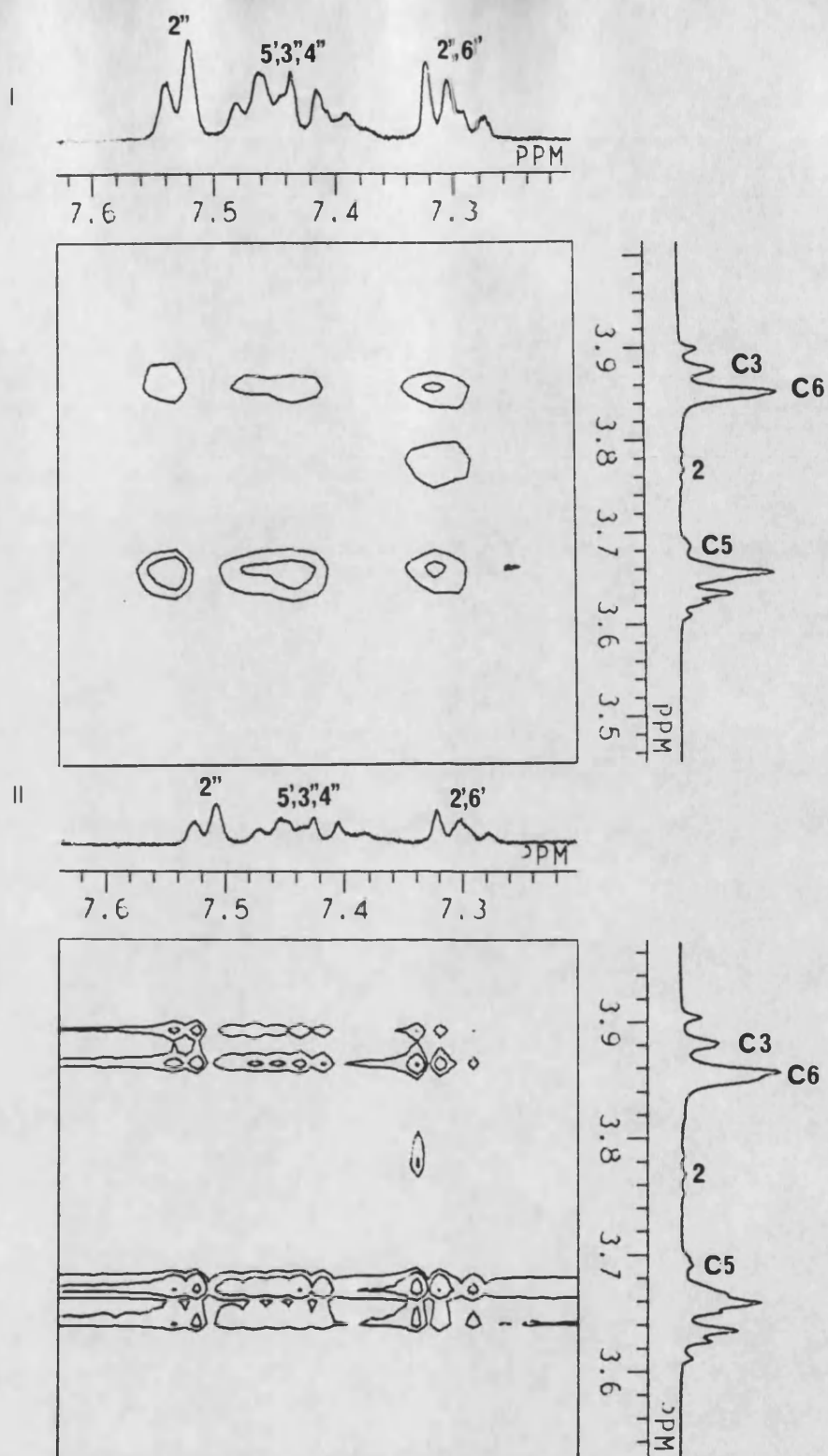


Figure 4.23 Expanded regions of 400MHz ROESY spectra of a 0.014M solution of flurbiprofen sodium in the presence of a mole equivalent of  $\beta$ -cyclodextrin in  $D_2O$  at  $30^\circ C$ . (i) resolution = 7.81Hz and (ii) folded with resolution = 3.88Hz. C denotes cyclodextrin resonances

correlations, the carrier frequency was moved by 500Hz to high and low field of its initial position, which represents the maximum shift compatible with simultaneously maintaining resolution and all resonances within the spectral width. TOCSY correlations within the cyclodextrin resonances remained prominent in each of these spectra, however, and do not therefore allow the presence of false ROESY cross peaks to be ruled out.

These TOCSY correlations remain in the folded spectrum, which allowed distinction of both aromatic resonances of flurbiprofen sodium and the H3 and H6 resonances of the cyclodextrin (Figure 4.22). Intermolecular ROESY correlations are, however, again weak despite a 4-fold increase in the number of scans versus the non-folded experiments, and was again thought to be a consequence of baseline distortions. Cross-peaks which can be distinguished indicate correlation of all aromatic resonances to the H3, H6 and presumably H5 resonances of the cyclodextrin, that of H5 lying partially obscured beneath that of cyclodextrin H2, Figure 4.23. Additional correlations to the cyclodextrin H2 or H4 resonance must be the result of combined TOCSY-ROESY interaction pathways, and suggests that other cross-peaks may similarly be false. Despite this inability to distinguish the true ROESY correlation from the false, it remains possible to conclude that both aromatic rings of the guest substrate penetrate the  $\beta$ -cyclodextrin cavity. Thus, false ROESY cross-peaks of resonances of one ring as a result of true correlation of the other are ruled out since the shortest  $^1\text{H}$  coupling pathway between the two rings is over 5 bonds, which effectively prohibits TOCSY interactions between the two. It is noted that no intra-aromatic ROESY correlation which would support the existence of a dimeric structure for the flurbiprofen sodium/ $\beta$ -cyclodextrin system, similar to that observed in the solid state, was apparent in this spectrum.

It has also been suggested that dimerisation may be an important feature of the complexation of naproxen sodium with  $\beta$ -cyclodextrin. A 1:1 mole ratio solution of naproxen sodium and  $\beta$ -cyclodextrin in  $\text{D}_2\text{O}$  examined using the

ROESY experiment similarly failed to show ROESY correlations within the naproxen sodium signals, however, which would support such a proposal. A number of intermolecular ROESY correlations were, however, present in this spectrum, which was acquired using a spin-lock field of 4kHz over a mixing period of 400ms. Figure 4.24 shows an expanded region of it together with assignments for each ROESY correlation.

It can be seen from these assignments that resolution in this matrix was insufficient to allow distinction between a number of signals. Thus, whilst aromatic H1' and H3' resonances of the naproxen sodium molecule were clearly resolved, those of H8' and H4' and H5' and H7' were partially overlapping in the high resolution <sup>1</sup>H spectrum and were not distinguished here. Additionally, a COSY-45 experiment revealed that the H2 resonance of this molecule was obscured beneath the cyclodextrin H3 and H6 resonances. Even so, Figure 4.24 shows that correlations of the aromatic H1' and H3' protons to it are readily discernible from those of other aromatic naproxen sodium resonances to the cyclodextrin H3 and H6 resonances either side of it.

The interpretation of these intermolecular ROESY correlations in terms of a unique structure of the β-cyclodextrin complex of naproxen sodium is not possible. Disregarding correlations assigned to the aromatic H4' and H8' resonances which could not be unequivocally assigned to either or both of these resonances, the weak correlation of H1' to the cyclodextrin H5 resonance only, together with the correlation of the aromatic resonances of H5' and/or H7' with the cyclodextrin H3 and H5 resonance suggests an orientation of the guest molecule in the β- cyclodextrin cavity opposed to that proposed to exist in d<sub>6</sub>-DMSO (Section 4.6.3). Additional cross-peaks observed between aromatic H5' and/or H7' and to the cyclodextrin H6 resonances are not, however, consistent with this model. The presence of false ROESY correlations was thought to offer a possible explanation for this discrepancy, since a strong TOCSY interaction was clearly present within

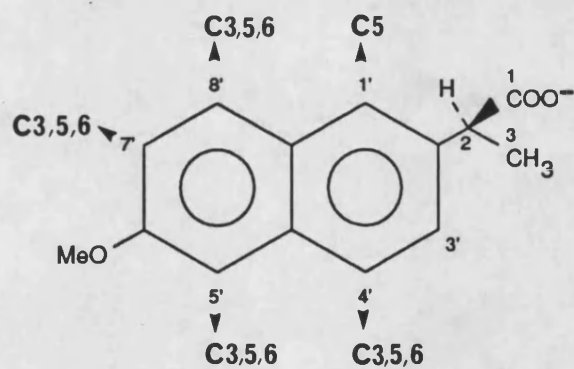
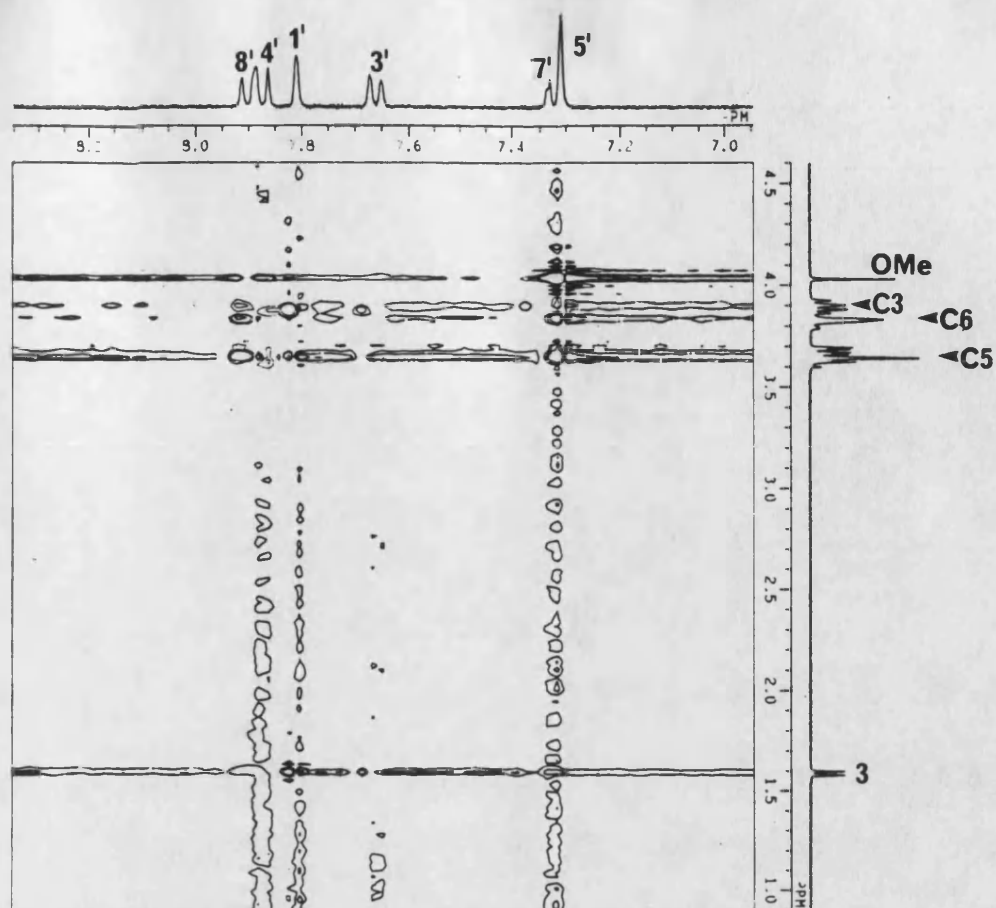


Figure 4.24 Expanded region of a 400MHz ROESY spectrum of a 0.014M solution of naproxen sodium in the presence of a mole equivalent of  $\beta$ -cyclodextrin in  $D_2O$  at  $30^\circ C$ . Intermolecular ROESY correlations are illustrated in the figure. C denotes resonances of the cyclodextrin

resonances of the  $\beta$ -cyclodextrin molecule. Test ROESY experiments on a concentrated 1:1 mole ratio solution of naproxen sodium and  $\beta$ -cyclodextrin in  $D_2O$  (0.055M in each reagent) were therefore carried out, using maximal transmitter off-sets to high and low field which allowed resolution in the 2D matrix to be maintained. Although the magnitude of the cyclodextrin TOCSY interaction was visibly reduced when the carrier was placed down field at approximately 5.9ppm, the failure to eliminate it completely prevented the presence of false ROESY cross-peaks to be ruled out. Increased separation of the H5' and H7' resonances of naproxen sodium for this more concentrated solution in these spectra did, however, indicate that correlations to the cyclodextrin H3,H5 and H6 resonances may be associated with each of the H5' and H7' resonances.

#### 4.8 Application of Measurements of $^{13}C$ $T_1$ to the Complexation of $\beta$ -Cyclodextrin with some 2-Arylpropionates in $D_2O$

Measurement of  $^{13}C$   $T_1$ s of cyclodextrins in the presence of a guest substrate in aqueous solution have been used by several authors to provide information regarding the structure and dynamics of the resulting inclusion complex [290-292]. The simplest interpretation of these values in terms of the motional characteristics of the complex requires that relaxation be dominated by the dipolar mechanism through some number N of directly attached protons and that molecular tumbling may be described by an isotropic correlation time,  $t_c$ . In the extreme narrowing limit,  $T_1$  may then be related to  $t_c$  according to,

$$\frac{1}{NT_1} \propto t_c \quad (4.7)$$

In practice, where complexation is not complete, the observed  $T_1$  is a population averaged sum of the  $T_1$  for the free and complexed states.

It was thought that the motional characteristics of a chiral guest might have important consequences in terms of chiral discrimination by a cyclodextrin host. Measurements of  $^{13}\text{C}$   $T_1$ s for the sodium 2-arylpropionate complexes of  $\beta$ -cyclodextrin were therefore undertaken.

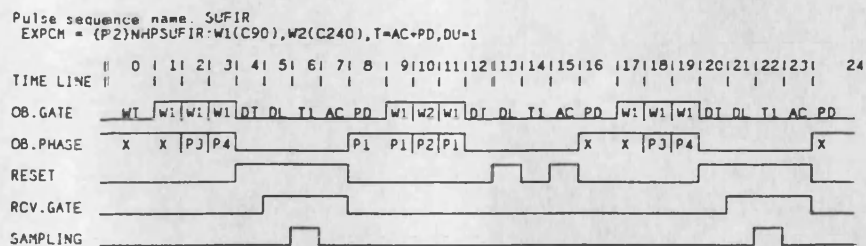
The low concentrations of the solutions ideally used in this work to avoid complex association ruled out use of the classical inversion-recovery sequence for measurement of  $^{13}\text{C}$  longitudinal relaxation times in a practicable experiment run time. Two recent methods intended for faster  $T_1$  measurements, namely the DESPOT and SUFIR methods described in Chapter 3, were therefore considered. The SUFIR method was considered the simplest and most appropriate of the two; its use requires only determination of the  $^{13}\text{C}$   $180^\circ$  pulse width, whereas the DESPOT sequence further requires determination of a pulse offset, which describes the deviation from proportionality of the pulse width and pulse angle. Additionally, the DESPOT sequence suffers with complications regarding the use of the lock circuitry of the spectrometer associated with the use of a homospoil pulse. Effective operation of the deuterium lock mechanism was considered essential for the long experiment times  $^{13}\text{C}$   $T_1$  measurements require.

#### 4.8.1 Implementation of the SUFIR sequence on a JEOL NMR Spectrometer

The SUFIR method has been relatively little used, and was not therefore available as a standard experimental sequence in the JEOL spectrometer software. The pulse sequence was therefore generated using the PEGS (Pulse Editing Graphics Software) program and is shown in Figure 4.25.

There are several important features of the sequence to be noted:

1. Continuous broad-band  $^1\text{H}$  decoupling is achieved by use of the WAUGH sequence [293]. Heteronuclear decoupling eliminates cross-relaxation between  $^{13}\text{C}$



Pulse sequence name. SUFIR  
EXPCM = {P2}NHPSUFIR:W1(C90),W2(C240),T=AC+PD,DU=1

Gate assignment

Spectrometer condition

PUCON	:	0
PULTS	:	0
OBCON	:	1
LCCON	:	1
IRRCO	:	3
TRRCO	:	1
OBOCO	:	0
OBOC2	:	0
IRSCO	:	1
IRSC2	:	0
TRSCO	:	0
TRSC2	:	0
LOCCO	:	0
OBAPC	:	1
IRAPC	:	13

Local symbol

T1	Type : S	Use :	1	List :	1
	Repeat :				
1 :	1.0 USEC				
X	Type : S	Use :	1	List :	1
	Repeat :				
1 :	0 DEG				

Figure 4.25 PEGS representation of the SUFIR experiment (continued overleaf)

P1	Type : M	Use :	8	List :	16
	Repeat : 1				
1 :	0 DEG	5 :	0 DEG		
2 :	90 DEG	6 :	90 DEG		
3 :	90 DEG	7 :	90 DEG		
4 :	0 DEG	8 :	0 DEG		
P2	Type : M	Use :	8	List :	16
	Repeat : 1				
1 :	90 DEG	5 :	90 DEG		
2 :	180 DEG	6 :	180 DEG		
3 :	180 DEG	7 :	180 DEG		
4 :	90 DEG	8 :	90 DEG		
P3	Type : M	Use :	1	List :	16
	Repeat : 8				
1 :	90 DEG				
P4	Type : M	Use :	2	List :	16
	Repeat : 4				
1 :	270 DEG				
2 :	90 DEG				
PUPHA	Type : P	Use :	1	List :	16
	Repeat : 1				
1 :	0 DEG				
APHAS	Type : A	Use :	1	List :	16
	Repeat : 1				
1 :	0 DEG				
GPHAS	Type : G	Use :	1	List :	32
	Repeat : 1				
	Arepeat : 1 @				
1 :	0 DEG				

PLX parameter

WT	=	INIWT
DT	=	DEADT
DL	=	DELAY
W1	=	PW1
W2	=	PW2
AC	=	ACQTM
PD	=	PD

Variable parameter

PLX	=	PI1
CNVRT	=	-1.0000

Figure 4.25 PEGS representation of the SUFIR experiment (continued from previous page)



and  $^1\text{H}$  nuclei which would otherwise cause deviation from mono-exponential behaviour of the measured  $T_1$  [244,294].

2. Preparation of the spin system requires the use of a single DUMMY sequence.

3. To ensure constancy of the time delay  $t$  between pulses, the central period is divided in the same manner as the two delays during which acquisition is carried out. This division into deadtime (DT), delay (DL), acquisition time (AC) and pulse delay (PD) requires the use of the RESET function (which resets the observation transmitter phase to  $0^\circ$ ) as a dummy event.

#### 4.8.2 Testing of the SUFIR Sequence

The SUFIR sequence was tested on a number of samples for which the  $^{13}\text{C}$   $T_1$  value from a classical inversion-recovery sequence was also measured. Test samples were chosen randomly, but were such that high sample concentrations were readily achieved to allow rapid measurement. Processing of inversion-recovery data is described in Chapter 5, and was achieved using calculation routines within the spectrometer software. A simple BASIC program, Figure 4.26, run on a BBC Archimedes computer allowed rapid calculation of  $T_1$  values from peak height measurements in the SUFIR method. The results are summarised in Tables 4.9 to 4.12.  $T_1$  values are given only for resonances which are clearly resolved and for which the necessary criteria for each experiment were satisfied; namely for the inversion-recovery experiment that  $T_1$  was less than a fifth of the largest value of the variable parameter  $t$ , and for the SUFIR method, that  $t/T_1$  lay in the range 0.5-3. Otherwise, entries are absent from these tables where calculation of  $T_1$  was not possible, since  $S_2 > S_1$  (see equation 3.11). This relationship between  $S_1$  and  $S_2$  was thought to be a result of errors in peak intensity measurement where  $S_2$  is little changed from  $S_1$ . In general, agreement between the inversion-recovery and SUFIR methods is good.

```

10 REM T1CALC:A SIMPLE PROGRAM FOR CALCULATING
15 REM T1 VALUES FROM THE SUFIR EXPERIMENT
20 REM CAROL MARCHANT 23-08-91
22 REM LINES 2610 AND 2660 ADDED 09-09-91
25 REM ENSURE PRINTER IS LOADED AND ON-LINE
30 REM BEFORE COMMENCING
40 *IGNORE
50 PRINT "PLEASE ENTER SAMPLE CODE"
100 INPUT CODE$
150 PRINT "PLEASE ENTER DFILE NAME"
200 INPUT DFILE$
250 PRINT "PLEASE ENTER TAU VALUE"
300 INPUT TAU
350 PRINT "PLEASE ENTER MXINTS1 VALUE"
400 INPUT MXINTS1
410 PRINT "PLEASE ENTER NGAIN1 VALUE"
420 INPUT NGAIN1
450 PRINT "PLEASE ENTER MXINTS2 VALUE"
500 INPUT MXINTS2
510 PRINT "PLEASE ENTER NGAIN2 VALUE"
520 INPUT NGAIN2
530 NF=NGAIN2-NGAIN1
540 NFP=2^NF
550 MXF=MXINTS2*NFP/MXINTS1
600 PRINT "PLEASE ENTER PEAK POSITION"
650 INPUT PEAK
700 PRINT "PLEASE ENTER S1 FOR THE CHOSEN PEAK"
750 INPUT S1
800 PRINT "PLEASE ENTER S2 FOR THE CHOSEN PEAK"
850 INPUT S2
900 SIGNAL_RATIO=S2*MXF/S1
950 PRELN=1-SIGNAL_RATIO
1000 IF PRELN>0 THEN GOTO 2250
1050 VDU2
1100 PRINT "SAMPLE ";CODE$
1150 PRINT "DFILE ";DFILE$
1200 PRINT "PEAK ";PEAK
1250 PRINT "TAU ";TAU
1300 PRINT "MXINTS1 ";MXINTS1
1350 PRINT "MXINTS2 ";MXINTS2
1850 PRINT "S1 ";S1
1900 PRINT "S2 ";S2
1950 PRINT "(1-S2/S1) ";PRELN

```

Figure 4.26 BASIC program for calculation of  $T_1$  values resulting from the SUFIR experiment from peak intensity data (continued overleaf)

```

1975 PRINT "LN ERROR"
2000 VDU1,10
2050 VDU1,10
2100 VDU1,10
2150 VDU3
2200 GOTO 3600
2250 LO=LN(PRELN)
2300 T1=-1*TAU/LO
2330 TAU_T1_RATIO=TAU/T1
2350 VDU2
2400 PRINT "SAMPLE ";CODE$
2450 PRINT "DFILE ";DFILE$
2500 PRINT "PEAK "; PEAK
2550 PRINT "TAU ";TAU
2600 PRINT "MXINTS1 ";MXINTS1
2610 PRINT "NGAIN1 ";NGAIN1
2650 PRINT "MXINTS2 ";MXINTS2
2660 PRINT "NGAIN2 "; NGAIN2
3250 PRINT "S1 ";S1
3300 PRINT "S2 ";S2
3350 PRINT "T1 ";T1
3370 PRINT "TAU/T1 ";TAU_T1_RATIO
3400 VDU1,10
3450 VDU1,10
3500 VDU1,10
3550 VDU3
3600 PRINT "DO YOU HAVE MORE PEAKS IN THIS DATA SET"
3650 PRINT "PLEASE ENTER Y TO CONTINUE"
3700 INPUT CONTINUE$
3750 IF CONTINUE$="Y" THEN GOTO 600
3800 PRINT "DO YOU HAVE MORE DATA FROM ANOTHER DATA SET"
3850 PRINT "PLEASE ENTER Y FOR A NEW DATA SET"
3900 INPUT NEWSET$
3950 IF NEWSET$="Y" THEN GOTO 50
4000 PRINT "END"

```

Figure 4.26 BASIC program for calculation of  $T_1$  values resulting from the SUFIR experiment from peak intensity data (continued from previous page)

$\delta/\text{ppm}$	$T_1/\text{s}$ inversion-recovery	$T_1/\text{s}$ ( $t/T_1$ ) SUFIR ( $t=5.4\text{s}$ )	$T_1/\text{s}$ ( $t/T_1$ ) SUFIR ( $t=10.4\text{s}$ )
29.2	4.5	3.9(1.4)	4.4(2.4)
26.4	3.8	3.4(1.6)	4.0(2.6)
19.0	4.8	4.6(1.2)	4.7(2.2)
18.4	5.0	5.4(1.0)	5.5(1.9)
8.5	6.2	4.7(1.2)	5.3(2.0)

Table 4.9 270MHz  $^{13}\text{C}$   $T_1$  measurements using the inversion-recovery and SUFIR methods for a concentrated solution of (+)camphor in  $\text{CDCl}_3$

$\delta/\text{ppm}$	$T_1/\text{s}$ inversion-recovery	$T_1/\text{s}$ ( $t/T_1$ ) SUFIR ( $t=2.0\text{s}$ )	$T_1/\text{s}$ ( $t/T_1$ ) SUFIR ( $t=5.5\text{s}$ )
129.5	2.9	2.8(0.7)	2.9(1.9)
120.9	2.1	2.1(0.9)	2.2(2.5)
115.2	2.9	2.9(0.7)	2.9(1.9)

Table 4.10 270MHz  $^{13}\text{C}$   $T_1$  measurements using the inversion-recovery and SUFIR methods for a concentrated solution of phenol in  $\text{CDCl}_3$

$\delta/\text{ppm}$	$T_1/\text{s}$ inversion-recovery	$T_1/\text{s}$ ( $t/T_1$ ) SUFIR ( $t=0.55\text{s}$ )	$T_1/\text{s}$ ( $t/T_1$ ) SUFIR ( $t=0.28\text{s}$ )
C1	0.16	-	0.18(1.6)
C4	0.17	-	0.16(1.7)
C3	0.17	-	0.18(1.6)
C5	0.17	0.20(2.7)	0.15(1.9)
C2	0.17	0.21(2.7)	0.16(1.8)
C6	0.10	-	0.11(2.5)

Table 4.11 270MHz  $^{13}\text{C}$   $T_1$  measurements using the inversion-recovery and SUFIR methods for a concentrated solution of  $\gamma$ -cyclodextrin in  $\text{D}_2\text{O}$ . Resonances were assigned by comparison with  $^{13}\text{C}$  data for aqueous solutions of  $\alpha$ - and  $\beta$ -cyclodextrin in  $\text{D}_2\text{O}$  [170]

$\delta/\text{ppm}$	$T_1/\text{s}$ inversion-recovery	$T_1/\text{s}$ ( $t/T_1$ ) SUFIR ( $t=5.5\text{s}$ )	$T_1$ ( $t/T_1$ ) SUFIR ( $t=3.0\text{s}$ )
127.6	3.2	3.0(1.8)	2.9(1.0)
126.4	2.0	1.9(2.9)	1.9(1.5)
124.8	3.1	3.0(1.8)	3.1(1.0)
69.1	2.8	2.5(2.1)	2.6(1.1)
24.5	1.2	-	1.2(2.5)

Table 4.12 270MHz  $^{13}\text{C}$   $T_1$  measurements using the inversion-recovery and SUFIR methods for a concentrated solution of *sec*-phenethyl alcohol in  $\text{CDCl}_3$

The *sec*-phenethyl alcohol sample was also used to investigate the reproducibility of the SUFIR method and its sensitivity to small errors in pulse width settings, since as a result of the poor sensitivity of  $^{13}\text{C}$  NMR it is often difficult to measure the pulse width with great accuracy.

Table 4.13 shows the results of consecutive measurements on the same sample under identical conditions and shows the method to be essentially reproducible.

Additionally, the effects of small variations in the  $^{13}\text{C}$  pulse in a range corresponding to a  $180^\circ$  pulse width of 15-19 $\mu\text{s}$ , compared with the measured value of 17 $\mu\text{s}$ , are shown in Table 4.14. These results confirm that the SUFIR method is not adversely affected by small errors in measurement of the  $^{13}\text{C}$  pulse width.

These observations together confirm the accuracy and robustness of the SUFIR method in the measurement of  $^{13}\text{C}$   $T_1$ , and support the validity of the application of the method to the  $\beta$ -cyclodextrin complexes of the sodium 2-arylpropionates studied in this work.

$\delta/\text{ppm}$	$T_1/s$ ( $t/T_1$ ) using the SUFIR method with $t=5.5s$		
	experiment 1	experiment 2	experiment 3
127.6	3.0(1.8)	2.9(1.8)	3.0(1.8)
126.4	1.9(2.9)	2.1(2.7)	1.9(2.8)
124.8	3.0(1.8)	3.2(1.7)	3.0(1.8)
69.1	2.5(2.1)	2.5(2.2)	2.8(1.9)

Table 4.13 Investigations of the reproducibility of the SUFIR method in the measurement of 270MHz  $^{13}\text{C}$   $T_1$  for a concentrated solution of *sec*-phenethyl alcohol in  $\text{CDCl}_3$

$\delta/\text{ppm}$	$T_1/s$ ( $t/T_1$ ) $\pi=17\mu s$	$T_1/s$ ( $t/T_1$ ) $\pi=16\mu s$	$T_1/s$ ( $t/T_1$ ) $\pi=18\mu s$	$T_1/s$ ( $t/T_1$ ) $\pi=15\mu s$	$T_1/s$ ( $t/T_1$ ) $\pi=19\mu s$
127.6	3.0(1.8)	3.0(1.8)	2.9(1.9)	3.1(1.8)	2.7(2.0)
126.4	1.9(2.9)	2.1(2.7)	1.9(2.8)	2.1(2.7)	1.7(3.2)
124.8	3.0(1.8)	3.2(1.7)	3.0(1.8)	3.3(1.7)	2.6(2.1)
69.1	2.5(2.1)	2.6(2.1)	2.5(2.2)	2.5(2.2)	2.5(2.2)

Table 4.14 Investigations of the sensitivity of the SUFIR method to small errors in pulse width in the measurement of 270MHz  $^{13}\text{C}$   $T_1$  for a concentrated solution of *sec*-phenethyl alcohol in  $\text{CDCl}_3$ . The  $180^\circ$  pulse width was mis-set from its measured value of  $17\mu s$ .

#### 4.8.3 $^{13}\text{C}$ $T_1$ Measurements of the Complexation of $\beta$ -Cyclodextrin with Ibuprofen Sodium in $\text{D}_2\text{O}$ using the SUFIR Sequence

Preliminary studies with the SUFIR sequence have compared  $^{13}\text{C}$   $T_1$  measurements of ibuprofen sodium in the presence and absence of a mole equivalent of  $\beta$ -cyclodextrin in  $\text{D}_2\text{O}$ . The solutions examined were of a comparatively high concentration (0.17M) in ibuprofen sodium to reduce initial experimental run times.



$^{13}\text{C}$  NMR data for ibuprofen sodium, referenced to a solution of DSS in  $\text{D}_2\text{O}$ , are given in Table 4.15. Resonances were assigned predominantly from a heteronuclear correlation experiment. Carbons  $\text{C1}'$  and  $\text{C4}'$  were assigned from weak correlations to the  $\text{H3}$  and  $\text{H1}''$  groups respectively in a long-range heteronuclear FLOCK experiment [295].

$\delta/\text{ppm}$	Assignment
186.8	C1
143.4	C1'
143.2	C4'
132.2	C3'
129.9	C2'
50.9	C2
46.9	C1''
32.5	C2''
24.4	C3''
21.2	C3

Table 4.15 270MHz  $^{13}\text{C}\{^1\text{H}\}$  data and assignments for a 0.17M solution of ibuprofen sodium in  $\text{D}_2\text{O}$

A heteronuclear correlation experiment of a 1:1 mole ratio solution of ibuprofen sodium and  $\beta$ -cyclodextrin in  $\text{D}_2\text{O}$  was also required to verify that the relative chemical shifts of these resonances were unchanged in the presence of  $\beta$ -cyclodextrin. An attempt to identify the resonances of carbons  $\text{C1}'$  and  $\text{C4}'$  in this case using the FLOCK experiment and the J coupling parameters of the ibuprofen sodium sample was, however, unsuccessful, perhaps as a result of enhanced rates of relaxation in the presence of the cyclodextrin [255]. Thus, it was unclear whether the single correlation which was observed between the lower field of these two resonances and  $\text{H2}'$  in this spectrum was the result of a 2 or 3 bond coupling pathway. The  $\text{C1}'$  and  $\text{C4}'$  resonances then remain unassigned.

As in  $^1\text{H}$  NMR spectroscopy, changes in chemical shift and chiral (or in the case of the isobutyl C3'' signal possibly prochiral) splittings of the ibuprofen sodium  $^{13}\text{C}$  resonances are observed in the presence of a mole equivalent of  $\beta$ -cyclodextrin. These are summarised in Table 4.16.

$^{13}\text{C}$ resonance	change in chemical shift/ppm	chiral splitting/ppm
C1	-0.9,-1.0	0.1
C1' and C4'	not assigned	0 or 0.1
C3'	-0.8	0
C2'	-0.5	0
C2	+0.2	0
C1''	+0.6	0
C2''	+0.4	0
C3''	+0.4,+0.3	0.1
C3	+0.7,+0.5	0.2

Table 4.16 Changes in chemical shift and chiral splittings of 270MHz  $^{13}\text{C}\{^1\text{H}\}$  resonances of a 0.17M solution of ibuprofen sodium in the presence of a mole equivalent of  $\beta$ -cyclodextrin in  $\text{D}_2\text{O}$

Splittings are all within the range of 0.1-0.2ppm and in the case of the C3 resonance and the unassigned C1' or C4' resonance are sufficient for baseline resolution to be achieved without recourse to the use of resolution enhancement functions. Their exploitation in the determination of optical purity is, however, hampered by the difficulties associated with quantitation in  $^{13}\text{C}$  NMR spectroscopy.

$^{13}\text{C}$   $T_1$  measurements for an aqueous solution of ibuprofen sodium were achieved using the SUFIR method. Two experiments with  $t$  delays of approximately 1.7s and 10s were found to be necessary to cover the range of  $T_1$ s within the substrate molecule. The results of these experiments are shown in Table 4.17. Entries are again absent from this table where calculation of  $T_1$  was not possible, either because, as above,  $S_2 > S_1$ , or because either  $S_1$  and/or  $S_2$  was of negligible peak intensity.



$^{13}\text{C}$ resonance	$T_1/s$ ( $t/T_1$ ) $t=10s$	$T_1/s$ ( $t/T_1$ ) $t=1.7s$
C1	19.3(0.52)	-
C1'	12.3(0.81)	-
C4'	11.3(0.88)	-
C3'	[1.9(5.27)]	2.0(0.87)
C2'	[2.1(4.74)]	2.1(0.82)
C2	-	1.8(0.97)
C1''	-	1.0(1.71)
C2''	[3.1(3.21)]	2.4(0.71)
C3''	-	1.5(1.11)
C3	3.5(2.89)	1.0(1.75)

Table 4.17 270MHz  $^{13}\text{C}$   $T_1$  for a 0.17M solution of ibuprofen sodium in  $\text{D}_2\text{O}$  measured using the SUFIR method. Calculated values for which  $t/T_1$  lies outside of its optimal range are given in parentheses

Cross-correlation effects, and consequent deviation from mono-exponential longitudinal relaxation [244,294], presumably account for a significant difference in the calculated  $T_1$  value for the C3 resonance from each experiment, since reasonable agreement is observed for other resonances where more than one determination of  $T_1$  was possible, even where the ratio of  $t/T_1$  lies outside its optimal range. Clearly, therefore, it must be considered essential when using the SUFIR method to carry out at least two determinations of  $T_1$  for each resonance using different  $t$  values, to ensure reproducibility of the calculated  $T_1$  and to establish mono-exponential relaxation, which is an important assumption of the SUFIR method.

As is generally the case, relaxation of the quaternary  $^{13}\text{C}$  nuclei was found to be significantly slower than that of other resonances, since the absence of directly attached protons reduces the efficiency of the dipolar relaxation mechanism. A further consequence of this absence is that nOe enhancement of the intensity of these resonances is also eliminated, and as a result of their small size, peak intensities, and therefore  $T_1$  values, for these nuclei are difficult to measure

with great accuracy. Although improvements in the signal-to-noise ratio of these quaternary signals may be anticipated with greater signal averaging, it is to be noted that for the solution of ibuprofen sodium examined here quaternary signals remained weak despite an approximately 9 hour acquisition period.

For a solution of ibuprofen sodium in the presence of a mole equivalent of  $\beta$ -cyclodextrin in  $D_2O$ , three SUFIR experiments were carried out to accommodate the range of  $^{13}C$   $T_1$  of host and guest. Results are summarised in Table 4.18. For shorter relaxation times, it was found necessary to halve the number of sampling points, leading to a reduction in spectral resolution, in order to achieve time delays which were sufficiently small.

$^{13}C$ resonance	$T_1/s$ ( $t/T_1$ ) $t=10s$	$T_1/s$ ( $t/T_1$ ) $t=1.7s$	$T_1/s$ ( $t/T_1$ ) $t=0.3s$
C1	8.0(1.25)	-	-
	6.1(1.65)	-	-
C1' or C4'	[3.3(3.07)]	-	-
	-	-	-
C1' or C4'	[2.1(4.73)]	2.3(0.75)	-
C3'	-	[0.5(3.13)]	0.5(0.57)
C2'	2.6(3.81)	0.6(2.78)	0.5(0.56)
C2	-	[0.5(3.71)]	-
C1''	-	-	0.3(0.85)
C2''	-	0.7(2.45)	-
C3''	-	0.8(2.12)	-
	-	0.8(2.09)	-
C3	-	[0.5(3.68)]	-
	[2.9(3.49)]	0.7(2.35)	-

Table 4.18 270MHz  $^{13}C$   $T_1$  for a 0.17M solution of ibuprofen sodium in the presence of a mole equivalent of  $\beta$ -cyclodextrin in  $D_2O$  using the SUFIR method. Calculated values for which  $t/T_1$  lies outside of its optimal range are given in parentheses

It is difficult to draw conclusive comparisons between  $T_1$  values given in Tables 4.17 and 4.18, since additional work is certainly required to establish their reproducibility. There are several points which may be made however. Thus, there appears to be a general reduction in  $^{13}\text{C}$   $T_1$  of drug resonances upon the addition of  $\beta$ -cyclodextrin, which for non-quaternary carbons may, from equation 4.7, be associated with an increase in  $t_c$  and a slowing of molecular reorientation. Measurement of solution viscosity would allow distinction between the contributions of drug inclusion and an increase in solution viscosity to this effect [290]. Accurate determination of the degree of complexation of ibuprofen sodium in the presence of cyclodextrin is furthermore required for detailed interpretation.

Relaxation times for the  $^{13}\text{C}$  resonances of  $\beta$ -cyclodextrin lie within the range 0.1-0.2s and are of the anticipated order of magnitude [291].  $^{13}\text{C}$   $T_1$  for the uncomplexed  $\beta$ -cyclodextrin macrocycle were not measured here, primarily because the limited solubility of the cyclodextrin does not allow preparation of solutions of the concentration achieved in the presence of ibuprofen sodium. Additionally, little change in the dynamics of the macrocycle was expected on formation of the inclusion complex, as has been observed in the presence of other substrates [291].

#### 4.9 Conclusion

The work reported here was directed towards greater understanding of the complexing and chiral discriminatory properties of the cyclodextrins. NMR spectroscopic methods have been used to examine the interaction of  $\beta$ -cyclodextrin with a series of 2-arylpropionates. Analysis of  $^1\text{H}$  chemical shift and coupling constant data in  $\text{D}_2\text{O}$  and  $d_6$ -DMSO allowed a common structure for the cyclodextrin with several of these guest substrates to be proposed. Whilst it was generally assumed in this interpretation that complexation of substrate and cyclodextrin was the result of interaction of a single molecule of each species, in

the case of flurbiprofen sodium results suggested that complexation in aqueous solution involved interaction of the guest with more than one molecule of cyclodextrin. Job plot studies in D<sub>2</sub>O confirmed a 1:1 stoichiometry of host and guest in the complex in all cases and lead to the proposal of a dimeric structure for the complex formed between flurbiprofen sodium and  $\beta$ -cyclodextrin. Chemical shift data from the continuous variation plot were insufficiently sensitive to the complexation process to distinguish the monomeric and dimeric inclusion complex directly, and illustrate a significant short-coming of the method. In general, previous reports have been inclined to overlook the possible formation of other than monomeric structures in NMR Job plot experiments, but in view of the undoubted tendency to association exhibited by the cyclodextrin macrocycle in the presence of certain substrates this remains an area for future study.

Measurement of the nuclear Overhauser effect for a more direct approach to information relating to the structure of the cyclodextrin complex was also undertaken. NOe difference spectroscopy was found to be unsuitable as a result of the inherently small size of the nOe, which is a consequence of the molecular correlation time of the inclusion complex. The ROESY experiment was thought to offer a promising alternative to the nOe difference experiment, since in this method positive nOes of a reasonable magnitude are observed regardless of molecular correlation time. Additionally, the 2D method eliminated the need to achieve selective perturbation of resonances as is required in 1D nOe experiments, and which was difficult to achieve here as a result of resonance overlap, the extent of which depended on the guest substrate. A disadvantage of the method resulted from the necessary reduction in spectral resolution in the 2D data matrix, which restricted interpretation, particularly through a failure to distinguish H3, H5 and H6 resonances of the cyclodextrin in certain cases. The H2 resonance of the guest substrate was also commonly obscured beneath resonances of the cyclodextrin and compounded this difficulty.

Distinction between the true and false ROESY cross-peaks in ROESY spectra also proved difficult, since for maximal resolution, the carrier necessarily lay close to the cyclodextrin resonances and promoted the TOCSY interactions which form the basis of the false ROESY cross-peak. Movement of the carrier position and a lowering of spin-lock power were largely unsuccessful in eliminating this problem and unequivocal interpretation of the resulting spectra in terms of unique structures of the cyclodextrin inclusion complexes of the 2-arylpropionates was not possible. We believe, therefore, that until variations of the ROESY experiment which allow the selective elimination of TOCSY pathways have been derived, application of this method to the study of the structure of the cyclodextrin inclusion complex is limited. Previous studies which have made use of the ROESY experiment in the elucidation of cyclodextrin complex structure have made little reference to the distinction of the true and false ROESY cross-peak. Additionally, fortuitous resolution of cyclodextrin  $^1\text{H}$  resonances, which facilitated spectral interpretation in these cases, is noted.

Preliminary studies with the SUFIR method allowed measurement of  $^{13}\text{C}$   $T_1$  values in a time considerably shorter than the classical inversion-recovery method would require. Application to the study of cyclodextrin inclusion complexation suggests that the method may be useful in providing additional structural and dynamic information relating to the complex.

#### Appendix 4.1

#### 400MHz $^1\text{H}$ NMR Data and Assignments for the Sodium Salts of some 2-Arylpropionic Acids at a Concentration of 0.014M in $\text{D}_2\text{O}$ at $30^\circ\text{C}$

##### 1. Sodium 2-phenylpropionate

<u>Chemical Shift/ppm</u> <u>(Coupling Constant/Hz)</u>	<u>Assignment</u>
7.472 (t,7.2)	H3'
7.434 (d,6.6)	H2'
7.376 (tt,6.8,2.0)	H4'
3.727 (q,7.2)	H2
1.487 (d,7.1)	H3

##### 2. Sodium 2-(4-chlorophenyl)propionate

<u>Chemical Shift/ppm</u> <u>(Coupling Constant/Hz)</u>	<u>Assignment</u>
7.456 (d,8.5)	H3'
7.389 (d,8.5)	H2'
3.711 (q,7.2)	H2
1.476 (d,7.1)	H3

The assignments of H3' and H2' in the free drug were confirmed by a  $^1\text{H}$  nOe difference experiment. Irradiation of the H2 and H3 resonances both lead to the observation of a positive nOe at the high field aromatic signal. Additionally, irradiation of the high field aromatic doublet gave a positive nOe at H2, whilst no enhancements were observed upon irradiation of the low field aromatic signal.

Assignment of aromatic resonances in the presence of  $\beta$ -cyclodextrin was not achieved. Two dimensional ROESY experiments aimed at their distinction through correlation to the H2 and H3 groups were unsuccessful. Additionally, the monitoring of shifts in aromatic signals through the analysis of Job plot data was prohibited by the strong coupling of these resonances exhibited at the lower field at which these plots were carried out (270MHz *versus* 400MHz).

### 3. Sodium 2-(4-nitrophenyl)propionate

<u>Chemical Shift/ppm</u> <u>(Coupling Constant/Hz)</u>	<u>Assignment</u>
8.292 (d,9.0)	H3'
7.614 (d,8.5)	H2'
3.864 (q,7.2)	H2
1.541 (d,7.3)	H3

Job plot data confirm that no change in relative position of the H2' and H3' resonances is observed in the presence of  $\beta$ -cyclodextrin. Aromatic resonances for the free salt are readily assigned from the large down-field shift associated with a phenyl proton *ortho* to a nitro substituent.

### 4. Ibuprofen Sodium

<u>Chemical Shift/ppm</u> <u>(Coupling Constant/Hz)</u>	<u>Assignment</u>
7.351 (d,8.3)	H2'
7.296 (d,8.1)	H3'
3.692 (q,7.2)	H2
2.562 (d,7.1)	H1''
1.922 (m,6.8)	H2''
1.470 (d,7.1)	H3
0.958 (d,6.8)	H3''

The aromatic resonances for ibuprofen sodium were assigned by an nOe difference experiment. Irradiation of the high field aromatic doublet gave a positive nOe at the isobutyl H2'' resonance, whilst irradiation of the low field signal gave an enhancement at H2. Correspondingly, irradiation at H2 gave a positive nOe at the low field aromatic resonance.

The assignment of these resonances in the complexed state was achieved from ROESY data. Clear correlations between the H3 resonance of the drug and the low field aromatic signal and the isobutyl H1'' group and the high field aromatic signal were observed in spectra used in the elucidation of the structure of the ibuprofen sodium inclusion complex with  $\beta$ -cyclodextrin.



## 5. Naproxen Sodium

<u>Chemical Shift/ppm</u> <u>(Coupling Constant/Hz)</u>	<u>Assignment</u>
7.929 (d,9.0)	H8'
7.901 (d,8.6)	H4'
7.841 (d,1.0)	H1'
7.570 (dd,8.5,2.0)	H3'
7.438 (d,2.7)	H5'
7.296 (dd,9.0,2.7)	H7'
4.024 (s)	OMe
3.864 (q,7.2)	H2
1.570 (d,7.1)	H3

Assignment of the naproxen sodium resonances, based on coupling constants and the up-field shift associated with aromatic protons *ortho* to an -OMe substituent, was confirmed by a combination of nOe difference and decoupling spectroscopy. Irradiation of the methoxy resonance in a  $^1\text{H}$  nOe difference experiment gave positive nOe enhancements at H5' and H7'. Irradiation of the H2 resonance then gave positive enhancements of H1' and H3'. Decoupling of the H7' resonance caused the collapse of H8' to a singlet and completed assignment.

Job plot spectra and a COSY-45 experiment supported the assignment of resonances observed in the presence of a mole equivalent of  $\beta$ -cyclodextrin.

## 6. Flurbiprofen Sodium

<u>Chemical Shift/ppm</u> <u>(Coupling Constant/Hz)</u>	<u>Assignment</u>
7.708 (d,8.3)	H2''
7.612 (t,7.4)	H3''
7.559 (t,8.2)	H5'
7.534 (tt,7.3,1.6)	H4''
7.318 (dd,7.9,1.6)	H6'
7.283 (dd,12.2,1.7)	H2'
3.773 (q,7.2)	H2
1.522 (d,7.3)	H3

Assignment of drug resonances was confirmed by a COSY-45 experiment with folding of the H3 resonance for improved spectral resolution. Aromatic proton resonances H2'' and H3'' were readily identified from their integral. COSY



cross-peaks between H2'' and H3'' and H4'' identified the latter so that the remaining triplet resonance could be identified as H5'. Correlation of the H5' resonance with that of H6' gave the H2' resonance by default.

Assignment of aromatic resonances in the presence of a mole equivalent of  $\beta$ -cyclodextrin was complicated by broadening and overlap of signals. The H2'' doublet was, however, clearly visible, and although exact chemical shifts could not be determined, the position of the overlapping H2' and H6' resonances were identified from Job plot spectra. Other resonances remain unassigned despite the use of COSY-45 spectroscopy.

## Appendix 4.2

### 400MHz $^1\text{H}$ NMR Data and Assignments for the Sodium Salts of some 2-Arylpropionic Acids at a Concentration of 0.014M in $d_6$ -DMSO at 30°C

#### 1. Sodium 2-phenylpropionate

<u>Chemical Shift/ppm</u> <u>(Coupling Constant/Hz)</u>	<u>Assignment</u>
7.261 (d,7.1)	H2'
7.174 (t,7.6)	H3'
7.064 (tt,7.3,1.3)	H4'
3.234 (q,7.1)	H2
1.231 (d,7.1)	H3

#### 2. Sodium 2-(4-chlorophenyl)propionate

<u>Chemical Shift/ppm</u> <u>(Coupling Constant/Hz)</u>	<u>Assignment</u>
7.277 (d,8.6)	H2'
7.222 (d,8.8)	H3'
3.235 (q,7.1)	H2
1.223 (d,7.1)	H3

#### 3. Ibuprofen sodium

<u>Chemical Shift/ppm</u> <u>(Coupling Constant/Hz)</u>	<u>Assignment</u>
7.162 (d,7.8)	H2'
6.955 (d,8.1)	H3'
3.204 (q,7.1)	H2
2.366 (d,7.3)	H1''
1.782 (m,6.8)	H2''
1.213 (d,7.1)	H3
0.851 (d,6.8)	H3''

#### 4. Flurbiprofen sodium

<u>Chemical Shift/ppm</u> <u>(Coupling Constant/Hz)</u>	<u>Assignment</u>
7.508 (d,8.3)	H2''
7.451 (t,7.6)	H3''
7.360 (tt,7.2,1.7)	H4''
7.329 (t,8.4)	H5'
7.179 (dd,12.8,1.6)	H2'
7.162 (dd,8.2,1.3)	H6'
obscured by residual water resonance	H2
1.277 (d,7.1)	H3

#### 5. Naproxen sodium

<u>Chemical Shift/ppm</u> <u>(Coupling Constant/Hz)</u>	<u>Assignment</u>
7.698 (d,8.8)	H8'
7.629 (d,8.6)	H4'
7.607 (s)	H1'
7.470 (dd,8.5,1.7)	H3'
7.211 (d,2.7)	H5'
7.072 (dd,8.9,2.6)	H7'
3.845 (s)	OMe
3.380 (q,7.1)	H2
1.319 (d,7.1)	H3

## CHAPTER 5

### Experimental Methods

#### 5.1 Chemical Suppliers

Reagents used in this work were supplied as follows: (+)-camphor (Aldrich); 2-(4-chlorophenyl)propionic acid (Janssen, MW=184.62); cumene (Aldrich);  $\alpha$ -cyclodextrin (Wacker, MW=972.86);  $\beta$ -cyclodextrin (Aldrich, MW=1135.01);  $\gamma$ -cyclodextrin (Wacker or Fluka, MW=1297.15); deuterated water (Goss or Merck); deuteriochloroform (Merck); 2,6- dimethyl- $\beta$ -cyclodextrin (Fluka, MW=1331.40); 2,2-dimethyl-2-silapentane-5- sulfonate (Aldrich);  $d_6$ -dimethylsulfoxide (Merck); flurbiprofen (Boots, MW=244.27); ibuprofen (Boots, MW=206.29); (R)-ibuprofen (Boots, MW=206.29); (S)-ibuprofen (Boots, MW=206.29); ibuprofen sodium (R P Scherer, MW=228.27); methanol, SLR grade (Fisons);  $\beta$ -methylphenethylamine (Aldrich); naproxen sodium (Sigma, MW=252.25); *sec*-phenethyl alcohol (Aldrich); phenol, AR grade (Fisons); 2-(4-nitrophenyl)propionic acid (Aldrich, MW=195.18); 2-phenylpropionic acid (Aldrich, MW=150.18); sodium chloride, AR grade (Fisons); sodium deuterioxide, 30% solution in D<sub>2</sub>O (Aldrich); sodium hydroxide pellets, AR grade (Fisons); sodium hydroxide, 0.1M Convol (BDH); sodium hydroxide, 0.1M Volucon (May and Baker); tween 80 (BDH)

All reagents were used as supplied, except in the case of methanol, which was distilled before use.

#### 5.2 Preparation of the Salts of the 2-Arylpropionic Acids

Ibuprofen and naproxen were supplied as the sodium salt. For all other 2-arylpropionic acids, the sodium salt was prepared by the following general procedure.

Typically, 5 or 10 ml of a standardised Convol or Volucon solution of 0.1M sodium hydroxide prepared in distilled water was added to a mole equivalent of the appropriate 2-arylpropionic acid dissolved in 5-10ml of distilled methanol. Following stirring and filtration through a plug of cotton wool, the solutions were taken to dryness on a rotary evaporator and dried under vacuum at a temperature of 100-120°C for several hours. Salts of (R)-ibuprofen and (S)-ibuprofen were similarly prepared, but on a smaller scale as a result of the restricted availability of these compounds. Alternatively the sodium hydroxide solution was added directly to the 2-arylpropionic acid and taken to dryness prior to dissolution in distilled methanol.

### 5.3 Biological Fluid Studies with Ibuprofen

#### 5.3.1 *in vivo* Studies with Ibuprofen

An oral dose of 400mg ibuprofen (Inoven™) was ingested with approximately 100ml of water by a healthy adult female. A urine sample was collected immediately and at approximately 4 hours and 8 3/4 hours thereafter and stored frozen until use.

Following defrosting to room temperature, 5ml aliquots of these samples were taken and 0.2ml of a 0.014M solution of DSS in distilled water added to them. These were then freeze-dried and reconstituted with 1ml D<sub>2</sub>O or an approximately 0.07M solution of NaOD in D<sub>2</sub>O, before being transferred directly to 5mm NMR tubes.

#### 5.3.2 *in vitro* Studies with Ibuprofen Sodium

*in vitro* studies of the discrimination of the enantiomers of ibuprofen sodium in human urine with DMCD were carried out using a urine sample collected from a healthy adult female. 1ml aliquots of this sample were freeze-

dried, either immediately following collection or after freezer storage, and reconstituted with 0.65ml of either D<sub>2</sub>O, a 1mg/ml (0.0044M) solution of ibuprofen sodium in D<sub>2</sub>O, or of a 1mg/ml solution of ibuprofen sodium in D<sub>2</sub>O to which the appropriate weight of DMCD had been added. Reconstituted samples were transferred directly to 5mm NMR tubes.

#### 5.4 *in vivo* Studies with Flurbiprofen

1. Two male Wistar rats of approximately 380g were starved over-night prior to oral dosing with 0.38ml of either a 1% solution of tween 80 or an approximately 10mg/ml suspension of flurbiprofen in a 1% solution of tween 80. The rats were kept in individual metabolism cages and allowed access to food and water. Urine samples were collected at approximately 0-7 1/2 and 7 1/2- 24 hours and stored frozen. Additionally, 1ml blood samples were taken at approximately 1 1/4 hours after dosing under an ether anaesthetic, but were not used in the work reported here.

0.3 or 0.4ml of these urine samples were taken following defrosting and 100µl of a 0.007M solution of DSS in D<sub>2</sub>O added to them. Samples were then freeze-dried and reconstituted with 0.4 or 0.5ml of an approximately 0.07M solution of NaOD in D<sub>2</sub>O. Reconstituted control rat urine was subsequently spiked with 0.1ml of a 0.029M solution of flurbiprofen in approximately 0.07M NaOD in D<sub>2</sub>O, followed by 0.1ml of a 0.11M solution of DMCD also prepared in 0.07M NaOD in D<sub>2</sub>O.

2. Two male Wistar rats of approximately 300g were starved over-night and orally dosed with 0.9ml of either distilled water or a 16.6mg/ml aqueous solution of flurbiprofen, converted to its salt *in situ* by addition of an equivalent of sodium hydroxide prepared as an aqueous solution. Animals were kept in individual metabolism cages following dosing and allowed access to food and water. Urine

samples were collected at approximately 0-7 and 7-24 hours and stored frozen prior to use.

### 5.5 Preparation of Non-biological NMR Samples

Non-biological samples for NMR analysis were commonly prepared by weighing of the sodium 2-arylpropionate and/or cyclodextrin and subsequent addition of an appropriate volume of deuterated solvent. Routinely, solutions were of a concentration 0.014M in host and/or guest, so that for 0.8ml of solution 1.9-2.9mg of guest substrate and 12.5mg of, for example,  $\beta$ -cyclodextrin were required. In studies of the effects of the presence of ionic salts on cyclodextrin complexation, solutions of sodium 2-arylpropionate and  $\beta$ -cyclodextrin prepared in this manner were then added quantitatively to an appropriate amount of the salt sodium chloride. Solutes generally dissolved readily on shaking, except in the case of dissolution of  $\beta$ -cyclodextrin in  $D_2O$ , where warming was sometimes required. Samples were generally filtered through a plug of cotton wool into 5mm NMR tubes.

Alternatively, solutions were prepared by volumetric addition of a quantitative solution of the cyclodextrin or sodium 2-arylpropionate in the deuterated solvent of choice to the other preweighed reagent.

Job plot studies were carried out by the quantitative mixing of individual, approximately 0.0078M, solutions of the sodium 2-arylpropionate and  $\beta$ -cyclodextrin in  $D_2O$  in volumes of 0.25 and 0.75ml, 0.33 and 0.67ml, 0.50 and 0.50ml, 0.67 and 0.33ml and 0.75 and 0.25ml respectively. In this case, solutions were not filtered during transfer to 5mm NMR tubes.

Test samples for the SUFIR sequence were not prepared quantitatively, but were all of high concentration.

## 5.6 NMR Methods

NMR spectra were routinely acquired on a JEOL JNM GX400 FT NMR spectrometer, sited in the Department of Chemistry, University of Bristol, and operating at a frequency of 399.65MHz for  $^1\text{H}$  and 54.10MHz for  $^{17}\text{O}$ . The spectrometer was equipped with a 5mm dedicated proton or tunable probe and a NM-GVT3 variable temperature controller.

Spectra were acquired at 30°C ( $\pm 1^\circ\text{C}$ ), except where stated, following an equilibration period of at least 10 minutes.

$^1\text{H}$  data were collected over a spectral width of 4000Hz following application of a pulse of 1.5 $\mu\text{s}$ , corresponding to a pulse angle of approximately  $8^\circ$  or  $18^\circ$  depending on the probe in use. 32K data points were transformed using a 0.12Hz exponential broadening factor combined with a trapezoidal apodization function\* (T1=0%, T2=0%, T3=90%, T4=100%) to give a final resolution of

---

\* The trapezoidal window function is here described in terms of four time parameters, T1-T4, which are expressed as a percentage of the acquisition time. These parameters define the co-ordinates of the four corners of the desired trapezium-shaped transformation function.

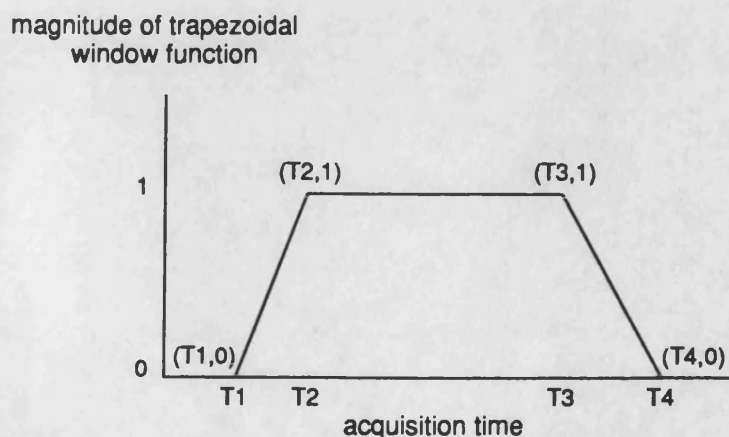


Figure 5.1 Parameters describing the trapezoidal window function



0.24Hz. Typically, 64 scans were collected using a pulse delay of 1 or 2s. Spectra were referenced to the residual solvent resonance.

Solvent suppression was achieved, where necessary, under equivalent conditions using the homogated decoupling sequence and an increased pulse delay of 5s, to ensure adequate saturation of the solvent resonance during this period. Continuous homonuclear decoupling spectra were similarly acquired with a delay of 5s following application of a pulse corresponding to a pulse angle of approximately  $40^\circ$ .

NOe difference spectra were similarly acquired over a spectral width of 4000Hz by interleaving the collection of 16 scans at each irradiation point following a pulse typically corresponding to an angle of approximately  $45^\circ$ . The pulse delay for such experiments was again increased to 5s. 16K data points were collected, zero-filled and transformed using a 2Hz exponential broadening factor combined with a trapezoidal apodization function ( $T1=0\%$ ,  $T2=0\%$ ,  $T3=90\%$ ,  $T4=100\%$ ) prior to spectral subtraction, giving a resolution of 0.24Hz. Typically, 64-384 scans were collected for each irradiation point.

Homonuclear 2D data sets were generally collected in matrices of size 1024 x 256 points and zero-filled in  $f_1$  prior to transformation, which for a standard spectral width of 4000Hz gave a resolution of 7.81Hz in each dimension. Typically 8 scans per slice were collected, using a pulse delay of 1s.

COSY-45 spectra were acquired in the absolute value mode and were transformed using a sine-bell window function.

ROESY spectra were acquired in the phase-sensitive mode using either a continuous spin-locking period, or an intermittent field of 10% duty cycle and composed of pulses corresponding to an angle of approximately  $30^\circ$ . Typically, this field was of strength 3.8-5.3kHz, and applied for a period of 400ms. Transformation was achieved using a trapezoidal apodization function ( $T1=0\%$ ,

T2=0%, T3=70%, T4=100%) in each dimension. Preliminary spectra were acquired with a reduced 2D matrix size of 512 x 128 points.

$^{17}\text{O}$   $T_1$  measurements were made using the inversion-recovery sequence and processed with the spectrometer software. Data were the result of the accumulation of 512 scans at each of 6 values of the variable time delay  $t$ , and the method of least squares was used to calculate  $T_1$  (equation 3.2) using an exponential weighting function. Data points in these calculations were rejected where the change in peak intensity was less than 20% of its maximum possible value. Spectra were collected over a frequency width of 50000Hz using a pulse delay of 0.05s. 8K data points were acquired and transformed using an exponential broadening factor of 1.5Hz combined with a trapezoidal apodization function (T1=0%, T2=0%, T3=90%, T4=100%) to give a resolution of 3.05Hz.

Alternatively, spectra were acquired on a JEOL JNM GX270 FT NMR spectrometer, sited in the School of Pharmacy and Pharmacology, University of Bath, and operating at a frequency of 270.05MHz for  $^1\text{H}$  and 67.80MHz for  $^{13}\text{C}$ . The spectrometer was equipped with a 5mm dual  $^{13}\text{C}/^1\text{H}$  or tunable probe, but had no temperature control capabilities. Solutions were therefore necessarily examined at ambient temperature.

For  $^1\text{H}$  spectra typically 256 scans were acquired using a 5 $\mu\text{s}$  pulse, corresponding to an angle of approximately  $28^\circ$  and a pulse delay of 0.541s. 32K data points were collected over a spectral width of 3001.2Hz and were transformed using a 0.1Hz exponential broadening factor in conjunction with a trapezoidal apodization function (T1=0%, T2=0%, T3=90%, T4=100%) to give a resolution of 0.18Hz. Spectra were referenced to the residual solvent resonance or to DSS where added.

$^{13}\text{C}$  spectra were acquired using a pulse of  $4\mu\text{s}$  equivalent to an angle of approximately  $45^\circ$  and a pulse delay of 0.213s. Continuous broad-band  $^1\text{H}$  decoupling was achieved using the WAUGH sequence. 16K data points were collected over a spectral width of 18050.5Hz corresponding to a resolution of 2.2Hz and were transformed using an exponential broadening factor of 1.1Hz combined with a trapezoidal apodization function ( $T_1=0\%$ ,  $T_2=0\%$ ,  $T_3=90\%$ ,  $T_4=100\%$ ). Spectra were referenced to the residual solvent resonance, or where this was inappropriate, to a sample of DSS in  $\text{D}_2\text{O}$ . The number of transients collected was largely dependent on sample concentration.

$^{13}\text{C}$ - $^1\text{H}$  heteronuclear correlation experiments were recorded using a matrix size of 1024 x 128 points, and assuming a  $^1J_{\text{CH}}$  value of approximately 139Hz. 64 scans per slice were acquired with a pulse delay of 2s, and data sets zero-filled in the  $f_1$  domain prior to transformation with a 4Hz exponential broadening factor in  $f_2$  combined with a trapezoidal window function ( $T_1=0\%$ ,  $T_2=10\%$ ,  $T_3=70\%$ ,  $T_4=100\%$ ) in both dimensions. Resolution in the  $f_1$  and  $f_2$  domains was 19.38Hz x 11.7Hz and 35.25Hz x 11.7Hz for ibuprofen sodium in the presence and absence of a mole equivalent of  $\beta$ -cyclodextrin respectively.

Long-range  $^{13}\text{C}$ - $^1\text{H}$  heteronuclear correlation experiments were acquired using the FLOCK experiment, the pulse sequence for which was provided by Martin Kipps, ICI Plant Protection Division, Bracknell. 112 scans per slice were collected for a matrix of 2048 x 128 points, using a pulse delay of 1s, and assuming  $^1J_{\text{CH}}$  and  $^2J_{\text{CH}}$  of approximately 139Hz and 8Hz respectively. Data were zero-filled in  $f_1$  prior to transformation with a 4Hz exponential broadening factor in  $f_2$  combined with a trapezoidal window function ( $T_1=0\%$ ,  $T_2=10\%$ ,  $T_3=70\%$ ,  $T_4=100\%$ ) in both dimensions, to give a final resolution of 9.69Hz x 11.7Hz.

$^{13}\text{C}$   $T_1$  measurements were made using either the inversion-recovery or SUFIR methods. Broad-band  $^1\text{H}$  decoupling was obtained in all cases using the WAUGH sequence. Spectra were acquired over a spectral width of 18050.5Hz and

typically collected into 16K data points and transformed using an exponential broadening factor of 1.1Hz combined with a trapezoidal apodization function ( $T_1=0\%$ ,  $T_2=0\%$ ,  $T_3=90\%$ ,  $T_4=100\%$ ) to give a resolution of 2.2Hz.

Determinations using the inversion-recovery method were the result of 8-128 scans for each of 8-10 values of the variable parameter  $t$ . Processing was achieved in a manner analogous to that described for measurements of  $^{17}\text{O}$   $T_1$ .

$T_1$  values from peak intensity measurements resulting from the SUFIR experiment were calculated on a BBC Archimedes Computer (Chapter 4). For test samples 8-128 scans were typically collected.  $T_1$  measurements of ibuprofen sodium samples were the result of 800-1100 scans.

$^{19}\text{F}$  data presented in this thesis were kindly recorded by Martin Kipps, ICI Plant Protection Division, Bracknell. For non- biological samples, spectra were acquired on a JEOL JNM GSX270 FT NMR spectrometer, operating at 254.05MHz for  $^{19}\text{F}$ . Broad-band proton-decoupled spectra were the result of the accumulation of 16 scans. 16K data points were acquired over a spectral width of 3001.2Hz giving a resolution of 0.37Hz. Fourier transformation was achieved using an exponential broadening factor of 0.2Hz combined with a trapezoidal apodization function ( $T_1=0\%$ ,  $T_2=0\%$ ,  $T_3=90\%$ ,  $T_4=100\%$ ).

$^{19}\text{F}$  spectra for biological samples were acquired on a JEOL JNM GX400, operating at 376.05MHz for  $^{19}\text{F}$ . 16K data points were acquired over a spectral width of 7530.1Hz. Data were zero-filled and transformed using an exponential broadening factor of 0.2Hz combined with a trapezoidal apodization function ( $T_1=0\%$ ,  $T_2=0\%$ ,  $T_3=90\%$ ,  $T_4=100\%$ ) to give a resolution of 0.46Hz. Spectra were recorded in either the proton-coupled or selective proton-decoupled mode, and were the result of the collection of 256 scans for urine samples spiked with flurbiprofen, or of 9000 scans for samples containing metabolized drug. Spectra

were referenced to a sample of  $D_2O$  containing a capillary of fluorotrichloromethane.

## REFERENCES

1. E.J. Ariëns and E.W. Wuis, *Clin. Pharmacol. Ther.* **42** 361-363 (1987)
2. *British National Formulary*, (September 1991)
3. *Goodman and Gilman's The Pharmacological Basis of Therapeutics*, 7th Edition, ed. A. Goodman Gilman, L.S. Goodman, T.W. Rall and F. Murad, Macmillan (1985)
4. R.O. Day, G.G. Graham, K.M. Williams and P.M. Brooks, *Drugs* **36** 643-651 (1988)
5. E.J. Ariëns, *Trends Pharmacol. Sci.* **7** 200-205 (1986)
6. E.J. Ariëns, *Eur. J. Clin. Pharmacol.* **26** 663-668 (1984)
7. E.J. Ariëns, *Med. Res. Rev.* **6** 451-466 (1986)
8. E.J. Ariëns, *Pharmacol. Toxicol.* **64** 319-320 (1989)
9. A.M. Evans, R.L. Nation, L.N. Sansom, F. Bochner and A.A. Somogyi, *Br. J. Clin. Pharmacol.* **26** 771-780 (1988)
10. J. Gal, *Clin. Pharmacol. Ther.* **44** 251-253 (1988)
11. B. Testa and W.F. Trager, *Chirality* **2** 129-133 (1990)

12. G.T. Tucker and M.S. Lennard, *Pharmacol. Ther.* **45** 309-329 (1990)
13. K. Williams and E. Lee, *Drugs* **30** 333-354 (1985)
14. C.A.M. Van Ginneken, J.F. Rodrigues de Miranda and A.J. Beld in *Stereochemistry and Biological Activity of Drugs*, ed. E.J. Ariëns, W. Soudijn and P.B.M.W.M. Timmermans, Blackwell Scientific (1983)
15. L. Borgström, L. Nyberg, S. Jönsson, C. Lindberg and J. Paulson, *Br. J. Clin. Pharmacol.* **27** 49-56 (1989)
16. J.H. Lin, D.M. Cocchetto and D.E. Duggan, *Clin. Pharmacokinet.* **12** 402-432 (1987)
17. S. Iwakawa, H. Spahn, L.Z. Benet and E.T. Lin, *Biochem. Pharmacol.* **39** 949-953 (1990)
18. J.H. Perrin, *J. Pharm. Pharmacol.* **25** 208-212 (1973)
19. P.J. Hayball and P.J. Meffin, *J. Pharmacol. Exp. Ther.* **240** 631-636 (1987)
20. M.P. Knadler, D.C. Brater and S.D. Hall, *J. Pharmacol. Exp. Ther.* **249** 378-385 (1989)
21. A.M. Evans, R.L. Nation, L.N. Sansom, F. Bochner and A.A. Somogyi, *Eur. J. Clin. Pharmacol.* **36** 283-290 (1989)

22. S. Rendic, T. Alebic-Kolbah, F. Kajfez and V. Sunjic, *Farmaco, Ed. Sci.* **35** 51-59 (1980)
23. M.E. Jones, B.C. Sallustio, Y.J. Purdie and P.J. Meffin, *J. Pharmacol. Exp. Ther.* **238** 288-294 (1986)
24. E.J.D. Lee, K. Williams, R. Day, G. Graham and D. Champion, *Br. J. Clin. Pharmacol.* **19** 669-674 (1985)
25. B.W. Berry and F. Jamali, *J. Pharm. Sci.* **78** 632-634 (1989)
26. J. Caldwell and M. Varwell Marsh, *Biochem. Pharmacol.* **32** 1667-1672 (1983)
27. R. Fears, K.H. Baggaley, R. Alexander, B. Morgan and R. M. Hindley, *J. Lipid Res.* **19** 3-11 (1978)
28. D.J. Porubek, S.M. Sanins, J.R. Stephens, M.P. Grillo, D.G. Kaiser, G.W. Halstead, W.J. Adams and T.A. Baillie, *Biochem. Pharmacol.* **42** R1-R4 (1991)
29. K. Williams, R. Day, R. Knihinicki and A. Duffield, *Biochem. Pharmacol.* **35** 3403-3405 (1986)
30. B.C. Sallustio, P.J. Meffin and K.M. Knights, *Biochem. Pharmacol.* **37** 1919-1923 (1988)
31. J. Caldwell, A.J. Hutt and S. Fournel-Gigleux, *Biochem. Pharmacol.* **37** 105-114 (1988)



32. D.H. Chatfield and J.N. Green, *Xenobiotica* **8** 133-144 (1978)
33. A. Rubin, P. Warrick, R.L. Wolen, S.M. Chernish, A.S. Ridolfo and C.M. Gruber Jr., *J. Pharmacol. Exp. Ther.* **183** 449-457 (1972)
34. P.C. Risdall, S.S. Adams, E.L. Crampton and B. Marchant, *Xenobiotica* **8** 691-704 (1978)
35. G.F. Lockwood and J.G. Wagner, *J. Chromatogr.* **232** 335-343 (1982)
36. L.M. Fuccella, G.C. Goldaniga, E. Moro, V. Tamassia, G.P. Tosolini and G. Valzelli, *Eur. J. Clin. Pharmacol.* **6** 256-260 (1973)
37. E.J. Segre, *J. Clin. Pharmacol.* **15** 316-323 (1975)
38. J. Pottier, D. Berlin and J.P. Raynaud, *J. Pharm. Sci.* **66** 1030-1036 (1977)
39. F. Jamali, A.S. Russell, C. Lehmann and B.W. Berry, *J. Pharm. Sci.* **74** 953-956 (1985)
40. C.G. Gibson and P. Skett, *Introduction to Drug Metabolism*, Chapman and Hall (1986)
41. M. El Mouelhi, H.W. Ruelius, C. Fenselau and D.M. Dulik, *Drug Metab. Dispos.* **15** 767-772 (1987)
42. Y. Nakamura and T. Yamaguchi, *Drug Metab. Dispos.* **15** 529-534 (1987)

43. D.G. Kaiser, G.J. Vangiessen, R.J. Reischer and W.J. Wechter, *J. Pharm. Sci.* **65** 269-273 (1976)
44. S. Fournel and J. Caldwell, *Biochem. Pharmacol.* **35** 4153-4159 (1985)
45. T. Yamaguchi and Y. Nakamura, *Drug Metab. Dispos.* **15** 535-539 (1987)
46. C.-S. Chen, T. Chen and W.-R. Shieh, *Biochim. Biophys. Acta* **1033** 1-6 (1990)
47. S.J. Lan, K.J. Kripalani, A.V. Dean, P. Egli, L.T. DiFazio and E.C. Schreiber, *Drug Metab. Dispos.* **4** 330-339 (1976)
48. F. Jamali, *Eur. J. Drug. Metab. Pharmacokinet.* **13** 1-9 (1988)
49. W.J. Wechter, D.G. Loughhead, R.J. Reischer, G.J. VanGiessen and D.G. Kaiser, *Biochem. Biophys. Res. Commun.* **61** 833-837 (1974)
50. R.D. Knihinicki, K.M. Williams and R.O. Day, *Biochem. Pharmacol.* **38** 4389-4395 (1989)
51. K.M. Knights, R. Drew and P.J. Meffin, *Biochem. Pharmacol.* **37** 3539-3542 (1988)
52. J.M. Mayer, C. Bartolucci, J.-M. Maître and B. Testa, *Xenobiotica* **18** 533-543 (1988)
53. J.M. Mayer, M. Young, B. Testa and J.-C. Etter, *Helv. Chim. Acta* **72** 1225-1232 (1989)

54. S.M. Sanins, W.J. Adams, D.G. Kaiser, G.W. Halstead, J. Hosley, H. Barnes and T.A. Baillie, *Drug. Metab. Dispos.* **19** 405-410 (1991)
55. R.G. Simmonds, T.J. Woodage, S.M. Duff and J.N. Green, *Eur. J. Drug Metab. Pharmacokinet.* **5** 169-172 (1980)
56. F. Jamali, R. Mehvar and A.S. Russell, *Pharm. Res.* **5** S-158 PP1238 (1988)
57. R. Mehvar and F. Jamali, *Pharm. Res.* **5** 76-79 (1988)
58. S.R. Cox, *Clin. Pharmacol. Ther.* **43** 146 PIIA-3 (1988)
59. Y. Nakamura, T. Yamaguchi, S. Takahashi, S. Hashimoto, K. Iwatani and Y. Nakagawa, *J. Pharmacobio-Dyn.* **4** S1 (1981)
60. J.W. Cox, S.R. Cox, G. VanGiessen and M.J. Ruwart, *J. Pharmacol. Exp. Ther.* **232** 636-643 (1985)
61. S.M. Sanins, W.J. Adams, D.G. Kaiser, G.W. Halstead and T.A. Baillie, *Drug Metab. Dispos.* **18** 527-533 (1990)
62. M.P. Knadler and S.D. Hall, *Chirality* **2** 67-73 (1990)
63. J.D. Bell, J.C.C. Brown and P.J. Sadler, *Chem. Br.* 1021-1024 (1988)
64. J.R. Bales, D.P. Higham, J.K. Nicholson and P.J. Sadler, *Med. Lab. World* **11**, 13, 15-16, 54 (1984)

65. S.K. Branch and A.F. Casy, *Prog. Med. Chem.* **26** 355-436 (1989)
66. J.C. Lindon, *J. Pharm. Biomed. Anal.* **4** 137-145 (1986)
67. M.C. Malet-Martino and R. Martino, *Xenobiotica* **19** 583-607 (1989)
68. J.K. Nicholson and I.D. Wilson in *Drug Metabolism: from Molecules to Man*, ed. D.J. Benford, J.W. Bridges and G.G. Gibson, Taylor and Francis (1987)
69. J.K. Nicholson and I.D. Wilson, *Prog. Drug Res.* **31** 427-479 (1987)
70. O.A.C Petroff, *Comp. Biochem. Physiol., B: Comp. Biochem.* **90** 249-260 (1988)
71. J.R. Bales, J.D. Bell, J.K. Nicholson, P.J. Sadler, J.A. Timbrell, R.D. Hughes, P.N. Bennett and R. Williams, *Magn. Reson. Med.* **6** 300-306 (1988)
72. J.L. Bock, *Clin. Chem.* **28** 1873-1877 (1982)
73. G. Vermeersch, J. Marko, B. Cartigny, F. Leclerc, P. Roussel and M. Lhermitte, *Clin. Chem.* **34** 1003-1004 (1988)
74. J.R. Everett, K.R. Jennings, G. Woodnutt and M.J. Buckingham, *J. Chem. Soc., Chem. Commun.* 894-895 (1984)
75. P. Kestell, M.H. Gill, M.D. Threadgill, A. Gescher, O.W. Howarth and E.H. Curzon, *Life Sci.* **38** 719-724 (1986)

76. K. Tulip, J.A. Timbrell, J.K. Nicholson, I. Wilson and J. Troke, *Drug Metab. Dispos.* **14** 746-749 (1986)
77. K. Tulip, J.K. Nicholson and J.A. Timbrell, *Adv. Exp. Med. Biol.* **197** (Biol. React. Intermed. 3 ) 941-950 (1986)
78. M.C. Malet-Martino, J.-P. Armand, A. Lopez, J. Bernadou, J.-P. Béteille, M. Bon and R. Martino, *Cancer Res.* **46** 2105-2112 (1986)
79. J.P. Vialaneix, M.C. Malet-Martino, J.S. Hoffmann, J. Pris and R. Martino, *Drug Metab. Dispos.* **15** 718-724 (1987)
80. E.L. Hahn, *Phys. Rev.* **80** 580-594 (1950)
81. H.Y. Carr and E.M. Purcell, *Phys. Rev.* **94** 630-638 (1954)
82. S. Meiboom and D. Gill, *Rev. Sci. Instrum.* **29** 688-691 (1958)
83. J.K.M. Sanders and B.K. Hunter, *Modern NMR Spectroscopy: A Guide for Chemists*, OUP (1988)
84. J.D. Bell, J.C.C. Brown, G. Kubal and P.J. Sadler, *F.E.B.S. Lett.* **235** 81-86 (1988)
85. D. Meynial, A. Lopez, M.C. Malet-Martino, J.S. Hoffmann and R. Martino, *J. Pharm. Biomed. Anal.* **6** 47-59 (1988)

86. I.D. Wilson and J.K. Nicholson, *J. Pharm. Biomed. Anal.* **6** 151-165 (1988)
87. R. Freeman, *A Handbook of Nuclear Magnetic Resonance*, Longman (1988)
88. J.R. Everett, J.W. Tyler and G. Woodnutt, *J. Pharm. Biomed. Anal.* **7** 397-403 (1989)
89. J.R. Everett, K. Jennings and G. Woodnutt, *J. Pharm. Pharmacol.* **37** 869-873 (1985)
90. K.E. Wade, I.D. Wilson, J.A. Troke and J.K. Nicholson, *J. Pharm. Biomed. Anal.* **8** 401-410 (1990)
91. K. Misiura, A. Okruszek, K. Pankiewicz, W.J. Stec, Z. Czownicki and B. Utracka, *J. Med. Chem.* **26** 674-679 (1983)
92. D.R. Dohn, M.J. Graziano and J.E. Casida, *Biochem. Pharmacol.* **37** 3485-3495 (1988)
93. R.E. Norman and P.J. Sadler, *Inorg. Chem.* **27** 3583-3587 (1988)
94. N.E. Preece, J.K. Nicholson and J.A. Timbrell, *Biochem. Pharmacol.* **41** 1319-1324 (1991)
95. J.R. Bales, J.K. Nicholson and P.J. Sadler, *Clin. Chem.* **31** 757-762 (1985)
96. S.M. Sanins, J.A. Timbrell, C. Elcombe and J.K. Nicholson, *Methodol. Surv. Biochem. Anal.* **18** (Bioanal. Drugs Metab.) 375-381 (1988)

97. I.D. Wilson and I.M. Ismail, *J. Pharm. Biomed. Anal.* **4** 663-665 (1986)
98. I.D. Wilson and J.K. Nicholson, *Anal. Chem.* **59** 2830-2832 (1987)
99. S. Yamaguchi in *Asymmetric Synthesis, Volume I, Analytical Methods*, ed. J.D. Morrison, Academic (1983)
100. G.R. Weisman in *Asymmetric Synthesis, Volume I, Analytical Methods*, ed. J.D. Morrison, Academic (1983)
101. R.R. Fraser in *Asymmetric Synthesis, Volume I, Analytical Methods*, ed. J.D. Morrison, Academic (1983)
102. B. Testa and P. Jenner in *Drug Fate and Metabolism: Methods and Techniques, Volume 2*, ed. E.R. Garrett and J.L. Hirtz, Marcel Dekker (1978)
103. J.A. Dale and H.S. Mosher, *J. Am. Chem. Soc.* **90** 3732-3738 (1968)
104. S. Yamaguchi, J.A. Dale and H.S. Mosher, *J. Org. Chem.* **37** 3174-3176 (1972)
105. D. Parker and R.J. Taylor, *J. Chem. Soc., Chem. Commun.* 1781-1783 (1987)
106. G.M. Whitesides and D.W. Lewis, *J. Am. Chem. Soc.* **92** 6979-6980 (1970)
107. C. Kutal in *Nuclear Magnetic Resonance Shift Reagents*, ed. R.E. Sievers, Academic (1973)

108. R.E. Rondeau and R.E. Sievers, *J. Am. Chem. Soc.* **93** 1522-1524 (1971)
109. T.J. Wenzel and R.E. Sievers, *J. Am. Chem. Soc.* **104** 382-388 (1982)
110. K. Kabuto and Y. Sasaki, *Chem. Lett.* 385-388 (1989)
111. K. Kabuto and Y. Sasaki, *J. Chem. Soc., Chem. Commun.* 316-318 (1984)
112. J. Bounoure and J. Souppe, *Analyst* **113** 1143-1144 (1988)
113. J. Reuben, *J. Chem. Soc., Chem. Commun.* 68-69 (1979)
114. J. Reuben, *J. Am. Chem. Soc.* **102** 2232-2237 (1980)
115. J.A. Peters, C.A.M. Vijerberg, A.P.G. Kieboom and H. van Bekkum, *Tetrahedron Lett.* **24** 3141-3144 (1983)
116. J. Granot and J. Reuben, *J. Am. Chem. Soc.* **100** 5209-5210 (1978)
117. J.F. DeBernardis, D.J. Kerkman, D.L. Arendsen, S.A. Buckner, J.J. Kyncl and A.A. Hancock, *J. Med. Chem.* **30** 1011-1017 (1987)
118. W.H. Pirkle, *J. Am. Chem. Soc.* **88** 1837 (1966)
119. C.P.R. Jennison and D. Mackay, *Can. J. Chem.* **51** 3726-3732 (1973)
120. C.A.R. Baxter and H.C. Richards, *Tetrahedron Lett.* 3357-3358 (1972)



121. D. Parker and R.J. Taylor, *Tetrahedron* **43** 5451-5456 (1987)
122. A. Dobashi, N. Saito, Y. Motoyama and S. Hara, *J. Am. Chem. Soc.* **108** 307-308 (1986)
123. J. Szejtli, *Cyclodextrins and their Inclusion Complexes*, Akadémiai Kiadó (1982)
124. H. Dugas, *Bioorganic Chemistry: A Chemical Approach to Enzyme Action*, 2nd Edition, Springer-Verlag (1989)
125. D.D. MacNicol and D.S. Rycroft, *Tetrahedron Lett.* **25** 2173-2176 (1977)
126. A.F. Casy and A.D. Mercer, *Magn. Reson. Chem.* **26** 765-774 (1988)
127. D. Greatbanks and R. Pickford, *Magn. Reson. Chem.* **25** 208-215 (1987)
128. K. Uekama, T. Imai, F. Hirayama, M. Otagiri, T. Hibi and M. Yamasaki, *Chem. Lett.* 61-64 (1985)
129. N.J. Smith, T.M. Spotswood and S.F. Lincoln, *Carbohydr. Res.* **192** 9-15 (1989)
130. T. Murakami, K. Harata and S. Morimoto, *Chem. Lett.* 553-556 (1988)
131. J.J. Richards and M.L. Webb in *Chirality in Drug Design and Synthesis*, ed. C. Brown, Academic (1990)

132. W.-S. Chung, N.J. Turro, J. Silver and W.J. le Noble, *J. Am. Chem. Soc.* **112** 1202-1205 (1990)
133. S.R. Abrams, M.J.T. Reaney, G.D. Abrams, T. Mazurek, A.C. Shaw and L.V. Gusta, *Phytochemistry* **28** 2885-2889 (1989)
134. N. Lamb and S.R. Abrams, *Can. J. Chem.* **68** 1151-1162 (1990)
135. R. McCague, M. Jarman, M.G. Rowlands, J. Mann, C.P. Thickitt, D.W. Clissold, S. Neidle and G. Webster, *J. Chem. Soc. , Perkin Trans. 1* 196-198 (1989)
136. E. Redenti, G. Bovis, G. Fronza and P. Ventura in *Minutes of the Fifth International Symposium on Cyclodextrins*, ed. D. Duchene, Editions Sante (1990)
137. M. Bernabé, J. Jiménez-Barbero, M. Martin-Lomas, S. Penadés and C. Vicent, *Carbohydr. Res.* **208** 255-259 (1990)
138. Y. Yamashoji, M. Tanaka and T. Shono, *Chem. Lett.* 945-948 (1990)
139. A. Taylor, D.A.R. Williams and I.D. Wilson, *J. Pharm. Biomed. Anal.* **9** 493-496 (1991)
140. A.W. Coleman, G. Tsoucaris, H. Parrot, H. Galons, M. Miocque, B. Perly, N. Keller and P. Charpin, *J. Chromatogr.* **450** 175-182 (1988)

141. R. Dyllick-Brezinger and J.D. Roberts, *J. Am. Chem. Soc.* **102** 1166-1167 (1980)
142. I. Orienti, C. Cavallari, V. Zecchi and A. Fini, *Arch. Pharm.* **322** 207-211 (1989)
143. K. Uekama, T. Imai, T. Maeda, T. Irie, F. Hirayama and M. Otagiri, *J. Pharm. Sci.* **74** 841-845 (1985)
144. D.D. Chow and A.H. Karara, *Int. J. Pharm.* **28** 95-101(1986)
145. G.P. Bettinetti, P. Mura, A. Liguori, G. Bramanti and F. Giordano, *Farmaco* **44** 195-213 (1989)
146. N. Kobayashi, *J. Chem. Soc., Chem. Commun.* 1126-1128 (1989)
147. T. Irie, K. Fukunaga, J. Pitha, K. Uekama, H.M. Fales and E.A. Sokolowski, *Carbohydr. Res.* **192** 167-172 (1989)
148. C.M. Spencer, J.F. Stoddart and R. Zarzycki, *J. Chem. Soc., Perkin Trans. 2* 1323-1336 (1987)
149. K. Koizumi, Y. Kubota, T. Utamura and S. Horiyama, *J. Chromatogr.* **368** 329-337 (1986)
150. Y. Kabuto, T. Tanimoto, S. Horiyama and K. Koizumi, *Carbohydr. Res.* **192** 159-166 (1989)

151. R.J. Abraham and P. Loftus, *Proton and Carbon-13 NMR Spectroscopy, An Integrated Approach*, Heyden (1981)
152. W. Kemp, *NMR in Chemistry, a Multinuclear Introduction*, Macmillan (1986)
153. C. Brevard and P. Granger, *Handbook of High Resolution Multinuclear NMR*, Wiley (1981)
154. I.M. Brereton, T.M. Spotswood, S.F. Lincoln and E.H. Williams, *J. Chem. Soc., Faraday Trans. 1* **80** 3147-3156 (1984)
155. P.V. Demarco and A.L. Thakkar, *J. Chem. Soc., Chem. Commun.* 2-4 (1970)
156. C.E. Johnson Jr. and F.A. Bovey, *J. Chem. Phys.* **29** 1012-1014 (1958)
157. J.W. Emsley, J. Feeney and L.H. Sutcliffe, *High Resolution Nuclear Magnetic Resonance Spectroscopy Volume I*, Pergamon (1967)
158. F. Djedaïni, S.Z. Lin, B. Perly, D. Wouessidjewe, *J. Pharm. Sci.* **79** 643-646 (1990)
159. T. Backensfeld, B.W. Müller, M. Wiese, J.K. Seydel, *Pharm. Res.* **7** 484-490 (1990)
160. Y. Kotake and E.G. Janzen, *J. Am. Chem. Soc.* **111** 2066-2070 (1989)
161. Y. Kotake and E.G. Janzen, *J. Am. Chem. Soc.* **111** 5138-5140 (1989)

162. *Blood and Other Body Fluids*, ed. D.S. Dittmer, Federation of American Societies for Experimental Biology (1961)
163. L. Eberson in *The Chemistry of Carboxylic Acids and Esters*, ed. S. Patai, Interscience (1969)
164. K. Harata, K. Uekama, M. Otagiri and F. Hirayama, *J. Inclusion Phenom.* **1** 279-293 (1984)
165. K. Harata, *J. Chem. Soc., Perkin Trans. 2* 799-804 (1990)
166. K. Kano, K. Yoshiyasu and S. Hashimoto, *J. Chem. Soc., Chem. Commun.* 1278-1279 (1989)
167. C.H. Dungan and J.R. Van Wazer, *Compilation of Reported  $F^{19}$  NMR Chemical Shifts: 1951 to Mid-1967*, Wiley Interscience (1970)
168. *Registry of Toxic Effects of Chemical Substances, 1981-2 Edition*, ed. R.L. Tatken and R.J. Lewis Sr., US Department of Health and Human Services (1983)
169. D.Y. Pharr, Z.S. Fu, T.K. Smith and W.L. Hinze, *Anal. Chem.* **61** 275-279 (1989)
170. Y. Yamamoto, M. Onda, Y. Takahashi, Y. Inoue, R. Chûjô, *Carbohydr. Res.* **170** 229-234 (1987)
171. D. Sybilska and J. Zukowski in *Chiral Separations by HPLC: Applications to Pharmaceutical Compounds*, ed. A.M. Krstulovic, Ellis Horwood (1989)

172. D.W. Armstrong, J.R. Faulkner Jr. and S.M. Han, *J. Chromatogr.* **452** 323-330 (1988)
173. S.M. Han and D.W. Armstrong in *Chiral Separations by HPLC: Applications to Pharmaceutical Compounds*, ed. A.M. Krstulovic, Ellis Horwood (1989)
174. V. Schurig, D. Schmalzing and M. Schleimer, *Angew. Chem., Int. Ed. Engl.* **30** 987-989 (1991)
175. V. Schurig and H.-P. Nowotny, *Angew. Chem., Int. Ed. Engl.* **29** 939-1076 (1990)
176. D.W. Armstrong, W. DeMond, A. Alak, W.L. Hinze, T.E. Riehl and K.H. Bui, *Anal. Chem.* **57** 234-237 (1985)
177. A.D. Cooper and T.M. Jefferies, *J. Pharm. Biomed. Anal.* **8** 847-851 (1990)
178. G. Vigh, G. Quintero and G. Farkas, *J. Chromatogr.* **506** 481-493 (1990)
179. F. Cramer and W. Dietsche, *Chem. Ber.* **92** 378-384 (1959)
180. S. Colonna, A. Manfredi, R. Annunziati, N. Gaggero and L. Casella, *J. Org. Chem.* **55** 5862-5866 (1990)
181. K. Hattori, K. Takahashi, M. Uematsu and N. Sakai, *Chem. Lett.* 1463-1466 (1990)

182. K.K. Chacko and W. Saenger, *J. Am. Chem. Soc.* **103** 1708-1715 (1981)
183. D. Duchene and D. Wouessidjewe, *Pharm. Technol.* **14** (6) 26,28,32,34 and **14** (8) 22,24,26,28,30 (1990)
184. A. Juhász, A. Salgó and A. Sebók in *Proceedings of the Fourth International Symposium on Cyclodextrins*, ed. O. Huber and J. Szejtli, Kluwer Academic (1988)
185. H. Hashimoto in *Proceedings of the Fourth International Symposium on Cyclodextrins*, ed. O. Huber and J. Szejtli, Kluwer Academic (1988)
186. R.J. Clarke, J.H. Coates and S.F. Lincoln, *Adv. Carbohydr. Chem. Biochem.* **46** 205-335 (1988)
187. D. French, A.O. Pulley, J.A. Effenberger, M.A. Rougvie and M. Abdullah, *Arch. Biochem. Biophys.* **111** 153-160 (1965)
188. T. Fujiwara, N. Tanaka and S. Kobayashi, *Chem. Lett.* 739-742 (1990)
189. D. French, *Adv. Carbohydr. Chem.* **12** 189-260 (1957)
190. P.R. Sundararajan and V.S.R. Rao, *Carbohydr. Res.* **13** 351-358 (1970)
191. C. Betzel, W. Saenger, B.E. Hingerty and G.M. Brown, *J. Am. Chem. Soc.* **106** 7545-7557 (1984)
192. K. Lindner and W. Saenger, *Angew. Chem., Int. Ed. Engl.* **17** 694-695 (1978)

193. K. Lindner and W. Saenger, *Carbohydr. Res.* **99** 103-115 (1982)
194. V. Zabel, W. Saenger and S.A. Mason, *J. Am. Chem. Soc.* **108** 3664-3673 (1986)
195. W. Saenger, C. Betzel, B. Hingerty and G.M. Brown, *Nature* **296** 581-583 (1982)
196. T. Fujiwara, M. Yamazaki, Y. Tomizu, R. Tokuoka, K. Tomita, T. Matsuo, H. Suga and W. Saenger, *Nippon Kagaku Kaishi* 181-187 (1983)
197. W. Saenger in *Inclusion Compounds Volume 2, Structural Aspects of Inclusion Compounds formed by Organic Host Lattices*, ed. J.L. Atwood, J.E.D. Davies and D.D. MacNicol, Academic (1984)
198. Y. Inoue, Y. Takahashi and R. Chûjô, *Carbohydr. Res.* **148** 109-114 (1986)
199. W.A. König, *Carbohydr. Res.* **192** 51-60 (1989)
200. G.M. Lipkind, A.S. Shashkov, S.S. Mamyan and N.K. Kochetkov, *Bioorg. Khim.* **13** 1075-1080 (1987)
201. B. Mulloy, T.A. Frenkiel and D.B. Davies, *Carbohydr. Res.* **184** 39-46 (1988)
202. M. Onda, Y. Yamamoto, Y. Inoue and R. Chûjô, *Bull. Chem. Soc. Jpn.* **61** 4015-4021 (1988)



203. M. St-Jacques, P.R. Sundararajan, K.J. Taylor and R.H. Marchessault, *J. Am. Chem. Soc.* **98** 4386-4391 (1976)
204. J.C. Christofides and D.B. Davies, *J. Chem. Soc., Chem. Commun.* 560-562 (1982)
205. N. Kobayashi, *J. Chem. Soc., Chem. Commun.* 918-919 (1988)
206. N. Kobayashi and T. Osa, *Carbohydr. Res.* **192** 147-157 (1989)
207. N. Kobayashi, *J. Chem. Soc., Chem. Commun.* 1126-1128 (1989)
208. A.F. Danil de Namor, R. Traboulssi and D.F.V. Lewis, *J. Chem. Soc., Chem. Commun.* 751-753 (1990)
209. A.F. Danil de Namor, R. Traboulssi and D.F.V. Lewis, *J. Am. Chem. Soc.* **112** 8442-8447 (1990)
210. M. Komiyama, *J. Am. Chem. Soc.* **111** 3046-3050 (1989)
211. O.S. Tee and J.J. Hoeven, *J. Am. Chem. Soc.* **111** 8318-8320 (1989)
212. C. Tanford, *The Hydrophobic Effect: Formation of Micelles and Biological Membranes*, Wiley-Interscience (1980)
213. K.W. Street Jr., *J. Liq. Chromatogr.* **10** 655-662 (1987)
214. M. Komiyama and M.L. Bender, *J. Am. Chem. Soc.* **100** 2259-2260 (1978)

215. R.L. VanEtten, J.F. Sebastian, G.A. Clowes and M.L. Bender, *J. Am. Chem. Soc.* **89** 3242-3253 (1967)
216. M. Sakurai, M. Kitagawa, H. Hoshi, Y. Inoue and R. Chûjô, *Carbohydr. Res.* **198** 181-191 (1990)
217. M. Kitagawa, H. Hoshi, M. Sakurai, Y. Inoue and R. Chûjô, *Carbohydr. Res.* **163** c1-c3 (1987)
218. P.C. Manor and W. Saenger, *J. Am. Chem. Soc.* **96** 3630-3639 (1974)
219. W. Saenger, *Nature* **279** 343-344 (1979)
220. B. Klar, B. Hingerty and W. Saenger, *Acta Crystallogr.* **B36** 1154-1165 (1980)
221. W. Saenger and K. Lindner, *Angew. Chem., Int. Ed. Engl.* **19** 398-399 (1980)
222. K. Lindner and W. Saenger, *Acta Crystallogr.* **B38** 203-210 (1982)
223. M. J. Gidley and S.M. Bociek, *J. Chem. Soc., Chem. Commun.* 1223-1226 (1986)
224. M. J. Gidley and S.M. Bociek, *Carbohydr. Res.* **183** 126-130 (1988)
225. I. Tabushi, Y. Kiyosuke, T. Sugimoto and K. Yamamura, *J. Am. Chem. Soc.* **100** 916-919 (1978)

226. I. Tabushi, *Acc. Chem. Res.* **15** 66-72 (1982)
227. R.I. Gelb, L.M. Schwartz, M. Radeos and D.A. Laufer, *J. Phys. Chem.* **87** 3349-3354 (1983)
228. R.I. Gelb, L.M. Schwartz, B. Cardelino, H.S. Fuhrman, R.F. Johnson and D.A. Laufer, *J. Am. Chem. Soc.* **103** 1750-1757 (1981)
229. D.W. Griffiths and M.L. Bender, *Adv. Catal.* **23** 209-261 (1973)
230. A. Buvári and L. Barcza, *Acta Chim. Hung.* **126** 455-462 (1989)
231. F.H. Allen, O. Kennard and R. Taylor, *Acc. Chem. Res.* **16** 146-153 (1983)
232. K. Uekama, F. Hirayama, T. Imai, M. Otagiri and K. Harata, *Chem. Pharm. Bull.* **31** 3363-3365 (1983)
233. K. Uekama, T. Imai, F. Hirayama, M. Otagiri and K. Harata, *Chem. Pharm. Bull.* **32** 1662-1664 (1984)
234. K. Harata, K. Uekama, M. Otagiri and F. Hirayama, *J. Inclusion Phenom.* **2** 583-594 (1984)
235. J.A. Hamilton and L. Chen, *J. Am. Chem. Soc.* **110** 4379-4391 (1988)
236. J.A. Hamilton and L. Chen, *J. Am. Chem. Soc.* **110** 5833-5841 (1988)

237. A.M. Stalcup and D.W. Armstrong in *Minutes of the Fifth International Symposium on Cyclodextrins*, ed. D. Duchene, Editions Sante (1990)
238. P. Macaudière, M. Lienne, A. Tambuté and M. Caude in *Chiral Separations by HPLC: Applications to Pharmaceutical Compounds*, ed. A.M. Krstulovic, Ellis Horwood (1989)
239. D.W. Armstrong, W. Li, C.-D. Chang and J. Pitha, *Anal. Chem.* **62** 914-923 (1990)
240. W.A. König, S. Lutz and G. Wenz in *Proceedings of the Fourth International Symposium on Cyclodextrins*, ed. O. Huber and J. Szejtli (1988)
241. J. Drabowicz, B. Dudzinski, P. Lyzwa and M. Mikolajczyk in *Proceedings of the Fourth International Symposium on Cyclodextrins*, ed. O. Huber and J. Szejtli, Kluwer Academic (1988)
242. J. Michon and A. Rassat, *J. Am. Chem. Soc.* **101** 995-996 (1979)
243. M. Mikolajczyk and J. Drabowicz, *J. Am. Chem. Soc.* **100** 2510-2515 (1978)
244. M.L. Martin, G.J. Martin and J.-J. Delpuech, *Practical NMR Spectroscopy*, Heyden (1980)
245. R.L. Vold, J.S. Waugh, M.P. Klein and D.E. Phelps, *J. Chem. Phys.* **48** 3831-3832 (1968)
246. S.W. Homans, *A Dictionary of Concepts in NMR*, Clarendon (1989)

247. R. Freeman and H.D.W. Hill, *J. Chem. Phys.* **54** 3367-3377 (1971)
248. J.L. Markley, W.J. Horsley and M.P. Klein, *J. Chem. Phys.* **55** 3604-3605 (1971)
249. K.A. Christensen, D.M. Grant, E.M. Schulman and C. Walling, *J. Phys. Chem.* **78** 1971-1977 (1974)
250. J. Homer and M.S. Beevers, *J. Magn. Reson.* **63** 287-297 (1985)
251. J. Homer and J.K. Roberts, *J. Magn. Reson.* **74** 424-432 (1987)
252. D. Canet, J. Brondeau and K. Elbayed, *J. Magn. Reson.* **77** 483-490 (1988)
253. D. Neuhaus and M.P. Williamson, *The Nuclear Overhauser Effect in Structural and Conformational Analysis*, VCH (1989)
254. R. Richarz and K. Wüthrich, *J. Magn. Reson.* **30** 147-150 (1978)
255. A.E. Derome, *Modern NMR Techniques for Chemistry Research*, Pergamon (1987)
256. F. Heatley, L. Akhter and R.T. Brown, *J. Chem. Soc., Perkin Trans. 2* 919-924 (1980)
257. G.A. Morris and R. Freeman, *J. Magn. Reson.* **29** 433-462 (1978)

258. A. Kumar, R.R. Ernst and K. Wüthrich, *Biochem. Biophys. Res. Commun.* **95** 1-6 (1980)
259. J.W. Keepers and T.L. James, *J. Magn. Reson.* **57** 404-426 (1984)
260. A.A. Bothner-By, R.L. Stephens, J. Lee, C.D. Warren and R.W. Jeanloz, *J. Am. Chem. Soc.* **106** 811-813 (1984)
261. H. Kessler, C. Griesinger, R. Kerssebaum, K. Wagner and R.R. Ernst, *J. Am. Chem. Soc.* **109** 607-609 (1987)
262. A. Bax and D.G. Davis, *J. Magn. Reson.* **63** 207-213 (1985)
263. C.J. Bauer, T.A. Frenkiel and A.N. Lane, *J. Magn. Reson.* **87** 144-152 (1990)
264. D. Neuhaus and J. Keeler, *J. Magn. Reson.* **68** 568-574 (1986)
265. A. Bax, *J. Magn. Reson.* **77** 134-147 (1988)
266. Y. Yamamoto and Y. Inoue, *J. Carbohydr. Chem.* **8** 29-46 (1989)
267. Y. Yamamoto, M. Onda, M. Kitagawa, Y. Inoue and R. Chûjô, *Carbohydr. Res.* **167** c11-c16 (1987)
268. Y. Yamamoto, M. Onda, Y. Takahashi, Y. Inoue and R. Chûjô, *Carbohydr. Res.* **182** 41-52 (1988)
269. S. Hamai, *J. Chem. Phys.* **94** 2595-2600 (1990)

270. T. Imai, T. Irie, M. Otagiri, K. Uekama and M. Yamasaki, *J. Inclusion Phenom.* **2** 597-604 (1984)
271. J. Sunamoto, H. Okamoto, K. Taira and Y. Murakami, *Chem. Lett.* 371-374 (1975)
272. R.C. Couch and G.E. Martin, *J. Magn. Reson.* **92** 189-194 (1991)
273. L. Poppe and H. van Halbeek, *J. Magn. Reson.* **93** 214-217 (1991)
274. D.J. Wood, F.E. Hruska and W. Saenger, *J. Am. Chem. Soc.* **99** 1735-1740 (1977)
275. C. Hervé du Penhoat, A. Imberty, N. Roques, V. Michon, J. Mentech, G. Descotes and S. Pérez, *J. Am. Chem. Soc.* **113** 3720-3727 (1991)
276. C. Altona and C.A.G. Haasnoot, *Org. Magn. Reson.* **13** 417-429 (1980)
277. P. Job, *Ann. Chim.* **9** 113-203 (1928)
278. V.M.S. Gil and N.C. Oliveira, *J. Chem. Educ.* **67** 473-478 (1990)
279. M. Suzuki and Y. Sasaki, *Chem. Pharm. Bull.* **32** 832-838 (1984)
280. S. Hamai, *Bull. Chem. Soc. Jpn.* **55** 2721-2729 (1982)

281. H. Shigekawa, T. Morozumi, M. Komiyama, M. Yoshimura, A. Kawazu and Y. Saito, *J. Vac. Sci. Technol.* **B9** 1189-1192 (1991)
282. M.C.R. Symons, J.A. Benbow and J.M. Harvey, *Carbohydr. Res.* **83** 9-20 (1980)
283. H. Uedaira, M. Ikura, H. Uedaira, *Bull. Chem. Soc. Jpn.* **62** 1-4 (1989)
284. H. Uedaira, M. Ishimura, S. Tsuda and H. Uedaira, *Bull. Chem. Soc. Jpn.* **63** 3376-3379 (1990)
285. Y. Inoue, Y. Kanda, Y. Yamamoto, R. Chûjô and S. Kobayashi, *Carbohydr. Res.* **194** c8-c13 (1989)
286. W. Saka, Y. Yamamoto, Y. Inoue, R. Chûjô, K. Takahashi and K. Hattori, *Bull. Chem. Soc. Jpn.* **63** 3175-3182 (1990)
287. G. Esposito, W.A. Gibbons and R. Bazzo, *J. Magn. Reson.* **80** 523-527 (1988)
288. M. Rance, *J. Magn. Reson.* **74** 557-564 (1987)
289. M. Rance and J. Cavanagh, *J. Magn. Reson.* **87** 363-371 (1990)
290. Y. Inoue, F.-H. Kuan and R. Chûjô, *Bull. Chem. Soc. Jpn.* **60** 2539-2545 (1987)
291. M. Suzuki, H. Takai, J. Szejtli and E. Fenyvesi, *Carbohydr. Res.* **201** 1-14 (1990)



292. A. Neszmélyi in *Proceedings of the First International Symposium on Cyclodextrins*, ed. J. Szejtli, Reidel (1982)
293. J.S. Waugh, *J. Magn. Reson.* **50** 30-49 (1982)
294. J. Brondeau and D. Canet, *J. Chem. Phys.* **67** 3650-3654 (1977)
295. W.F. Reynolds, S. McLean, M. Perpich-Dumont and R.G. Enríquez, *Magn. Reson. Chem.* **27** 162-169 (1989)